CORA Cork Open Research Archive
Cartlann Taighde Oscailte Chorcaí

Title	A study on the impact of primary packaging interfaces on protein adsorption and stability
Authors	Downey, John D.
Publication date	2024
Original Citation	Downey, J. D. 2024. A study on the impact of primary packaging interfaces on protein adsorption and stability. PhD Thesis, University College Cork.
Type of publication	Doctoral thesis
Rights	© 2024, John Downey. - https://creativecommons.org/licenses/by/4.0/
Download date	2026-11-03 11:18:48
Item downloaded from	https://hdl.handle.net/10468/17585



UCC
University College Cork, Ireland
Coláiste na hOllscoile Corcaigh

Ollscoil na hÉireann, Corcaigh

National University of Ireland, Cork



A Study on the Impact of Primary Packaging Interfaces on Protein Adsorption and Stability

Thesis presented by

John Downey, MSc

0000-0001-9929-5555

for the degree of

Doctor of Philosophy

University College Cork

School of Pharmacy

Head of School: Prof. Brendan Griffin

Supervisors: Dr Katie Ryan & Prof. Abina Crean

2024

For Eleanor,

I hope I made you proud

Table of Contents

Table of Contents ..... Page i
Declaration of Authorship ..... Page iv
Abstract ..... Page v
Acknowledgements ..... Page vii
Publications & Presentations ..... Page ix
List of Figures ..... Page x
List of Tables ..... Page xiv
List of Abbreviations ..... Page xv
Thesis Outline ..... Page xvii

Chapter One

1. General Introduction ..... Page 1
1.1 Background ..... Page 2
1.1.1 Therapeutic proteins ..... Page 2
1.1.2 Protein stability considerations ..... Page 2
1.1.3 Protein formulations ..... Page 10
1.1.4 Primary packaging ..... Page 11
1.1.5 Mitigating protein adsorption ..... Page 16
1.1.6 Analysing protein adsorption and stability ..... Page 17
1.1.7 Proteins investigated in this thesis ..... Page 18
Aims & Objectives ..... Page 20

Chapter Two

2. Impact of Protein Adsorption During Biopharmaceutical Manufacture & Storage ..... Page 21
2.1 Abstract ..... Page 22
2.2 Introduction ..... Page 23
2.3 Factors impacting protein adsorption ..... Page 25
2.4 Protein adsorption during fill-finish and storage operations ..... Page 28
2.4.1 Challenges in downstream bioprocessing ..... Page 28
2.4.2 Fill-finish interfaces ..... Page 30
2.4.3 Primary packaging interfaces during storage ..... Page 34
2.5 Formulation strategies to reduce protein adsorption ..... Page 39
2.5.1 Excipient selection ..... Page 39
2.5.2 Surfactants ..... Page 40
2.5.3 Other excipients ..... Page 43
2.6 Conclusions ..... Page 49

Chapter Three

3. Lysozyme Adsorption to Borosilicate: Influence of Buffer pH & Composition ..... Page 50

3.1 Abstract ..... Page 51

3.2 Introduction ..... Page 52

3.3 Materials & methods ..... Page 54

3.3.1 Materials ..... Page 54

3.3.2 Methods ..... Page 54

3.4 Results ..... Page 58

3.4.1 Lysozyme analysis in buffered solutions ..... Page 58

3.4.2 Lysozyme adsorption behaviour ..... Page 64

3.5 Discussion ..... Page 69

3.6 Conclusion ..... Page 73

Chapter Four

4. Influence of Packaging Interface and Leucine Concentration on BSA Stability ..... Page 74

4.1 Abstract ..... Page 75

4.2 Introduction ..... Page 76

4.3 Materials & methods ..... Page 79

4.3.1 Materials ..... Page 79

4.3.2 Methods ..... Page 79

4.4 Results ..... Page 82

4.4.1 Thermal unfolding studies ..... Page 82

4.4.2 Impact of vial orientation and storage conditions on the stability of BSA ..... Page 85

4.4.3 Evaluation of the effect of leucine concentration on BSA stability under thermal agitation conditions ..... Page 91

4.5 Discussion ..... Page 99

4.6 Conclusion ..... Page 102

Chapter Five

5. Application of a Phosphorylcholine Polymer on Vial Stoppers Using a Cold Plasma Deposition Process ..... Page 103

5.1 Abstract ..... Page 104

5.2 Introduction ..... Page 105

5.3 Materials & methods ..... Page 108

5.3.1 Materials ..... Page 108

5.3.2 Methods ..... Page 108

5.4 Results ..... Page 115

5.4.1 Optimizing coating parameters using design of experiments ..... Page 115

5.4.2 Microscopic analysis of poly(MPC-*co*-BMA)-coated stoppers Page 119
5.4.3 Spectroscopic analysis of poly(MPC-*co*-BMA) coatings Page 123
5.4.4 BSA formulation compatibility with coated stoppers Page 128
5.5 Discussion Page 132
5.6 Conclusion Page 137

Chapter Six
6. General Discussion Page 138
6.1 Research objectives and outcomes Page 139
6.1.1 Thesis findings Page 140
6.1.2 Thesis highlights Page 147
6.1.3 Limitations Page 147
6.1.4 Future work Page 148
6.1.5 Conclusions Page 149

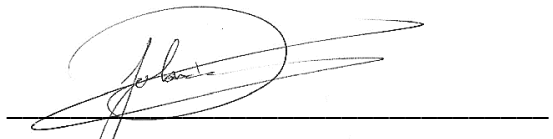
References Page 151
Appendix Page 178
S3 Supplementary Information for Chapter Three Page 178
S3.1 Supporting Methods Page 178
S3.2 Supporting Results Page 179
S4 Supplementary Information for Chapter Four Page 182
S4.1 Supporting Results Page 182
S5 Supplementary Information for Chapter Five Page 184
S5.1 Supporting Methods Page 184
S5.2 Supporting Results Page 184
S6 Supplementary Information for Chapter Six Page 193

Declaration of Authorship

This is to certify that the work I am submitting is my own and has not been submitted for another degree, either at University College Cork or elsewhere. All external references and sources are clearly acknowledged and identified within the contents. I have read and understood the regulations of University College Cork concerning plagiarism and intellectual property.

The following contributions were made to **Chapter Five**. Dr Denis O'Sullivan, TheraDep Ltd. assisted in selecting the plasma process parameters for investigation. Chloe Frewen, TheraDep Ltd. performed the coating of the elastomeric closures and their atomic force microscopy analysis. Dr Richard Unitt, School of Biological, Earth & Environmental Sciences UCC, performed chemical analysis of the elastomeric closures using Raman hyperspectral imaging. Hazel Neill, Tyndall National Institute, assisted in scanning electron microscopy with energy-dispersive X-ray spectroscopy of the elastomeric closures.

This thesis has emanated from research supported partly by a research grant from Science Foundation Ireland (SFI). It was co-funded under the European Regional Development Fund [grant numbers 12/RC/2275(P2) and 18/EPSRC-CDT/3587] and the Engineering and Physical Sciences Research Council UK [grant number EP/S023054/1]. For open access, the author has applied a CC BY public copyright license for any publications arising from this thesis.



John D. Downey

Abstract

Protein-based therapies represent a transformative class of biotherapeutics, yet their stability remains a critical challenge. Therapeutic proteins are intrinsically unstable molecules owing to their structural complexity and amphiphilic properties and potential to adsorb to interfaces present during the product development lifecycle and shelf-life. Protein adsorption promotes unfolding and aggregation which can result in altered bioactivity of the therapeutic moiety or particle formation in solution. Consequently, there is an increased risk of deleterious effects such as lack of efficacy upon administration or an adverse immunogenic reaction. To overcome these challenges, rational formulation design and selection of compatible packaging materials can minimise protein adsorption. However, the excipients used in biological medicines have drawbacks such as poor chemical stability in aqueous solution and the potential to degrade packaging coatings. Moreover, owing to the stringent requirements for primary packaging materials, innovative packaging solutions have not received significant attention to date.

The overall aim of this thesis is to explore the impact of packaging interfaces and formulation on the adsorption and stability of two model proteins, lysozyme and bovine serum albumin (BSA), and develop novel formulation and packaging mitigation strategies to minimise the adverse impacts arising from protein-packaging interactions.

Chapter One introduces protein therapeutics, focusing on their higher order structure, the impact of various stresses on protein physicochemical stability and formulation requirements to maintain stability. It also considers primary packaging for liquid parenterals and the impact of the protein formulation on container/closure compatibility.

Chapter Two reviews prior literature on protein adsorption-induced instability during fill pumping and storage. Topics include factors influencing protein adsorption behaviour, interfaces present during unit operations, pump and tubing types, primary packaging materials, excipient-packaging incompatibility, and formulation considerations. **Chapters Three**, **Four** and **Five** focus on investigating the gaps in the formulation and packaging approaches to reduce protein adsorption and instability identified in **Chapter Two**.

Chapter Three principally explores the effect of buffer type and pH on lysozyme adsorption to borosilicate glass. Lysozyme adsorption to borosilicate was found to be

mediated by electrostatic interactions owing to the ionisation of glass in aqueous solutions generating an anionic material interface. Buffer type did not have a significant impact on the quantity of adsorbed lysozyme, but it was found to influence the properties of the adsorbed protein layer.

Chapter Four examines the effect of vial orientation (upright versus inverted storage) on BSA stability under different storage conditions over one week. Inverted storage in vials with polydimethylsiloxane-coated stoppers at 40°C under agitation resulted in greater protein unfolding and aggregation. Packaging and formulation mitigation strategies of altering the vial stopper to an ethylene tetrafluoroethylene coating and including leucine as an aggregation suppressor were shown to be unsuitable for maintaining BSA in its native conformation under these storage conditions.

Chapter Five focuses on developing an innovative vial stopper coating to reduce protein instability where sustained contact with vial stoppers occurs. A copolymer, poly(MPC-*co*-BMA), comprised of 2-methacryloyloxyethyl phosphorylcholine and butyl methacrylate was used to deposit a thin film coating to bromobutyl rubber stoppers using an innovative aerosol-assisted cold plasma deposition technique. Plasma process parameters (flow rate, speed and voltage) were found to affect coating coverage as indicated by changes in stopper hydrophobicity. BSA compatibility with poly(MPC-*co*-BMA)-coated stoppers was found to be comparable to commercial polydimethylsiloxane and ethylene tetrafluoroethylene stopper coatings over a 3-month storage period.

Chapter Six provides a general discussion of the research performed and presents the key findings, limitations, future work and conclusions of this thesis. In brief, this thesis investigates how packaging interfaces and formulations affect protein adsorption and stability, focusing on strategies to mitigate protein instability. This thesis found that for the lysozyme, adsorption can be controlled by the solution pH and that for BSA, interfacial stress plays a minor role while storage environments significantly impact stability. Additionally, aerosol-assisted, low-temperature plasma is a viable thin film coating deposition technique for pharmaceutical packaging but requires further research to determine the long-term stability of the coating in the presence of liquid protein formulations.

Acknowledgements

A PhD, despite its solitary nature, cannot be accomplished in isolation, and the success of a project relies on the culmination of efforts from a dedicated group of people. To that effect, acknowledging those who have contributed to this thesis is of the utmost importance.

First, I would like to thank my supervisors, Dr Katie Ryan and Prof. Abina Crean, for teaching me what it means to be an independent scientist and the importance of collaboration and teamwork. Thank you always for your advice, support, and understanding. Thank you for this opportunity, I am deeply grateful for your mentorship. I do have to add, now that I'm well into the new job, you trained me well for a SciComm role!

To my family, who believe I work at both McDonald's and CUH despite being in UCC since 2015. Thank you for being interested, rarely asking what's next, listening to me, and supporting me over the years. A special thank you to my grandparents, John and Nancy, who are always there for me with acceptance. To my Mom and Dad for unwavering love and for being there to celebrate my success.

To everyone in UCC who offered support, encouragement, and time throughout the years. Dr Michael Cronin, Dr Ken Devine, and Dr Fatma Farag, thank you for always assisting with my research and teaching me instrument engineering. Michael, thank you for all the discussions and advice. Ken, I am very sorry for constantly complaining about the HPLCs. Dr Sonja Vucen, for always being someone I can talk to without judgement. To Aisha and Kathleen, who were always willing to help and lend an ear for a chat. To Prof. Brendan Griffin for the recommendation.

To the pharmaceutics, SSPC and CDT cohorts. Khaled, Theo and Andrew, friends I never knew I needed. Khaled, thank you for always helping me think through the noise. Andrew, for all the time spent playing Seven, Uno Flip, Mario Kart, pool, bowling and trips to the Borough Market. Theo, for the shared sense of humour. Lianne, Rasha, Omar and Fatma for what I believe will be a lifelong friendship. Jack, for a memorable time in Vienna. To Laura, Maja, Nancy, Aida, Claudia, Callum, Lotte, Michael, Chengbin, Miguel, Sophia, and Francisca, thank you for your kindness and friendship. For all the pub quizzes, birthdays and parties. Kate, for the glasses of red and white wine with conference dinners, for being thoughtful and considerate, and for always having a nice thing to say. Maria, Cristina, and Aswathy, thank

you for the fun shared at every CDT event and conference. Maria, for the shared love of Baldur's Gate 3 and good Chinese food. To the UK students, namely Emily, Colm, Lewis, Grazia, Alfredo, Merryn and Fiona, for the laughs and banter shared. To the Italians in Tyndall for unexpected friendships.

I want to give a special mention to Tracy Gallagher, Prof. Anne-Marie Healy, Prof. Steven Ferguson, and Prof. Snow Stolnik for their leadership, mentorship, and kindness. I also thank Martin, Louise, Sarah and Graham who were always extremely helpful. I thank the SSPC and CDT for funding my research, allowing me to see the world, and supporting my extracurricular activities. I also want to thank Evan Healy for always having an open door.

To everyone who directly assisted with my research. Without Dr Liam O'Neill, Chloe Frewen, Dr Richard Unitt and Dr Denis O'Sullivan, I likely wouldn't have finished my PhD. Prof. Maria Santos-Martinez, for being an all-around amazing human being and scientist. Xavier Thiry, for providing the stoppers. Dr Ciaran Maguire, Prof. Mischa Zelzer, Dr Patrick O'Dwyer and Dr Evin Allen for advice and support. Dr Fathima Laffir for XPS, Dr Brendan Sheehan and Dr Long Jiang for AFM. Dr Davinder Singh and Dr Farzan Gity for SEM-EDX. Dr Anna Hogan for providing access to the fluorimeter, Dr Dmitri Papkovsky for giving access to the Nanodrop, and Dr Eoin Fleming for access to the PCR. Will Daly and Dr Simon Lawrence for advice throughout. Aine Healy, Dr Anja Tetzner and Dr Sinead Kerins for all the demonstrating hours.

Most importantly, to Hazel, whom I promise never to speak to again about proteins for the rest of our lives. Nothing I could write could express my gratitude for your support and love. I love you despite your claims that you "ground me" and make me "humble", whatever that means. I will be there for your PhD every step of the way. I'm so proud of you.

Publications & Presentations

Peer Reviewed Journals**:**

- Review article entitled 'Impact of Protein Adsorption During Biopharmaceutical Manufacture & Storage' submitted in part to the European Journal of Pharmaceutics. Status: *under review*
- Review article entitled 'Application of a Phosphorylcholine Polymer on Vial Stoppers Using a Cold Plasma Deposition Process' submitted in part to Colloids and Surfaces B: Biointerfaces. Status: *under revision*

Oral Presentations**:**

- Probing the impact of protein/peptide adsorption onto solid substrates on functional behaviour and stability. UKICRS Virtual Symposium 2021.
- Lysozyme Adsorption to Borosilicate: Influence of Buffer pH and Composition. Particular Sciences QCM-D Roadshow University of Limerick 2024.

Poster Presentations**:**

- Probing the impact of protein/peptide adsorption onto solid substrates on functional behaviour and stability. UKICRS Virtual Symposium 2021.
- Investigating Buffer Effects on Lysozyme Adsorption to Borosilicate. APS Conference 2022.
- Dynamic analysis of lysozyme adsorption to Borosilicate. UKICRS Symposium 2023.
- Design, Optimisation & Analysis of a Biocompatible Vial Stopper Polymer Coating. PBP World Meeting 2024.

List of Figures

Figure 1.1: Overview of protein higher order structure. Created using BioRender.com.

Figure 1.2: Scheme describing the mechanisms of physicochemical protein degradation. Created using BioRender.com. Adapted from *Wang*, *Int*. *J*. *Pharm*., *2006*.

Figure 1.3: Illustration of interface-induced physical denaturation of a therapeutic antibody on a hydrophobic surface. Created using BioRender.com. Adapted from *Latour*, *Colloids Surf*. *B Biointerfaces*, *2020.*

Figure 1.4: C-laser differential interference contrast images of commercial glass primary packaging after different processing conditions which can result in defects on the glass surface. The figure is reprinted from the reference with permission of the publisher.

Figure 1.5: The figure depicts lysozyme (**A**) and BSA (**B**) structures as a cartoon and is coloured as follows: blue, α-helix; yellow, β-sheet; white, other structures. They are enclosed in an outer shell illustrating hydrophobicity in blue. Lysozyme and BSA were visualised using their protein data bank files 1LYZ and 3V03 for lysozyme and BSA, respectively.

Figure 2.1: The effect of protein adsorption to a solid-liquid interface and the consequences for therapeutic protein manufacture, bioactivity, and patient safety. Created with BioRender.com.

Figure 2.2: Formulation and fill-finish process flow. Created with BioRender.com.

Figure 2.3: Schematic presentation of select biopharmaceutical fill pumping systems: rotary piston pump (**A**), radial peristaltic pump (**B**) and linear peristaltic pump (**C**). The figure is reprinted from the reference with permission of the publisher.

Figure 2.4: The most common primary packaging and container systems used for liquid parenteral protein formulations and their associated surface coatings.

Figure 2.5: Cross-linked silicone coating applied to primary packaging surfaces. This coating technique ensures a tighter, more uniform layer thickness, significantly reducing silicone particle leachables compared to traditional silicone coatings. Inspired by *Depaz et al*. Created with BioRender.com.

Figure 2.6: Sizing and chemical identification of particles produced from pharmaceutical vial stoppers analysed by FTIR microscopy. Sizing identified particles of ≥25 µm in length suitable for chemical analysis (rectangular boxes), scale bar 100 µm. FTIR analysis identified protein, protein-PDMS and fluoropolymer particles. The figure is reprinted from the reference with permission of the publisher.

Figure 2.7: Excipients used to mitigate protein adsorption and their associated mechanisms. Illustration of surfactant pathways used to prevent protein adsorption where either surfactant engages in interfacial binding as a mechanism of anti-adsorptive behaviour (**A**) or surfactant forms protein-surfactant complexes of low adsorption affinity (**B**). Additionally, charged amino acids such as arginine can participate in molecular crowding (**C**), and hydrophobic amino acids such as leucine can reduce the surface tension (**D**). Created with BioRender.com.

Figure 3.1: Representative CD spectra of buffered lysozyme (1 mg/mL) solutions (**A**). Control represents lysozyme in deionised water, heat stressed refers to lysozyme, which was heated to 75°C. Percent secondary structural content obtained from spectral deconvolution by CDNN (**B**). Three independent samples were analysed, and data in (**B**) represents mean ± SD, n=3.

Figure 3.2: Melt temperature of buffered lysozyme (1 mg/mL) solutions. Control represents lysozyme in deionised water. Data represents mean ± SD, n=3. Statistical analysis was conducted using one-way ANOVA with Tukey's post hoc test, **p<0.01, ***p<0.001, ****p<0.0001.

Figure 3.3: Representative chromatograms of buffered lysozyme (1 mg/mL) solutions categorised by pH, pH 7.4 (**A**), pH 5,5 (**B**), pH 3.6 (**C**). Control represents lysozyme in deionised water. Three independent samples, n=3, were evaluated for each buffered solution.

Figure 3.4: Zeta potential determination of buffered lysozyme (1 mg/mL) solutions and buffered borosilicate microparticle suspensions. Data represents mean ± SD, n=3.

Figure 3.5: Mass of adsorbed lysozyme per unit area (ng/cm^2) from buffered lysozyme (1 mg/mL) solutions quantified by the Sauerbrey equation (**A**) and representative mass plot organised by pH (**B**). Buffers chosen for (**B**) were Na-Phos, pH 7.4, L-His, pH 5.5 and Na-Cit, pH 3.6. Dashed lines indicate the buffer equilibration step (BE), initial lysozyme adsorption during perfusion (LA) and reversibility assessment by buffer perfusion (BP). Data is represented by mean ± SD, n=3. Statistical analysis was conducted using one-way ANOVA with Tukey's post-hoc test, *p<0.05, **p<0.01.

Figure 3.6: Representative frequency and dissipation curves for lysozyme at 25 mg/mL in 10 mM histidine HCl monohydrate, pH 6, and lysozyme at 1 mg/mL in 10 mM L-His, pH 5.5. Frequency (black and dark blue lines) and dissipation (grey and light blue lines) correspond to the left and right y axes, respectively. All measurements were performed using three independent replicates, n=3. Arrows on the 25 mg/mL frequency plot indicate adsorption events.

Figure 3.7: Impact of glass type and storage conditions on lysozyme (25 mg/mL) adsorption expressed as adsorption per unit area (µg/cm^2) to commercial primary packaging vials. Mass adsorbed (blue bars) and percent adsorbed (blue diamonds and hexagons) correspond to the left and right y axes, respectively. The data shown is mean ± SD, n=3. Statistical analysis was conducted using two-way ANOVA with Tukey's post-hoc test, *p<0.05.

Figure 4.1: Thermal ramp profile of BSA 50 mg/mL in Na-Phos as measured by CD spectroscopy (**A**) and DLS (**B**). For (**A**), the percent alpha helix content (light blue circles) corresponds to the left y-axis, and mdeg intensity at 222 nm (dark blue squares) corresponds to the right y-axis. For CD analysis, the samples were diluted 50-fold to 1 mg/mL in Na-Phos before analysis. Data represents mean ± SD, n=3. For (**B**), Z-Avg (blue bars) and PDI (open blue diamonds) correspond to the left and right axes, respectively. Data represents mean ± SD, n=3. Representative intensity plot of the DLS thermal unfolding studies (**C**).

Figure 4.2: Representative CD spectra of BSA 50 mg/mL solutions in Na-Phos stored for 7 days in Fiolax Type 1 Plus® vials under refrigerated, ambient and thermal agitation conditions in both upright and inverted positions (**A**) and percent alpha helix content for reference and thermal agitation samples stored upright and inverted (**B**). Before CD analysis, BSA samples were diluted 50-fold to a final concentration of 1 mg/mL. Three independent samples were

evaluated for (**A**), and data represents mean ± SD, n=3, for (**B**). Statistical analysis was conducted using a one-way ANOVA with Tukey's post-hoc test, *p<0.05.

Figure 4.3: Z-Average and PDI (**A**) and representative intensity plot (**B**) of BSA 50 mg/mL solutions after 7 days storage in Fiolax Type 1 Plus® vials in refrigerated, ambient and thermal agitation conditions in both upright and inverted positions. Z-Avg (blue bars) and PDI (open blue hexagons) correspond to the left and right axes, respectively. For (**A**), data represents mean ± SD, n=3.

Figure 4.4: Representative size-exclusion chromatogram (**A**) and percent HMWs (**B**) of BSA 50 mg/mL solutions after 7 days storage in Fiolax Type 1 Plus® vials in refrigerated, ambient and thermal agitation conditions in both upright and inverted positions. Before analysis, BSA samples were diluted 50-fold to a final concentration of 1 mg/mL. Data represents mean ± SD, n=3, for (**B**). Statistical analysis was conducted using a one-way ANOVA with Tukey's post-hoc test, *p<0.05.

Figure 4.5: Percent alpha helix content determined by CDNN for BSA 50 mg/mL solutions after 7 days storage in Fiolax Type 1 Plus® vials under thermal agitation conditions in both upright and inverted positions. Before analysis, BSA samples were diluted 50-fold to a final concentration of 1 mg/mL. Data represents mean ± SD, n=3. Grey dashed lines represent the values for the alpha-helical content of BSA prepared fresh in Na-Phos. Statistical analysis was conducted using a two-way ANOVA with Tukey's post-hoc test ($\alpha = 0.05$).

Figure 4.6: Z-Avg (**A**) and PDI (**B**) of BSA 50 mg/mL solutions after 7 days storage in Fiolax Type 1 Plus® vials under thermal agitation conditions in both upright and inverted positions. Data represents mean ± SD, n=3. Grey dashed lines represent values for BSA prepared fresh in Na-Phos. Statistical analysis was conducted using a two-way ANOVA with Tukey's post-hoc test, ***p<0.001, ****p<0.0001.

Figure 4.7: Representative intensity plot for the BSA formulations stored under thermal agitation conditions either upright (**A**) or inverted (**B**). Particle size distribution of peak 2 (blue bars) and peak 3 (open crossed circles) are shown for upright (**C**) and inverted (**D**). Data represents mean ± SD, n=3, for (**A**-**B**). For peak 3 sizes, all replicates are shown (zero values and particles >5 µm were excluded). Reference represents BSA prepared fresh in Na-Phos. Statistical analysis was conducted using a two-way ANOVA with Tukey's post-hoc test, **p<0.01.

Figure 4.8: Z-Avg and PDI (**A**), intensity plot for ETFE (**B**), PDMS (**C**), and size distribution (**D**) for the BSA formulations stored under thermal agitation conditions in an inverted position. Z-Avg (blue bars) and PDI (open circles and squares) correspond to the right and left y-axes, respectively. The particle size distribution of peak 2 (blue bars) and peak 3 (open crossed and dotted circles) are shown for the ETFE or PDMS-coated stoppers. Data represents mean ± SD, n=3, for the Z-Avg, PDI and peaks 2 and 3 size distributions. For peak 3 sizes, all replicates are shown (zero values and particles > 5 µm were excluded). Statistical analysis was conducted using a two-way ANOVA with Tukey's post-hoc test, *p<0.05, **** p<0.0001.

Figure 5.1: Water contact angle measurements (**A**) and %RSD of WCA measurements across six coated stoppers (**B**). Stoppers were coated with poly(MPC-*co*-BMA) according to a 2^4 DoE approach. He activated represents helium-activated control. Data represents mean ± SD, n=6, each measured in duplicate.

Figure 5.2: Main effects plots for water contact angle (**A**) and %RSD between repeat WCA measurements for the coated stoppers in each run (**B**) and significant two-factor interaction plots for significant binary mixtures (**C-E**).

Figure 5.3: SEM images of stopper surfaces. Uncoated (**A**) and poly(MPC-*co*-BMA)-coated stopper (**B**), scale bar 10 µm. Higher magnification images of uncoated (**C**) and poly(MPC-*co*-BMA)-coated (**D**) stoppers, scale bar 2 µm.

Figure 5.4: Energy-dispersive X-ray elemental maps of uncoated (**A**) and poly(MPC-*co*-BMA)-coated (**B**) stoppers.

Figure 5.5: Representative AFM images showing 50 x 50 µm area on the uncoated (**A**) and poly(MPC-*co*-BMA)-coated (**B**) surfaces. Each sample was evaluated in duplicate and n=3 independent samples were analysed for the uncoated and coated halobutyl rubber flange septas.

Figure 5.6: Representative FTIR spectra of poly(MPC-*co*-BMA) raw material and coatings produced on NaCl discs by wet and plasma deposition methods (**A**) and poly(MPC-*co*-BMA) immobilised on the stopper surface (**B**). Three independent samples were evaluated for each coating process to the NaCl discs.

Figure 5.7: Raman hyperspectral images of the drug contact area of uncoated (**A**) and poly(MPC-*co*-BMA)-coated (**B**) stopper plugs. Red colouring indicates the signal of TiO_2 near the surface, green represents the TiO_2 signal at the midpoint, and blue denotes the signal at the lowest depth measured (2 µm). The black represents areas where the Raman signal was oversaturated due to intense autofluorescence. Topographic images of uncoated (**C**) and poly(MPC-*co*-BMA)-coated (**D**) stopper plugs. Scale bar 50 µm in all images.

Figure 5.8: Raman hyperspectral image of the reference stopper plug (**A**), after autoclavation at 121°C for 15 minutes (**B**), immersion in water for 24 hours (**C**), and 4 weeks exposure to a placebo formulation under thermal agitation stress (**D**). Red colouring indicates the signal of TiO_2 near the surface, green is the TiO_2 signal at the midpoint, and blue is the signal at the lowest depth measured (2 µm). The black represents areas where the Raman signal was oversaturated due to intense autofluorescence. Scale bar 50 µm in all images.

Figure 5.9: Z-Avg (blue bars) and PDI (crossed blue circles) correspond to the left and right axes, respectively (**A**), representative intensity plot of the BSA formulation stored under thermal stress conditions for each stopper type (**B**), representative light microscopy image of an isolated gel-like particle captured on an Isopore™ 0.8 µm polycarbonate membrane, scale bar 200 µm (**C**) and Raman hyperspectral image of reference (**D**), refrigerated (**E**) and thermal stress (**F**) poly(MPC-*co*-BMA)-coated stoppers after 3 months contact with the model formulation, scale bar 50 µm (**D**). Data in (**A**) represents mean ± SD, n=3, measured in duplicate. Statistical analysis was conducted using a two-way ANOVA, correcting for multiple comparisons with Tukey's post-hoc test, **p<0.01.

List of Tables

Table 1.1: Conditions affecting protein stability and their route of instability. Adapted from *Wang*, *Int*. *J*. *Pharm*., *2006*.

Table 1.2: Generally accepted mechanisms proposed to explain protein adsorption. Adapted from *Rabe et al.*, *Adv. Colloid Interface Sci*., *2011*.

Table 1.3: Summary of the excipient categories included in liquid and lyophilised protein formulations. Adapted from *Gervasi et al.*, *Eur*. *J*. *Pharm*. *Biopharm*., 2018.

Table 1.4: Techniques commonly applied to study protein adsorption and stability.

Table 2.1: Summary of the critical protein, solution and interfacial factors that govern protein absorption and the associated effect.

Table 2.2: Summary of the critical factors impacting protein stability during formulation, fill-finish and storage operations.

Table 2.3: Excipients, mechanisms for reducing protein adsorption, advantages and critical considerations.

Table 3.1: Frequency and dissipation data determined for lysozyme (1 mg/mL) at time=30 min using QCM-D. Data represents mean ± SD, n=3.

Table 4.1: BSA storage conditions investigated in this study.

Table 5.1. Storage conditions to assess BSA formulation-stopper compatibility.

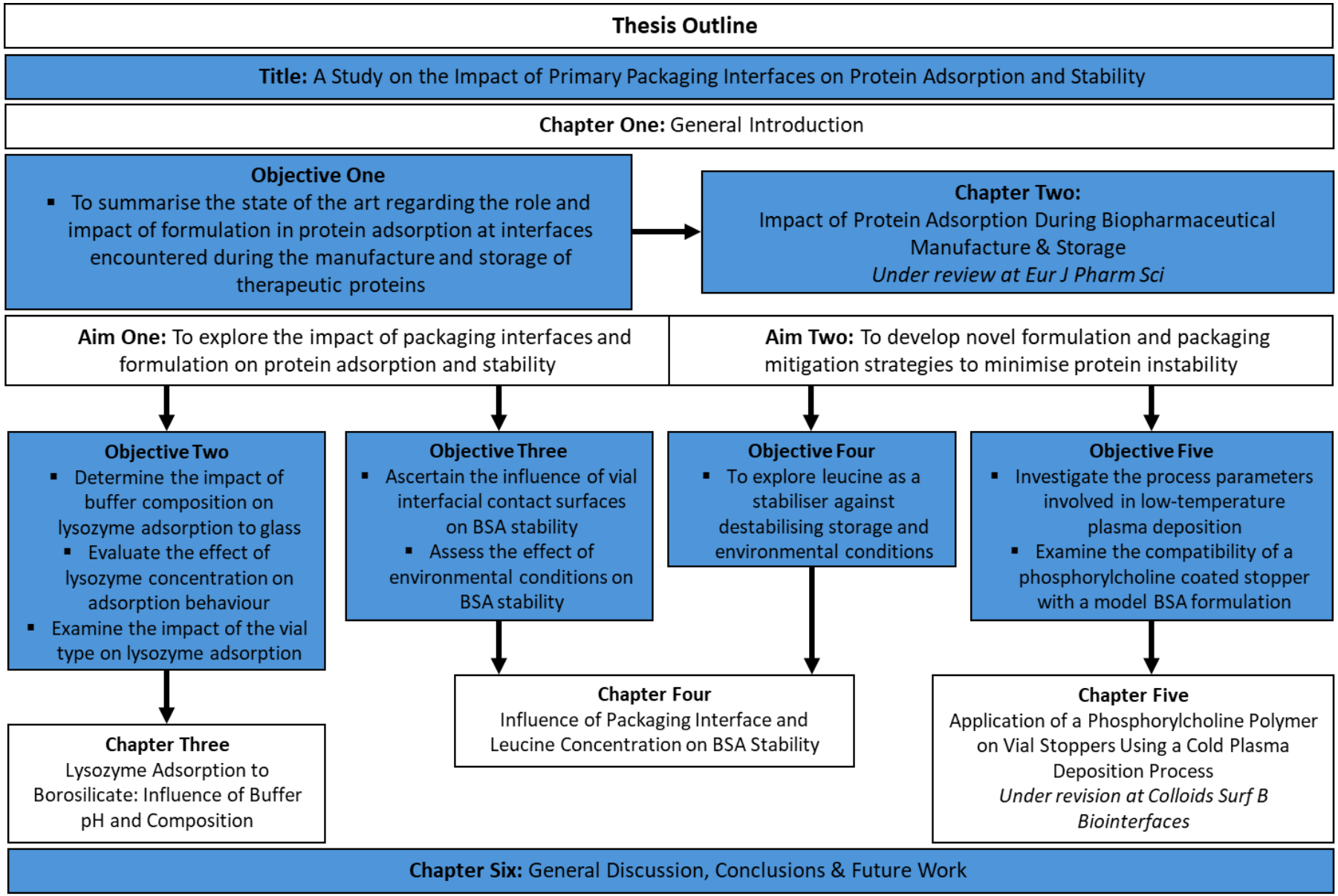
Table 5.2. Storage conditions to assess BSA formulation-stopper compatibility.

Table 5.3: AFM analysis of representative uncoated and poly(MPC-*co*-BMA)-coated surfaces. Data represents mean ± SD, n=3.

List of Abbreviations

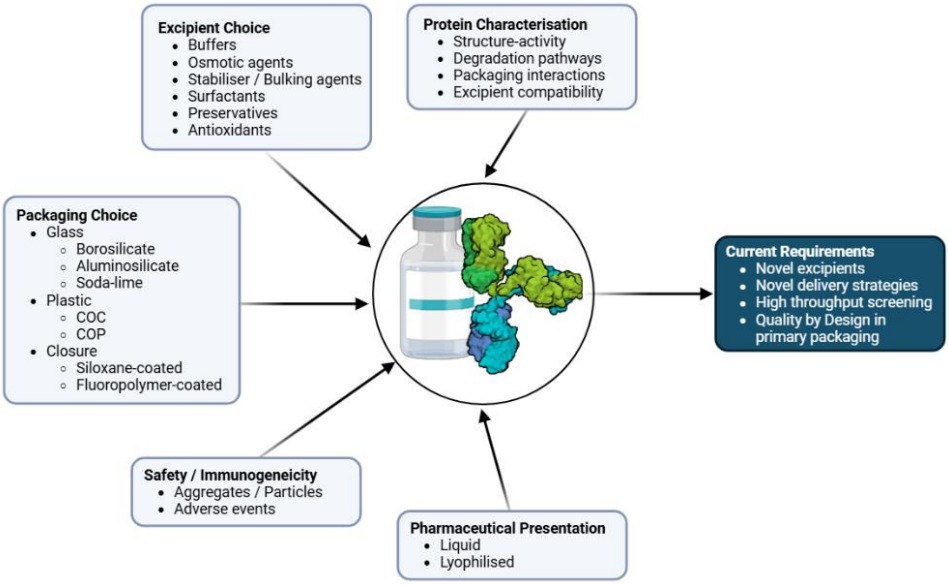
3D	Three-Dimensional
AFM	Atomic Force Microscopy
BMA	Butyl Methacrylate
Brij 35®	Polyoxyethylene Lauryl Ether
Brij 58®	Polyoxyethylene Cetyl Ether
BSA	Bovine Serum Albumin
CD	Circular Dichroism
CDNN	Circular Dichroism Neural Networking
DLS	Dynamic Light Scattering
DoE	Design of Experiments
DSF	Differential Scanning Fluorimetry
ΔD	Change in Dissipation
EDX	Energy-dispersive X-ray
ETFE	Ethylene Tetrafluoroethylene
ΔF	Change in Frequency
FEP	Fluorinated ethylene propylene
FTIR	Fourier-transform Infrared
FM1000	N-myristoyl Phenylalanine Polyether Amine Diamide
ΔG	Change in Gibbs Free Energy
HCl	Hydrochloric Acid
He	Helium
HEX	Hexachlorofluorescein
HLB	Hydrophilic-Lipophilic Balance
HWMs	Higher Molecular Weight Species
Hz	Hertz
IEP	Isoelectric Point
Ig	Immunoglobulin
KCl`	Potassium Chloride
MPC	2-Methacryloyloxyethyl Phosphorylcholine
NaCl	Sodium Chloride

NaOH	Sodium Hydroxide
Na-Phos	Sodium Phosphate Buffer (10 mM, pH 7)
PBS	Phosphate Buffered Saline (147 mM, pH 7.4)
PDI	Polydispersity Index
PDMS	Polydimethylsiloxane
PEG	Poly(ethylene glycol)
PTFE	Polyethylene Tetrafluoroethylene
%RSD	Percent Relative Standard Deviation
Poly(MPC-*co*-BMA)	Poly[2-methacryloyloxyethyl phosphorylcholine-*co*-*n*-butyl methacrylate]
QCM-D	Quartz Crystal Microbalance with Dissipation
SE-HPLC	Size-exclusion Chromatography High Performance Liquid Chromatography
SEM	Scanning Electron Microscopy
SiO_2	Silicon Dioxide
Slm	Standard Litres per Minute
TiO_2	Titanium Dioxide, Anatase
WCA	Water Contact Angle
Z-Avg	Z-Average Hydrodynamic Diameter


Thesis Outline
Title: A Study on the Impact of Primary Packaging Interfaces on Protein Adsorption and Stability
Chapter One: General Introduction
Objective One
To summarise the state of the art regarding the role and impact of formulation in protein adsorption at interfaces encountered during the manufacture and storage of therapeutic proteins
Chapter Two:
Impact of Protein Adsorption During Biopharmaceutical Manufacture & Storage
Under review at Eur J Pharm Sci
Aim One: To explore the impact of packaging interfaces and formulation on protein adsorption and stability
Aim Two: To develop novel formulation and packaging mitigation strategies to minimise protein instability
Objective Two
Determine the impact of buffer composition on lysozyme adsorption to glass
Evaluate the effect of lysozyme concentration on adsorption behaviour
Examine the impact of the vial type on lysozyme adsorption
Objective Three
Ascertain the influence of vial interfacial contact surfaces on BSA stability
Assess the effect of environmental conditions on BSA stability
Objective Four
To explore leucine as a stabiliser against destabilising storage and environmental conditions
Objective Five
Investigate the process parameters involved in low-temperature plasma deposition
Examine the compatibility of a phosphorylcholine coated stopper with a model BSA formulation
Chapter Three
Lysozyme Adsorption to Borosilicate: Influence of Buffer pH and Composition
Chapter Four
Influence of Packaging Interface and Leucine Concentration on BSA Stability
Chapter Five
Application of a Phosphorylcholine Polymer on Vial Stoppers Using a Cold Plasma Deposition Process
Under revision at Colloids Surf B Biointerfaces
Chapter Six: General Discussion, Conclusions & Future Work

Chapter One

1. General Introduction



1.1 Background

1.1.1 Therapeutic proteins

Biological medicines encompass various biotherapeutic molecules that are used to treat multiple clinical conditions. Therapeutic proteins are the largest class of commercial biotherapeutic molecules and include monoclonal antibodies, vaccines, fusion proteins, hormones, enzymes, and cytokines. These molecules are formulated in either the liquid or solid state for varying routes of administration.[1] Since their discovery, therapeutic proteins have been increasingly developed commercially for various diseases and clinical applications. They offer transformative potential for conditions for which no treatments were previously available.[2]

Therapeutic proteins are predominantly formulated as liquid parenteral injections. This route of administration offers significant benefits compared to other routes because it avoids the gastrointestinal tract and can deliver therapeutics directly into systemic circulation, which achieves a rapid onset of action.[3] Irrespective of the route of administration, a principal concern for protein delivery includes maintaining protein stability. Proteins are highly labile moieties and stable only within a narrow range of concentration, pH, ionic strength, acidity, and temperature conditions, making them highly prone to physicochemical instability.[4,5]

1.1.2 Protein stability considerations

Protein higher order structure

Proteins are comprised of amino acid residues in either single- or multi-chain compositions that fold into a specific three-dimensional (3D) conformation, which is essential for its specific activity or function. The protein structure can be described at distinct levels of primary, secondary and tertiary structures, **Figure 1.1**. Additionally, quaternary structures can be observed if several protein chains or subunits organise into a closely packed arrangement, but this is protein dependent.[6]

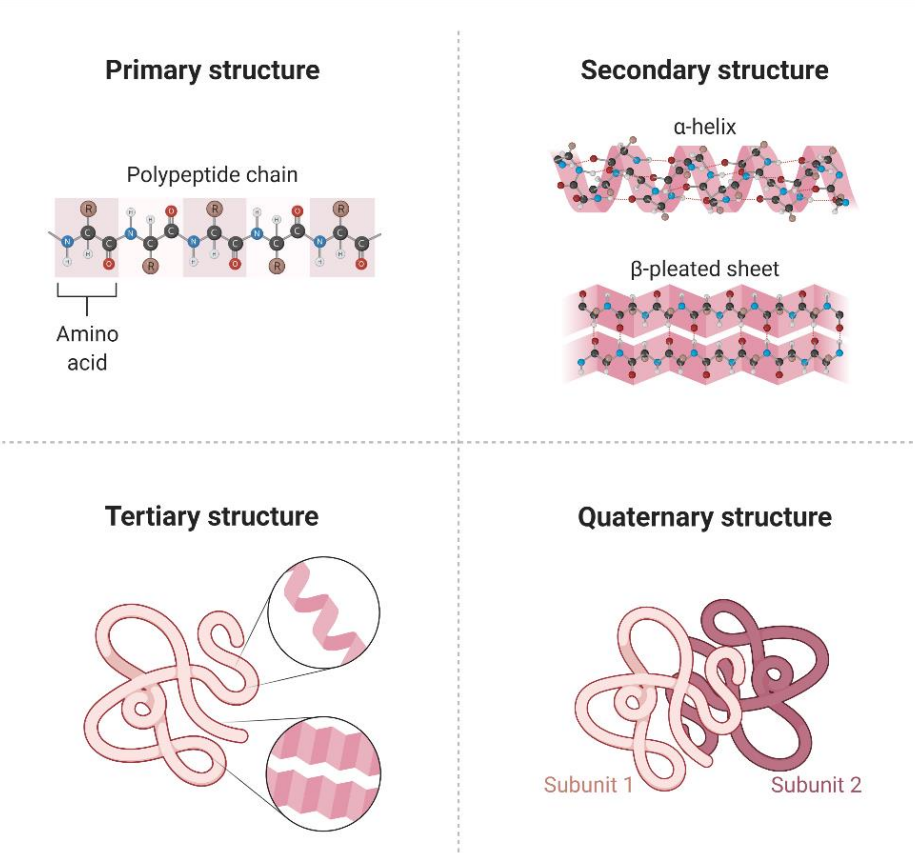


Figure 1.1: Overview of protein higher order structure. Created using BioRender.com.

The primary structure is simply the protein's linear sequence of amino acids formed due to covalent amide linkages. The secondary structure refers to the local spatial conformation of the polypeptide backbone where, through hydrogen bonding, alpha-helix and beta-pleated sheet structures can form.[7] The tertiary structure is the overall 3D fold of the polypeptide chain in space. It is stabilised by external polar hydrogen and ionic bonds and internal hydrophobic interactions, salt bridges, and disulfide exchange.[7] The sequence of amino acid moieties and the 3D fold are the foundation of the protein's activity, which predominantly occurs through specific binding domains.[8] Combinations of secondary structural features facilitate binding events, allowing proteins to perform their function.

The shape in which a protein naturally folds is considered its native conformation, while a loss of conformation is referred to as unfolding. The transition from the native state to the unfolded state occurs through an intermediary phase, during which the protein is highly susceptible to aggregation and particle formation.[5] This is influenced by the protein's physicochemical properties, with hydrophobic and charged amino acids being associated with

protein-protein interactions.[9] The success of therapeutic proteins is strongly dependent on the folding and binding capabilities of the protein, where any disturbances may lead to partial or complete loss of bioactivity and increased immunogenicity.[10] The fold of a protein is impacted by several factors, namely temperature, mixing, stirring, shaking and adsorption. These factors can cause fragmentation, aggregation, and particle formation, which increases the risk of an immunogenic reaction or thromboembolic events.[11–14]

Protein aggregation pathways

Aggregation is recognised to occur through distinct pathways where either: (i) aggregates form through unfolded or intermediate unfolded moieties, (ii) by self-association or (iii) via chemical degradation, **Figure 1.2**.[5,15] As the protein unfolds, its hydrophobic core becomes exposed, facilitating increased protein-protein interactions and aggregation in solution.[16] Aggregated proteins typically consist of monomers or nanometre aggregates that interact to form oligomers (<100 nm) primarily through non-covalent interactions.[17] Oligomers can associate to form aggregates that are sub-visible, with particles of 0.1 µm to 1 µm in size classed as submicron, whereas particles of 1 µm to 100 µm are large sub-visible, micron aggregates.[18] Visible particles (>100 µm) have many different morphologies and are precipitants in solution.[18] Precipitation may be preceded by opalescence, which is a phase separation of unstable particles from stable soluble proteins.[19] Irreversible aggregates, which may be precipitants, typically form ordered fibrils, amorphous particulates or gels.[18,20] These aggregate morphologies are linked to temperature, pH, ionic strength and concentration but can be influenced by the type of interface present, as silicone oil-water interfaces can promote protein gelation.[21,22] However, protein aggregates will only precipitate from solution if a large population with reduced solubility limits is present. Protein solubility issues are mainly linked to solution pH and ionic strength in addition to intrinsic stability. While unfolded and intermediate unfolded moieties, driven by hydrophobic interactions, account for the primary reason for aggregate formation in liquid parenteral protein formulations, electrostatic associations can also occur without conformational changes.[23] This generally results in the formation of reversible aggregates, which can be affected by the solution's ionic strength and pH. However, reversible aggregates can readily act as a precursor for irreversible aggregation.[5]

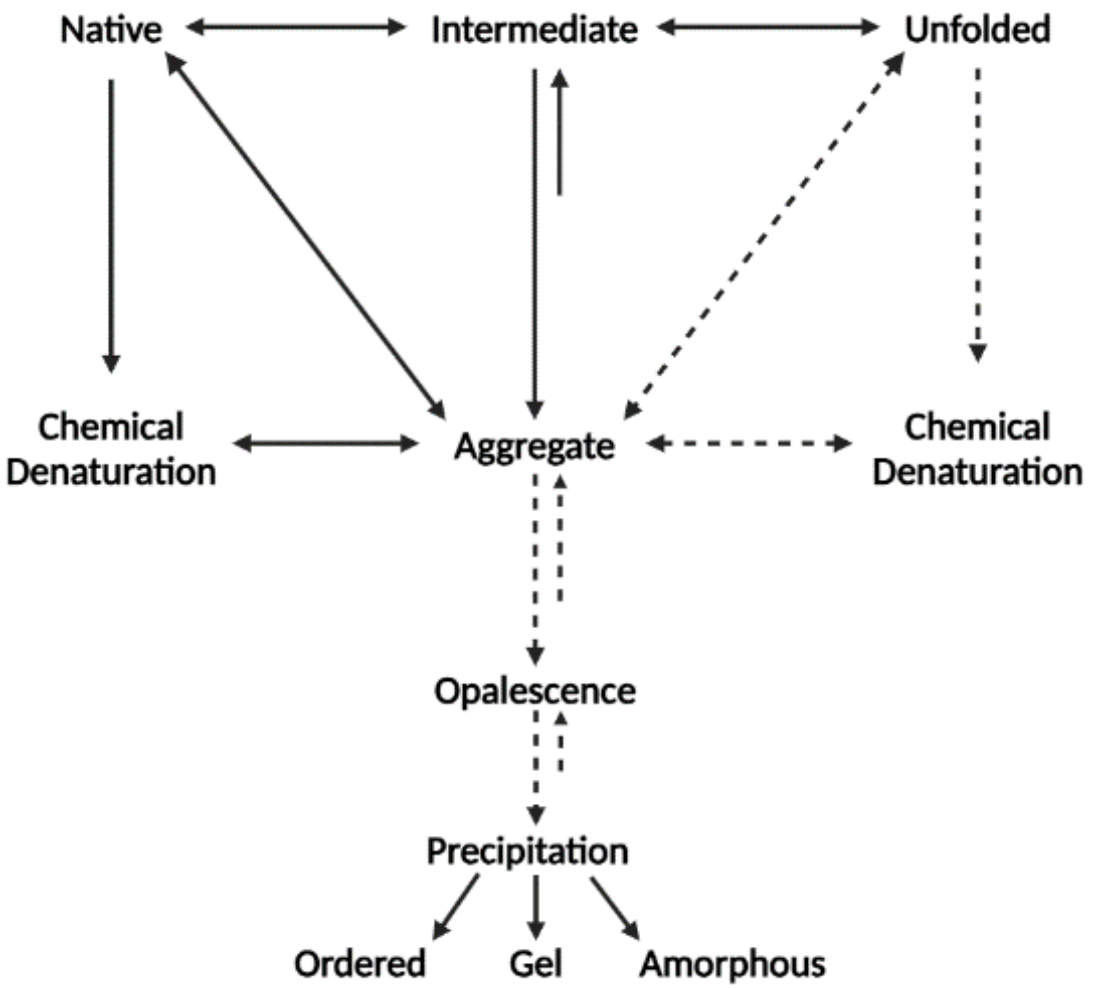


Figure 1.2: Scheme describing the mechanisms of physicochemical protein degradation. Created using BioRender.com. Adapted from *Wang*, *Int*. *J*. *Pharm*., *2006*.[5]

Chemical degradation is another source of aggregate formation.[24] Most notably, the oxidation of therapeutic proteins has been observed to occur through reactive sulfur residues found on the side chains of cysteine and methionine amino acids. However, oxidation of aromatic amino acids, such as tyrosine, tryptophan and phenylalanine, and the imidazole group of histidine, can also occur. The oxidation of these moieties requires the presence of reactive oxygen species, which can originate from oxygen ($O_2^{\bullet -}$), hydroxyl ($OH^{\bullet}$), alkoxyl ($RO^{\bullet}$) or peroxyl ($ROO^{\bullet}$) radicals.[25] External stressors such as metal ions, UV, and visible light can initiate or propagate the formation of reactive oxygen species.[5,26] Other chemical degradation pathways, such as hydrolysis, deamidation, and racemisation, can have similar effects. **Table 1.1** provides an overview of stress factors that can result in the instability of the therapeutic protein moiety.

Table 1.1: Conditions affecting protein stability and their route of instability. Adapted from *Wang*, *Int*. *J*. *Pharm*., *2006*.[5]

Stress condition	Route of instability	Impact on stability
Temperature e.g., ≥40°C	Physical: unfolding, aggregation	High temperatures can break non-covalent bonds.
Concentration e.g., ≥50 mg/mL	Physical: colloidal aggregation	High concentrations result in non-specific aggregation.
pH	Physical: unfolding, aggregation, fragmentation.	Alters protein ionisation, changing the native fold. Extreme pH values cause hydrolysis and fragmentation. pH near the isoelectric point can enhance self-association.
Ionic strength	Physical: aggregation	Alters electrostatic interactions between charged residues, influencing aggregation and precipitation.
Interfacial adsorption e.g., solid-liquid	Physical: unfolding, aggregation	Induces unfolding and aggregation mainly based on surface hydrophobicity and charge.
Chemical denaturants e.g., Urea, SDS, Guanidine HCl	Physical: unfolding, aggregation	Denaturants disrupt non-covalent interactions, promoting unfolding and aggregation.
Mechanical stress e.g., freeze-thaw, shear, dehydration	Physical: denaturation, aggregation, fragmentation	It can cause protein unfolding or aggregation through physical forces.
Pressure	Physical: denaturation, aggregation Chemical: degradation	High pressure can affect non-covalent interactions and compact the protein. It can also alter the solubility and hydration.
Redox conditions e.g., metal ions, peroxides	Chemical: degradation	Affects disulfide bond formation or cleavage and causes oxidation of aromatic and imidazole residues.
Light	Chemical: degradation	UV and visible light can lead to oxidation of amino acids and can break disulfide bonds.

Protein adsorption

Interfacial adsorption is another pathway that can lead to instability. However, it has only been recognised in recent years. Interfacial adsorption is a spontaneous phenomenon that occurs when a protein encounters an interface, whether solid-liquid or air-liquid.[27] Its role in unfolding, aggregation, and, most critically, particle formation has become widely investigated over the last two decades, with numerous factors identified as contributors to adsorption, **Chapter Two**, **Table 2.1**. Protein adsorption can be associated with unfolding and aggregation because hydrophobic and hydrophilic interfaces alike have been observed to induce conformational changes in the protein's higher order structure.[28,29] This is because protein moieties will undergo subtle biophysical changes to enable them to adsorb to the interface should the change in Gibbs free energy (ΔG) be favourable. These higher order structural changes include loss of secondary structure, dimerisation, cooperative effects, and even colloidal aggregation.[30–32]

However, adsorption to an interface does not necessarily mean that aggregation and particle formation will occur. Moreover, it also does not mean that the protein will undergo substantial unfolding either. For this reason, *Nakanishi* aptly described protein adsorption as a "common but very complicated phenomenon".[33] Adsorption is a common phenomenon because it will likely occur in every instance of interfacial contact. Still, it is regarded as complicated because, despite understanding protein adsorption behaviour, it is a multivariate issue. Therefore, decoupling intrinsic protein characteristics from external factors impacting adsorption is difficult.[34]

Fundamentally, protein adsorption involves various protein-water-interface interactions and is primarily driven by diffusion and non-covalent interactions, namely Coulombic and van der Waals forces, hydrogen and hydrophobic bonding, and electrostatic interactions.[35,36] Moreover, the gain in ΔG from releasing water molecules, solvent ions, or low molecular weight solutes from the solid interface is critical to adsorption behaviour.[37] Hydrophobic interactions are the most influential forces of these adsorption mechanisms because a protein's hydrophobic domain tends to be buried within the 3D structure when the protein is in solution. However, these domains become exposed to facilitate adsorption to hydrophobic interfaces, e.g., solid-liquid and air-liquid, because of disruption to the balance of intra-protein and protein-solvent interactions, **Figure 1.3**.[35] Additionally, adsorption at

hydrophobic interfaces, usually results in the protein undergoing more significant denaturation than that observed with hydrophilic interfaces.[28,38,39] This occurs due to the gain in ΔG, where the protein maximises its surface area through structural reorganisation. However, this is dependent on a protein's inherent internal stability.

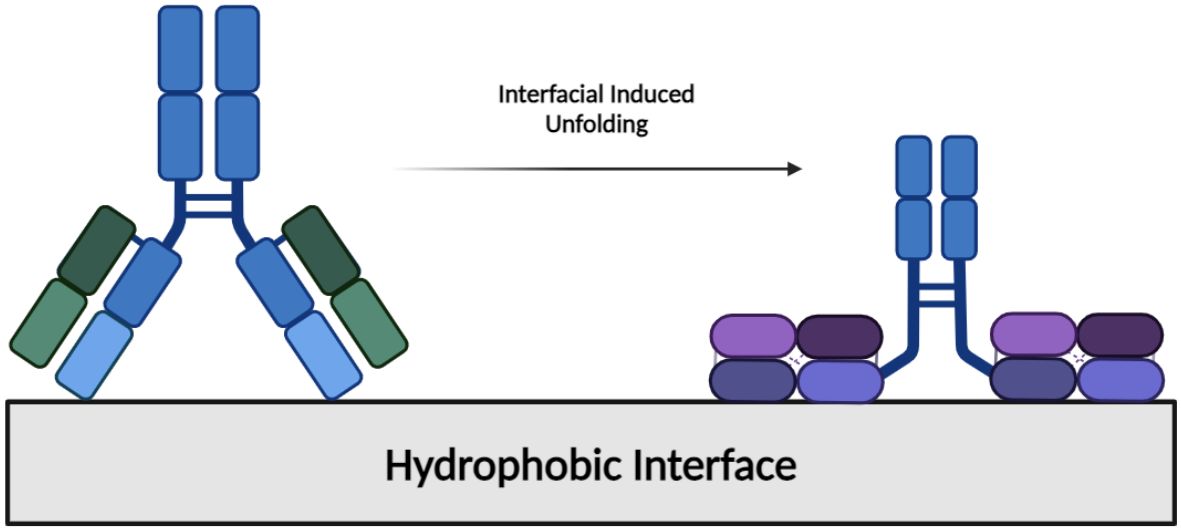


Figure 1.3: Illustration of interface-induced physical denaturation of a therapeutic antibody on a hydrophobic surface. Created using BioRender.com. Adapted from *Latour*, *Colloids Surf. B Biointerfaces*, *2020.*[35]

Adsorption is inherently more complex at hydrophilic interfaces, especially solid material interfaces. The most likely explanation for adsorption at these interfaces is biased diffusion toward the surface, followed by anchoring to the interfacial water layer, which allows the protein to penetrate the water layer and adsorb to the surface.[37] Thereafter, a stepwise lockdown mechanism has been proposed. This mechanism involves structural rotation of the molecule facilitated by the distribution of protein interfacial charges and surface-accessible amino acid residues that promote surface dehydration and adsorption.[40,41]

A protein's size, shape, and surface-accessible side chains can also significantly impact its adsorption behaviour. This behaviour can become increasingly complex when considering the many protein properties, such as folded state or charge, which can vary in different environmental conditions. Therefore, several molecular adsorption mechanisms have been proposed, **Table 1.2**. These mechanisms consider the random distribution of protein molecules at an interface in addition to site-directed adsorption.

Table 1.2: Generally accepted mechanisms proposed to explain protein adsorption. Adapted from *Rabe et al.*, *Adv. Colloid Interface Sci*., *2011*.[30]

Theory	Process
Langmuir	Adsorption to distinct binding sites
Random Sequential Adsorption	Adsorption to random available surfaces
Monomer-Dimer Exchange	Dimers in the bulk solution replace adsorbed monomers on the surface using size-exclusion effects
Surface Clusters	Two-dimensional clusters grow (reversibly) at the interface via proteins binding to pre-adsorbed monomers either horizontally (lateral) or vertically
Two-States Model	Conformational changes initiated by adsorption lead to an increased affinity for the surface. This occurs in two ways: (i) protein adsorbs (reversibly), unfolds, and denatures, or (ii) protein adsorbs (reversibly) or adsorbs and immediately denatures
Three-States Model	Protein adsorbs and transitions from an irreversible orientational bound state into a conformationally flexible bound state, leading to stretching along the interface
Multiple-States Model	Transition into states of surface denaturation along the surface
Rollover Model	Reorientation of end-on adsorbed proteins to side-on adsorbed proteins
Tracking Model	Cooperative adsorption due to the tracking of proteins to binding sites close to other pre-adsorbed proteins

A critical consideration related to protein native conformation includes its internal stability. Proteins with low internal stability are more prone to adsorption than proteins with high internal stability, as they are less resistant to interface-induced unfolding. *Robert Huber* described this as "Proteins may be rigid or flexible to various degrees as required for optimum function. Flexibility at the level of amino acid sidechains occurs universally and is important for binding and catalysis".[42] *Willem Norde* proposed another way to describe this concept based on "hard" and "soft" proteins.[43–45] Hard or rigid proteins undergo limited structural changes upon adsorption, while soft proteins subjected to significant structural changes may involve a reduction in ordered (secondary) structures upon adsorption. It is essentially the

difference in the balance of internal protein interactions competing with interfacial interactions.[46,47]

1.1.3 Protein formulation

Proteins are generally formulated as liquid dosage forms for parenteral administration. The balance between promoting conformational and colloidal stability and maintaining optimum biological activity must be determined for most therapeutic proteins. Excipients are employed to protect the protein from stress over its shelf-life.[48] The main excipient categories are summarised in **Table 1.3**.

Table 1.3: Summary of the excipient categories included in liquid and lyophilised protein formulations. Adapted from *Gervasi et al.*, *Eur. J. Pharm. Biopharm.*, 2018.[1]

Excipient class	Excipient	Concentration range (mg/mL)
Buffering agent (pH 3.1-8.15)	Non-amino acid: phosphate, citrate, acetate, succinate, tris, carbonate	0.2 to 14.8
	Amino acid: histidine, glutamate, aspartate, glycine	
Stabiliser	Amino acid: arginine, methionine, glycine, glutamate, proline	0.1 to 42.1
	Disaccharide/polyol: sucrose, trehalose, sorbitol, mannitol, glycerol	1.9 to 200
	Protein: recombinant human albumin	0.5 to 10
Surfactants	Polysorbate 80, polysorbate 20, poloxamer 188, poloxamer 171	0.01 to 8
Preservatives	Metacresol, phenol, benzyl alcohol	0.8 to 10
Tonicifiers	NaCl, KCl	0.2 to 11.7

Two common hypotheses were identified for the excipient stabilisation of protein moieties: (i) preferential hydration and (ii) preferential interaction.[49] Preferential hydration refers to excluding the excipient from the protein's hydrodynamic radius owing to its hydrodynamic size, where water directly interacts with the protein to maintain its stability. Preferential interaction can partially exclude water from the protein's hydrodynamic radius

and directly interact with the protein through non-covalent interactions. In this case, a specific concentration is required to ensure homogenous interactions over the protein's surface. For buffers, tonicifiers and other osmolytes, the stabilisation mechanism involves transient hydrogen, hydrophobic and electrostatic interactions with external residues on the protein's surface and maintaining isotonicity, osmolality and pH.[50]

Surfactants primarily mitigate interfacial adsorption, but amino acids, namely arginine as well as cyclodextrins, show promise.[51–58] Polysorbate 80 (PS80) is the most well-known surfactant for interfacial stabilisation. It is employed in numerous liquid formulations to offer protection from air-liquid and solid-liquid interfaces. Polysorbate 20 (PS20), poloxamer 188 (PoL188) and poloxamer 171 (Pol171) are the only alternative approved surfactants present in commercial protein formulations.[1] Pol188 is typically used when mechanical and freezing stress is encountered or as an alternative to polysorbates where their stability is a concern.[59–61] It is not as effective as the polysorbates for interfacial stabilisation because of its lower hydrophobicity.[62–64]

1.1.4 Primary packaging

Injectable protein stability is challenged during formulation, filling, and storage. This is because the rational design, selection and investigation of sterile packaging systems are frequently ignored until compatibility problems occur that implicate the packaging system.[65] This can likely be attributed to the difficulty in deconvoluting the effects of inherent protein instability or solution and environmental stress from interfacial properties during stability testing.[34,66] However, only a limited number of packaging systems are employed for commercial protein products. They can be categorised into six primary packaging or container systems: (i) vials, (ii) syringes, (iii) cartridges, (iv) bags, (v) bottles and (vi) ampoules. The vials, syringes, cartridges and bags commonly used to store and deliver protein medicines are of significance.[67,68] Their general composition includes a glass or polymer container, an elastomeric closure and potentially a silicone oil emulsion surface coating.

Glass

Glass-based packaging materials (vials, syringes, and cartridges) are the most used for storage and delivery after commercial biopharmaceutical unit operations.[69] The primary disadvantage of glass-based packaging is the potential reactivity between the protein formulation and the packaging components.[70,71] This can result in particulate matter, leachables/extractables, protein adsorption and aggregation.[65,72] Polymeric storage materials also have drawbacks, mainly their reported higher oxygen permeability.[73]

Glass is primarily composed of silicon dioxide (SiO_2) with varying amounts of other oxides such as sodium, potassium, calcium, magnesium, aluminium, barium, zinc, boron and iron.[65] Many different glass compositions have been approved for use. Still, Type 1 borosilicate and aluminosilicate glasses are the most employed due to their high composition of SiO_2, boric oxide and aluminium oxide.[74,75] Borosilicate and aluminosilicate form inert networks with a low coefficient of thermal expansion, meaning the risk of leachables is relatively low.[76] Type 2 and Type 3 glasses are composed of soda-lime, with Type 2 undergoing surface treatment with sulfur dioxide or other alkalisers to prevent leachables.[65] Soda-lime glass has high sodium oxide and calcium oxide compositions, posing a greater risk during use than Type 1. The chemical treatment of Type 2 glass is also highly susceptible to degradation during cleaning and sterilisation procedures, especially if subjected to repeated exposure.[65]

The basic structure of glass is a network formed from the silicon oxide tetrahedron. The boric oxide can enter this structure for borosilicate glass, but the other oxides will only be present at interstices.[65] These oxides are mobile and can leach into the formulation in contact with the glass. This can be a substantial issue under thermal stress conditions, especially for formulations stored in Type 2 and Type 3 glass materials.[72] Leaching of alkali ions occurs through an ion exchange diffusion process where hydrogen ions from the solution are exchanged for alkali ions at the glass surface. The immediate impact of this is the modification of the solution pH, where an increase in pH can typically be observed.

Obvious issues arising from this include changes in the pH of water for injection and altered stability in drug products with minimal buffering capacity. Further, the buffer type can also present some concerns, as phosphate and citrate buffers can attack the glass surface, causing delamination and flocculation.[77] Phosphate buffer ions can also form insoluble salts with the

divalent metal cations present at the surface of the glass, making it a particularly problematic buffering system for liquid protein formulations, notwithstanding its proven incompatibility with bioprocessing steps during biomanufacturing.[65,78] The risk of delamination, in addition to leachables, increases when formulations have a pH greater than pH 8. This can be exacerbated by issues caused during cleaning and sterilisation, as excessive heat exposure during depyrogenation can cause ion exchange, vaporisation and surface defects, resulting in a compromised surface, **Figure 1.4**.[65] During heating, the mobile oxide ions will migrate to the surface of the glass network and can readily leach on exposure to the solution/formulation.[79] The current mitigation approach uses acidic ammonium sulfate in the vapour state to form soluble salts that can be washed away. However, this is not cost-effective and does not guarantee a successful outcome.[65] It also presents the risk of sulfate leachables. Besides ion exchange effects and glass dissolution, chelating agents can also cause pit formation on the glass surface, and acidic environments below pH 4 can etch the surface.[65,76,80]

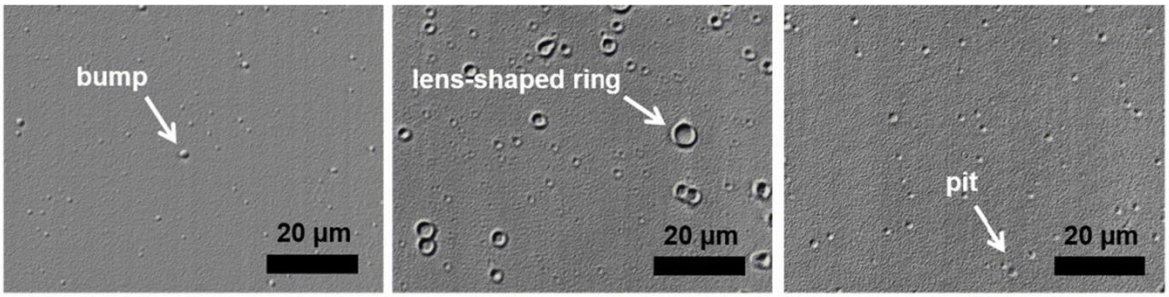


Figure 1.4: C-laser differential interference contrast images of commercial glass primary packaging after different processing conditions which can result in defects on the glass surface. The figure is reprinted from the reference with permission of the publisher.[81]

Moreover, owing to the hydrophilic characteristics of borosilicate, recovery of the total therapeutic dose from the vial can be challenging to achieve. Additionally, for self-administration devices (syringes, cartridges), the inner surface of the vial can present a high friction surface, making it challenging to release the formulation from the delivery device. Therefore, silicone coatings, generally silicone emulsions, are applied to the interior surface to generate a hydrophobic surface, allowing full dose recovery and ease of use. Siliconisation presents its challenges, which are discussed in detail in **Chapter Two**.

Rubber

The composition of pharmaceutical-grade rubber is less widely known compared to pharmaceutical glass. It has mainly been studied for its extractables and leachables profile, with only a few compounds identified in its composition.[72,82–85] An exemplary review by *Sacha et al*. was used to understand its production, physicochemical composition and critical quality attributes.[65]

In the liquid parenteral protein packaging and administration area, rubber is ubiquitously employed for various functionalities. Like glass, the choice of rubber product is dictated by the properties of the rubber material and its intended usage. Physicochemical properties such as elasticity, hardness, fragmentation or coring tendencies, oxygen and water vapour permeability, penetration force, self-sealing properties, structure retention, and leachables/extractables profile all influence the choice of rubber used.[65] The most critical factors from these physicochemical properties depend on the type of storage system, as break-loose glide force is vital for syringes and cartridges. In contrast, elasticity, hardness and permeability are more critical for vial stoppers. Secondary considerations affecting the choice of rubber product include the protein formulation properties.[86]

Rubber is a very complex material composed of various organic and inorganic components. The base material of rubber is the elastomer, which is made of natural or synthetic rubber and confers most of the material's physicochemical characteristics. Synthetic rubbers, which include styrene-butadiene, neoprene, nitrile, and butyl rubber, are used for pharmaceutical packaging.[65] Butyl rubber, mainly chlorobutyl and bromobutyl, is the most common elastomer used for injectables because it provides a superior oxygen/moisture barrier.[65] In addition to the elastomer, rubber formulations can contain a vulcanising agent, activator, filler and other components to control the curing rate and colour.[65] Vulcanising agents form the cross-links within the rubber, providing its shape and elasticity. The most common vulcanising agent is sulfur.[65] The activator tends to be a metal oxide, such as zinc oxide, with a fatty acid, such as stearic acid, accelerating the rate at which the sulfur reacts with the unsaturated elastomer.[65] Vulcanisation can also be controlled with other accelerating and retarding compounds such as sulfenimide, benzoic acid, salicylic acid and phthalic anhydride.[65] Fillers, such as carbon black, titanium dioxide, and calcium carbonate,

control colour and adjust hardness, among other functions.[65,82,84] Further, antioxidants and antiozonants can also be found in rubber formulations.

Rubber stoppers can be one of the most problematic interfaces in primary packaging because they contain a wide range of organic and inorganic materials.[87] Uncoated stoppers, due to incompatibility between the excipients and the stopper material, have been implicated in the incidence of pure red cell aplasia in chronic kidney disease patients treated with epoetins.[83] The most common leachables are vulcanising agents, 2-mercaptobenzo-thiazole, aluminium, nitrosamines, stearate, polynuclear aromatic hydrocarbons, iron and zinc.[65,82–84] However, this is stopper dependent.[88]

Rubber interfaces also face additional challenges, such as the adsorption of the active ingredient onto the surface, the absorption of formulation components into the rubber, and the permeation of formulation components through the rubber.[65] Additionally, like glass, rubber stoppers can be subjected to siliconisation but are subjected to tighter regulations as siliconised elastomeric closures are a root cause of silicone oil contamination and protein-silicone oil interactions.[89,90] Typically, siliconised stoppers are washed in a drum or spray-coated with polydimethylsiloxane (PDMS) to create a layer on the stopper surface. However, this layer is poorly adherent and PDMS has been observed to leach into protein formulations.[91] To counteract this and to reduce the risk of leachables, fluoropolymer coatings such as polytetrafluoroethylene (PTFE), ethylene tetrafluoroethylene (ETFE), and fluorinated ethylene propylene (FEP) can be applied to stoppers and plungers however, they are reported to induce adsorption, unfolding, aggregation and fibrillation.[92–94] This is a surface and protein-dependent effect as some protein-fluoropolymer laminate film interactions are stabilising compared to uncoated or siliconised surfaces.[86,95] Additionally, using fluoropolymer laminate films eliminates the need for silicone oil, decreases particulate matter and extractable levels.[96] However, laminate films still use silicone coatings, known as B2, albeit with a significant reduction in free silicone due to the cross-linking method.[97,98] Fluoropolymer laminate films are typically applied by a thermal laminate process to create a thick, strongly adherent stopper film which is responsible for improving container/closure integrity.

1.1.5 Mitigating protein adsorption

Owing to the complexity of pharmaceutical packaging and the significant drawbacks of protein adsorption, the adsorption process must be minimised for commercial products. Several decades ago, a set of molecular-level characteristics for protein-resistant surfaces was proposed, known as Whitesides rules. These identified four critical characteristics for protein-resistant surfaces: (i) strong hydrophilic properties, (ii) the presence of hydrogen bond acceptors, (iii) the absence of hydrogen bond donors, and (iv) the presence of a net neutral charge.[99,100] To date, several adsorption-inhibiting coatings have been explored but have not been applied to pharmaceutical packaging. They can be divided into two major categories: phosphorylcholine and polysaccharide-based coatings or synthetic hydrophilic polymer coatings such as poly(ethylene glycol) (PEG).[101] These surface coatings are considered passive adsorption reduction techniques that aim to create a thin, hydrophilic, non-charged layer between the protein and the interface. This reduces the intermolecular attraction between adsorbing protein molecules and the interface. Alternative approaches focus on physical surface modifications such as nanopatterning, sacrificial proteins and chemical surface modifications.[102] However, all approaches have limitations, such as being inconsistent, non-homogenous and time-consuming.

Phosphorylcholine-based coatings are a promising approach to achieving compatibility with primary packaging interfaces and protein formulations. These surface coatings are reportedly strongly protein-resistant because of the phosphocholine moieties neutral net charge, which helps reduce long-range electrostatic attraction between the surface and proteins in aqueous solution.[103] Further, water adsorbed to the phosphorylcholine headgroup produces a low-energy interface in aqueous media, which decreases the likelihood of the adsorbing protein's penetration of the water layer.[104] Moreover, polysaccharide coatings are also of interest but require modifications to have a hydrophobic backbone to ensure sustained adherence to the material surface.[105]

A central limitation to the application of these coatings is their long-term surface stability. Formulation components can readily degrade surface coatings and compromise surface adhesion in aqueous solution.[106,107] However, plasma chemical vapour deposition techniques can overcome these issues, producing consistent, homogenous and fast application of surface coatings as proven by SCHOTT's Type 1 Plus® vials and SiO_2 Medical Products pre-filled

syringes. These products have an inert inner SiO_2 coating resistant to protein adsorption.[108,109] While the issues associated with pharmaceutical glass can be overcome by the choice of glass composition, appropriate protein formulation and vial coatings, the elastomeric materials remain of considerable concern. Despite the inertness of fluoropolymer laminate films, they are still reported to adsorb significant amounts of protein from aqueous solution.[94] There appear to be no commercial adsorption-resistant coatings for pharmaceutical-grade rubber packaging materials therefore, the current limitations still need to be adequately addressed.

1.1.6 Analysing protein adsorption and stability

Several techniques exist for studying protein adsorption and stability in injectable protein formulations. **Table 1.4** outlines some fundamental techniques that can be employed to investigate adsorption and stability behaviour. Spectroscopic analytical techniques are typically employed to measure protein formulations. Various protein-light interaction effects can be measured, such as absorbance, transmittance, reflectance, fluorescence, and scattering, which confer information about concentration, conformation and aggregation. The solvent environment strongly influences the choice of analytical technique, as buffers and excipients can interfere with detection and reduce the sensitivity. Additional techniques that rely on the change in mass or phase behaviour can be used to determine the physicochemical properties of the protein, such as its melt temperature, surface charge, hydrophobicity, and adsorptive capacity.

Table 1.4: Techniques commonly applied to study protein adsorption and stability.

- **Conformation:**
  - IR
  - CD
  - Fluorescence
  - Raman
- **Thermal:**
  - Differential Scanning Fluorimetry
- **Colloidal:**
  - Light Scattering
  - Size-exclusion Chromatography
  - Flow Imaging
  - Light Obscuration
- **Surface Charge:**
  - Zeta Potential
  - Isoelectric Focusing
- **Quantification:**
  - Reverse-phase HPLC
  - BCA Assay
- **Adsorption**
  - Quartz Crystal Microbalance
  - Surface Plasmon Resonance

1.1.7 Proteins investigated in this thesis

Two model proteins, lysozyme and BSA, **Figure 1.5**, were evaluated in this thesis. Lysozyme was chosen because it has a moderately hydrophobic surface, is small, and is ellipsoidal at a size of about 14 kDa.[110] It also has a high isoelectric point (IEP) of approx. pH 10 owing to its large composition of positively charged amino acids.[111] Its secondary structure predominantly comprises alpha helices and disordered regions with some ordered beta structure content. It is reported to possess a very high level of internal stability, evidenced by its high melt temperature of approx. ≥70°C.[112,113] Owing to this, it is highly conformationally stable and is not an aggregate-prone protein. Lysozyme offers considerable benefits for use as a model protein primarily because it retains a net positive charge within the pH range typically employed for liquid parenteral protein formulations.[1,111] This is useful because therapeutic antibodies, the largest class of biotherapeutic products, can only be formulated within a very narrow window (approx. pH 5-6) which results in these molecules retaining a net positive charge.[1] This net charge increases the potential for protein adsorption to charged interfaces. Therefore, lysozyme can be used to model the adsorption behaviour of therapeutic antibodies in the presence of primary packaging interfaces such as the vial surface which presents an anionic interface in aqueous media.[114] Additionally, it can be used to determine the effect of excipients on protein surface charge which has implications for adsorption behaviour.

On the other hand, BSA is a large heart-shaped protein of about 66 kDa in size.[115] Its surface is hydrophilic, and it has a very low level of internal stability, which is linked to solution pH, making it highly susceptible to unfolding and aggregation.[116] It also has a low to moderate melt temperature of approx. ≤63°C.[117] BSA is known to be an adsorption-prone protein owing to the combination of its surface-accessible amino acids and low internal stability. Its IEP is also considerably lower and ranges between pH 4.5-5.5 which makes BSA susceptible to physical degradation by the solution conditions.[115] Unlike lysozyme, BSA's stability is highly comparable to that of therapeutic antibodies owing to its lower melt temperature, propensity for adsorption and its aggregate prone behaviour.[116,117] BSA stability is representative of a broader range of biotherapeutic molecules including human albumins and as a result, can be used to model the behaviour of therapeutic proteins when exposed to different solution and environmental conditions. Furthermore, in contrast to lysozyme, BSA can be used to model the stability of therapeutic proteins in the presence of packaging interfaces as BSA is

adsorption-prone, positioning it as a useful model for therapeutic proteins when assessing packaging coatings on protein stability.[118]

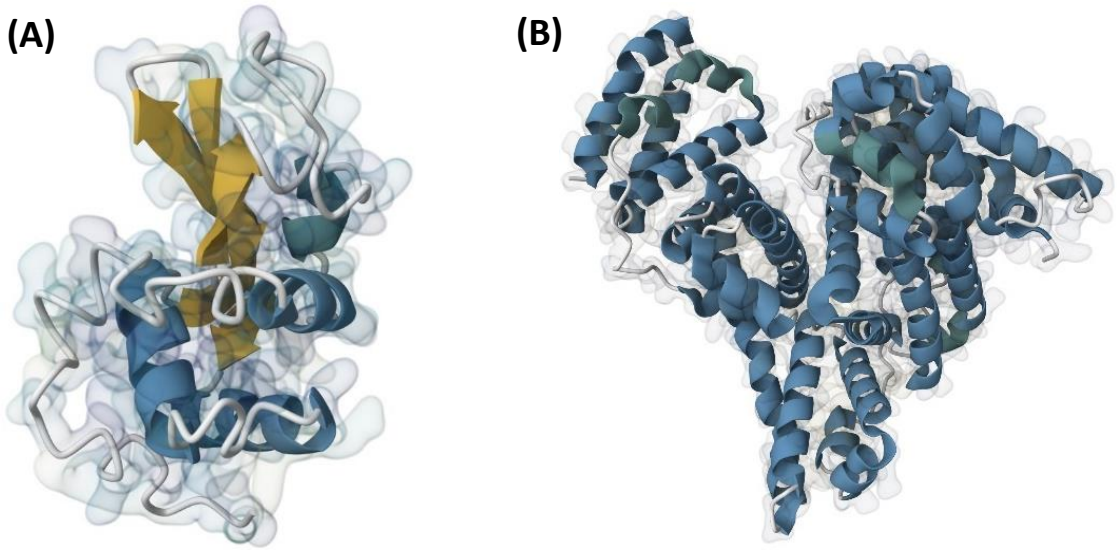


Figure 1.5: The figure depicts lysozyme (**A**) and BSA (**B**) structures as a cartoon and is coloured as follows: blue, α-helix; yellow, β-sheet; white, other structures. They are enclosed in an outer shell illustrating hydrophobicity in blue. Lysozyme and BSA were visualised using their protein data bank files 1LYZ and 3V03 for lysozyme and BSA, respectively.[119,120]

Aims and Objectives

The overall aim of this thesis is to explore the impact of packaging interfaces and formulation on the adsorption and stability of two model proteins, lysozyme and BSA, and develop novel formulation and packaging mitigation strategies to minimise the adverse impact of protein-packaging interactions.

The following objectives were established to achieve this aim.

Chapter Two:

- To summarise the state of the art regarding the role and impact of formulation in protein adsorption at interfaces encountered during the manufacture and storage of therapeutic proteins.

Chapter Three:

- To examine the influence of the solution environment, namely buffer type and pH, on lysozyme adsorption and stability.
- To determine the influence of lysozyme concentration on adsorption behaviour.
- To understand the role of storage conditions and vial coating on lysozyme adsorption from a high-concentration formulation.

Chapter Four:

- To determine the role of different vial interfacial contact surfaces on BSA stability when stored upright and inverted.
- To evaluate leucine as a novel stabiliser against BSA aggregation induced by vial interfacial contact surfaces.

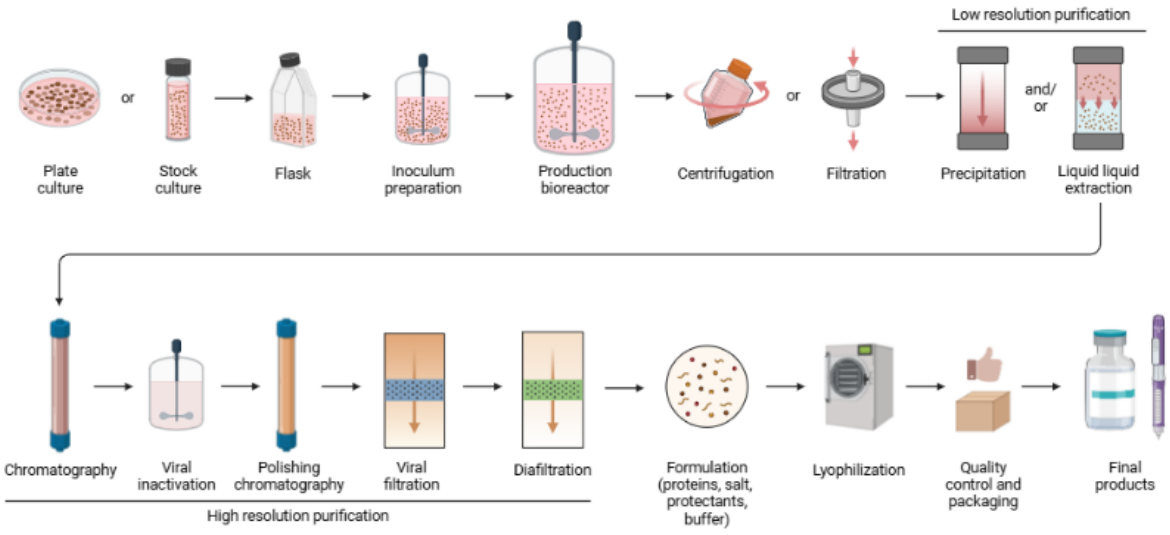
Chapter Five:

- To explore a novel phosphorylcholine vial stopper coating to mitigate BSA instability induced by stopper interfacial contact during storage.
- To determine the suitability of aerosol-assisted low-temperature plasma process parameters for applying a thin phosphorylcholine film to the surface of vial stoppers

Chapter Two

2. Impact of Protein Adsorption During Biopharmaceutical Manufacture & Storage

Submitted in Part to the European Journal of Pharmaceutical Sciences



2.1 Abstract

Protein therapeutics contact multiple interfaces during formulation, filtration, fill-finish, and storage processes. Interactions at these interfaces can compromise the protein's conformational and colloidal stability through surface adsorption, potentially leading to aggregation and particle formation. Surface-induced conformational changes in protein higher order structures, influenced by interfacial hydrophobicity and charge, are critical drivers of these effects. The resulting loss of active protein and increased aggregation risk pose significant challenges to the efficacy and safety of the final biotherapeutic product. Thus, developing strategies that minimise protein-surface interactions that compromise protein conformational and colloidal stability during manufacturing and storage is imperative. This review focuses on current research on biotherapeutic protein behaviour at interfaces encountered during fill-finish and storage. Furthermore, the review introduces the factors influencing protein adsorption and interfacial stability and current methodologies and advancements in mitigating interfacial adsorption, emphasising rational formulation design strategies.

2.2 Introduction

The landscape of biopharmaceutical therapeutics has undergone significant changes driven by the transformative role of protein and peptide-based therapies in disease treatment.[2] Unlike small molecule drugs, a protein's therapeutic efficacy depends on its higher order structure. Disruption of this structure can profoundly impact a protein's therapeutic profile.[121] Therefore, preserving protein stability is paramount during both manufacturing and storage processes. Proteins have a strong tendency to adsorb to interfaces, leading to a potential loss of target concentration and alterations in conformational and colloidal stability.[27,122] From cell harvesting to fill-finish and storage processes, therapeutic proteins are exposed to various interfacial stresses such as the air-liquid, solid-solid, ice-liquid and oil-liquid interfaces.[123] Understanding the underlying factors contributing to protein adsorption behaviour is critical to maintaining its medical value and therapeutic efficacy and circumventing the consequences of interfacial adsorption, **Figure 2.1**.

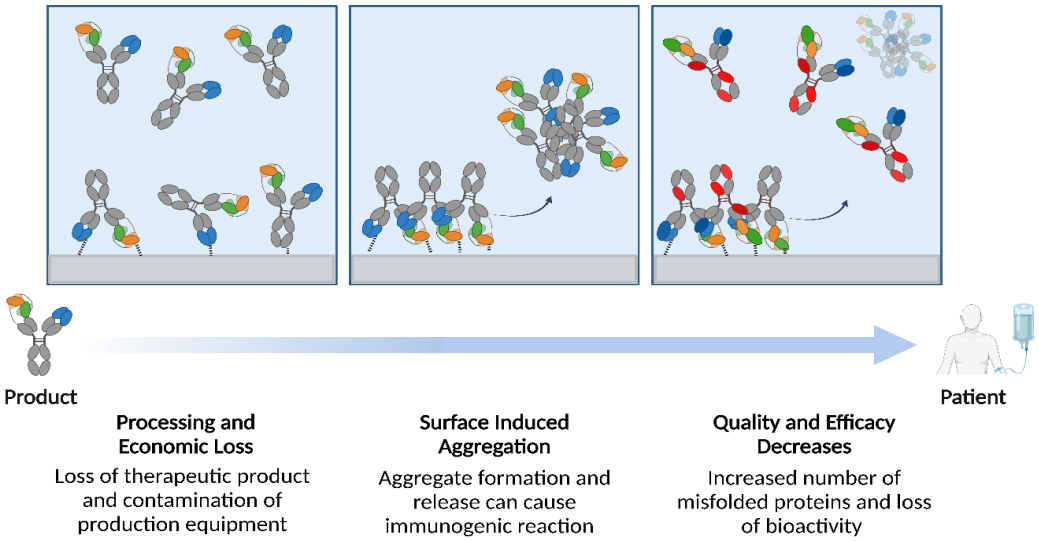


Figure 2.1: The effect of protein adsorption to a solid-liquid interface and the consequences for therapeutic protein manufacture, bioactivity, and patient safety. Created with BioRender.com.

There have been considerable advancements in elucidating the specific mechanisms which govern protein adsorption behaviour, leading to an increased understanding of how intrinsic and external factors affect adsorption characteristics. However, the impact of

protein-formulation interactions on protein adsorption behaviour during key processing steps such as filtration, fill pumping, and storage is of considerable interest owing to the complex interactions and the implications on product stability.[124] Understanding how excipients influence inherent protein characteristics, including their adsorption behaviour, enables the development of formulations that effectively control this phenomenon during biomanufacturing and, critically, storage. Protein adsorption behaviour can be influenced by poor excipient stability and formulation design, including excipient-surface incompatibility, creating environments favourable for interfacial adsorption and protein instability.[125] Moreover, inadequate consideration of the surface properties of manufacturing and storage materials, specifically their surface hydrophobicity and charge, can lead to surface-induced conformational and colloidal instability.[35]

To date, many specialised reviews have focused on various aspects of protein adsorption during commercial biopharmaceutical manufacture and product storage, such as antibody adsorption, the impact of interfacial stress on adsorption behaviour, the effects of high shear, extractables and leachables, packaging, drug formulation, and delivery.[27,72,123,126–132] Several reviews also focus on providing a fundamental understanding of protein adsorption behaviour, discussing specific mechanisms of adsorption and technologies to study the behaviour.[30,35,37,133,134] However, this review provides an overview of protein adsorption during fill-finish operations and storage and provides insights into formulation effects on this adsorption behaviour.

2.3 Factors impacting protein adsorption

Several adsorption models discuss random and direct surface distributions of adsorbed protein molecules.[30,133,135] They interrogate the many different facets of adsorption behaviour supported by simulations.[40,41,136–139] However, the fundamental parameters which affect protein adsorption can be simplified into three distinct groups: (i) protein, (ii) solution/environment, and (iii) surface properties. The effect of each of these groups on adsorption behaviour is summarised in **Table 2.1**.

Molecular interactions are the fundamental forces underpinning protein adsorption. Electrostatic interactions, including van der Waals forces and hydrogen bonding, are the primary forces governing protein adsorption to hydrophilic and charged materials.[36] The magnitude of these interactions depends on buffer composition, pH, and ionic strength and is influenced by the distribution of amino acids on the protein's surface. Hydrophobic interactions can also occur. The protein's hydrophobic domain tends to be buried within the 3D structure when the protein is in an aqueous solution. However, these domains become exposed and adhere to hydrophobic interfaces, disrupting the balance of intra-protein and protein-solvent interactions.[35] Protein-surface interactions at hydrophobic surfaces can also result in significant protein denaturation which is not typically observed for hydrophilic interfaces.[140] However, this depends on several factors, including temperature, interfacial properties, pH, ionic strength, handling, protein concentration, charge, stability, and excipients.[44,141]

However, once proteins form a surface bond, their charge and concentration can dictate the formation of mono- and multi-layers at an interface.[30] Monolayer formation occurs because of weak or repulsive protein-protein interactions. It depends on the strength of the electrostatic repulsions between the protein and surface and the mass of protein adsorbed.[30] Meanwhile, multilayer formation is typically observed under specific solution and environmental conditions.[141,142] The layer formation and thickness are also influenced by the protein's surface orientation, density, lateral protein interactions, and concentration.[30,110,111,143]

Table 2.1: Summary of the critical protein, solution and interfacial factors that govern protein absorption and the associated effect.[27,30,35,37,144]

Factor	Property	Effect
Protein	Size/shape	Proteins diffuse slowly in aqueous media with increasing size but have potentially more sites of interaction with the interface.
	Charge	Proteins preferentially adsorb to interfaces bearing an opposite net charge. However, even if the net charge of the surface is the same as the protein, adsorption can still occur, as most proteins will have localised sites of both positive and negatively charged residues.
	Hydrophobicity	Polar domains adsorb to polar or charged interfaces, while hydrophobic domains adsorb to hydrophobic interfaces only. Proteins with low internal stability may expose their internal hydrophobic core to facilitate adsorption.
	Hydrodynamic radius	Proteins are precluded from entering and adsorbing to sites smaller than their hydrodynamic radius.
	Stability	Proteins with low internal stability will adsorb in higher quantities and display higher degrees of denaturation and activity loss.
	Concentration	Low protein concentrations in aqueous solutions can form a thin film, leading to greater unfolding on interfacial adsorption. High concentrations lead to more significant protein adsorption and the formation of viscoelastic films.
Solution/environmental	Temperature	Higher temperatures result in the thermal unfolding of the protein and an increased diffusivity toward the interface. Unfolding can lead to more interaction sites with the material and promote induced denaturation.
	Buffer composition	Buffers maintain the pH of a solution but can modify the protein's surface charge, hydrophobicity or stability. Buffers can also modify interfacial properties.
	pH	Altering the pH can modulate the charge of the interface and the protein, which can give rise to electrostatic interactions. pH near the IEP of the protein can also induce adsorption.

	Ionic strength	High ionic strength solutions can result in electrostatic shielding of protein-interface interactions. However, the choice of tonicifer, their charge screening capacity and surface hydrophobicity are critical.
	Excipients	Excipients can modify the protein's physicochemical properties in addition to the solution and interfacial conditions altering protein-interface interactions.
Surface	Composition	The chemical makeup of an interface will determine the types of protein-interface interactions: polar, electrostatic, etc. Specific chemical groups present on the surface can influence this.
	Topography	Increased roughness provides a larger surface area for protein adsorption and may lead to spreading and denaturation along the interface.
	Surface energy	An interface with a high surface energy promotes adsorption, whereas low surface energy may repel proteins from the surface due to weaker forces.
	Wettability	Surfaces with a water contact angle ≤65° adsorb less protein due to the inability of the protein to displace interfacial water, whereas ≥65° adsorption is expected to be more significant. Hydrophobic materials are also known to induce a greater degree of protein unfolding and aggregation. However, some hydrophobic surfaces can be adsorption resistant.

2.4 Protein adsorption during fill-finish and storage operations

2.4.1 Challenges in downstream bioprocessing

Therapeutic proteins are exposed to considerable stresses during production, including interfacial adsorption, which is widely recognised as a driving force for protein unfolding, aggregation, and particle formation.[20,127,128,145,146] Therefore, to minimise the impact of protein adsorption on stability during downstream biomanufacturing and storage, it is essential to carefully control the conditions under which the protein is processed and stored. The focus of this review is to provide an update on the current research on protein adsorption behaviour during fill-finish and storage, **Figure 2.2**, specifically the impact of fill pumping and primary packaging interfaces.

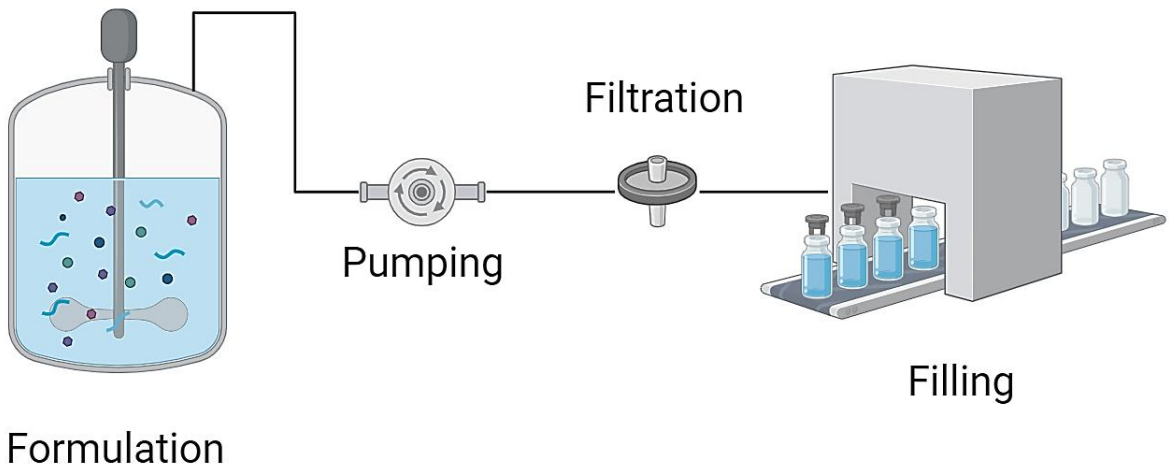


Figure 2.2: Formulation and fill-finish process flow. Created with BioRender.com.

Fill pumping is a critical concern in the biopharmaceutical manufacturing process.[128,147] Protein adsorption to filling surfaces after bulk formulation and sterile filtration can induce instability in the final product. Additionally, any particulates generated during fill pumping can remain in the biopharmaceutical product, potentially triggering further instability upon exposure to secondary stressors during storage. Instability induced during the transition from drug substance manufacture to drug product manufacture, such as the bulk freeze-thaw process, can also affect the protein's adsorption behaviour and overall stability throughout its production lifecycle and shelf-life.[130,148–158] Key parameters affecting protein stability during unit operations, transport and storage are summarised in **Table 2.2**. Filtration

processes, which occur before fill pumping and storage, can also present issues related to filter particle shedding and their adsorption-associated concerns.[159–170] For example, studies on filtration systems have identified incompatibilities with the screen/membrane type used for ultrafiltration/diafiltration and the system hydraulics, which can induce protein instability and operational failure.[171] Further, *Deringer et al*. showed that aggregates formed during pumping could block the filter membrane, and the tubing type was also implicated.[161] Innovative mitigation strategies have focused on membrane functionalisation in the case of protein-specific separation. Different approaches have included anion-exchange adsorption and pH-controlled effects or increasing the hydrophilicity of the filter membrane.[172–176] Additionally, single-use bioprocess technologies require consideration for their impact on protein adsorption and stability during biomanufacturing, as their use poses a risk for leachables and particulate formation.[67,177,178]

Table 2.2: Summary of the critical factors impacting protein stability during formulation, fill-finish and storage operations.[65,123,130,179]

Unit operation	Interface	Stress	Impact on stability
Bulk freeze-thaw	Ice-liquid, air-liquid, solid-liquid	Cryoconcentration, excipient crystallisation, pH shift, interfacial unfolding, temperature, cold denaturation	Aggregation due to ice crystal formation, pH-induced denaturation, interfacial unfolding and aggregation, thermal-induced unfolding and aggregation
Formulation/ mixing	Air-liquid, liquid-liquid, solid-liquid	Shear, interfacial adsorption, phase separation, foaming, excipient loss/degradation, raw material impurities, leachables, foreign matter	Shear-induced denaturation, interfacial unfolding and aggregation, excipient loss
Filtration	Solid-liquid	Interfacial adsorption, shear, excipient loss/degradation	Loss in target concentration, interfacial unfolding and aggregation, shear-induced denaturation, contamination

Filling	Solid-liquid, air-liquid, solid-solid	Shear, cavitation, foaming, occlusion, temperature, leachables, interfacial adsorption, foreign matter, light, excipient adsorption/degradation	Shear and cavitation-induced denaturation, foaming, occlusion causing physical damage, thermal-induced unfolding and aggregation, contamination, interface-induced particles
Packaging/ labelling	Air-liquid, solid-liquid, liquid-liquid	Agitation, light, temperature	Agitation-induced aggregation, light exposure causing degradation, thermal-induced unfolding and aggregation, interface-induced particles
Transport	Air-liquid, solid-liquid, liquid-liquid	Mechanical shock, cavitation	Shock-induced denaturation, supercooled drug formulations can freeze, leachabes, opalescence, precipitation
Storage	Air-liquid, solid-liquid, liquid-liquid	Container interactions, leachables, interfacial adsorption, excipient-container/closure incompatibility	Interface-induced aggregation, leachables, excipient incompatibility leading to particle formation, glass lamellae formation, coating delamination due to formulation

2.4.2 Fill-finish

Fill-finish procedures involve filling protein therapeutics into their final primary packaging containers, such as vials, syringes, or cartridges. This complex mechanical engineering process includes fluid filling and sealing systems, where the interplay between shear forces and interfacial adsorption can significantly alter protein stability downstream.[180] Several material interfaces encountered during these production steps, notably stainless-steel, can influence protein adsorption behaviour and result in surface-induced aggregation. Factors such as surface composition, heat in the pump head, oxidative stress due to cavitation, mechanical stress from occlusion, and particle shedding can also induce protein instability.[181–185]

Stainless-steel is widely used for production equipment and is associated with inducing therapeutic protein instability.[72] Stainless-steel can be problematic in fill-finish operations

due to its anionic characteristics in aqueous solution.[186,187] Due to electrostatic mediated adsorption, therapeutic proteins can adsorb in high quantities to this material interface.[186,187]

Interfacial adsorption of therapeutic proteins to the surface of biomanufacturing equipment such as stainless-steel can result in irreversible interactions and interface-induced degradation.[188] This can be compounded through exposure of the protein moiety to varying shear rates and environmental conditions. Degradation induced by interfacial shear rates can be affected by the concentration of the therapeutic protein, and the combination of solution and environmental factors can cause significant particle formation depending on the interfacial composition. *Kalonia et al*. demonstrated this effect using IgG1*,* where exposure to alumina or stainless-steel substrates in the presence of varying protein concentrations impacted subvisible particle formation.[189] It was found that IgG stability was concentration dependent. At concentrations ≥50 g/L, more protein adsorbed to the stainless-steel, which induced conformational changes and increased protein-protein interactions. Interestingly, the shedding of adsorbed protein particles from the different interfaces due to interfacial shear was implicated in generating these subvisible particles. Only a small fraction of adsorbed protein was required for this to occur.[189] *Wu* and *Randolph* also observed similar findings for intravenous immunoglobulin (Ig) adsorption to steel pump surfaces and attributed the particle count to the charge of the stainless-steel interface.[186] However, the shedding of adsorbed protein films is not always a prerequisite for particle formation.

Stainless-steel is commonly employed in fill-finish operations as pumping apparatuses. In biopharmaceutical fill-finish operations and downstream purification processes, various types of steel pumps control the transfer of fluids. Typically, these pumps operate as either lobe, rotary piston, rolling diaphragm, time-pressure filler, or peristaltic pumps.[190–192] **Figure 2.3** illustrates an example of the commonly used fill pumping units. Fill pumping poses a concern due to the potential effects of friction, shear, pressure, cavitation, occlusion, and heat produced by the pumping process on protein stability.[193] However, the effect of these processes, particularly shearing, on protein stability during the short-filling process is likely negligible.[186,192,194–198]

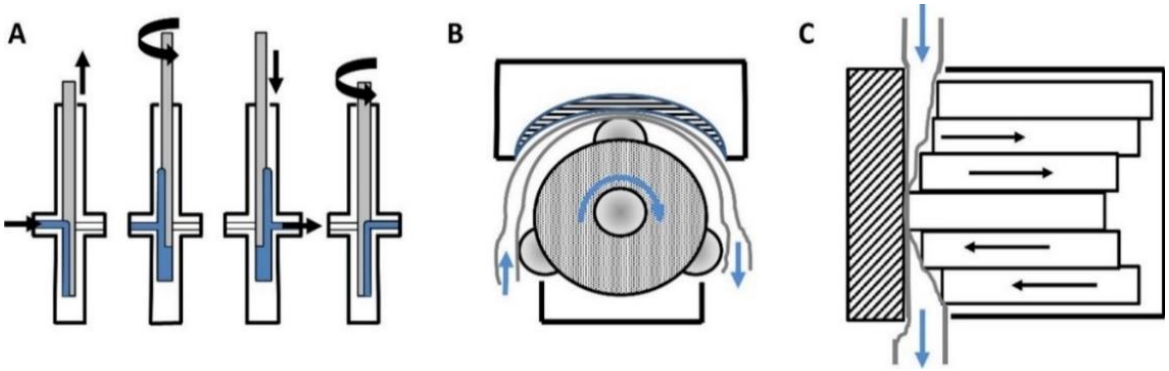


Figure 2.3: Schematic presentation of select biopharmaceutical fill pumping systems: rotary piston pump (**A**), radial peristaltic pump (**B**) and linear peristaltic pump (**C**). The figure is reprinted from the reference with permission of the publisher.[190]

The incompatibilities between fill pumping and protein stability can stem from the combination of the pumping processes with unwanted protein adsorption to the type of pump utilised for filling.[190] *Nayak et al*. highlighted this factor, stating that the rolling diaphragm pump, peristaltic pump, and time-pressure filler generated fewer IgG1 subvisible particles than a rotary piston pump.[191] *Roffi et al*. also demonstrated that more protein particles were generated in a rotary piston pump than in a peristaltic pump.[196] *Defante et al*. observed similar issues for stainless-steel rotary piston pumps.[199] While, *Corvari et al*. identified that the rotary piston pump and time-pressure filler contributed to sub-visible particle formation.[200] It is worth noting that lobe pumping has also been implicated in the formation of protein aggregation, likely owing to exposure of the protein solution to a large stainless-steel interface. The piston pump-induced protein instability mechanism was identified by *Dreckmann et al*., who indicated that piston pumps generate a recirculation zone.[190] This zone leads to incomplete fluid exchange in the cylinder of the piston pump, causing repetitive exposure of the product to stress. While peristaltic pumping offers advantages over rotary piston pumps due to its more straightforward fluid path flow, adsorption and film abrasion remain significant issues.

While proteins avoid the stainless-steel interface during peristaltic pumping, they can still adsorb to the tubing materials used for fluid transfer.[183] The heat produced due to speed and occlusion, vapour phase hydrogen peroxide, and tubing characteristics can contribute to protein adsorption and instability during filling using this pumping technique.[184,201–203] The influence of tubing material and properties has recently been implicated as a problematic

interface during fill-pumping procedures, as it can affect the number of particles generated.[55] Additionally, tubing can shed particles into the solution, acting as nucleation sites for additional protein adsorption and aggregation when combined with steel or filter particles.[72,162,181,182,204] However, tubing material shedding can be avoided using materials with low surface roughness and high abrasion resistance.

Deiringer and *Friess* identified that post-pumping particle levels differed substantially between tubing types precisely due to the combination of material composition and hardness.[184] *The authors* found that protein particle formation was linked to the stretching of silicone tubing, and aggregation increased with higher strain beyond the breaking point of the adsorbed protein film. Additionally, more hydrophobic tubing materials can result in faster protein film renewal, leading to repetitive adsorption and desorption cycles that can increase the particle count. While more rigid tubing materials appear more suitable for peristaltic pumping, they can lead to the formation of larger protein particles.[184] *Fanthom et al*. also found that solid-solid contact of the tubing materials disrupted adsorbed protein films, leading to monomer loss and aggregation during pumping.[201] Abrasion of adsorbed protein films from the fill pump tubing can occur as described by *Deiringer* and *Friess* in three distinct ways: (i) stretching of the outer wall and compression of the inner wall by insertion into the pump head, (ii) transversal stretching during squeezing of the tubing and (iii) longitudinal stretching and compression during pump roller movement.[184,201]

Mitigating the impact of pump- and tube-induced aggregation and particle formation is relatively straightforward. Alterations to the pumping process, including surfactants or charge screening molecules, can help reduce and prevent protein adsorption and film abrasion. Interestingly, *Roffi et al*. proposed a ceramic piston pump with an optimised clearance factor and surface roughness for piston pumps to minimise protein adsorption and particle formation.[205] With interchangeable pistons, this design yielded a customisable pumping system that could be modified on a protein-by-protein basis. For peristaltic pumping, the mitigation process is also relatively straightforward. In cases where hydrodynamic flow and solid-solid contact cause abrasion of adsorbed protein films from hydrophobic tubing, using a hydrophilic tubing material can reduce protein adsorption. *Deiringer* and *Friess* proposed a polymer coating consisting of a PDMS backbone and (PEG) side chain, which can be applied to both traditional silicone and modern thermoplastic elastomer-based tubing.[206] Including

surfactants, cyclodextrins, or amino acids such as arginine can limit adsorption where tubing characteristics cannot be altered.

2.4.3 Primary packaging during storage

Once the protein product has been filled and packaged into sterile, inert materials for storage, **Figure 2.4**, there is further potential for protein adsorption and instability. Adsorption to the surface of the primary packaging is limited by the properties of the packaging material, the drug contact surface area and the properties of the protein moiety. Surface-adsorbable protein can undergo conformational and colloidal changes and desorb into the bulk media after exposure to secondary stressors, where aggregation and particle formation can readily occur. It also poses a risk for proteins in aqueous solution to exhibit altered bioactivity.

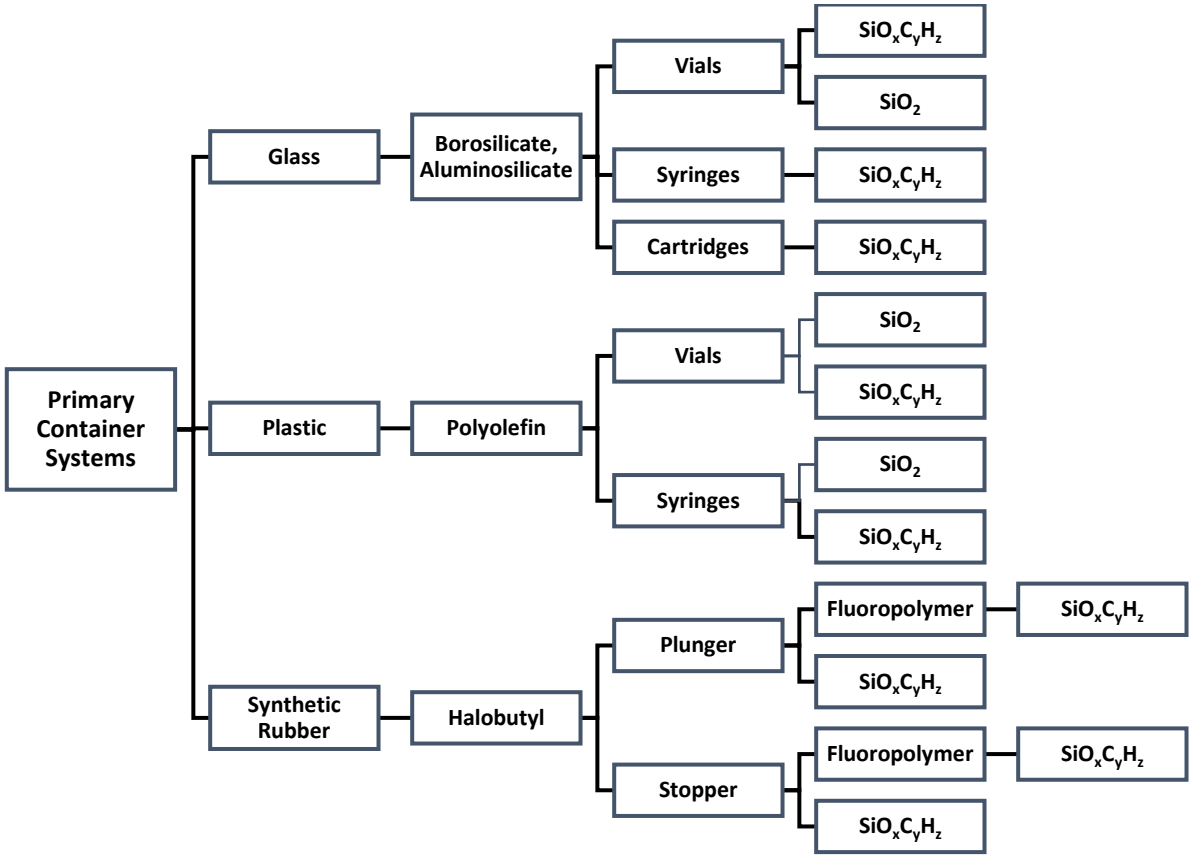


Figure 2.4: The most common primary packaging and container systems used for liquid parenteral protein formulations and their associated surface coatings.[65,69] SiO_2: silicon dioxide; $SiO_xC_yH_z$: siloxane.

Concerns also exist regarding the shedding of glass particles, alkali leachables, tungsten, needle glue and rubber extractables arising from glass vial packaging systems and the elastomeric closures used for syringe plungers and vial stoppers.[65,71,72,75,84,89,90,207,208] Elastomeric closures represent some of the most complex primary packaging materials. These materials are known for leaching organic compounds into parenteral protein products, causing pH shifts and destabilising the protein moiety.[65,82,209] The most common strategy to address this includes surface coating the packaging material with fluoropolymer materials, e.g., PTFE, ETFE, and FEP. However, this approach requires assessment on a case-by-case basis, as fluoropolymer-induced instability has previously been observed.[92,210]

Elastomeric closures are widely associated with silicone oil, primarily used as an interfacial lubricant. Their purpose is to facilitate the easy insertion of the stopper into the vial or improve the glide force for self-delivery devices.[211] Silicone oil comprises PDMS but can also contain trace levels of cyclic polymers such as octamethylcyclotetrasiloxane.[65,72] Although the use of siliconisation for elastomeric closures and glass surfaces is established, concerns exist owing to its propensity to leach into parenteral protein formulations.[212,213] Moreover, siliconised interfaces also introduce hydrophobic sites for surface adsorption, which can result in denaturation and instability.[214] Interestingly, silicone oil droplet formation has recently been linked to the age of the delivery device. Older syringes show reduced droplet migration, likely owing to greater annealing of the silicone oil over time.[215] Further, the syringe source, siliconisation process, excipient type, and concentration significantly contribute to oil droplet migration into the formulation.[216]

Covalently bonded, baked and cross-linked siliconisation methods have been developed to address concerns related to the exposure of the therapeutic cargo to the oil-water interface.[97,217,218] These methods are superior to the conventional spray-on or liquid silicone oil application techniques in reducing silicone oil leachables, protein particle formation, and protein-PDMS particle formation.[98,217,219,220] Exposure to autoclaving post-coating can change the surface topography of siliconised surfaces prepared with bake-on methods.[221] *Moll et al*. showed that autoclaving can turn a homogenous silicone coating into a non-homogenous, micro-structured surface with increased protein adsorption, particularly at high sterilisation temperatures.[221] Nevertheless, the bake-on approach is a viable alternative to sprayed-on silicone oil coatings. Further, the use of cross-linked silicone is reported to be advantageous

over baked-on silicone coatings because it has superior adhesion to the glass and elastomeric closures, **Figure 2.5**, reducing migration of silicone oil droplets into the solution owing to resistance to chemical attacks by the formulation and is compatible with staked needle devices.[97,98,218] Plasma deposition has also been shown to covalently bond inert silicon-based coatings to primary packaging systems.[108,109] Notably, it has been shown that silicone oil alone is often insufficient to trigger aggregation.[222] Still, lower molecular weight silicones can lead to the most rapid denaturation and aggregation.[129,223]

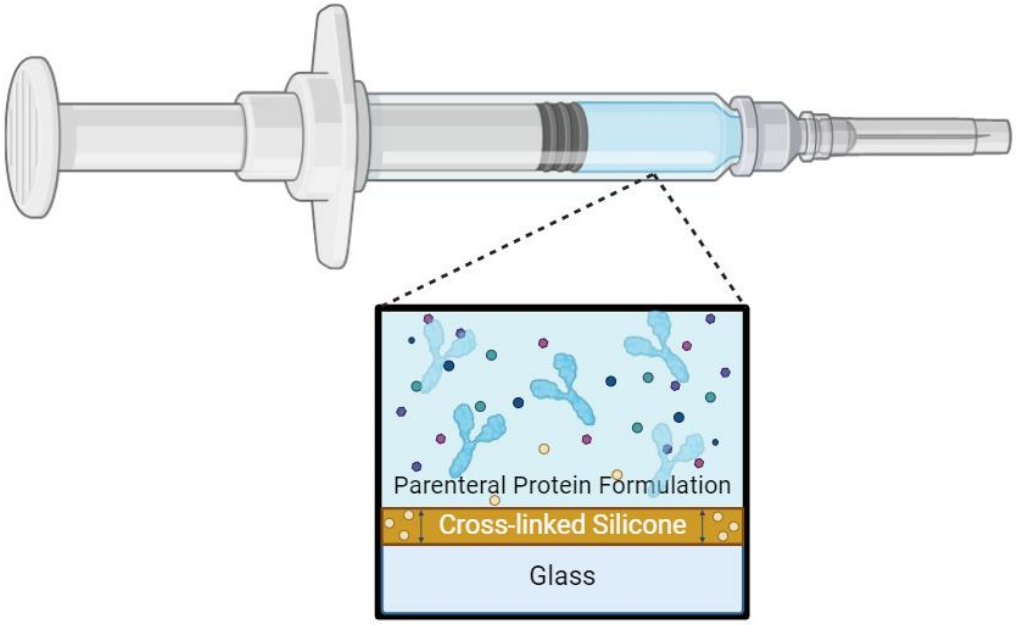


Figure 2.5: Cross-linked silicone coating applied to primary packaging surfaces. This coating technique ensures a tighter, more uniform layer thickness, significantly reducing silicone particle leachables compared to traditional silicone coatings. Inspired by *Depaz et al*.[98] Created with BioRender.com.

While there is an impetus to improve siliconisation techniques for primary packaging systems, silicone-free devices are the subject of increased research interest owing to the need for packaging devices for silicone-sensitive medicines. Current research into silicone-free packaging devices focuses on two packaging solutions: (i) polymeric storage materials and (ii) uncoated borosilicate glass with fluoropolymer elastomeric closures. Several studies have compared glass and polyolefin materials and their subsequent impact on protein adsorption and stability. *Yoneda et al*. investigated adalimumab and abatacept adsorption at the syringe

interface in both borosilicate and cycloolefin polymer syringes.[224] Both proteins were found to form multi-layered structures consisting of two distinct layer types. Proteins adsorbed on the surface of the syringe material, and proteins adsorbed on top of the proteins on the syringe surface. A pH-dependent, electrostatic interaction was the dominant force for protein adsorption onto the glass surface, while hydrophobic effects were dominant for protein adsorption on the polymer surface. Interestingly, when the repulsive forces between proteins were weak, protein adsorption increased for both materials and protein aggregation increased. *Maruno et al*. highlighted that the olefin polymer syringe barrels were superior at preventing protein interfacial binding compared to glass while *Werner et al*. suggested that polyolefin syringes could effectively replace glass syringes because they offer similar chemical stability over long-term storage.[73]

These polymeric storage devices offer a viable alternative for packaging biologicals where more stringent storage requirements are needed.[225,226] Their primary limitations include a higher oxygen permeability and a propensity for sterilisation-induced radical generation, which heightens the risk of oxidative damage for liquid parenteral proteins.[227] However, secondary packaging, such as an oxygen absorber and nitrogen-filled aluminium pouches, can help address this issue.[73,228] SiO_2-coated polymer packaging has also been developed to harness the benefits of polymeric storage materials and glass packaging devices without their respective drawbacks.[229,230]

The vial stopper and syringe plunger have also been scrutinised due to studies determining that these materials are significant sites for protein adsorption and instability. *Soeda et al*. implicated the vial stopper as a site for surface-induced protein aggregation. When coated with silicone oil, visible protein-PDMS particles can release in the bulk solution.[89] Modifying the siliconisation method or applying a fluoropolymer coating have been employed as risk mitigation strategies, as mentioned earlier. *Teska et al*. compared the effects of accelerated stress conditions on protein stability in contact with a novel fluoropolymer surface and the typical siliconised surface.[95] *The authors* showed that protein particle formation was much lower during agitation with the fluoropolymer surface than the siliconised surface. Reduced particle formation and consistent break-loose gliding forces were also found for glass-PTFE syringe plunger systems.[96] However, *Grapentin et al*. showed that despite the potential benefits of fluoropolymer coatings, there are inherent limitations due

to the risk of fluoropolymer particles shedding from the surface, indicating susceptibility to degradation by the formulation over time. Recovery of filtered solutions showed that microscopic fluoropolymer particles, **Figure 2.6**, were detected as identified by Fourier-transform infrared spectroscopy (FTIR).[90] One of the critical causes of this particle formation is mechanical shock during transport and handling.[230–233] Additionally, scope exists to mitigate protein adsorption to primary packaging by developing innovative surface coatings, as seen with polyglycerol, PEG and SiO_2 coatings to pharmaceutical glass.[105,108,206]

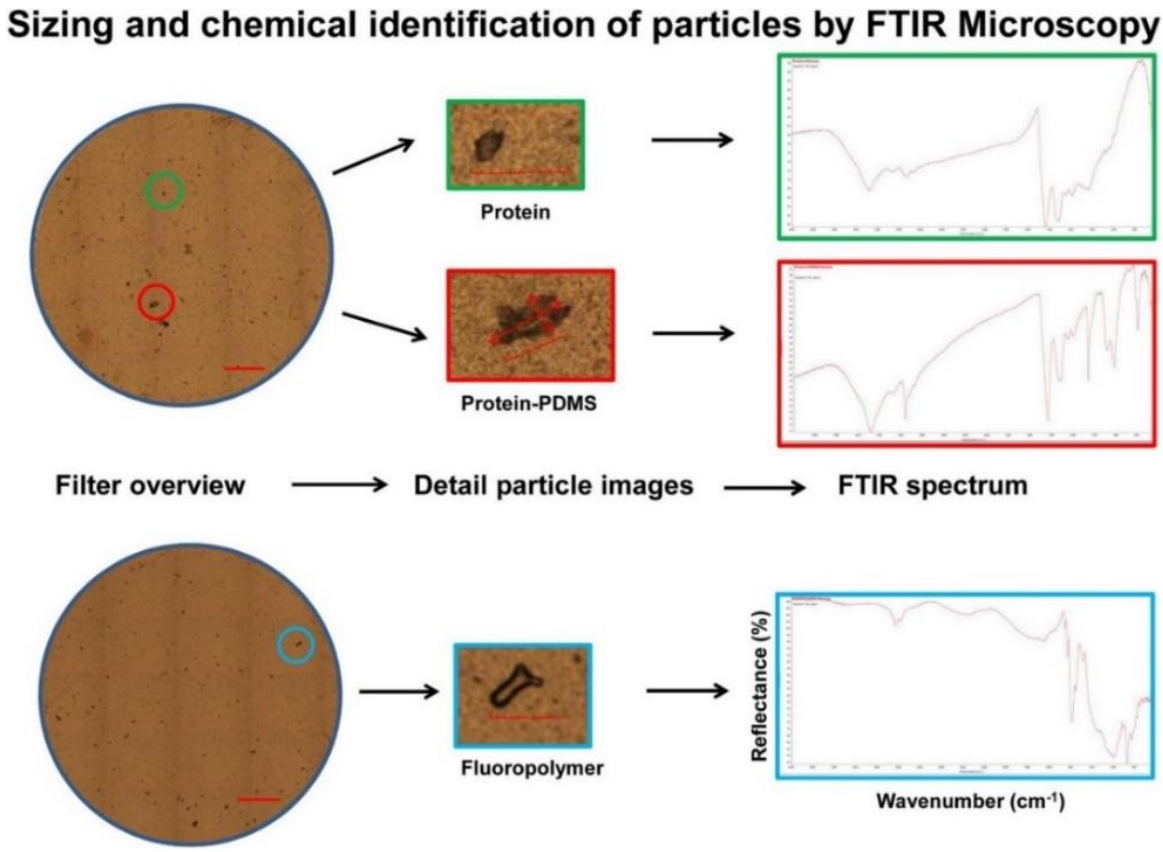


Figure 2.6: Sizing and chemical identification of particles produced from pharmaceutical vial stoppers analysed by FTIR microscopy. Sizing identified particles of ≥25 µm in length suitable for chemical analysis (rectangular boxes), scale bar 100 µm. FTIR analysis identified protein, protein-PDMS and fluoropolymer particles. The figure is reprinted from the reference with permission of the publisher.[90]

2.5 Formulation strategies to reduce protein adsorption

2.5.1 Excipient selection

Excipients are crucial in pharmaceutical formulations, particularly in stabilising protein-based therapeutics. They can act as competitive surface-active agents or mitigate undesirable protein interactions at interfaces, **Figure 2.7**.[63] Surfactants and recombinant human albumin are the primary excipient choice to mitigate adsorption especially for low concentration liquid parenteral protein formulations. However, other excipients, like buffers and amino acids, can also potentially protect the protein from interfacial adsorption.

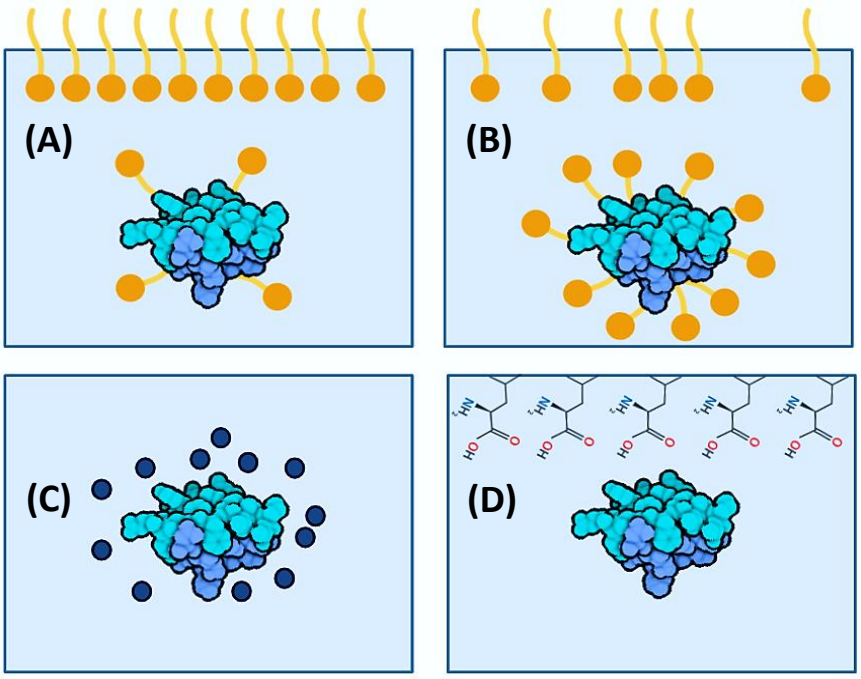


Figure 2.7: Excipients used to mitigate protein adsorption and their associated mechanisms. Illustration of surfactant pathways used to prevent protein adsorption where either surfactant engages in interfacial binding as a mechanism of anti-adsorptive behaviour (**A**) or surfactant forms protein-surfactant complexes of low adsorption affinity (**B**). Additionally, charged amino acids such as arginine can participate in molecular crowding (**C**), and hydrophobic amino acids such as leucine can reduce the surface tension (**D**). Created with BioRender.com.

2.5.2 Surfactants

Surfactants are widely used in biomanufacture and biopharmaceutical products as anti-adsorptive agents due to their established role in interfering with protein-surface interactions **Table 2.3**.[51] The surfactants used are typically small, non-ionic surfactants. They compete with the therapeutic cargo for space at the interface, displace adsorbed proteins or form complexes with the protein, inhibiting surface adsorption.[234,235] However, the efficacy of many surfactants can be influenced by the packaging surface's composition.[62] Further, surfactant effectiveness can depend strongly on formulation pH, buffer and salt composition, and interface hydrophobicity and charge.[54,236] Four surfactants, PS80, PS20, Pol188 and Pol171, have been approved and included in commercial liquid parenteral protein formulations.[1]

PS80 is the most widely used surfactant in protein formulations owing to its interfacial stabilising properties.[1,237,238] It has been used for many studies to assess protein interfacial stability both for fill pumping and storage conditions. *Her* and *Carpenter* studied the effect of PS80 on the interfacial binding of Ig to three commercial peristaltic fill pumping tubing materials.[239] In agreement with other literature, *the authors* found that adsorption occurred depending on material type, and protein film abrasion resulted in particulate formation. However, including PS80 0.1% w/v effectively prevented the interaction between the interface and the protein. Interestingly, it was also observed that with the appropriate choice of buffer, particle formation could be significantly reduced. *Deiringer et al*. also showed that protein particle formation and size distribution were influenced by the formulation parameters, specifically ionic strength, for protein adsorption to silicone rubber tubing.[185] Like *Her* and *Carpenter*, surfactant use, in this case, PS20, could effectively screen against protein-surface interactions by increasing the hydrophilicity of the tubing. However, using polysorbates as an interfacial stabiliser does not guarantee success in mitigating adsorption-induced instability. As observed by *Wu* and *Randolph,* the inclusion of PS80 did not prevent surface-induced particle formation when a piston pump apparatus for biotherapeutic fill pumping was used.[186]

Additionally, it is well known that polysorbate surfactants are associated with chemical instability because of the hydrolysis of the ester bond, auto-oxidation, and cleavage of the

ethylene oxide subunit.[61,125,240] The formulation has also been shown to impact degradation, with buffer choice accelerating oxidation.[236] Further, glass leachables such as aluminium have also been associated with causing free fatty acid particle formation due degradation of polysorbate surfactants.[71,241] Additionally, polysorbates are associated with visible and sub-visible particle formation in polysorbate-based biotherapeutic products. A recent study by *Poumarede et al*. observed the accelerated oxidation of PS80 in a polysorbate-containing formulation in contact with platinum-cured silicon tubing during filling for an extended period (~1 h).[242] This was attributed to the leaching of radical initiators from the platinum-cured silicon tubing, which *the authors* suggested were organosilicon peroxides decomposed by iron. Polysorbate oxidation has been reported to initiate degradation during storage, which can significantly affect protein stability.[243] The primary mitigation strategy proposed by *the authors* is to avoid iron traces, add a chelating agent such as ethylenediaminetetraacetic acid or reduce the filling time. Using a peristaltic pump, *the authors* also evaluated the impact of a thermoplastic elastomer-based tubing on PS80 stability and filling performance. This tubing type proved to be more rigid and required higher oscillations for filling, which is undesirable despite the reduced particle formation.[242] Only Pol188 has been considered a meaningful alternative to polysorbate surfactants in protein formulations due to its similar stabilising efficacy to PS80 and its potential for bulk freezing and fill pumping where other mitigation strategies fail.[55,59,60]

Beyond formulation, surfactants also present limitations in biomanufacture. Surfactant adsorption to the mixing, filter and pumping materials leads to a loss in the available concentration.[166,244,245] While this can help prevent interface-mediated protein instability by altering the substrate's surface properties, it can potentially present issues during storage due to insufficient surfactant concentration.[166,179,246]

Despite the evidence for the protein-stabilising effects of surfactants, they can also have a detrimental impact on primary packaging materials, specifically their surface coatings.[69] *Kannan et al*. studied the effects of PS20 (0.01% w/v or 0.1% w/v) on the silicone oil-liquid interface in a pre-filled syringe and compared its results with Pol188. PS20 produced lower interfacial tension than Pol188, which made PS20 more effective at mitigating adsorption to the oil-water interface.[64] Additionally, the presence of PS20 lowered the aggregation propensity of IgG1. However, despite the apparent advantage of PS20 use over Pol188, the

lower interfacial tension led to more oil droplets in the agitated mixtures. Another concerning aspect of surfactant-packaging interactions is the effect of the formulation components on the syringe and cartridge plunger break-loose glide force. Excipients such as buffers, sugars and surfactants can all affect the break-loose glide forces due to their interactions with the silicone oil coating on the surface of the glass.[247] Specifically, PS80 has been identified to increase the glide force owing to induced changes in the structure of the silicone oil lubricant after exposure to thermal stress.[247,248] However, Pol188 does not have the same impact on device functionality due to its lower interfacial activity.[64,249] Proteins have recently been observed to have a similar effect depending on their physicochemical characteristics.[107] While there is a rationale for Pol188 use in siliconised pre-filled devices because of the limited air phase, its use in vials warrants caution. This is because poloxamer has been reported to have lot-to-lot variability, specifically exhibiting differences in the surfactant's hydrophobicity.[250] As mentioned earlier, protein-PDMS mixed visible particles have also been observed where Pol188 is employed as a surfactant in liquid parenteral protein formulations stored in contact with the stoppers of glass vial containment systems. This can also be attributed to this surfactant type's higher hydrophilic-lipophilic balance (HLB) value.

Novel surfactants are required to overcome the limitations of those currently available.[251] In terms of interfacial adsorption and stability, Brij® surfactants, notably polyoxyethylene cetyl ether (Brij® 58) and polyoxyethylene lauryl ether (Brij® 35) as well as sugar-based surfactants and cyclodextrins, namely 2-hydroxypropyl-β-cyclodextrin, **Table 2.3**, have been indicated as potential alternatives to polysorbate surfactants for biotherapeutic manufacture and storage.[53,55,56,62,125,252–262] Interestingly, combining cyclodextrins with polysorbates may also provide a route to optimal stabilisation.[263] Additionally, lyso-phosphatidycholine has recently been identified as an alternative to polysorbate surfactants, displaying similar interfacial stabilisation properties.[264] Another promising surfactant, N-myristoyl phenylalanine polyether amine diamide (FM1000), which incorporates a phenylalanine moiety into its structure, has exhibited significantly faster adsorption dynamics at interfaces than traditional surfactants, improving stabilisation against agitation-induced aggregation.[265–267] Research into FM1000's molecular mechanisms highlighted the critical role of its hydrophobic tail length, with the 14-carbon chain proving optimal for reversible protein adsorption and enhanced stability.[268] Furthermore, its stability in downstream processing

steps, e.g., ultrafiltration/diafiltration and its compatibility with parenteral packaging exposed to external stressors suggest its suitability for biotherapeutic production.[269,270]

2.5.3 Other excipients

While surfactants are the predominant class of excipients that can minimise protein adsorption, other excipients (buffers, tonicifer, albumin and bulk stabilisers) also act to inhibit protein-surface interactions, **Table 2.3**.[38,271] There has been an increased focus on excipients like sugars, polyols, and amino acids, which prevent protein adsorption due to their ability to suppress electrostatic interactions between the protein and interface. Additionally, they can stabilise the protein by preferential exclusion or binding. Disruption of the protein's hydration layer can impact its adsorption to hydrophilic and hydrophobic surfaces, thus altering its adsorption behaviour. Arginine is effective in preventing aggregation and the binding of proteins to surfaces.[49] Moreover, arginine has been shown to displace adsorbed proteins and slow the kinetics of irreversible adsorption.[57,272] The prevailing theory is that arginine can bind to the surface of a protein and suppress protein-surface interactions by hindering hydrophobic and electrostatic interactions.[273] Arginine is proposed to adhere to the protein's aromatic residues implicated in surface adsorption.[57] A key limitation to arginine's application is the high molar concentration required to see appreciable effects. Moreover, the choice of counterion is also essential, as arginine HCl has been reported to destabilise proteins.[274] Arginine aspartate or arginine glutamate has been reported to offer superior stabilising effects.[275] Lysine was also explored as an adsorption suppressor and similar anti-adsorption properties were noted, but weaker effects were observed compared to arginine.[57] Glycine was shown to be ineffective because it has no additional side chains/functional groups that could disrupt protein-interface interactions.[57] While not investigated for their adsorption-reducing properties to our knowledge, hydrophobic amino acids such as leucine and valine can lower the interfacial tension at air-liquid interfaces.[58,276] Phenylalanine, has been investigated for freeze-dried formulations, may also display similar properties.[277] They could be viable excipients for protecting proteins from hydrophobic interfaces.[58,276]

Sugars have been investigated in several protein adsorption studies for their potential to reduce adsorption. *Wendorf et al*. probed the effect of trisaccharides, disaccharides, monosaccharides, and 6-carbon polyols on the adsorption behaviour of three model

proteins.[278] As the concentration of sugar increased, the amount of protein adsorption decreased. At equivalent concentrations, the ability of the sugar to reduce adsorption followed the trend where trisaccharides > disaccharides > 6-carbon polyols > monosaccharides. *The authors* proposed that the heat of the solution of amorphous saccharides correlated to the relative protein stability within the formulation and was responsible for reducing surface adsorption. Similar results were seen for trehalose, sucrose, glucose, glycerol, and dextran.[57,279,280] Sugars and amino acids are attractive protein formulation excipients because they can increase the therapeutic protein's conformational and thermal stability and act as an interfacial binding inhibitor.

Albumin is another stabiliser used to prevent the interfacial adsorption of therapeutic proteins. It has been employed as a sacrificial protein in commercial formulations to coat primary packaging to inhibit the adsorption of the therapeutic moiety.[38,271] Protein-albumin interactions have been reported to occur and alter the bioactivity of the active protein.[281] Albumin's use has declined owing to concern over disease transmission. However, the development of recombinant albumin, helped address these concerns, and consequently it has regained attention as an excipient.[282]

Buffers can also help preserve a protein's stability, and buffer choice should be considered in conjunction with the protein's physicochemical properties, e.g., IEP.[50] Buffers are primarily responsible for maintaining solution pH and are usually formulated with tonicifiers such as NaCl or KCl to maintain ionic strength.[1] Buffer type, pH, and ionic strength greatly influence protein adsorption as they can alter the charge of the protein and the substrate depending on their respective IEPs. Different buffers can have varying ionic strengths and affinities for proteins and surfaces, affecting protein interactions with solid interfaces. Adding tonicity agents to buffered solutions adds another layer of complexity to adsorption behaviour. *Mathes* and *Frieß* demonstrated that IgG1 adsorption to Fiolax® Type 1 borosilicate glass vials depended on formulation pH and ionic strength and, to some degree, on the tonicifer type.[114] Adsorption was highest at pH 4, and it steadily decreased with increasing pH due to the change in the zeta potential of both the protein and the glass surface. At pH 7.2 and pH 8.6, an increase in the NaCl concentration led to a decrease in the amount of IgG adsorbed owing to a screening effect from the Cl^- ions. In contrast, at pH 4.0, adsorption increased because of increased hydrophobic interactions between IgG and the surface caused by the NaCl.

Substitution of sodium sulfate for NaCl produced similar adsorption profiles at pH 7.2 and 8.6. However, at pH 4.0, sodium sulfate led to a more significant increase in adsorption. Similar ion effects have been noted for siliconised surfaces and polyolefin surfaces.[54,91,283] Some buffers can considerably affect therapeutic protein stability by altering the formulation pH when exposed to thermal stress, such as freezing.[78,284] Therefore, choosing the correct salts based on the intended use and required solution pH is paramount to minimise the effect on protein adsorption and stability.

Table 2.3: Excipients, mechanisms for reducing protein adsorption, advantages and critical considerations.

Excipient	Mechanism	Advantages	Considerations
Surfactants	• Compete with proteins for space at the interface • Form complexes with proteins to reduce adsorption • Displace proteins from the interface • Alter the surface properties, e.g., lower surface energy, steric barrier	• Highly effective at preventing adsorption • Can desorb proteins from interfaces • Compatible with a range of solution conditions • Low concentration required • Can increase protein stability and solubility • Effective for a range of interfaces	• Chemical instability (hydrolysis, oxidation)[125,240,243,285] • Varying efficiency based on buffer, pH, ionic strength and interface[54,62,236] • Can degrade or be degraded by siliconised surfaces[216,248,286] • Require high HLB value to be fully effective[64]
Cyclodextrins	• Form inclusion complexes with proteins • Compete with proteins for space at the interface	• Enhance thermal and conformational stability • Effective in a wide range of solution conditions	• Potential for interactions with other excipients • Weak interfacial stabiliser[287] • Some derivatives can be destabilising[56] • May be more effective if combined with other excipients[263] • Specific effects can vary and may be limited[257] • Similar degradation concerns to disaccharides and polyols[125]

Amino acids	• Suppresses hydrophobic and electrostatic interactions • Act as molecular crowders • Alter the surface properties, e.g., lower interfacial tension	• Enhances protein stability and solubility • Can desorb proteins from interfaces	• Specific effects can vary and may be limited • High concentrations required[57] • Potential to destabilise protein[274,288] • May require mixtures to be effective[288,289]
Albumin	• Compete with proteins for space at the interface • Can displace adsorbed proteins • Alter the surface properties, e.g., increased hydrophilicity	• Readily adsorbs to surfaces • Functional with a diverse range of surfaces and solution conditions	• Highly unstable with a tendency to self-associate • May form a non-uniform heterogeneous layer • Requires other excipients to maintain stability[290] • Risk of interaction with the therapeutic protein[291–293] • Potential to alter the bioactivity[281]
Disaccharides & Polyols	• Increase protein stability via a protective hydration shell • Increase solution viscosity	• Enhance thermal and conformational stability • Higher viscosity reduces protein mobility in aqueous solution • Functional with a diverse range of solution conditions	• Can be prone to degradation under certain conditions[125] • May require surfactants to provide adequate stabilisation • Limited effectiveness

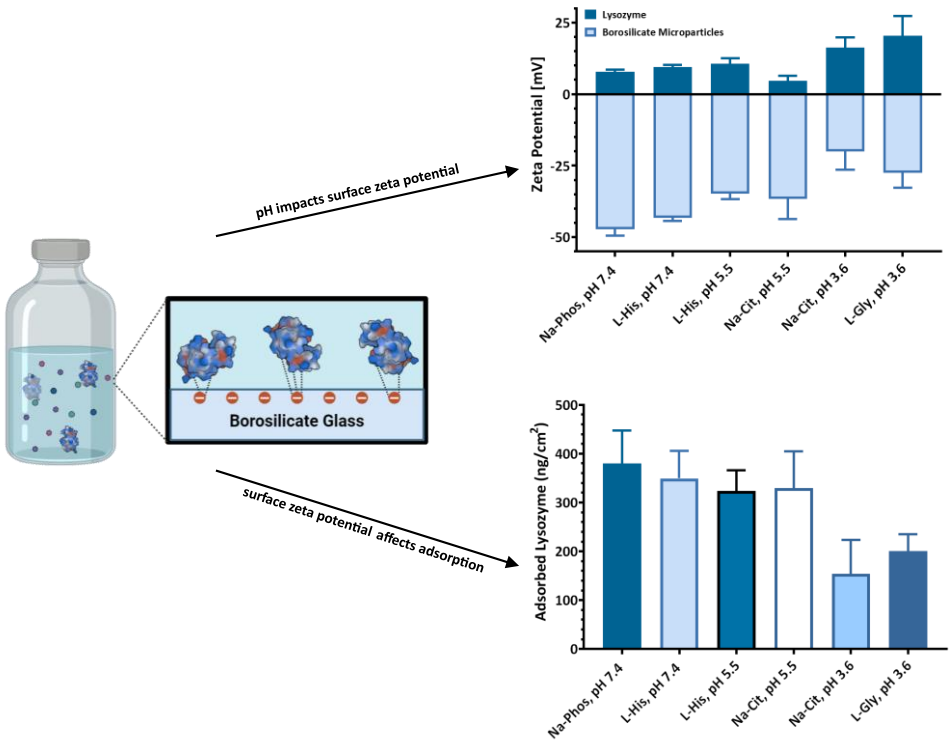
Buffers	• Maintain solution pH • Alter the surface properties, e.g., surface charge, surface hydrophobicity • Can alter protein surface charge or hydrophobicity	• Can reduce adsorption when optimised • Can control the charge imbalance between the protein and the surface • Can stabilise the protein against unfolding and aggregation • Wide range of buffers	• Choice of buffer critical to minimise adverse interactions[54,114,236] • Challenging to balance the chemical properties of the surface with those of the protein • Limited effectiveness • Potential concentration effects Interface dependant
Tonicifiers	• Maintain ionic strength and osmotic pressure of the solution • Can alter protein surface charge or hydrophobicity	• Can screen protein interaction with the interface • Functional in a range of solution environments and surfaces • Wide range of salts	• Incorrect selection or concentration may lead to instability, reduced solubility or increased adsorption[54,114,283] • May conform to Hofmeister series effects • Potential concentration and pH effects • Limited effectiveness • Interface dependant

2.6 Conclusions

Protein adsorption presents significant challenges within the pharmaceutical industry, particularly in the manufacturing and storage of biotherapeutics. The interfacial adsorption of protein molecules can lead to the formation of protein particles, which are implicated in adverse immune responses. This necessitates diligent mitigation strategies throughout the bulk freeze-thaw, formulation/mixing, filtration, fill-finish, transport, and storage stages to avoid increased processing costs, alterations in bioactivity, and a decline in therapeutic quality and efficacy. The complex interplay of factors influencing adsorption behaviour, such as the type of interface and the stresses encountered, must be carefully managed. Further, it must be recognised that excipient-interfacial incompatibility can induce protein instability during the production lifecycle and product shelf-life. Formulation compatibility studies are required to determine the suitability of the different production interfaces with therapeutic protein stability. Moreover, it is critical to assess excipient-packaging interactions before storage as evidence for surfactant-container/closure coating incompatibility, which has been identified as a root cause of particle formation. Opportunity exists for developing and optimising novel filter membranes, fill pumping units, tubing types, packaging materials, surface coatings, and, most importantly, introducing novel excipients. Additionally, there is strong evidence for the rational selection of buffer and tonicifer salts to control adsorption and stability, particularly during storage. It is imperative to design biotherapeutic products to consider the impact of interfacial stress and the interplay between protein stability and formulation. Overall, this review extends the scope of current literature by integrating discussions on formulation approaches, fill-finish unit operations, and primary packaging considerations.

Chapter Three

3. Lysozyme Adsorption to Borosilicate: Influence of Buffer pH and Type



3.1 Abstract

Due to the ionic nature of borosilicate glass, electrostatic interactions between therapeutic proteins and glass packaging materials can readily occur. These interactions can be altered by formulation parameters such as solution pH, ionic strength, and salt choice. Buffers control the pH of protein formulations and contribute to protein stabilisation, but their role in protein-glass interactions has yet to be characterised. This study aims to understand protein adsorption to borosilicate glass by examining the influence of buffer type at pH values from pH 3.6-7.4. Protein stability, concentration, storage conditions, and vial coating on lysozyme adsorption were also evaluated. Changes in solution pH altered the zeta potential of both borosilicate glass and lysozyme, indicating potential differences in electrostatic interactions with buffer pH. Quartz crystal microbalance with dissipation (QCM-D) examined lysozyme adsorption behaviour on the borosilicate surface. At low lysozyme concentrations, layer formation on the surface was thin and rigid, while at high concentrations, it was viscoelastic. QCM-D revealed lysozyme's adsorption insensitivity to buffer type but confirmed sensitivity to buffer pH. More significant adsorption occurred at higher pH due to increased electrostatic interactions. In commercial vials, adsorption was marginally higher in uncoated vials than in SiO_2-coated vials and increased when lysozyme was exposed to higher storage temperatures. The findings show that while buffer pH can alter lysozyme adsorption behaviour in its native form due to electrostatic interactions, higher storage temperatures can lead to more significant adsorption.

3.2 Introduction

Protein adsorption is a spontaneous phenomenon that occurs when a protein encounters an interface. Several factors contribute to adsorption, including solution environment, interfacial properties, and inherent protein characteristics.[27,30,44,294] This phenomenon poses a challenge for therapeutic protein production and storage due to the quantitative loss of therapeutic cargo.[126,178] This loss can be exacerbated if the formulation design and interfaces encountered during the protein's manufacture and storage promote adsorption.[186] Additionally, changes in protein stability due to interfacial adsorption can affect the protein's therapeutic efficacy.[27,123] Therefore, understanding the factors that govern protein adsorption is crucial when developing stable therapeutic protein formulations and selecting suitable materials for their manufacturing and storage.

Investigations into the influence of solution conditions on protein adsorption to borosilicate glass packaging have highlighted the effects of formulation pH and ionic strength.[54,114] pH effects on protein adsorption are well characterised and depend on the formulation pH relative to the protein's IEP and the substrates. At pH values in the region of the protein's IEP, hydrophobic interactions or surface-induced structural changes can occur.[114] Ionic strength has been found to reduce adsorption through charge screening effects, except under acidic pH conditions where the opposite effect may be observed.[114] The choice of salt type for modulating ionic strength can significantly impact adsorption, especially in acidic conditions where salts with high charge screening capacity can increase protein-surface interactions.[114] Similar ion effects have been observed for alternative packaging surfaces such as siliconised and polyolefin materials.[54,91,283] Moreover, pH, ionic strength, and salt type can affect the physical stability of therapeutic proteins, and formulation approaches that destabilise the protein can further induce adsorption to solid interfaces.[295]

Due to the confounding effects of pH, ionic strength, and salt type on protein adsorption, buffer type is crucial in protein formulations. Buffers can play a role in influencing protein adsorption primarily through transient hydrodynamic, hydrophobic, and electrostatic interactions.[50,296] Despite the widely recognised impact of buffer type on protein stability, scope exists to further focus on the relationship between buffer components and protein adsorption to primary packaging.[50] Furthermore, with the growing use of amino acids in

parenteral protein products, exploring the adsorption behaviour of proteins from amino acid-based buffer formulations, particularly with borosilicate glass packaging, is required.[1]

Borosilicate glass possesses numerous properties, making it the ideal choice for packaging liquid parenteral protein products. However, its strong anionic characteristics in aqueous solutions can result in irreversible protein-surface interactions.[29,65,114] To mitigate protein-glass interactions, inert coatings such as SiO_2 may be applied to the glass inner surface. However, these coatings may still acquire a protein film over time.[108] If uncoated, the composition of the vial contact surface may be affected by the formulation composition or storage environment, which can also alter protein adsorption behaviour.

This study examines the influence of buffer type and pH on the adsorption behaviour of the model protein, lysozyme, to borosilicate glass. Lysozyme was chosen for its IEP of approx. pH 10-11, making it weakly cationic in the buffering media commonly used for parenteral formulations.[111,297] This allows for the modelling of the adsorption behaviour of therapeutic proteins such as mAbs to borosilicate glass. mAbs are commonly formulated to be cationic to maintain stability, but their charge can be readily influenced by buffer type.[298] Buffers can cause charge inversion or neutralisation which has the potential to produce an altered adsorption profile especially in the presence of glass-based primary packaging.[114]

To evaluate the impact of buffer type and pH on lysozyme adsorption behaviour, QCM-D was employed. QCM-D can provide information on the mass of adsorbed protein, adsorption kinetics and the properties of the adsorbed protein layer.[299] Mass adsorbed is monitored by observing changes in frequency (ΔF), where a decrease denotes mass gain, and layer properties are measured by an increase in dissipation (ΔD). Additionally, the physical stability of lysozyme in each buffer system was determined, as changes in protein stability can affect its adsorption behaviour.[27,295] Electrostatic and, to a lesser extent, hydrophobic interactions are reported to influence adsorption to glass.[114] Therefore, the zeta potential of lysozyme and borosilicate was evaluated in the buffer media. Finally, the study compared the mass of lysozyme adsorbed to uncoated (Fiolax® Type 1) and SiO_2-coated (Fiolax Type 1 Plus®) borosilicate glass vials under ambient and elevated temperature storage conditions using a high-concentration protein formulation.

3.3 Materials & Methods

3.3.1 Materials

Formulation components, reagents and consumables were purchased from Merck, Ireland unless otherwise stated. SYPRO® orange dye (Invitrogen™) was supplied by ThermoFisher Scientific, Ireland. Clear, non-skirted, 96-well PCR plates and clear thermal seals were purchased from Bio-Rad, Ireland. The borosilicate sensors for QCM-D were purchased from Particular Sciences Ltd., Ireland. SCHOTT 10R/10 mL Fiolax® Type 1 and Fiolax Type 1 Plus® borosilicate vials and 20 mm freeze-dry vial stoppers were obtained from Adelphi Healthcare Packaging, UK.

3.3.2 Methods

Buffer preparation

L-histidine (L-His) and L-glycine (L-Gly), 10 mM buffers, were prepared by dissolving histidine, histidine HCl or glycine in deionised water and adjusting to the relevant pH by addition of 1 M HCl or 1 M NaOH. Sodium phosphate (Na-Phos) and sodium citrate (Na-Cit) 10 mM buffers were prepared by adding sodium phosphate dibasic and sodium phosphate monobasic or citric acid and sodium citrate tribasic dihydrate to deionised water. All buffer solutions were filtered using a 0.45 µm polyvinylidene fluoride filter before use. The pH of all buffers was confirmed using a Jenway 3510 benchtop pH meter (Cole Palmer, Ireland). All protein solutions were filtered through a 0.22 µm polyethersulfone filter. Sample handling was performed in Eppendorf® low adsorption tubes.

Lysozyme and borosilicate characterisation

Lysozyme secondary structure

Far-UV circular dichroism (CD) spectroscopy analysis of lysozyme solutions (1 mg/mL) was conducted using a CD spectrophotometer at 25°C (Chirascan, Applied Photophysics). The CD spectra were measured with a path length of 0.01 cm ranging from 185 nm to 260 nm, bandwidth 1 nm, spectral resolution 1 nm and 1 s/point at 25°C. The average of three spectra was obtained, and a 5-point smoothing algorithm was applied after correction of the solvent

baseline for each independent replicate. Histidine buffered solutions were not analysed due to the strong absorptive behaviour at the wavelength range of interest. All measurements were performed using three independent replicates, n=3. Lysozyme in deionised water was used as a positive control, and a heat stressed aqueous solution of lysozyme (1 mg/mL) was used as a negative control. Heat stressed samples were prepared by heating the sample at 5°C/min from 20-75°C within the instrument. Protein conformational information was quantified using CD neural networking (CDNN) software over the wavelength range of interest, 195-260 nm.

Lysozyme thermal stability

Differential scanning fluorimetry (DSF) was performed using a CFX96™ RT-qPCR (Bio-Rad) instrument and SYPRO® Orange Dye. Lysozyme (1 mg/mL) solutions (48 µL) were dispensed into clear 96-well PCR plates with SYPRO™ orange dye (2 µL), diluted 100-fold and overlaid with a clear thermal seal to prevent evaporation. Fluorescence was measured using the hexachlorofluorescein (HEX) (560-580 nm) filter with an excitation wavelength of 515-535 nm. During the DSF experiment, the temperature was increased from 20-95°C in 0.5°C steps with 10 s hold time for equilibration at each step. Data was collected using three independent replicates, n=3, and lysozyme (1 mg/mL) in deionised water as a positive control. Melt curve determination was performed using Bio-Rad CFX Maestro.

Lysozyme size distribution

Lysozyme (1 mg/mL) solutions were prepared fresh before size exclusion chromatography (SE-HPLC) analysis. Analysis was performed using an Agilent 1200 Series HPLC equipped with a Phenomenex BioSep SEC-s2000 column. Measurements were performed using 20 mM Na-Phos buffer pH 5.9 supplemented with 300 mM NaCl and 10% acetonitrile as the mobile phase at a 1.0 mL/min flow rate. The injection volume was 10 µL, and the total run time was 20 min with a detection wavelength of 280 nm. Data was collected using three independent replicates, n=3, and lysozyme (1 mg/mL) in deionised water was used as a positive control. Data analysis and processing were performed using OpenLabs CDS.

Determination of zeta potential of lysozyme and borosilicate microparticles

The zeta potential of lysozyme (1 mg/mL) in each buffer solution was measured with disposable folded capillary cells (DTS1070) with the minimum required volume of 750 µL using a Zetasizer nano ZS (Malvern Panalytical) operated in protein analysis mode with 60 s delay between measurements. The settings were as follows: protein as material (refractive index 1.450 and absorption 0.001) and water as dispersant (viscosity 0.8872 cP, refractive index 1.330) at 25°C. Three independent replicates, n=3, of each sample type, were analysed in triplicate. Zeta potential measurements were also performed for borosilicate glass suspensions. Borosilicate suspensions were prepared in the following manner. Borosilicate substrates (glass coverslips) were cleaned in an ultrasonic bath with acetone followed by isopropanol. Then, three washes were performed in ultrapure water for 15 minutes each and left to air dry. Borosilicate glass was then ground in a mortar and pestle until a fine powder was obtained. The powder was separated using a molecular sieve (Retsch) with a pore size of 38 µm. The borosilicate particles were divided equally (20 mg) into 2 mL tubes and suspended in 2 mL of each buffer solution. The vials were allowed to rest until the particles sedimented, and the supernatant was collected for zeta potential analysis as described.

Quartz crystal microbalance with dissipation monitoring of lysozyme adsorption

Lysozyme adsorption onto borosilicate sensors was measured using a Q-Sense® E4 QCM-D system. For all measurements, the sensors were washed with 2% sodium dodecyl sulfate, 70% ethanol and deionised water in an ultrasonic bath and then gently dried under nitrogen before mounting on the instrument. Buffer was subsequently passed over all sensors for a further 15 min to aid cleaning, followed by equilibrating for 5 min to establish the baseline frequency and dissipation. Thereafter, lysozyme solutions (1 mg/mL or 25 mg/mL) in the different buffers were introduced separately, perfusing for 15 min. During measurement, ΔF and ΔD were recorded. Sensors were flushed with the corresponding buffer for 10-15 min to determine the reversibility of adsorption. All experiments were conducted at a flow rate of 100 µL/min. Average values of ΔF and ΔD (overtone #7-harmonic 7 above the fundamental note) were reported for analysis as no differences in overtones were obtained. As the ΔD were near zero and the ΔF harmonics overlapped (**Figure S3.1**) at the 1 mg/mL concentration, the mass of lysozyme layers was calculated based on the Sauerbrey equation and

quantification was performed at time=30 min using QTools software. Three independent replicates, n=3, were analysed for each sample type. Dissipation values less than or at $0*10^{-6}$ were excluded from the analysis. The equations for quantification (Eq. 1) and dissipation (Eq. 2) are provided in the Appendix.

Quantitation of lysozyme adsorbed to borosilicate vials

Lysozyme (25 mg/mL) solution in 10 mM histidine buffer pH 6 was aliquoted in 3 mL volumes into the borosilicate vials (Fiolax® Type 1) and borosilicate vials with a chemically bonded SiO_2 coating (Fiolax Type 1 Plus®). This corresponds to an approximate contact surface area of 8.74 cm^2 for the Type 1 and 8.64 cm^2 for the Type 1 Plus® vials. The vials were stored for 7 days at ambient temperature (between 15-25°C) on a shelf out of direct sunlight and in the oven (APOLLO HP50 shaker oven) at 40°C. At the end of the study, the lysozyme solutions were emptied from the vials and thrice aspirated with fresh buffer. An eluting buffer (3 mL), which comprised of phosphate buffered saline (PBS) containing 10 mM Na-Phos, 137 mM NaCl, 2.7 mM KCl with 0.05% v/v PS20, was added to the vials and adsorbed lysozyme eluted over 15 min in an ultrasonic bath. Lysozyme content in the eluted samples was measured by RP-HPLC using a Poroshell 300SB-C8 column on an Agilent 1120 Compact LC using a 5 µL injection volume and a detection wavelength of 280 nm. Chromatographic analysis was performed using water with 0.1% trifluoroacetic acid (Mobile Phase A) and acetonitrile with 0.07% trifluoroacetic acid (Mobile Phase B) using a linear gradient of 10-100% B over 3 min at 70°C. Data was collected using three independent replicates, n=3. Data analysis and processing were performed using OpenLabs CDS.

Data process and statistical analysis

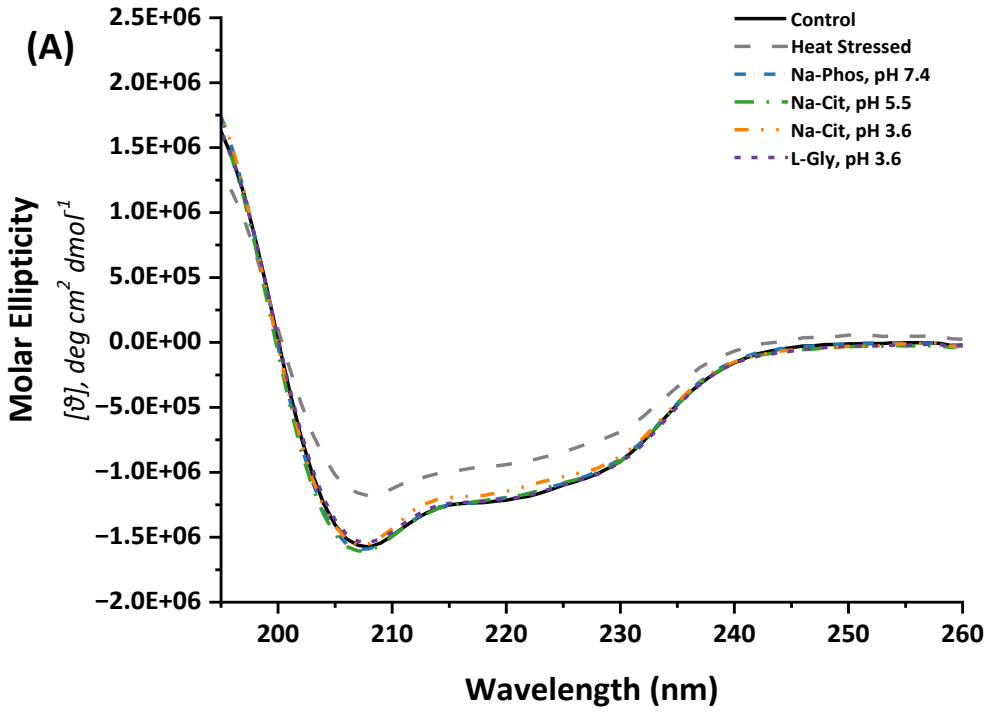
The data was processed and graphed in OriginPro® 2022 version 9 or GraphPad Prism 8®. All statistical analysis was performed using GraphPad Prism 8®. The datasets were analysed by conducting either a one-way or two-way ANOVA (alpha threshold = 0.05; C.I = 95%) and Tukey's post-hoc test. Pearson correlation coefficient was also calculated for adsorption measured by QCM-D, thermal stability, and zeta potential data.

3.4 Results

3.4.1 Lysozyme analysis in buffered solutions

Lysozyme secondary structure

Lysozyme's secondary structure was analysed by CD spectroscopy to ascertain any buffer and pH effects on lysozyme conformation, which could alter adsorption behaviour, **Figure 3.1A**. Two minima peaks at 208 nm and 222 nm were observed, characteristic of alpha-helical structures. The spectral results indicated no significant structural changes signifying that lysozyme's structure was stable over the pH range of pH 3.6-7.4 using the buffered systems employed in this study. The heat stressed control of lysozyme in deionised water heated to 75°C displayed a marginal loss of spectral intensity and showed resilience to peak shift, indicating high internal stability. Spectral deconvolution was performed using CDNN, and the percent secondary structure content was measured, **Figure 3.1B**. The buffered lysozyme solutions showed equivalent alpha helix, random coil, and beta content compared to the control, similar to what has been reported for lysozyme in the literature.[110,111,300]



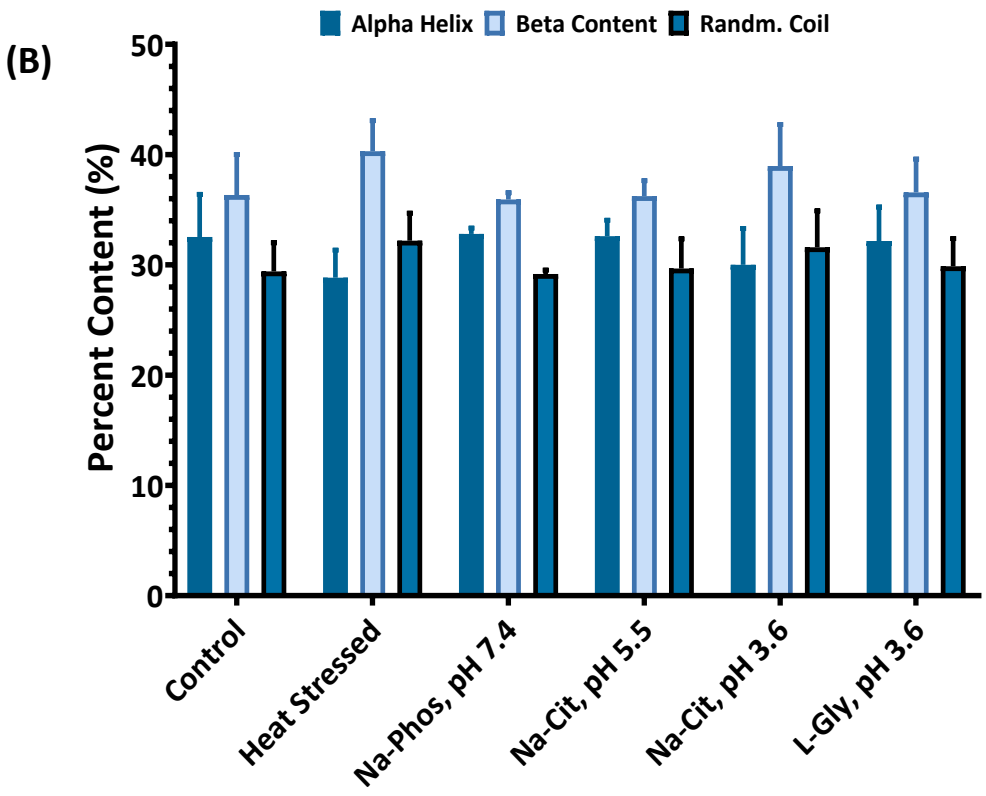


Figure 3.1: Representative CD spectra of buffered lysozyme (1 mg/mL) solutions (**A**). Control represents lysozyme in deionised water, heat stressed refers to lysozyme, which was heated to 75°C. Percent secondary structural content obtained from spectral deconvolution by CDNN (**B**). Three independent samples were analysed, and data in (**B**) represents mean ± SD, n=3.

Lysozyme thermal stability

To probe the impact of buffer and pH on the thermal stability profile of lysozyme in each buffer system, DSF was employed to determine the melt temperature. As seen in **Figure 3.2**, there were differences in lysozyme's melt temperature depending on the solution pH and buffer type. Lysozyme's thermal stability was lowest at pH 7.4 and increased at pH 5.5 and 3.6. Differences between buffer types were observed at each pH value, with the amino acid buffers displaying higher melt temperatures.

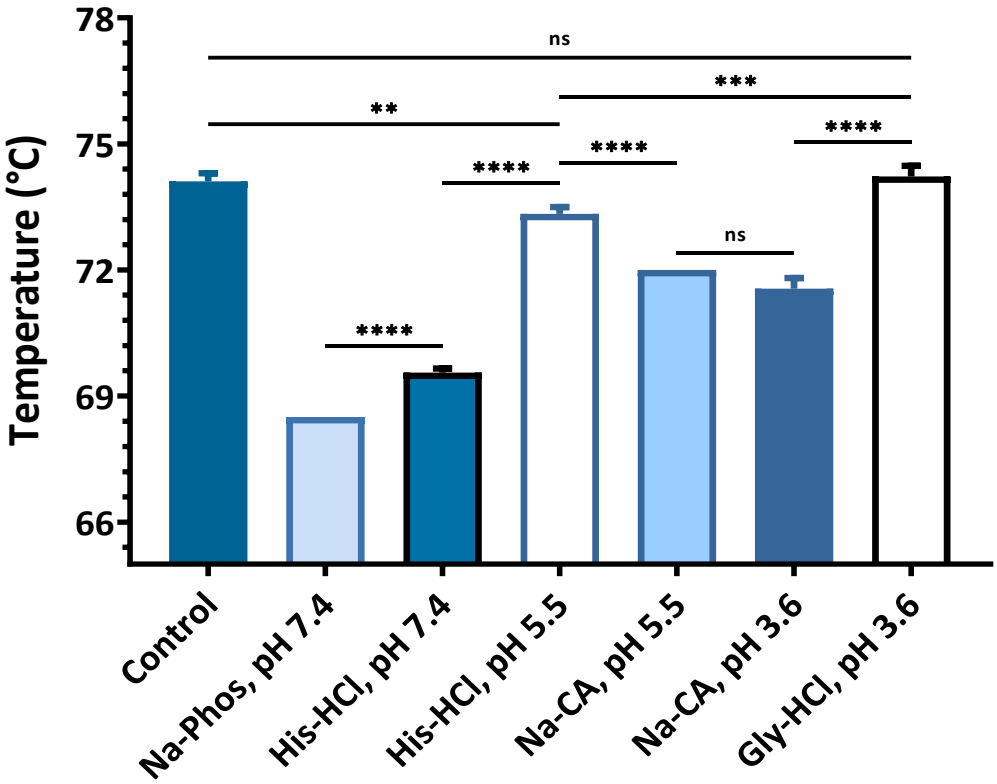
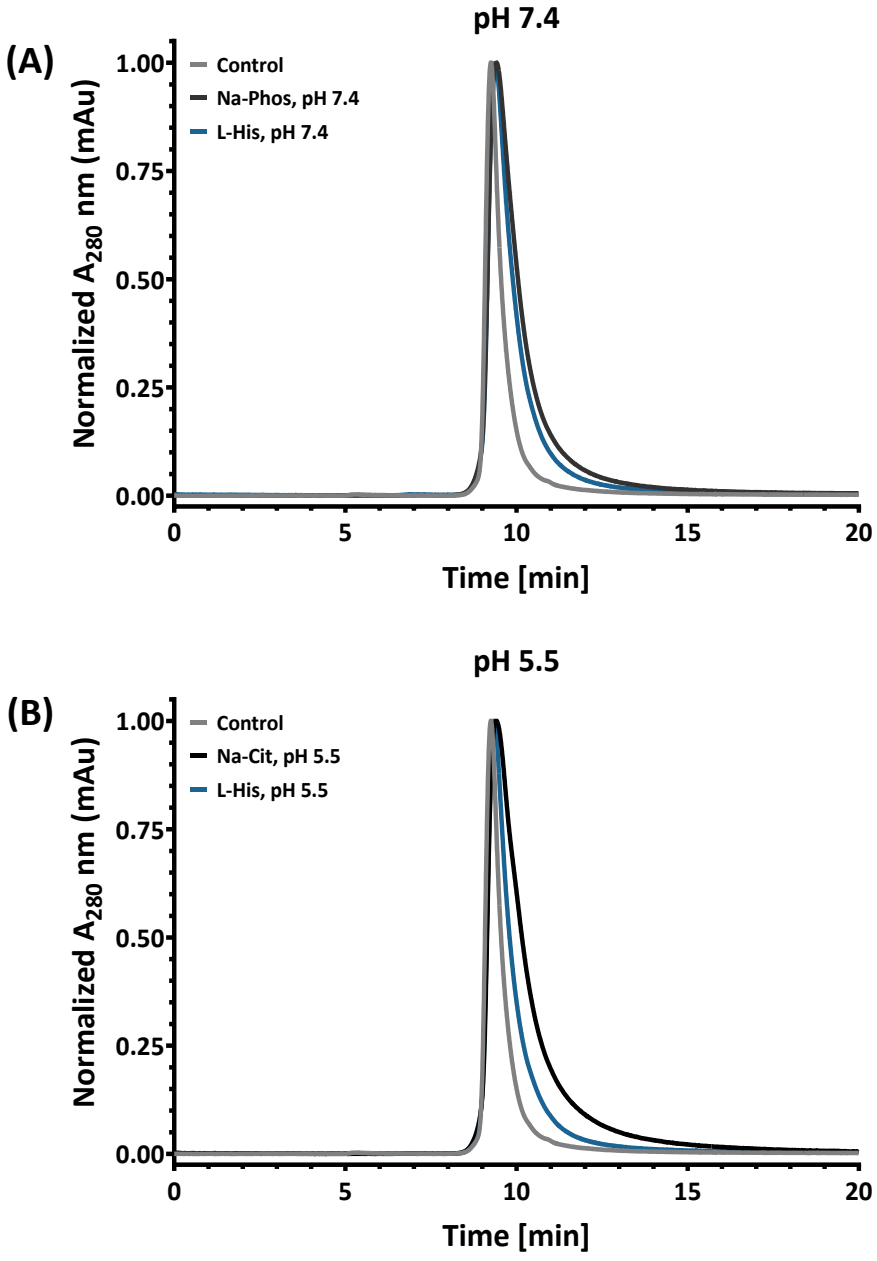


Figure 3.2: Melt temperature of buffered lysozyme (1 mg/mL) solutions. Control represents lysozyme in deionised water. Data represents mean ± SD, n=3. Statistical analysis was conducted using one-way ANOVA with Tukey's post hoc test, **p<0.01, ***p<0.001, ****p<0.0001.

Lysozyme size distribution

The size distribution of lysozyme was evaluated in buffered and control solutions using SE-HPLC. A representative chromatogram for each buffer organised by solution pH is shown in **Figure 3.3**. No changes in lysozyme size distribution were detected in any buffered solutions for the chosen pH range. However, lysozyme displays an extended elution profile for each buffered solution compared to the aqueous control. The altered elution profile may result from the buffers causing increased secondary interactions between the lysozyme and the column, likely due to changes in the protein's hydrodynamic radius or ion exchange effects.



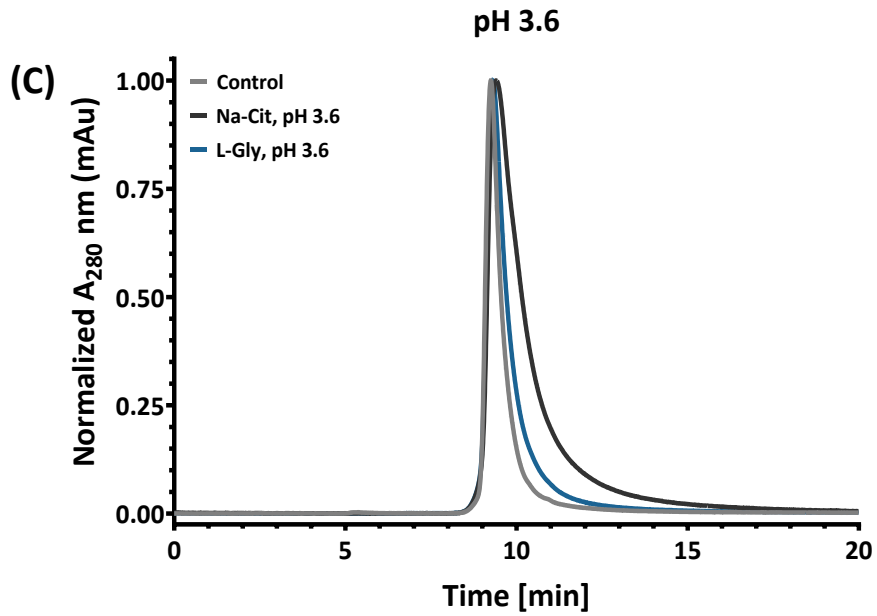


Figure 3.3: Representative chromatograms of buffered lysozyme (1 mg/mL) solutions categorised by pH, pH 7.4 (**A**), pH 5,5 (**B**), pH 3.6 (**C**). Control represents lysozyme in deionised water. Three independent samples, n=3, were evaluated for each buffered solution.

Zeta potential analysis of lysozyme and borosilicate microparticles

The zeta potential of lysozyme and borosilicate in each buffer system was also explored to investigate the impact of buffer type and pH, **Figure 3.4**. As the pH decreases from pH 7.4-3.6, there is a positive increase in lysozyme's zeta potential. The zeta potential of the borosilicate microparticles in each buffer system was also analysed to understand the potential effect of electrostatic interactions on lysozyme adsorption. A trend showing a decrease in the negative zeta potential of borosilicate microparticles suspended in the buffer solution was observed as the pH decreased from pH 7.4-3.6.

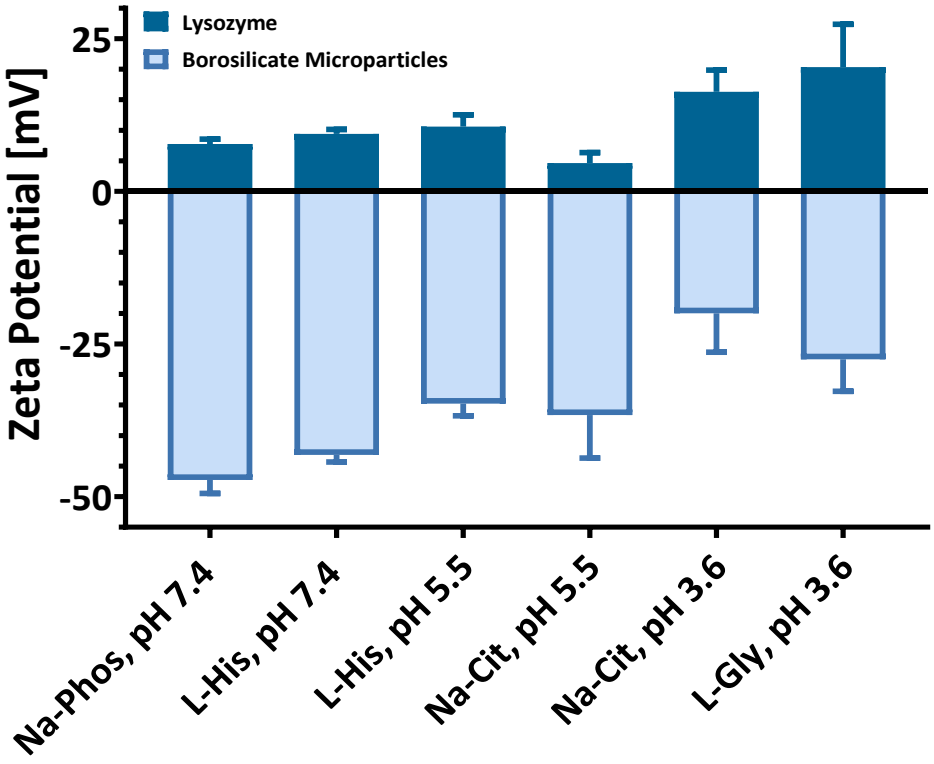


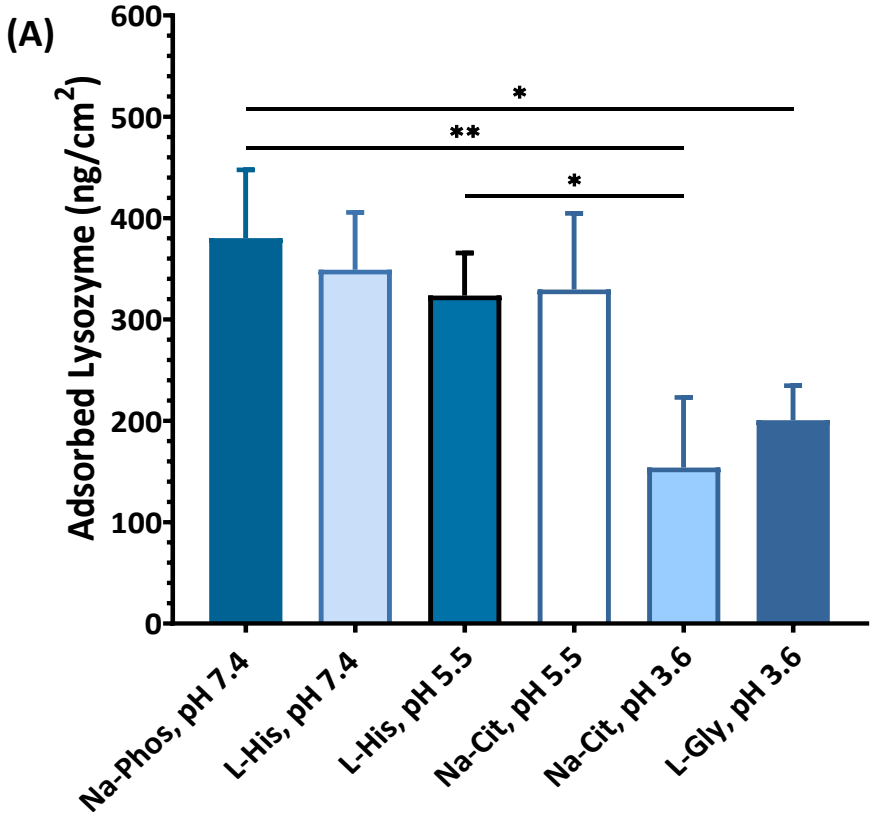
Figure 3.4: Zeta potential determination of buffered lysozyme (1 mg/mL) solutions and buffered borosilicate microparticle suspensions. Data represents mean ± SD, n=3.

3.4.2 Lysozyme adsorption behaviour

QCM-D analysis of lysozyme adsorption

QCM-D was used to monitor the adsorption behaviour of lysozyme to a borosilicate sensor and to assess layer formation *in-situ*. Adsorbed lysozyme (ng/cm^2) calculated by the Sauerbrey equation shows that adsorption was impacted by pH and that there were no significant differences between buffer type at each pH, **Figure 3.5A**. Statistical analysis indicated a difference in adsorption between pH 7.4/5.5 and pH 3.6. The QCM-D analysis also showed that lysozyme adsorption to the borosilicate sensors resulted from strong interactions as minimal protein was desorbed during the buffer rinse step, **Figure 3.5B**, suggesting lysozyme behaved like a solid film.

The relationship between adsorption and both borosilicate (R^2 0.9282) and lysozyme (R^2 0.7268) zeta potential values showed a strong correlation, whereas a weak correlation was observed for lysozyme melt temperature (R^2 0.3170), **Figure S3.2**. Regression analysis of the combined adsorption and zeta potential values at each pH, further indicated that adsorption followed a linear trend (R^2 0.9193) where a reduction in solution pH resulted in a decrease in the surface zeta potential of the borosilicate glass, thus reducing adsorption.



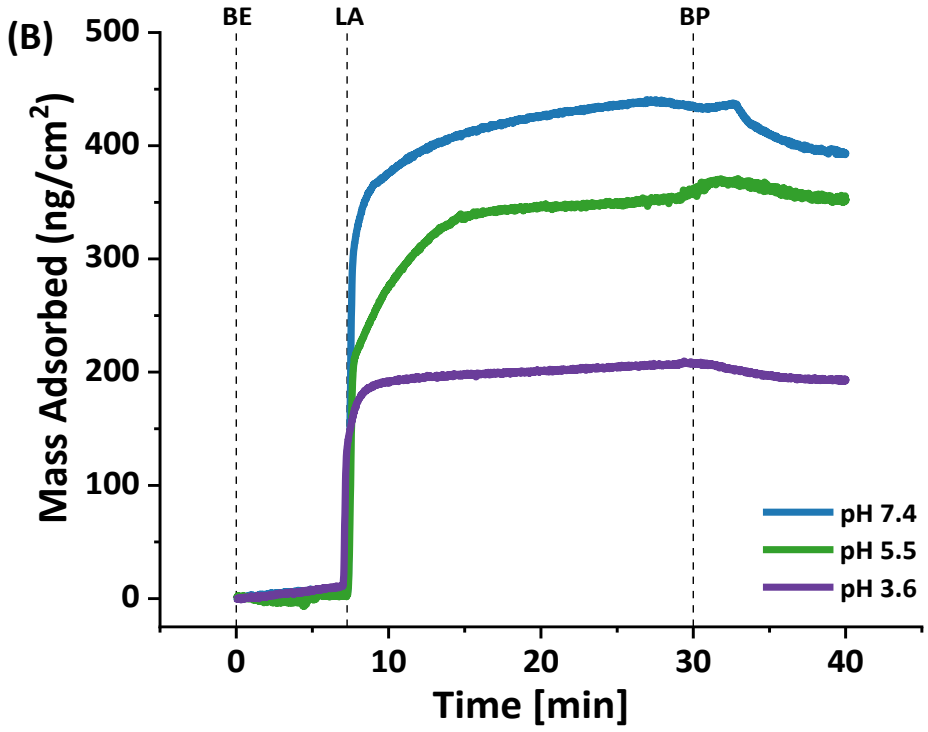


Figure 3.5: Mass of adsorbed lysozyme per unit area (ng/cm^2) from buffered lysozyme (1 mg/mL) solutions quantified by the Sauerbrey equation (**A**) and representative mass plot organised by pH (**B**). Buffers chosen for (**B**) were Na-Phos, pH 7.4, L-His, pH 5.5 and Na-Cit, pH 3.6. Dashed lines indicate the buffer equilibration step (BE), initial lysozyme adsorption during perfusion (LA) and reversibility assessment by buffer perfusion (BP). Data is represented by mean ± SD, n=3. Statistical analysis was conducted using one-way ANOVA with Tukey's post-hoc test, *p<0.05, **p<0.01.

In addition to the mass adsorbed data, the QCM-D also determined the type of layer formation using ΔD, which indicates layer viscoelasticity. In general, negative frequency and positive dissipation values are characteristic of surface binding and layer formation. Further, depending on the dissipation value obtained, it can indicate if the layer is thin and rigid (ΔD~0) or soft and viscoelastic (ΔD>0).[301] All samples produced a ΔD ≤1*10^{-6} for the buffered solutions investigated, signifying that all films made were stiff and relatively inelastic. As seen in **Table 3.1**, buffer composition and pH appear to have a negligible impact on layer formation except for histidine buffer pH 5.5, which is slightly more hydrated. This is supported by the higher D/F ratio value obtained. Owing to the similarity in the overtones for frequency and

dissipation, **Figure S3.1**, and the rigidity of the layer, a partial or full monolayer likely formed on the glass surface.

Table 3.1: Frequency and dissipation data determined for lysozyme (1 mg/mL) at time=30 min using QCM-D. Data represents mean ± SD, n=3.

Sample	pH	ΔF	ΔD	D/F	ng/cm^2
Na-Phos	7.4	-21.67 ± 3.87	0.23 ± 0.13	1.06	380.26 ± 67.42
L-His		-19.90 ± 3.27	0.14 ± 0.15	0.70	349.06 ± 56.63
L-His	5.5	-18.45 ± 2.4	0.78 ± 0.23	4.23	323.53 ± 42.08
Na-Cit		-18.79 ± 4.28	0.24 ± 0.27*	1.23	329.52 ± 75.13
Na-Cit	3.6	-8.78 ± 3.95	0.15 ± 0.09	1.71	153.94 ± 69.21
L-Gly		-11.44 ± 1.95	0.22 ± 0.21*	1.92	200.58 ± 34.12

*Denotes n=2 independent replicates

To investigate the influence of protein concentration, lysozyme was formulated at 25 mg/mL in a 10 mM histidine HCl monohydrate buffer at pH 6 and analysis by QCM-D was repeated. Histidine buffer pH 6 was chosen due to its relevance in formulating therapeutic proteins, including monoclonal antibodies.[1,237,238] QCM-D analysis showed a considerable change in frequency (ΔF, -80.44 ± 4.11 Hz), dissipation (ΔD, 9.20 ± 0.47 * 10^{-6}) and D/F ratio (11.44 10^{-8} 1/Hz) for the higher protein concentration (25 mg/mL) compared to the 1 mg/mL lysozyme samples (**Table 3.1**). This indicates that the mass adsorbed and layer viscoelasticity can change as a function of lysozyme concentration.

The ΔF and ΔD profiles of the 25 mg/mL lysozyme solution pH 6 were also compared with the 1 mg/mL lysozyme in histidine buffer pH 5.5, **Figure 3.6**, owing to the negligible buffer composition effects observed within the pH range of pH 5.5-7.4. Interestingly, at the higher concentration, lysozyme adsorption was evidenced to occur through a two-step adsorption process (**Figure S3.3**). The dissipation values for the overtones investigated at the 25 mg/mL concentration were also variable, **Figure S3.3**, suggesting a softer, multilayer adsorption behaviour. After completing the buffer rinse, significantly greater changes in the frequency and dissipation can be observed for the 25 mg/mL solution compared to the 1 mg/mL sample, indicating layer disruption and protein desorption.

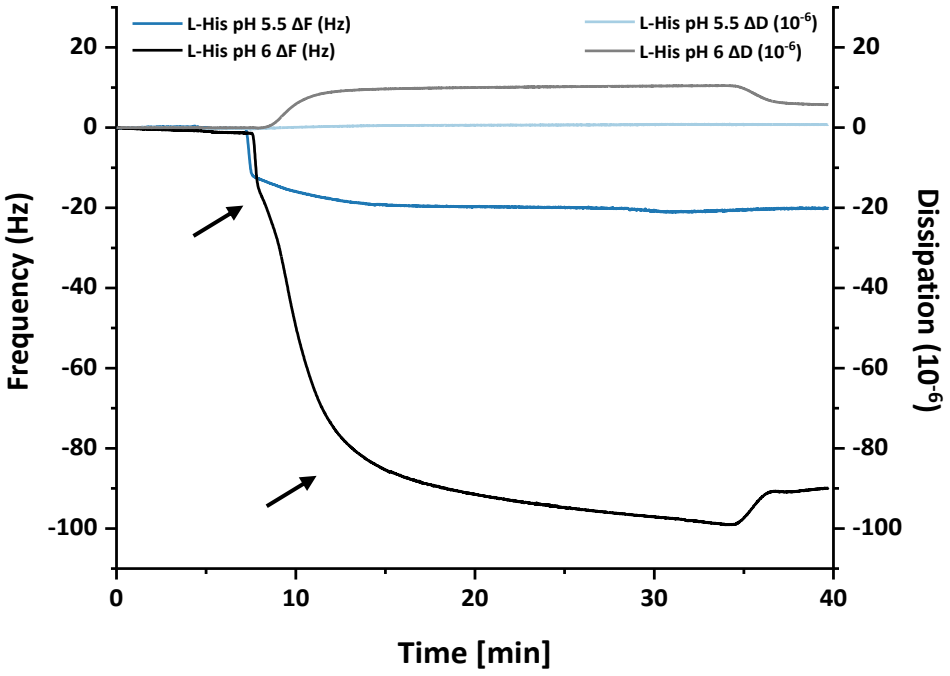


Figure 3.6: Representative frequency and dissipation curves for lysozyme at 25 mg/mL in 10 mM histidine HCl monohydrate, pH 6, and lysozyme at 1 mg/mL in 10 mM L-His, pH 5.5. Frequency (black and dark blue lines) and dissipation (grey and light blue lines) correspond to the left and right y axes, respectively. All measurements were performed using three independent replicates, n=3. Arrows on the 25 mg/mL frequency plot indicate adsorption events.

Lysozyme adsorption to pharmaceutical borosilicate vials

Lysozyme adsorption to pharmaceutical vial containers was evaluated in 10 mM histidine buffer at pH 6 at 25 mg/mL. Uncoated (Fiolax® Type 1) and SiO_2-coated vials (Fiolax Type 1 Plus®) were utilised to assess the impact of vial surface composition on lysozyme-container interactions. The effect of storage temperature, ambient (15-20°C) and thermal stress (40°C) on lysozyme adsorption was also investigated over a 7-day storage period. At ambient temperature, adsorbed lysozyme on Fiolax® Type 1 vials was higher and more variable than the SiO_2-coated vials. The increased storage temperature resulted in a significant increase in adsorption for the Fiolax® Type 1 vials. However, the increase in the SiO_2-coated vials was not significant. The percent of adsorbed lysozyme was also calculated, **Figure 3.7**, indicating mass loss to adsorption is below 0.1% of the total protein formulation.

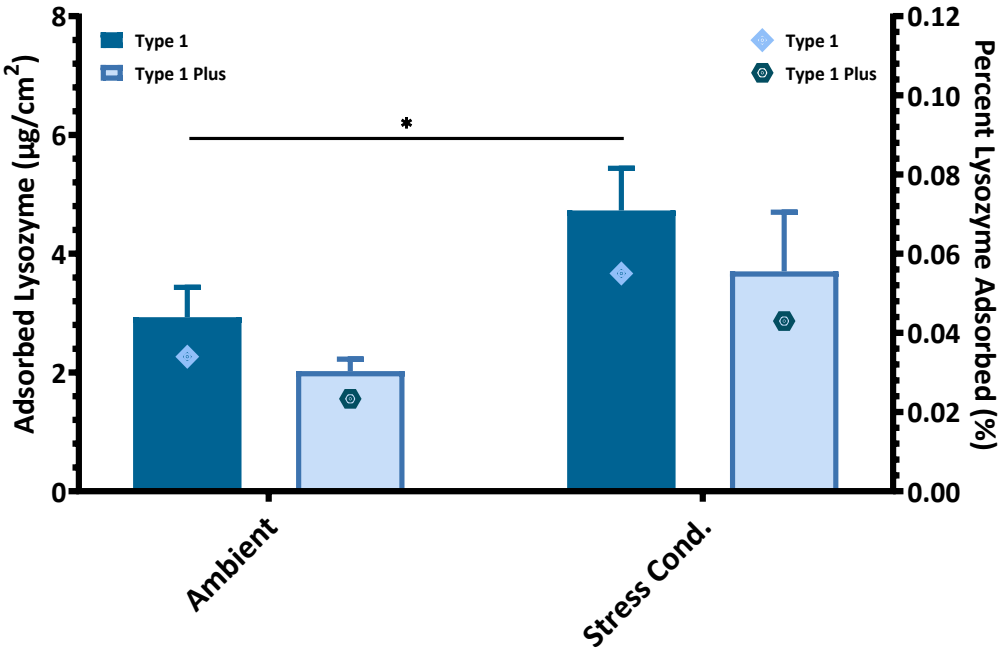


Figure 3.7: Impact of glass type and storage conditions on lysozyme (25 mg/mL) adsorption expressed as adsorption per unit area (µg/cm^2) to commercial primary packaging vials. Mass adsorbed (blue bars) and percent adsorbed (blue diamonds and hexagons) correspond to the left and right y axes, respectively. The data shown is mean ± SD, n=3. Statistical analysis was conducted using two-way ANOVA with Tukey's post-hoc test, $^*p<0.05$.

3.5 Discussion

As previously reported, protein-borosilicate interactions can occur predominantly via electrostatic interactions.[54,114] Therefore, the excipient choice for protein formulations can alter this interaction. In this study, we examined the adsorption behaviour of lysozyme in different buffered solutions to ascertain how buffer composition influenced lysozyme adsorption to borosilicate using QCM-D. In advance of these studies, the effect of the different buffers on lysozyme's physical stability was investigated because any change in protein stability due to the solution environment or in the preparation of the proteins solutions can result in altered protein adsorption behaviour.[44] No significant changes in the secondary structure were observed across the solution conditions investigated (**Figure 3.1**). However, DSF determined lower thermal stability at pH 7.4 and increased thermal stability in the amino acid buffers (**Figure 3.2**). The lower thermal stability can likely be attributed to the reduced surface zeta potential of the protein, which can cause increased protein-protein interactions in solution and the higher thermal stability in the amino acid buffers can likely be attributed to hydrophobic stabilisationC.[302] A slightly extended elution profile for the citrate buffers was also observed using SE-HPLC but this does not signify a change in the stability (**Figure 3.3**). Overall, lysozyme was identified as a protein with high stability under the conditions investigated.

Lysozyme displayed a net positive zeta potential, increasing between pH 7.4/5.5 and pH 3.6 (**Figure 3.4**). Citrate buffer pH 5.5 deviated from this trend, which can be attributed to lysozyme-citrate binding in aqueous solution, as seen with monoclonal antibodies in a study by *Roberts et al*.[298] The borosilicate's zeta potential was negative and exhibited a reducing trend as the pH was reduced to pH 3.6 (**Figure 3.4**). This decrease relates to the pH approaching the point of zero charge, which is reportedly below pH 3 for borosilicate.[54,114] The borosilicate zeta potential was highest at pH 7.4 and lowest at pH 3.6, which mirrors the trend for lysozyme adsorption observed with the QCM-D, with more significant adsorption at pH 7.4 compared to pH 3.6 (**Figure 3.5A**). The relationship between zeta potential and lysozyme adsorption suggests that the charge of the substrate and, therefore, electrostatic interactions, as suggested by *Mathes* and *Friess*, are the dominant forces governing protein adsorption to borosilicate glass.[114]

To understand buffer types and pH effects, QCM-D was employed to evaluate protein adsorption to borosilicate and ascertain the protein's layer formation at the interface.[299] The QCM-D data indicated that protein-borosilicate adsorption was predominately irreversible (**Figure 3.5B**) and showed low dissipation energy with overlapping overtones at 1 mg/mL. The dissipation energy indicated a thin, rigid, and non-viscoelastic protein layer at the borosilicate interface (**Table 3.1**). At pH 3.6, owing to the low dissipation energy, frequency values and poor reversibility, lysozyme adsorption on the surface is likely sparse. However, at pH 7.5 and pH 5.5, the lower frequency values would suggest a more dense, rigid film, likely monolayer or potentially sub-monolayer in nature, in agreement with *Nezu et al*. and *Komorek et al*.[110,304] However, it is important to note potential influences from the protein and buffer environment on the dissipation. Buffers can alter the layer stiffness or localise at the sensor surface and the protein may change conformation or orientation when adsorbed on the solid interface.[111,141,304,305] Interestingly, similar to this study, lysozyme's adsorption insensitivity to buffer types has also been shown for other solid surfaces.[306]

Increasing the protein concentration affected not only the adsorbed mass but also the layer formation. Significantly, by increasing the protein concentration 25-fold, the mass of adsorbed lysozyme was considerably increased, and the layer formation was softer and more hydrated and viscoelastic, as evidenced by the increase in dissipation, spreading of the overtones and increase in the D/F ratio (**Figure 3.6**). Adsorption in the high-concentration lysozyme solution also occurred in a two-step process, suggesting multilayer film formation. Multilayer formation would also explain the partial desorption observed during the buffer rinse step, as the shear forces could disrupt lysozyme's self-association. These results agree with an earlier study performed by *Wang et al*. in which similar trends for changes in frequency and dissipation as a function of lysozyme concentration were observed for borosilicate glass using QCM-D.[244] Characterisation of protein layer properties in protein product development is critical because abrasion of protein films can lead to increased particle formation during storage and cause issues with delivery, such as altered flow rate, increased friction, or blockages.[127,148,180,189,196]

A limitation of this study is that the QCM-D analysis was performed over 30 minutes, which is a relatively short duration and does not account for the fact that adsorption can increase as a function of time.[307] Yet, conducting the study for a longer duration would likely

not have yielded significantly different results, given the plateau observed in the frequency curves. Moreover, with the proven robustness of lysozyme and its capacity for rapid film renewal, changes in the dissipation or structural stability of the protein was unlikely to occur under the conditions investigated. However, this study provides information on adsorption behaviour on the initial introduction of the protein solution to a borosilicate surface. QCM-D provides an opportunity to probe protein-surface phenomena *in-situ* and can help inform how proteins will interact with primary packaging materials. QCM-D also considers interfacial water, a significant factor for adsorption, as proteins are generally dispersed in aqueous solutions in parenteral formulations.[35,37] While understanding mass adsorption events and layer formation can inform judicious formulation design, evaluating adsorption with the actual packaging system is required to confirm protein-container compatibility.[299]

Therefore, lysozyme adsorption to vials used for primary packaging was also evaluated in 10 mM histidine buffer pH 6 at a protein concentration of 25 mg/mL (**Figure 3.7**). Uncoated borosilicate vials were initially assessed due to their similarity in composition to the borosilicate sensor. Lysozyme adsorption to SiO_2-coated borosilicate vials was also evaluated to investigate any impact of surface coating on adsorption. SiO_2-coated borosilicate vials have been reported to have adsorption-reducing effects owing to the inert and dense SiO_2 ion-barrier coating.[108] As expected, the estimated protein adsorption was higher for uncoated borosilicate vials than for SiO_2-coated vials. Further, under thermal stress conditions, it was found that adsorption was increased for both vial types, likely due to the protein's accelerated diffusivity in solution at 40°C.[308] However, the increase was only significant for uncoated borosilicate vials. *Schwarzenbach et al*. also reported a decrease in protein adsorption for the SiO_2-coated vials relative to the uncoated vials.[108] Although a limitation of this study is that the conformation of adsorbed lysozyme was not investigated, other reports in the literature have demonstrated that protein-glass interactions do not significantly alter protein conformation owing to the surface hydrophilicity.[29,303] Additionally, the stability of the bulk lysozyme was not studied despite the prolonged exposure (7 days) to elevated temperature conditions as lysozyme can readily refold into its native confirmation once removed from degradation conditions.[309]

While differences in the experimental design exist between the QCM-D and pharmaceutical vial experiments, both studies indicate lysozyme adsorption to borosilicate

glass is minimal. Moreover, the application of an inner SiO_2 coating to pharmaceutical vials can reduce adsorption however, exposure to elevated temperatures can promote lysozyme-packaging interactions. Additionally, DSF revealed that simple high throughput assays can be effective for optimising buffer systems for protein stability and highlighted the superior stabilising efficacy of amino acid buffers over conventional buffer systems. QCM-D analysis proved to be a valuable analytical tool to provide insight into the adsorption kinetics and relative affinities of proteins to solid interfaces when exposed to different solution environments and has significant potential to act as a predictive tool for protein adsorption to primary packaging materials.[299]

3.6 Conclusion

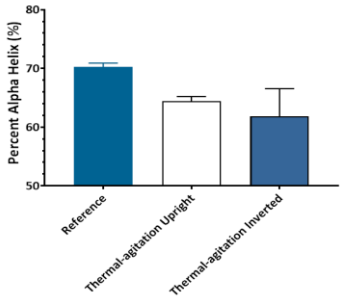
This study found that buffer pH influenced protein adsorption behaviour, but buffer type did not however, adsorption was numerically greater in the amino acid buffer at pH 3.6 Buffer type primarily influenced the hydration of the protein layer and the thermal stability of lysozyme, highlighting the potential risk and benefits of amino acid buffers. Solution pH affected the glass packaging material's zeta potential, indicating an electrostatic mechanism driving adsorption behaviour. Higher protein concentrations notably increased lysozyme adsorption onto the glass sensors, where a change in layer formation was also observed. QCM-D proved helpful in this study as a screening tool to assess protein, buffer, and borosilicate compatibility regarding protein adsorption. Such an approach has a broader potential to screen other formulation components and contact surfaces. The limited impact of buffer type in this study suggests that the predominant factor impacting lysozyme adsorption is the glass zeta potential. Interestingly, protein adsorption to the glass vial packaging revealed marginal differences due to vial surface chemistry and much greater sensitivity to storage conditions driven by elevated temperature. Further investigation encompassing the influence of buffer pH and type on lysozyme adsorption to other primary packaging surfaces, for example, vial stoppers, is warranted before optimisation of buffer type to minimise lysozyme adsorption.

Chapter Four

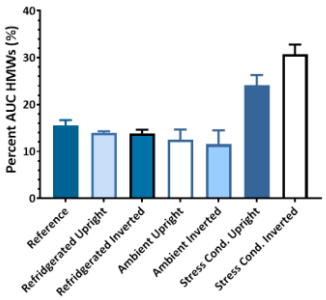
4. Influence of Packaging Interface and Leucine Concentration on BSA Stability



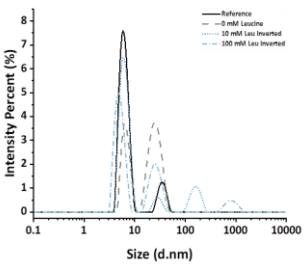
Inverted storage caused greater BSA unfolding



Inverted storage produced more aggregates



Inclusion of leucine resulted in aggregates >100 nm



4.1 Abstract

Significant advances have been made in the formulation of protein therapeutics to enable safe and effective biological medicines to be available to patients however, stability challenges during storage, such as interface-induced aggregation, remain a concern. Amino acids, used as multifunctional excipients, may help counteract this issue. However, there is a lack of understanding regarding the use of hydrophobic amino acids as liquid parenteral protein stabilisers and their compatibility with primary packaging materials. This study aimed to explore the potential of leucine to stabilise the model protein BSA when subjected to thermal agitation conditions (40°C, 150 rpm) in both upright and inverted vial orientations. This was performed as contact with different primary packaging interfaces, such as the vial stopper during vial inversion, can affect protein stability. The study evaluated the effectiveness of leucine in preventing thermal-induced unfolding and aggregation at concentrations ranging from 10-150 mM using CD spectroscopy and dynamic light scattering (DLS). Initial thermal unfolding studies indicated that BSA's native conformation is compromised around 50°C, with unfolding and denaturation causing aggregation above 60°C. BSA stability was evaluated without leucine under different vial storage conditions to establish a model for studying leucine's potential as a stabiliser. This revealed greater unfolding and aggregation occurred on sustained contact with the siliconised vial stopper under thermal agitation conditions. Leucine addition demonstrated variable effects on BSA stability. It did not prevent thermal-induced unfolding but reduced BSA instability when stored upright, as determined by DLS at 50 mM and 100 mM leucine concentrations. Aggregated particles >100 nm were not detected in these formulations. To address BSA's instability when stored inverted, ETFE-coated stoppers were also investigated but proved ineffective. Stabilisation of BSA by the addition of leucine proved inadequate during storage under thermal stress. Vial stopper effects on BSA stability warrant further investigation to evaluate the contribution of BSA adsorption to its aggregation behaviour.

4.2 Introduction

Protein and peptide therapeutics play an important role in the treatment of many clinical conditions.[1,237,238,310] However, a key challenge is maintaining their stability during storage, especially by minimising aggregation arising due to unintended packaging interactions.[311,312] Protein instability can arise due to protein-packaging interactions through protein adsorption to the primary container surface.[127] Adsorption can result in conformational changes in the protein's higher order structure, promoting aggregation and film formation, which, if ruptured, can release particles into solution.[224,313] The interaction between therapeutic protein moieties and packaging interfaces, notably elastomeric closures and siliconised surfaces, is a widely recognised factor contributing to protein instability during storage.[64,89,90,107] Moreover, with increasing evidence implicating formulation components such as surfactants in the degradation of siliconised packaging, it has become essential to account for packaging interfaces in formulation development studies. This is crucial for understanding protein-excipient-packaging interactions and for minimising protein adsorption and particle formation in liquid parenteral protein formulations.

Despite known issues, the most common approach in commercial protein products to reduce adsorption and aggregation is the inclusion of surfactant excipients, such as PS80, PS20, and Pol188.[1] However, in addition to the potential to degrade primary packaging coatings, these surfactants have further limitations.[125] Polysorbates are prone to chemical degradation during storage, and poloxamers have lower interfacial activity and may not effectively protect against adsorption.[51,59,64,240,314] Additionally, in the presence of poloxamer 188 or surfactant-free formulations, protein-induced depletion of siliconised packaging coatings has also been observed and identified as a cause of protein-PDMS particle formation.[89,107] Innovations in packaging materials, such as silicone oil-free containers, offer promising alternatives to mitigate against this particle type.[73,95,315] However, scope remains to investigate alternative surface-active excipients. Recent studies have highlighted a range of novel surfactants, namely Brij® 58, Brij® 35 and FM1000. These surfactants are more effective at stabilising protein formulations at lower concentrations than polysorbate and poloxamer surfactants.[62,252,253,265,267] Yet, despite research into these alternative surfactants, current formulations still predominantly use polysorbate and poloxamer surfactants as stabilisers.

The opportunity exists to explore the application of amino acids as stabilisers against interfacial stress. Several amino acids, such as leucine and arginine, have been studied as therapeutic protein stabilisers to prevent aggregation and for their ability to minimise protein adsorption and interfacial tension.[57,58,273,316] Amino acids are employed in commercial protein formulations as osmoprotective molecules, buffers, thermal stabilisers, tonicifiers, antioxidants and viscosity reduction agents.[1,125,317] Combinations of amino acids may display synergistic effects, and their degradation pathways are well-defined.[11,125,289,318] Hydrophobic amino acids like leucine and charged amino acids like arginine show promise as interfacial stabilisers owing to their zwitterionic, aliphatic and amphiphilic nature.[58,276] However, their ability to protect against interfacial stress induced by the primary packaging system has not been fully explored, and their influence on protein stability in contact with primary packaging interfaces has also received little attention.

Stabilisation of therapeutic proteins by charged amino acids, glycine and proline are well reported.[1] Hydrophobic amino acids are relatively unexplored as excipients for liquid parenteral protein formulations. However, *Szenczi et al*. reported that leucine can offset aggregation by reducing the protein's tendency to self-associate when exposed to thermal-induced unfolding.[316] These effects were observed after 4 weeks at 37°C, and the delay in the aggregation process was postulated to result from hydrophobic stabilisation. *Horn et al*. also identified the suitability of leucine as a bulking agent for lyophilised protein formulations and detected no aggregation after the freeze-drying process.[277] However, neither study evaluated the impact of primary packaging contact surfaces on the stability of the protein in the presence or absence of leucine.

In this study, the potential of leucine to function as a liquid parenteral protein stabiliser when in contact with commercial primary packaging interfaces was evaluated. Leucine was chosen for investigation as stabilisation by hydrophobic, aliphatic amino acids may protect proteins against hydrophobic interface-induced instability. It has also shown some capacity to lower the surface tension of water, similar to that of other hydrophobic amino acids like valine.[58,276] Broader consideration of leucine's stabilising effects has not been investigated, especially when contact with the vial stopper is maintained. This is important because the vial stopper is known to adsorb formulation components onto the rubber surface, posing a protein stability risk during storage.[65,319] To mitigate this, commercial fluoropolymer laminate

films have been developed, however, there are limited studies evaluating the impact of these stopper interfaces on protein stability.

This study explored leucine's potential to stabilise the model protein, BSA, stored under thermal agitation conditions (40°C, 150 rpm) in both upright and inverted vial orientations in SiO_2-coated borosilicate vials capped with either PDMS or ETFE-coated stoppers. Leucine was examined using BSA as a model because of BSA's alpha-helix rich composition. BSA's shape is influenced by the three helical domains which act as the proteins hydrophobic core. These regions are highly susceptible to unfolding, which in turn, leads to aggregation, and are leucine rich zones. Therefore, the inclusion of leucine as a free excipient in solution has the potential to protect these regions from instability through preferential interaction and hydrophobic stabilisation. The ability of leucine to inhibit thermal-induced unfolding and aggregation was evaluated at various concentrations ranging from 10-150 mM. Initially, thermal unfolding studies were performed on BSA to provide some baseline data on the effect of elevated temperature on BSA stability. Then, BSA's conformation and colloidal stability in the absence of leucine were measured under different vial storage orientations and temperatures to establish an appropriate model to investigate leucine's potential to act as a stabiliser. The packaging materials investigated consisted of Fiolax Type 1 Plus® vials, which have an inner SiO_2 coating to reduce adsorption, and bromobutyl rubber stoppers, which have either a PDMS or ETFE-coated surface.[108] CD spectroscopy and DLS were used to monitor protein conformational and colloidal stability, while size exclusion chromatography was employed to quantify aggregation.

4.3 Materials & Methods

4.3.1 Materials

Unless otherwise stated, all chemicals and materials were purchased from Merck, Ireland. The 10R/10 mL Fiolax Type 1 Plus® vials and 20 mm bromobutyl stoppers, which were siliconised with a PDMS coating, were obtained from Adelphi Healthcare Packaging, UK. ETFE laminate film-coated stoppers were obtained from Aptar, France.

4.3.2 Methods

Formulation preparation

10 mM Na-Phos pH 7 was prepared by adding sodium phosphate dibasic and sodium phosphate monobasic to deionised water. All pH measurements were performed using a Jenway 3510 pH meter (Cole Palmer, Ireland). To ascertain the effects of leucine concentration on BSA stability, leucine in the concentration range of 10-150 mM was employed for this study. For leucine-containing solutions, solubilisation of leucine was performed using a mixture of sonication (15 min at 60°C) and vortexing (800 rpm for 60 s). All buffer solutions with and without leucine were filtered using a 0.45 µm polyvinylidene fluoride filter before preparing the BSA formulations. BSA formulations were prepared by adding BSA 50 mg/mL to Na-Phos with and without leucine. Sample handling was performed in Eppendorf® low adsorption tubes.

Formulation storage

All BSA formulations were filtered through a 0.22 µm polyether sulfone filter into Fiolax Type 1 Plus® vials up to a 3 mL fill volume, stoppered and crimp sealed. Samples were then stored for 7 days, either upright or inverted, under the conditions outlined in **Table 4.1**. In the case of ambient conditions, vials were quiescently stored at room temperature on a shelf out of direct sunlight. Thermal agitation samples were subject to shaking conditions of 150 rpm at 40°C, using an APOLLO HP50 orbital shaker oven.

Table 4.1: BSA storage conditions investigated in this study.

Storage Conditions	Storage Details
Reference	Freshly prepared BSA in Na-Phos under ambient conditions
Heat Stressed	Reference heated to 70°C for 15 min
Refrigerated	Storage at 2-8°C
Ambient	Storage at 15-25°C
Thermal agitation	Storage at 40°C shaking at 150 rpm

BSA stability evaluation

Investigation of protein secondary structure using circular dichroism spectroscopy

Far-UV CD spectroscopy measurements of BSA solutions diluted 50-fold to 1 mg/mL in Na-Phos were obtained using a CD spectrophotometer (Chirascan, Applied Photophysics, Leatherhead, UK). The CD spectra were measured with a path length of 0.01 cm in the range 190-260 nm, bandwidth of 1 nm, spectral resolution of 1 nm and 1 s/point. The temperature was held at 25°C. The average of three spectra was obtained, and a 5-point smoothing algorithm was applied after correction of the solvent baseline for each independent replicate. BSA 1 mg/mL prepared fresh in Na-Phos was used as a reference, and heat stressed BSA was used as a negative control. Heat stressed samples were prepared by holding the temperature of the internal cell at 70°C for 15 min before spectral acquisition. Spectral deconvolution was performed using CDNN in the 190-260 nm wavelength range. Thermal unfolding was measured at a single wavelength (222 nm) over an increasing temperature range of 20°C to 90°C at a heating rate of 5°C/min.[320] Data was collected using three independent replicates, n=3, with each replicate analysed in triplicate.

Investigation of protein particle formation using dynamic light scattering

The Z-average hydrodynamic diameter (Z-Avg) and polydispersity index (PDI) of BSA were measured without dilution in disposable 1 mL poly(methyl methacrylate) cuvettes with the minimum required volume of 500 µL in the protein analysis mode. The analysis involved 120 s equilibration, 30 s delay between measurements and a minimum of 13 runs of 10 s using a Zetasizer nano ZS (Malvern Panalytical). The settings were as follows: protein as material

(refractive index 1.450 and absorption 0.001) and water as dispersant (viscosity 0.8872 cP, refractive index 1.330) at 25°C. BSA 50 mg/mL prepared fresh in Na-Phos was used as a reference, and heat stressed samples were prepared by holding the internal cell temperature at 70°C for 15 min before data acquisition. Thermal analysis was performed by increasing the temperature from 45-75°C at a heating rate of 6°C/min in quartz cuvettes. Data was collected using three independent replicates, n=3, with each replicate analysed in duplicate.

Investigation of protein aggregation using size-exclusion chromatography

BSA samples were diluted 50-fold to 1 mg/mL in Na-Phos before injection onto the column for SE-HPLC. Analysis was performed using an Agilent 1120 Compact LC equipped with a UV detector at a detection wavelength of 214 nm and an Agilent Bio-Sec 5 column. The mobile phase consisted of Na-Phos supplemented with 150 mM NaCl and a flow rate of 1.0 mL/min was employed. The injection volume was 5 µL, and the total run time was 25 min. BSA 1 mg/mL prepared fresh in Na-Phos was used as a positive control. Data analysis and processing were performed using OpenLabs CDS.

Data process and statistical analysis

The data was processed and graphed in OriginPro® 2022 version 9 or GraphPad Prism 8®. All statistical analysis was performed using GraphPad Prism 8®. The quantification datasets were analysed by conducting a one or two-way ANOVA (alpha threshold = 0.05; C.I = 95%) and Tukey's post-hoc test. Pearson correlation coefficient was also calculated for percent alpha helix content, Z-Avg, PDI and particle size versus leucine concentration..

4.4 Results

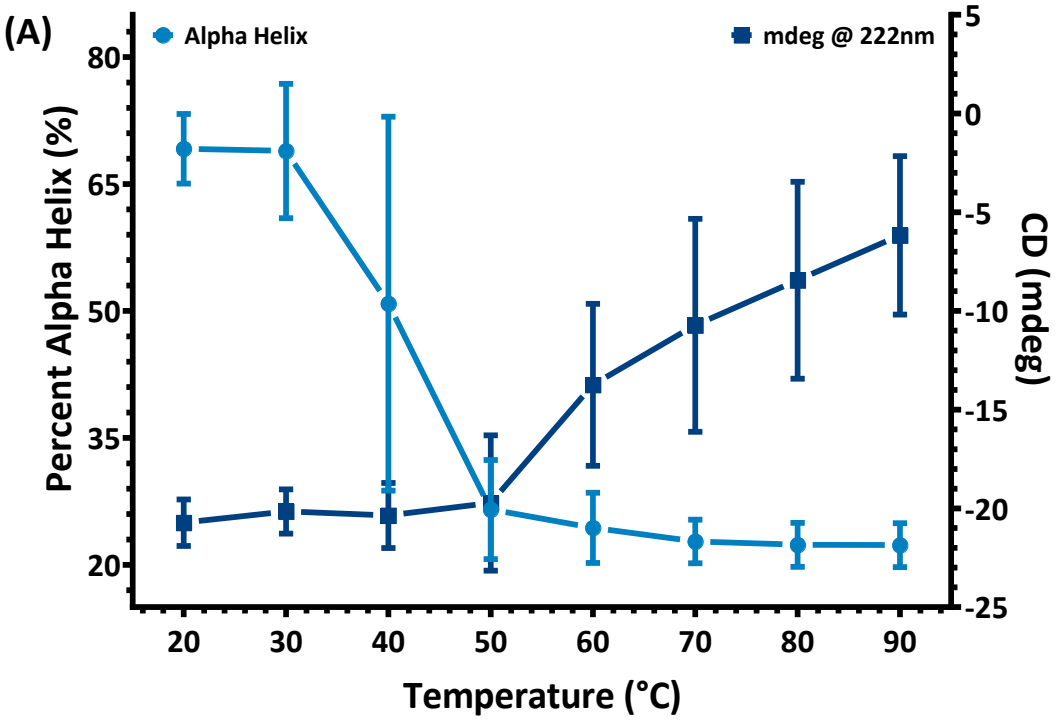
4.4.1 Thermal unfolding studies

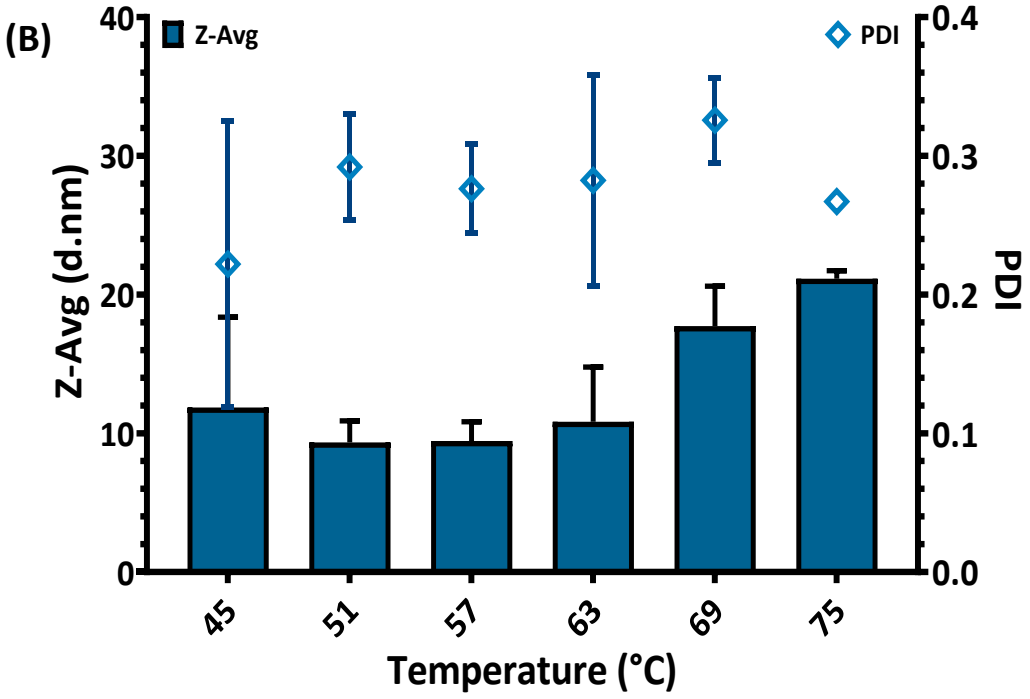
Thermal unfolding studies were performed on the freshly prepared solutions of BSA in 10 mM Na-Phos, pH 7 to provide baseline data on the effect of elevated temperature on BSA stability.

CD spectroscopy and dynamic light scattering

The thermal unfolding properties of BSA were assessed by CD spectroscopy by measuring changes at 222 nm as a function of temperature. This approach has previously been used to determine the melt temperature of BSA.[320] As seen in **Figure 4.1A**, the onset of thermal unfolding begins between 40°C and 50°C, with a significant loss in spectral intensity at 222 nm observed after 50°C. Additionally, a loss in alpha-helical content was observed to occur earlier from 30°C.

Owing to the large change in mdeg from 50-60°C, a thermal ramp study using DLS was performed over a 45-75°C temperature range to determine if BSA unfolding related to BSA aggregation. There were no significant changes in the Z-Avg or PDI from 45-63°C, **Figure 4.1B**. However, an increased Z-Avg after 63°C suggests aggregation driven by protein unfolding has occurred. The intensity plots were examined to better understand the particle sizer distributions. **Figure 4.1C** reveals that BSA's native state is characterised by a bi-modal size distribution with a significant monomeric peak at 8 nm and a prominent secondary peak at approx. 40 nm. With heating, the particle size profile changed to a tri-modal distribution at 45°C with a reduction in the monomeric peak and the appearance of two peaks of reduced intensity at larger particle sizes of approximately 15 nm and 60 nm. Further heating caused an additional decrease in the monomer peak and a more prominent broad peak of about 30 nm in size.


(A)
Alpha Helix
mdeg @ 222nm
Percent Alpha Helix (%)
CD (mdeg)
Temperature (°C)
80
65
50
35
20
5
0
-5
-10
-15
-20
-25
20
30
40
50
60
70
80
90


(B)
Z-Avg
PDI
Z-Avg (d.nm)
PDI
Temperature (°C)
40
30
20
10
0
0.4
0.3
0.2
0.1
0.0
45
51
57
63
69
75

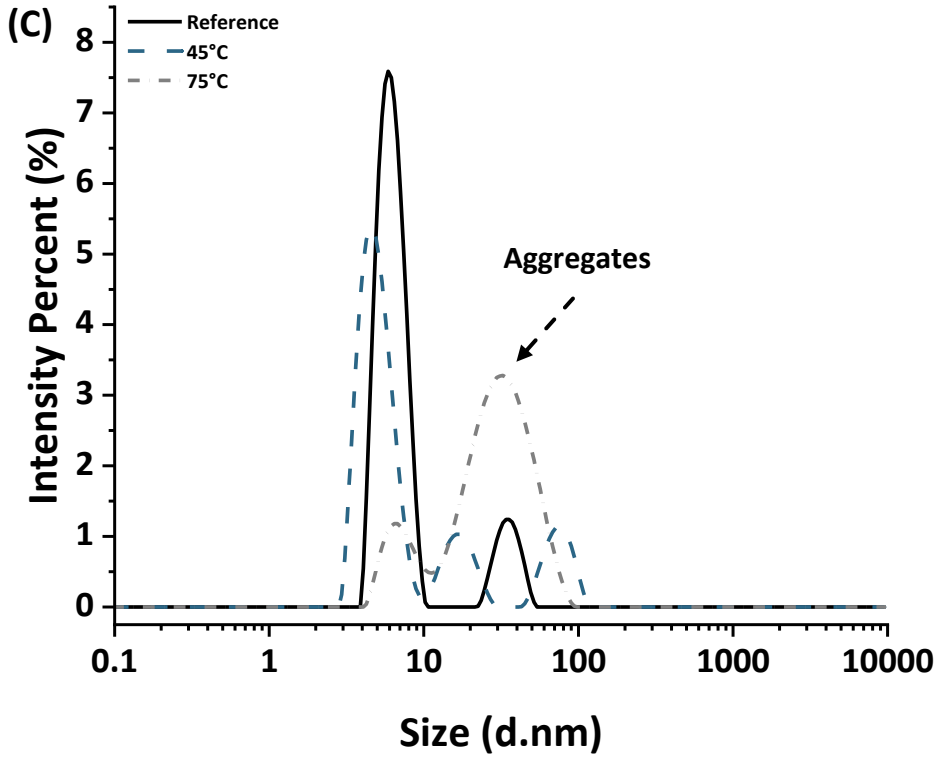


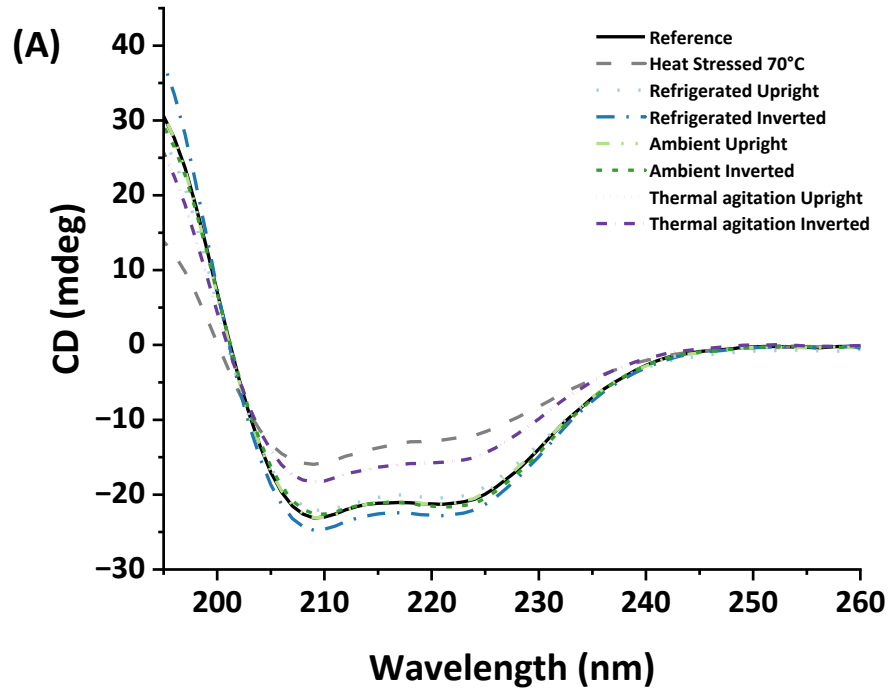
Figure 4.1: Thermal ramp profile of BSA 50 mg/mL in Na-Phos as measured by CD spectroscopy (**A**) and DLS (**B**). For (**A**), the percent alpha helix content (light blue circles) corresponds to the left y-axis, and mdeg intensity at 222 nm (dark blue squares) corresponds to the right y-axis. For CD analysis, the samples were diluted 50-fold to 1 mg/mL in Na-Phos before analysis. Data represents mean ± SD, n=3. For (**B**), Z-Avg (blue bars) and PDI (open blue diamonds) correspond to the left and right axes, respectively. Data represents mean ± SD, n=3. Representative intensity plot of the DLS thermal unfolding studies (**C**).

4.4.2 Impact of vial orientation and storage conditions on the stability of BSA

To address the impact of vial and stopper interfacial contact surfaces on BSA stability, upright and inverted storage orientations were evaluated under different temperature conditions.

CD spectroscopy

CD spectroscopy in the far-UV region was used to analyse BSA's secondary structure to ascertain the vial orientation and storage environment effects on BSA's conformation, **Figure 4.2A**. Two minima peaks at 208 nm and 222 nm were observed, which are characteristic peaks for alpha helices. A loss in spectral intensity indicated unfolding was observed at both vial orientation conditions for the thermal agitation conditions. Spectral deconvolution was performed using CDNN to quantify the percent alpha helix content and showed a 6-8% loss in alpha helix content compared to the reference, **Figure 4.2B**. The reduction in alpha-helical content was considerable for samples stored under thermal agitation conditions but was statistically significant for inverted vial storage only.



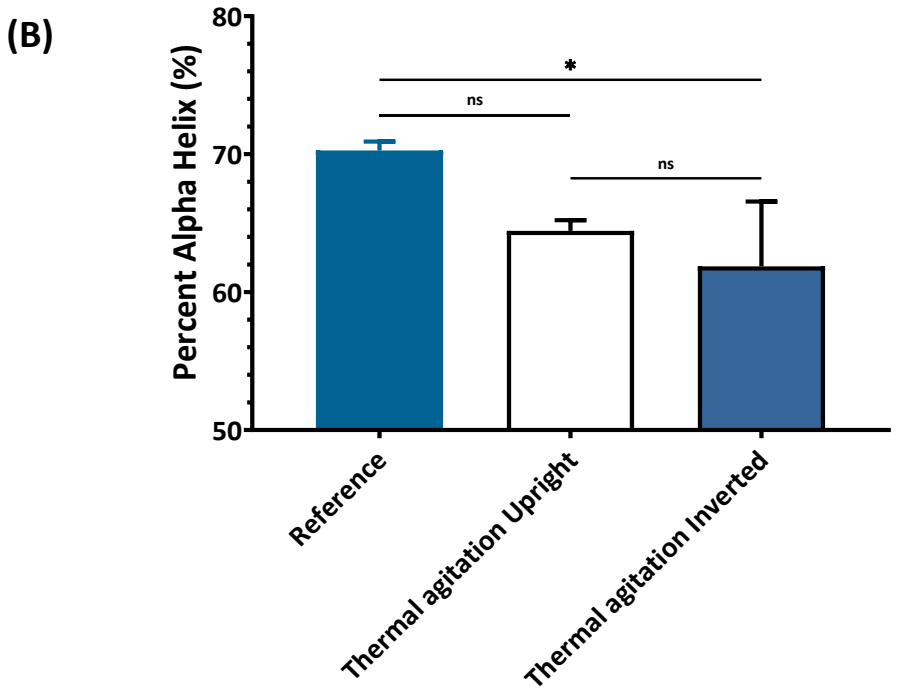
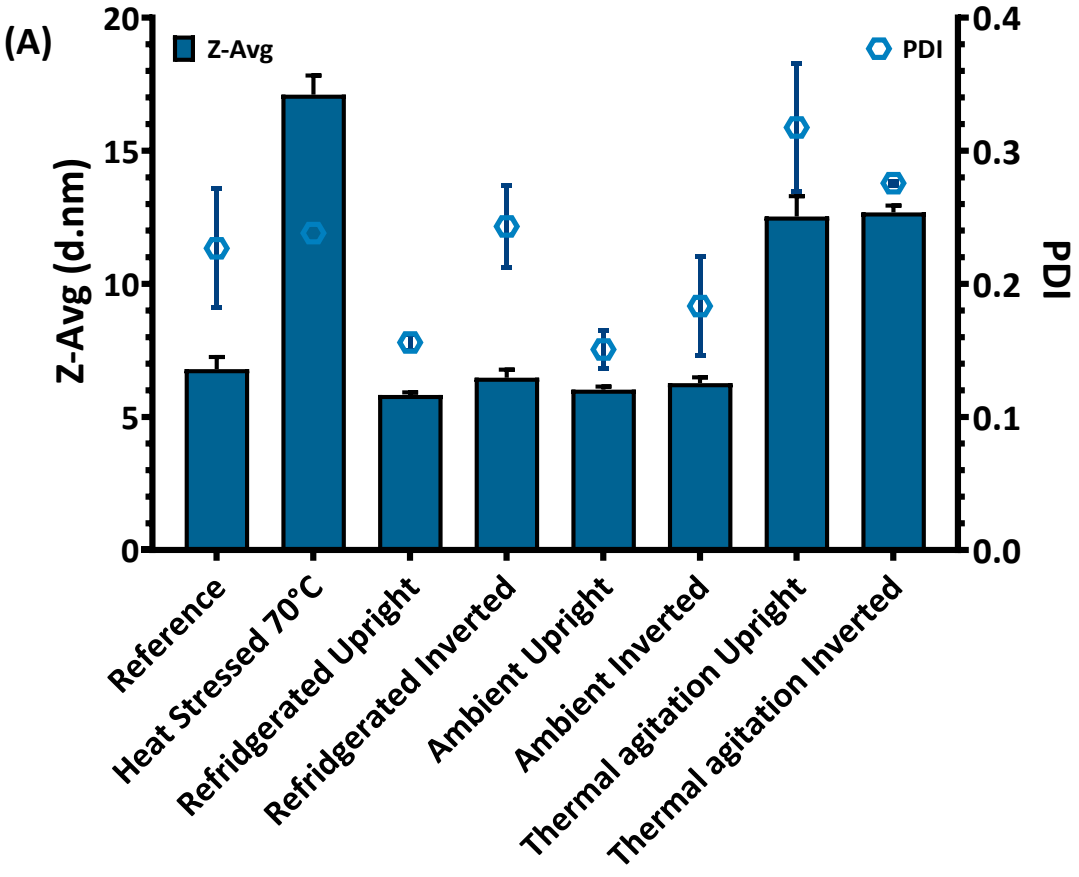


Figure 4.2: Representative CD spectra of BSA 50 mg/mL solutions in Na-Phos stored for 7 days in Fiolax Type 1 Plus® vials under refrigerated, ambient and thermal agitation conditions in both upright and inverted positions (**A**) and percent alpha helix content for reference and thermal agitation samples stored upright and inverted (**B**). Before CD analysis, BSA samples were diluted 50-fold to a final concentration of 1 mg/mL. Three independent samples were evaluated for (**A**), and data represents mean ± SD, n=3, for (**B**). Statistical analysis was conducted using a one-way ANOVA with Tukey's post-hoc test, $^{*}p<0.05$.

Dynamic light scattering

The colloidal stability of BSA was assessed using DLS, where the reference BSA solution displayed a Z-Avg of 6.8 nm and a PDI of 0.23, **Figure 4.3A**. Storage orientation for the refrigerated and ambient conditions did not result in significant changes in the Z-Avg however, the PDI was greater for the refrigerated sample stored under inverted conditions. The thermal agitation condition produced the highest change in Z-Avg (12.5-12.7 nm) and PDI (0.28-0.32), with both storage orientations producing similar effects on BSA's stability. To further understand the changes in stability, the intensity plots, **Figure 4.3B**, were also examined. The intensity plots for the reference show a bimodal distribution, as discussed in section 4.4.1. The samples stored under thermal agitation conditions were similar to the heat stressed negative control in terms of peak 2 size intensity but were more polydisperse in comparison. Additionally, the thermal agitation samples overlay each other and showed a greater reduction in the intensity of the monomeric BSA peak compared to the heat stressed control.



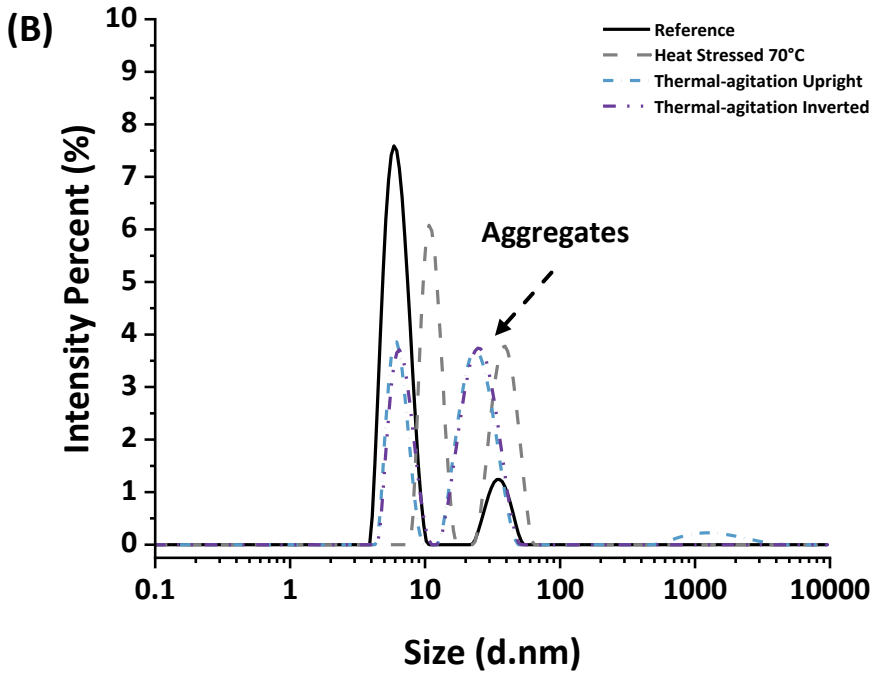
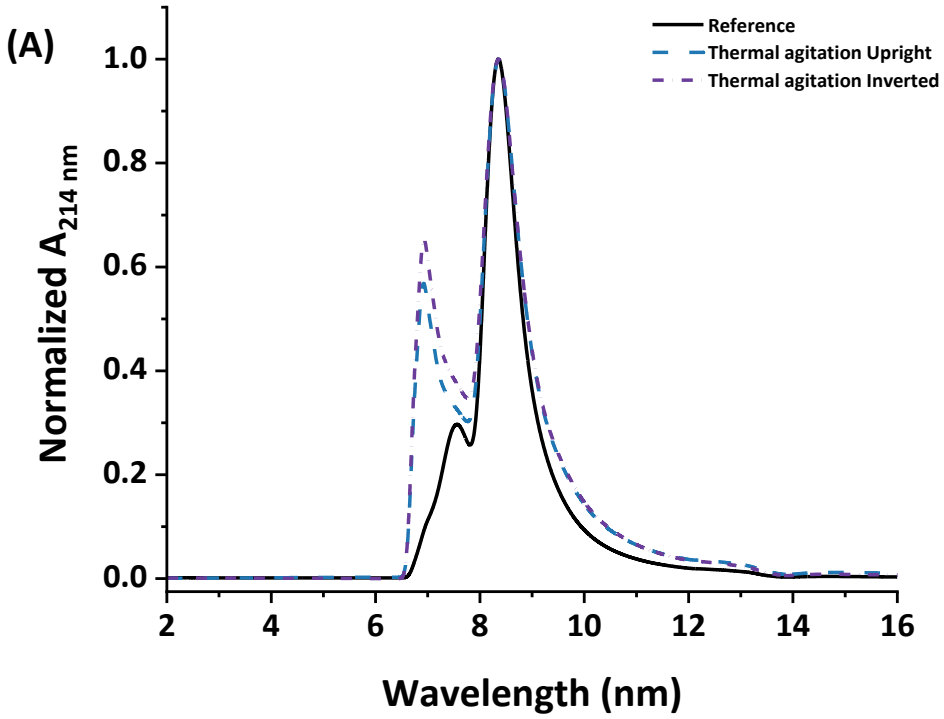


Figure 4.3: Z-Average and PDI (**A**) and representative intensity plot (**B**) of BSA 50 mg/mL solutions after 7 days storage in Fiolax Type 1 Plus® vials in refrigerated, ambient and thermal agitation conditions in both upright and inverted positions. Z-Avg (blue bars) and PDI (open blue hexagons) correspond to the left and right axes, respectively. For (**A**), data represents mean ± SD, n=3.

Size exclusion chromatography

SE-HPLC was used to quantify the size distribution of the BSA to assess the impact of vial orientation and storage conditions on its aggregation. Only under thermal agitation conditions were changes observed in the size distribution analysis, **Figure 4.4A**. Quantifying the percent content of high molecular weight species (HMWs) indicated that samples stored inverted under stress conditions, where contact with a PDMS-coated stopper was sustained, displayed statistically higher levels of HMWs than those stored upright, **Figure 4.4B**. The percent in HMWs increased from 15.5% from the reference to 24.2% and 30.7% for the samples stored upright and inverted under stress conditions, respectively.



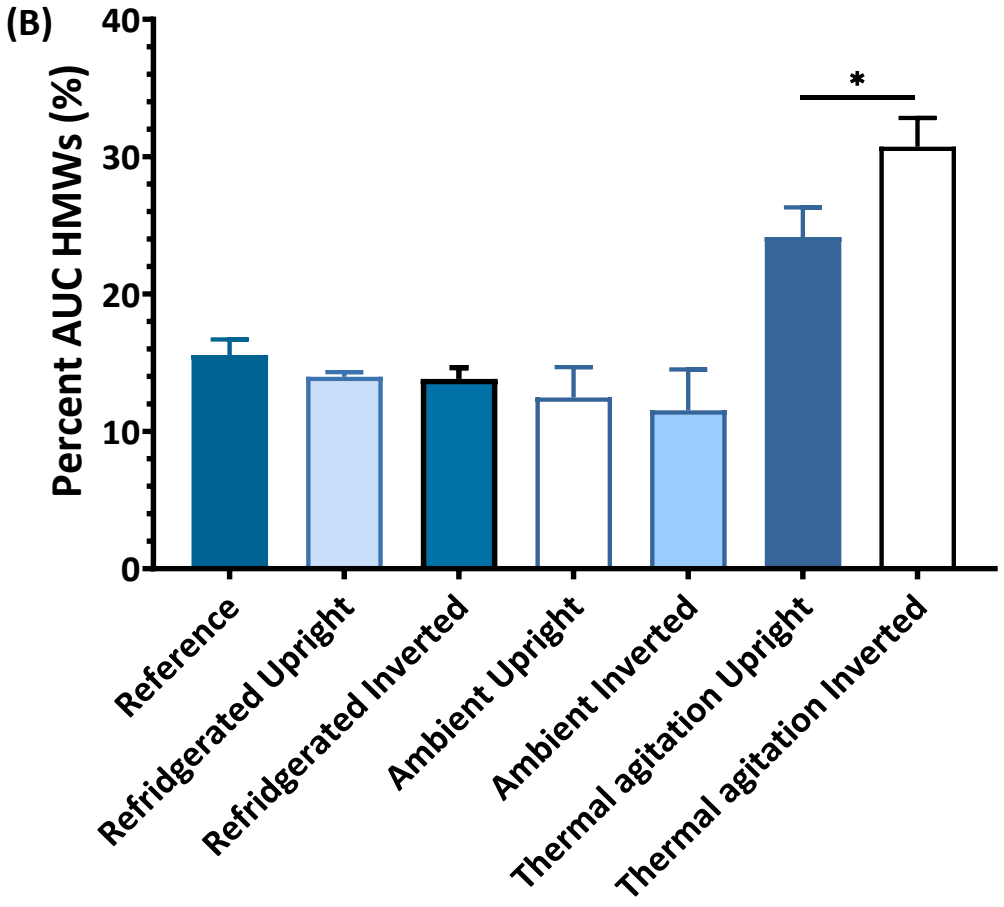


Figure 4.4: Representative size-exclusion chromatogram (**A**) and percent HMWs (**B**) of BSA 50 mg/mL solutions after 7 days storage in Fiolax Type 1 Plus® vials in refrigerated, ambient and thermal agitation conditions in both upright and inverted positions. Before analysis, BSA samples were diluted 50-fold to a final concentration of 1 mg/mL. Data represents mean ± SD, n=3, for (**B**). Statistical analysis was conducted using a one-way ANOVA with Tukey's post-hoc test, $^{*}p<0.05$.

4.4.3 Evaluation of the effect of leucine concentration on BSA stability under thermal agitation conditions

Leucine was included in the formulations over the concentration range of 10-150 mM and investigated for its impact on BSA stability, compared to the buffer-only formulation, when stored upright and inverted under thermal-agitation conditions for 7 days.

CD spectroscopy

Using the percent alpha-helix content as a marker, no statistically significant stabilising effects were observed due to the inclusion of leucine within the range employed, **Figure 4.5**. Further, no statistically significant vial orientation or leucine concentration effects were noted. Interestingly a strong negative correlation (R^2=0.9757) was found between leucine concentration and BSA stability where upright vial orientation was used. While not significant due to the 10mM data point, a similar downward trend in percent alpha helix content from 50-150mM can be seen for inverted vial storage, **Figure S4.1**.

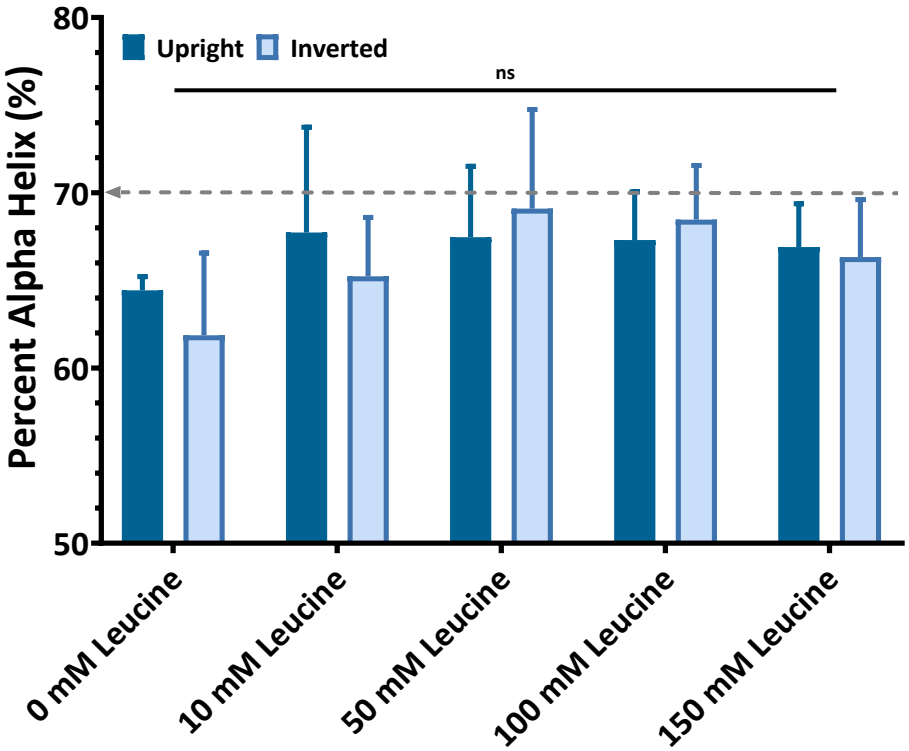
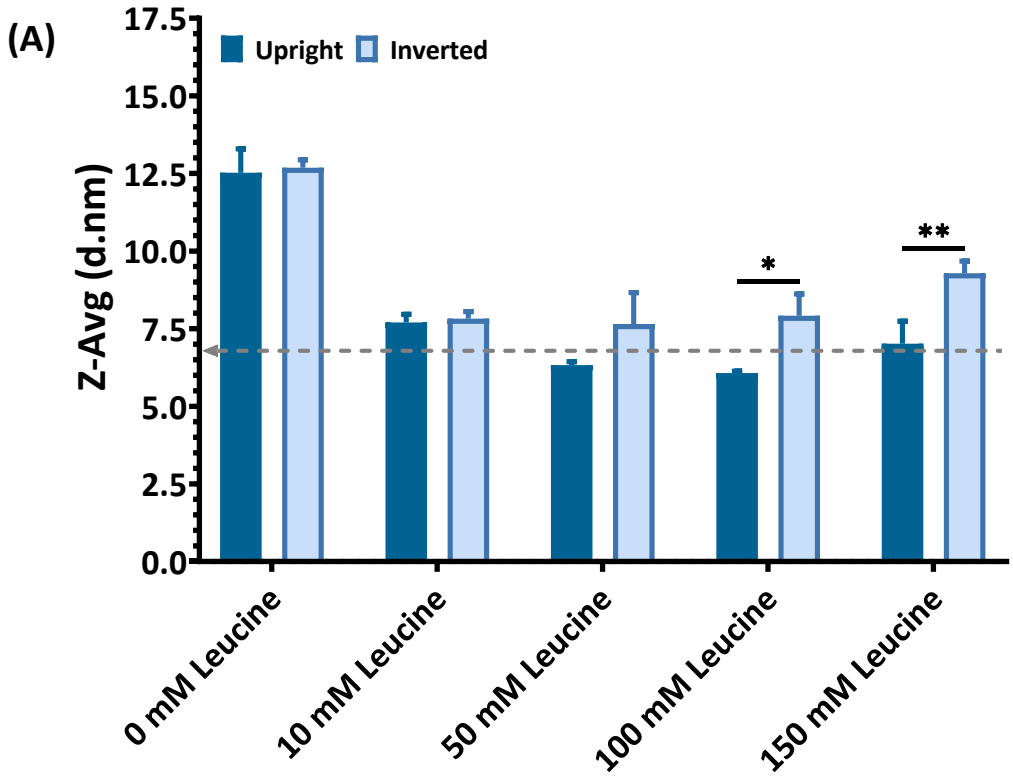


Figure 4.5: Percent alpha helix content determined by CDNN for BSA 50 mg/mL solutions after 7 days storage in Fiolax Type 1 Plus® vials under thermal agitation conditions in both upright

and inverted positions. Before analysis, BSA samples were diluted 50-fold to a final concentration of 1 mg/mL. Data represents mean ± SD, n=3. Grey dashed lines represent the values for the alpha-helical content of BSA prepared fresh in Na-Phos. Statistical analysis was conducted using a two-way ANOVA with Tukey's post-hoc test (α = 0.05).

Dynamic light scattering

The Z-Avg, **Figure 4.6A**, identified that including leucine within the range employed stabilised BSA against thermal agitation-induced aggregation irrespective of vial orientations. However, above 50 mM leucine, there were apparent orientational effects, where inverted storage (PDMS-coated stopper contact) results in a statistically higher Z-Avg than upright storage. A strong correlation (R^2=0.6803) was found for this effect but was not statistically significant, **Figure S4.2**. The PDI, **Figure 4.6B**, showed a similar trend, and there were significantly higher PDI values for inverted vial storage with increasing leucine concentration. This trend was found to be statistically significant, producing a strong correlation (R^2=0.9742) indicating that the greater the concentration of leucine in solution, the greater the heterogeneity in particle formation and size distribution, **Figure S4.2**. However, upright orientation produced the opposite effect but was not statistically significant.



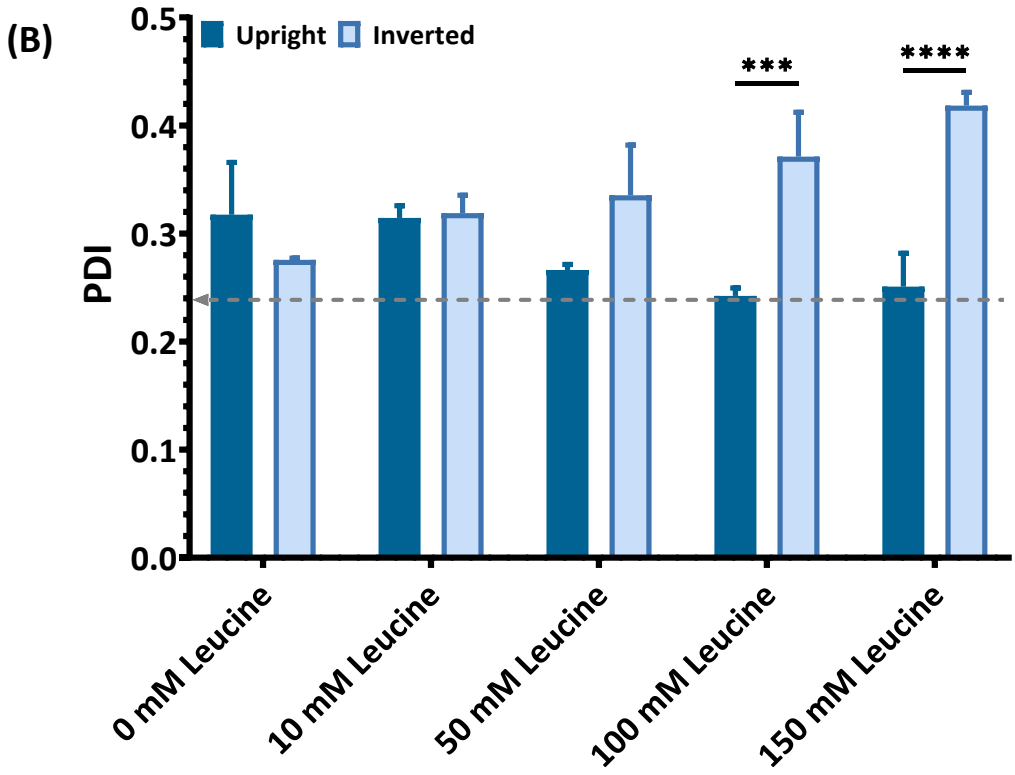
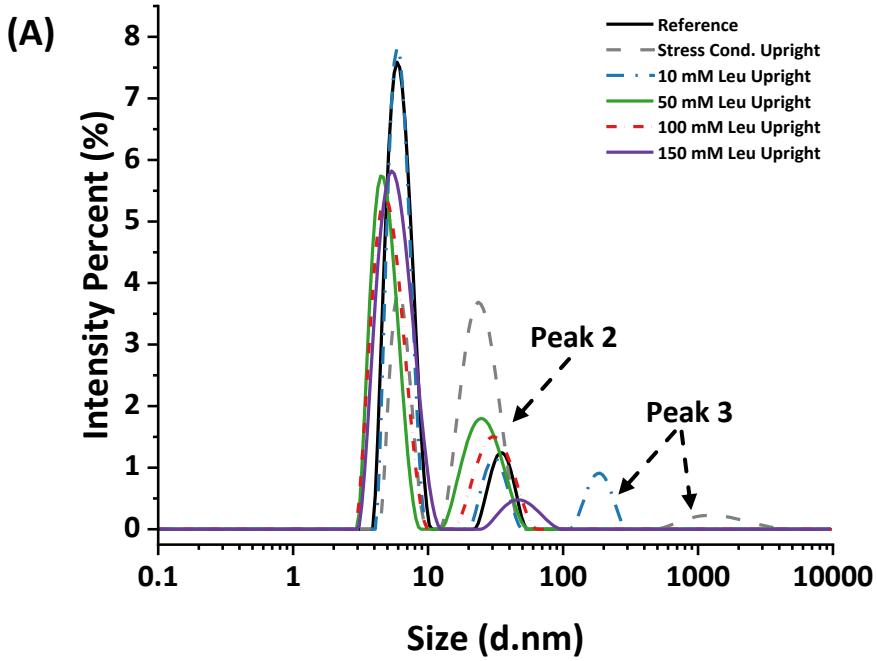
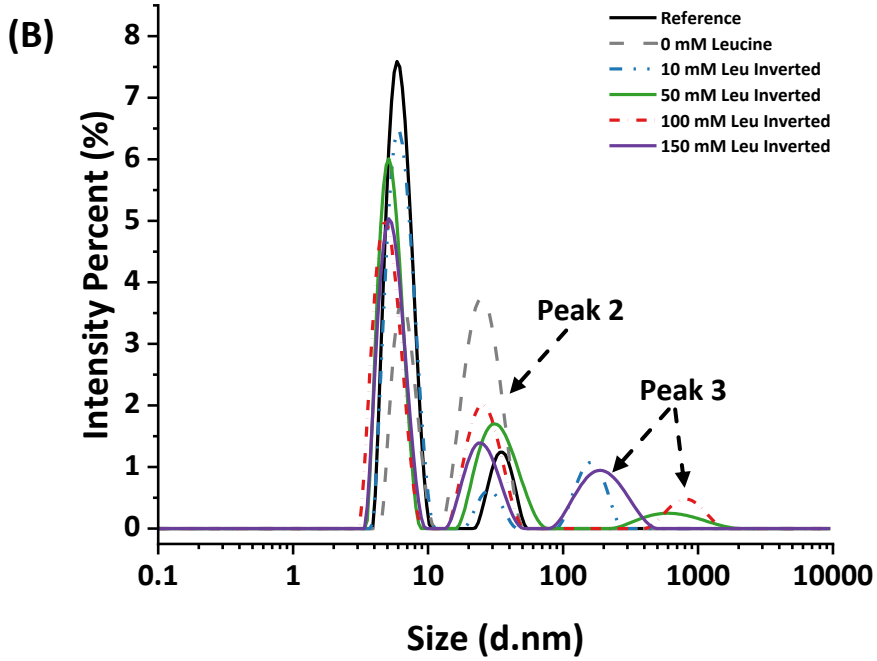


Figure 4.6: Z-Avg (**A**) and PDI (**B**) of BSA 50 mg/mL solutions after 7 days storage in Fiolax Type 1 Plus® vials under thermal agitation conditions in both upright and inverted positions. Data represents mean ± SD, n=3. Grey dashed lines represent values for BSA prepared fresh in Na-Phos. Statistical analysis was conducted using a two-way ANOVA with Tukey's post-hoc test, $^{***}p<0.001$, $^{****}p<0.0001$.

It should be noted that the intensity plots showed a smaller reduction of the monomeric peak for formulations with leucine compared to samples stored without leucine under thermal agitation conditions at both orientations. However, samples showed differences in aggregate profiles. For upright orientation, a bimodal distribution was observed for 50 mM and 100 mM leucine solutions, with 10 mM and 150 mM leucine samples showing a trimodal distribution, **Figure 4.7A**. Irrespective of leucine concentration, all inverted samples showed a trimodal distribution and similar peak polydispersity, **Figure 4.7B**. To enhance the interpretation of the heterogeneity and highlight the variability in the size distribution, the peak particle sizes for upright, **Figure 4.7C**, and inverted, **Figure 47D**, were plotted to highlight trends. Statistically significant differences in the distribution of the particles was not obtained

when BSA was stored upright however, for inverted storage 50mM leucine had a statistically higher particle size distribution.





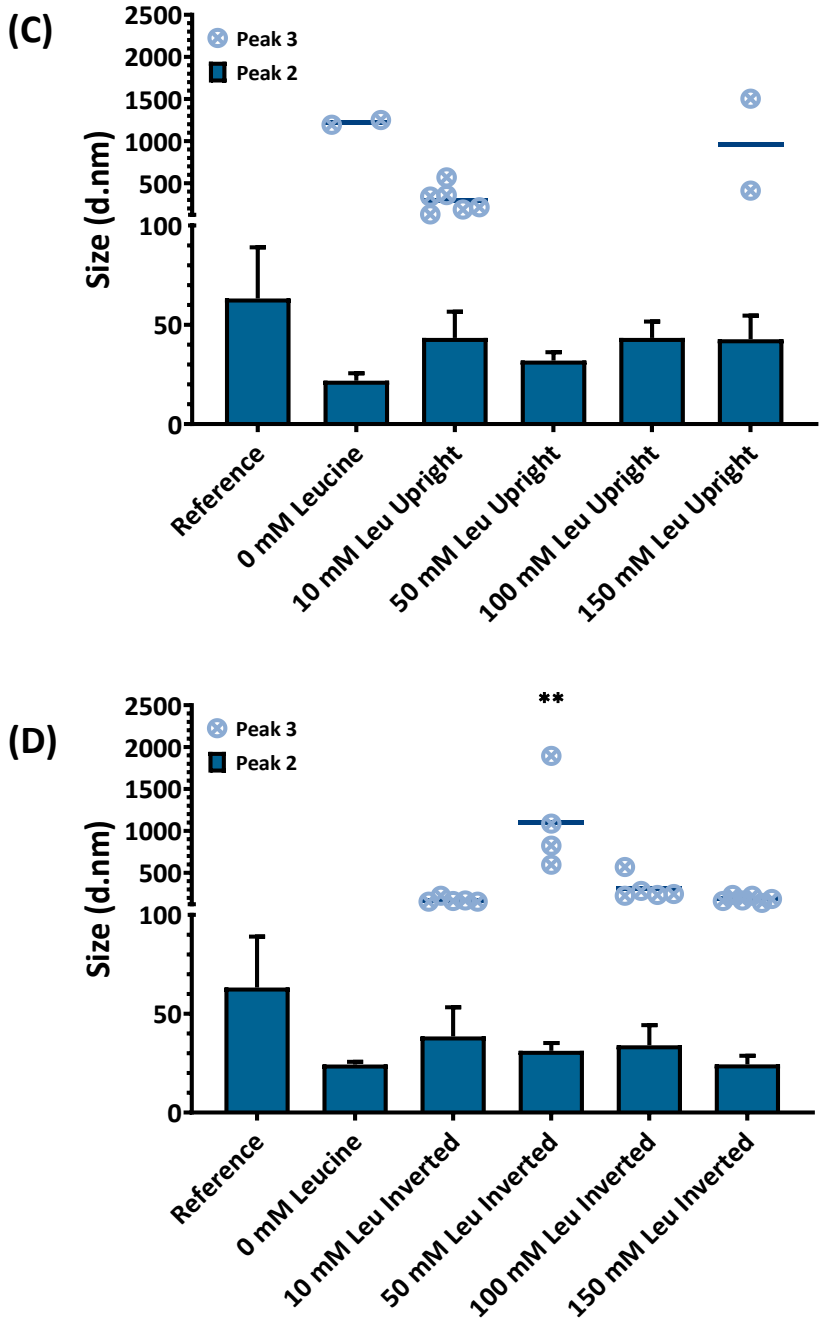
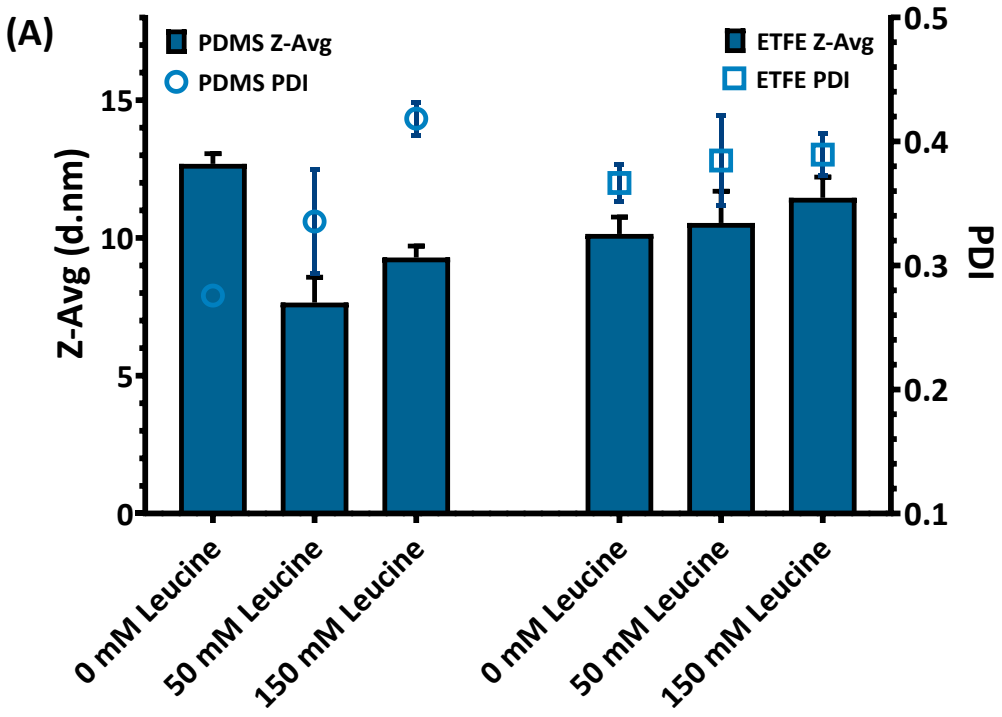
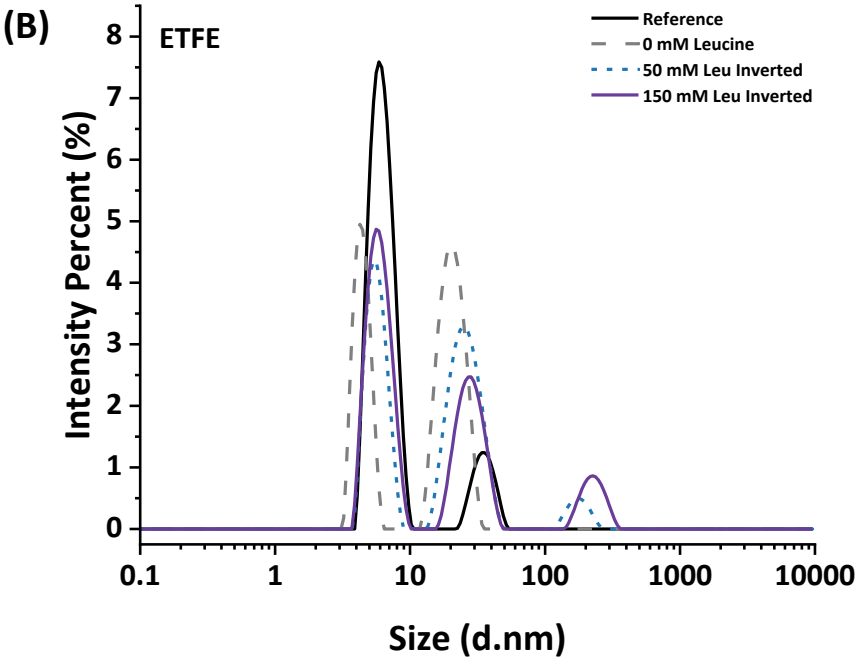
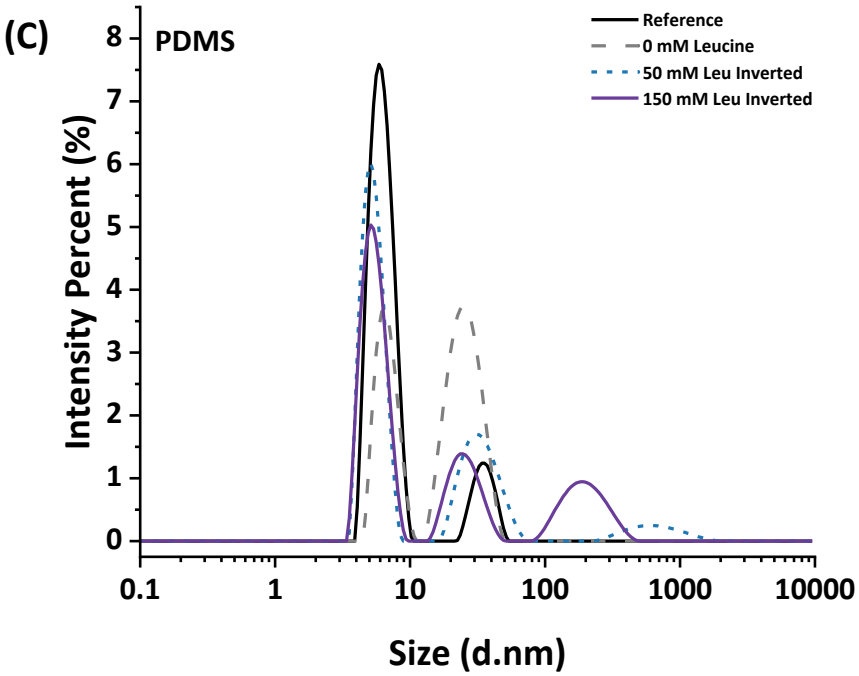


Figure 4.7: Representative intensity plot for the BSA formulations stored under thermal agitation conditions either upright (**A**) or inverted (**B**). Particle size distribution of peak 2 (blue bars) and peak 3 (open crossed circles) are shown for upright (**C**) and inverted (**D**). Data represents mean ± SD, n=3, for (**A**-**B**). For peak 3 sizes, all replicates are shown (zero values and particles >5 µm were excluded). Reference represents BSA prepared fresh in Na-Phos. Statistical analysis was conducted using a two-way ANOVA with Tukey's post-hoc test, $^{**}p<0.01$.

As inverted storage had a more destabilising effect on the stability of the BSA reference solution compared to upright storage under thermal agitation conditions (**Figure 4.4**), the impact of an alternative stopper material (ETFE coating) on BSA stability in the presence and absence of leucine at a moderate and high molar concentration was also evaluated. Compared to PDMS, ETFE coatings creates a contact surface with very low surface energy[321], which should minimise BSA-stopper interactions. However, ETFE is inherently hydrophobic, similar to PDMS. In both the presence and absence of leucine, BSA stability was similar for both stopper types, **Figure 4.8A**. However, BSA in the presence of ETFE stoppers produce a significantly (p-value <0.0001) higher Z-Avg value compared to PDMS at each leucine concentration. Additionally, the intensity plots, **Figure 4.8B** and **Figure 4.8C**, in the absence of leucine were also similar for both stopper types however, in the presence of the ETFE-coated stopper, there was a greater intensity in the peak 2 species. Interestingly, despite the differences in the intensity plot, the size distribution was similar for both stopper types, **Figure 4.8D**. Statistically significant differences in the distribution of particles were not obtained except that inverted storage using an ETFE stopper and 50mM leucine produced a statistically smaller particle size distribution.




(B)
ETFE
Reference
0 mM Leucine
50 mM Leu Inverted
150 mM Leu Inverted
Intensity Percent (%)
0
1
2
3
4
5
6
7
8
0.1
1
10
100
1000
10000
Size (d.nm)


(C)
PDMS
Reference
0 mM Leucine
50 mM Leu Inverted
150 mM Leu Inverted
Intensity Percent (%)
0
1
2
3
4
5
6
7
8
0.1
1
10
100
1000
10000
Size (d.nm)

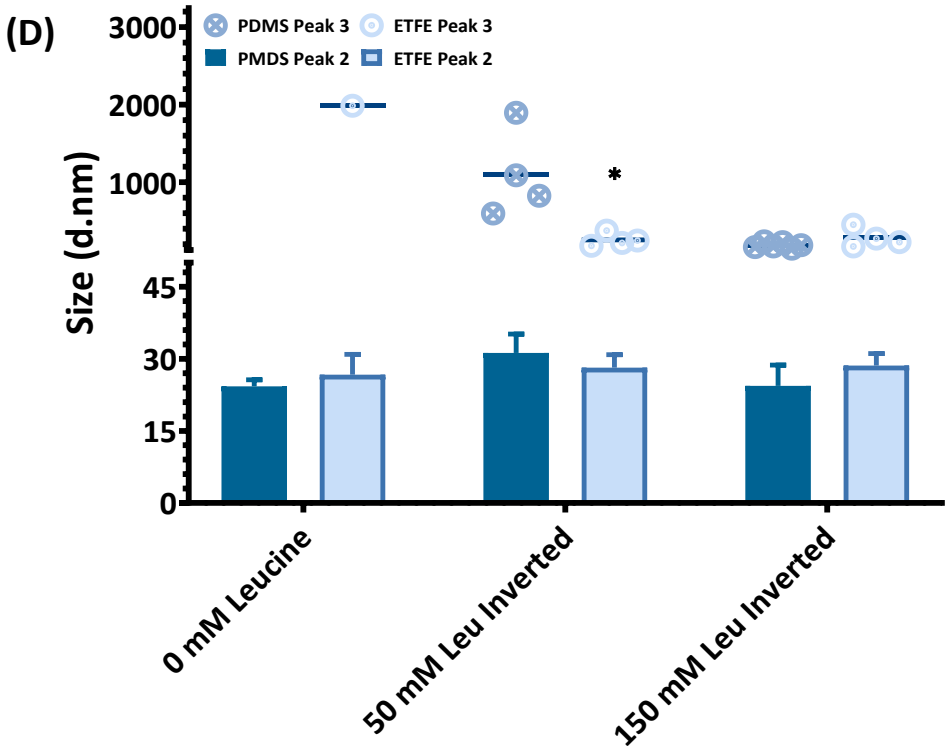


Figure 4.8: Z-Avg and PDI (**A**), intensity plot for ETFE (**B**), PDMS (**C**), and size distribution (**D**) for the BSA formulations stored under thermal agitation conditions in an inverted position. Z-Avg (blue bars) and PDI (open circles and squares) correspond to the right and left y-axes, respectively. The particle size distribution of peak 2 (blue bars) and peak 3 (open crossed and dotted circles) are shown for the ETFE or PDMS-coated stoppers. Data represents mean ± SD, n=3, for the Z-Avg, PDI and peaks 2 and 3 size distributions. For peak 3 sizes, all replicates are shown (zero values and particles > 5 µm were excluded). Statistical analysis was conducted using a two-way ANOVA with Tukey's post-hoc test, $^{*}p<0.05$, **** $p<0.0001$.

4.5 Discussion

Elastomeric closures such as vial stoppers pose considerable risk to the stability of biotherapeutic molecules because they are inherently hydrophobic materials. Stoppers may also be treated with surface coatings such as PDMS or fluoropolymers, which are reported to induce protein instability.[64,89,90,92,95,225] Moreover, current research on container/closure systems has revealed an association between excipients, mainly surfactants, and the degradation of PDMS coatings used for primary packaging.[64,247] In this study, investigating protein-excipient-container/closure compatibility, leucine was employed as an aggregation suppression excipient. Leucine demonstrated an inability to preserve BSA's colloidal stability due to thermal-induced unfolding. In limited circumstances, leucine appeared to reduce BSA's instability when stored in an upright orientation compared to buffer-only solutions. However, this was concentration-dependent (50 mM and 100 mM) as particles >100 nm were observed at 10 mM and 150 mM. This was likely due to either too little leucine being present at 10mM in solution to confer effective stabilisation and too much leucine at 150mM which, owing to the hydrophobicity of the excipient, could have accelerated BSA unfolding rather than prevented it. High concentrations of hydrophobic excipients can create localised microenvironments in solution where unfolding can be promoted.[322] This hypothesis is supported by the negative relationship between BSA alpha helix content and molar concentration of leucine in solution. This relationship would suggest that the higher the concentration of leucine in solution, the more likely BSA is to unfold under stress. Furthermore, the linear relationship between Z-Avg and PDI with increasing leucine concentration particularly for inverted storage would suggest that this unfolding can lead to more significant aggregation than when the vial is stored upright. Mitigating particle formation by changing the stopper material from a PDMS-coated stopper to an ETFE-coated stopper also proved ineffective, as BSA demonstrated greater sensitivity to the storage environment compared to the stopper interface. Ultimately, BSA proved to be an inherently thermosensitive protein, and its native conformation can be compromised between 40-50°C, with prominent unfolding and denaturation causing aggregation above 60°C.[323]

Short-term (7-day) storage studies in buffer-only solutions were performed to determine the impact of packaging interfaces on BSA aggregation (**Figure 4.1**). This was done to collect baseline data before evaluating the effect of leucine addition. These studies confirmed BSA's

sensitivity to thermal agitation stress, as evidenced by the increase in HMWs (**Figure 4.4**). Further, these storage conditions resulted in greater particle size distributions and an altered protein conformation in solution (**Figure 4.2** and **Figure 4.3**). This study also identified that exposure to the vial stopper under short-term, inverted storage had a greater impact on BSA's conformational and colloidal stability when exposed to thermal agitation conditions compared to upright storage (**Figure 4.2** and **Figure 4.4**).

The higher instability observed for BSA when stored in the inverted vial orientation could result from numerous individual factors or a combination. A likely explanation is that the exposure to two hydrophobic interfaces (vial headspace and stopper), may have caused more unfolding and aggregation (**Figure 4.2** and **Figure 4.4**) compared to upright storage, where only the air-liquid interface was present which is in line with a study by *Dasnoy et al*.[270] Moreover, the stoppers used to collect the baseline data were coated in a PDMS layer, which has previously been demonstrated by *Kannan et al*. to induce unfolding and aggregation for monoclonal antibodies.[64] Additionally, as agitation conditions were employed, this may have accelerated the destabilising effect of the PDMS surface as suggested work by *Thirumangalathu et al*. who showed that agitation was required to destabilise the protein in the presence of siliconised surfaces.[222]

Interestingly, despite the inert nature of fluoropolymers, BSA and other proteins have been reported to strongly adsorb to PTFE, which is chemically similar to ETFE, which was the laminate film coating present on the stoppers used in this study. This could explain why instability was still observed despite altering the packaging interface (**Figure 4.8**).[92,94,321,324–327] One notable study by *Teska et al*. found that the stability of Ig in contact with fluoropolymer and traditional siliconised stoppers was similar in terms of protein particle counts and soluble protein levels. *The authors* noted a decrease in total particle concentration when fluoropolymer stoppers were used, consistent with other studies.[95,96]

The addition of leucine was investigated to assess whether it could improve the stability of BSA in the packaging and storage configurations investigated. No major stabilising effect was observed due to the addition of leucine. The BSA-leucine solutions displayed unfolding for all conditions investigated (**Figure 4.5**), and particle formation >100 nm occurred more so where vial stopper contact was sustained (**Figure 4.6** and **Figure 4.7**). This result was observed for both stopper types investigated. A possible explanation for this effect is that the presence

of leucine could have altered the pathway to aggregation as leucine has been reported to influence the kinetics of aggregation.[316] However, it is more probable that intrinsic BSA instability in the elevated temperature environment acted as the driving force for the aggregation behaviour observed in this study and leucine was not successful in reducing this.

The influence of leucine on aggregation behaviour was reported by *Szenczi et al*. who discovered that leucine could prevent IgG aggregation by reducing its tendency to aggregate during thermal-induced unfolding. In the presence of leucine 3 mg/mL (23 mM), IgG aggregation took 50 seconds longer to occur. In our study, it was found that BSA does not fully aggregate in the leucine formulations which suggests it could have been maintained in an unfolded form under thermal agitation conditions as described by *Borzova et al*.[328] Therefore, it is possible leucine is imparting some effect on the aggregation behaviour but investigating leucine with other potential stabilisers such as polar amino acids or at lower storage temperatures may be a more beneficial approach for aggregate-prone, thermosensitive proteins.[276]

There were also several limitations in this study. Firstly, the quantity of BSA adsorbed to the glass and stopper interfaces or the potential for adsorption at the air-liquid interface was not evaluated. Further, the conformation of BSA at these interfaces was also not established. This would have provided useful information regarding the mechanism of BSA aggregation, as it is possible that the packaging interface played a more prominent role than detectable by the techniques applied in this study. Further studies using QCM-D with dissipation, surface tension, and interfacial rheology would be beneficial in examining the kinetics of the interactions and identifying leucine's role in adsorption. Particle counting technologies would also be essential to determine if the particle count changes in parallel to the size distribution. Lastly a comparison with PS80 as an additional control and studying PS80 with leucine would have been advantageous to determine if a combination of excipients could have stabilised BSA against particle formation during inverted storage given the protective effects of surfactants at hydrophobic interfaces.

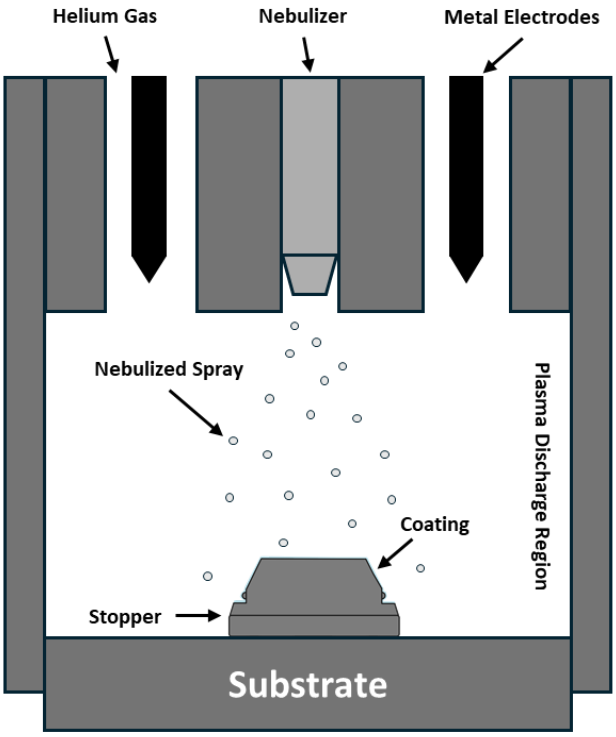
4.6 Conclusion

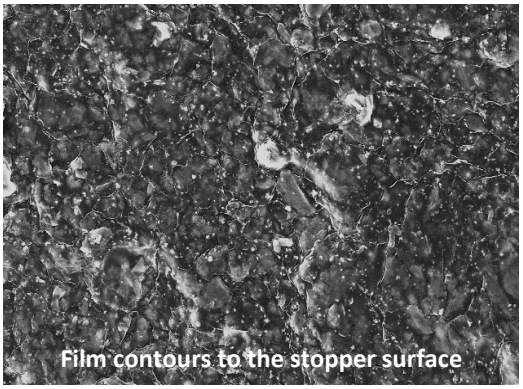
BSA is an inherently thermosensitive protein. Its native conformation can be compromised between 40-50°C, with prominent unfolding and denaturation causing aggregation above 60°C. Storage studies confirmed BSA's sensitivity to thermal agitation stress, as evidenced by the increase in HMWs. This study also identified that under short-term storage (7 days), inverted vial orientation had a greater effect on BSA's conformational and colloidal stability when exposed to thermal agitation conditions compared to upright storage. We postulate this is due to the compounding effects of the vial stopper and vial headspace interfaces and the high protein concentration used. The vial stopper presents a hydrophobic interface which are known to induce protein unfolding and interface-induced aggregation. In combination with the vial headspace, which adds an additional hydrophobic interface, interface-induced unfolding and aggregation effects can be accelerated and may also occur to a greater extent. Further, with the high protein concentration used, the movement of the BSA molecules in solution could be restricted, increasing the potential for protein-protein collision in both the bulk solution and at the vial stopper and headspace interfaces. The addition of leucine as a stabiliser demonstrated variable effects, a sensitivity to inverted storage, and an inability to stabilise BSA's conformation against thermal-induced aggregation. However, it had partial stabilising effects on BSA's stability when stored in an upright orientation under thermal agitation conditions, and this was concentration dependent, with larger aggregates observed at 10 mM and 150 mM leucine. Changing the stopper interface from PDMS to ETFE-coated stoppers proved ineffective, and intrinsic BSA instability induced by the hydrophobic interfaces, solution environment and storage conditions resulted in similar aggregation profiles.

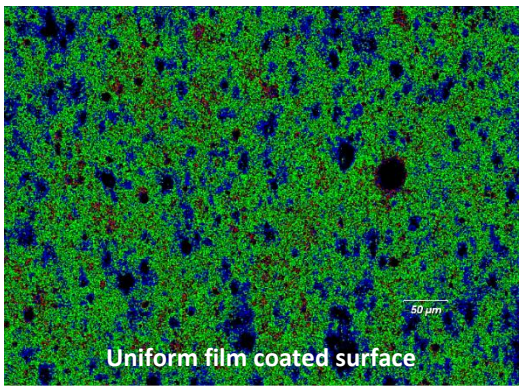
Chapter Five

5. Application of a Phosphorylcholine Polymer on Vial Stoppers Using a Cold Plasma Deposition Process

Submitted in Part to Colloids and Surfaces B: Biointerfaces







5.1 Abstract

Polymeric coatings are applied to vial stoppers used in the packaging of therapeutic proteins to aid lubricity, reduce leachables and increase protein-stopper compatibility. However, current stopper coatings have been implicated in product quality defects, such as the formation of protein-PDMS particles and the leaching of fluoropolymers into liquid parenteral products, impacting product integrity. Therefore, there is a need to investigate novel polymer coatings and coating techniques to enhance protein-stopper compatibility. This study examines the coating of vial stoppers using a copolymer, poly(MPC-*co*-BMA), which is comprised of 2-methacryloyloxyethyl phosphorylcholine (MPC) and butyl methacrylate (BMA), and its deposition using an innovative aerosol assisted cold plasma deposition technique. Stoppers were successfully coated, and plasma process parameters (flow rate, speed and voltage) were found to affect coating coverage as indicated by changes in stopper hydrophobicity measured by static water contact angle (WCA) analysis. A reduction in surface roughness post-coating was observed using atomic force microscopy (AFM). Attenuation of the Raman intensity for the titanium dioxide (TiO_2, Anatase) component in the coated stoppers provided a useful measure of coating distribution. Poly(MPC-*co*-BMA) coating compatibility with a model BSA protein formulation was benchmarked against commercial PDMS and ETFE-coated stoppers. No changes in BSA stability were observed after three months of refrigerated storage, even when exposed to agitation or freeze-thaw stresses. The protein compatibility with poly(MPC-*co*-BMA)-coated stoppers was comparable to commercial PDMS and ETFE coatings. This study highlights the potential of poly(MPC-*co*-BMA) as a stopper coating and demonstrates the effectiveness of atmospheric aerosol-assisted plasma in depositing these coatings.

5.2 Introduction

Interfacial stress significantly impacts protein stability and plays a pivotal role in particle formation, ranging from subvisible to visible-sized particles.[123] These particles form primarily during key manufacturing and handling stages, notably fill-finish operations, transport, and storage.[73,129,161,183,185,227,232] Given the risk that the generation of these particles pose to the therapeutic quality and safety, precise control over the storage interfaces and product handling is critical. Primary container systems used for the storage of protein formulations typically include glass vials, syringes, or cartridges, and include an elastomeric component (stopper or plunger) to protect against environmental factors and preserve the final product quality.[65] Borosilicate glass is a common packaging material used to contain liquid parenteral products and has many advantages, such as being inert, durable, and impermeable. However, concerns exist regarding the compatibility of protein formulations with the elastomeric closures used to maintain sterility in glass packaging systems, due to the risk of leachables, particle generation and product instability.[72,89,90] Recent evidence of interactions between vial stopper components and protein formulations emphasises the need for packaging that does not adversely affect product integrity.[89,90]

Uncoated closures are associated with the leaching of rubber components into the protein formulation.[83] Moreover, due to the hydrophobicity of closure materials, there is an increased risk of protein adsorption, which can lower the target protein concentration and compromise the therapeutic product's stability.[30] Further, owing to the friction present at the glass-rubber interface, closures may be coated with PDMS to enhance stopper lubricity. However, contact between the protein formulation and the PDMS interface during storage has been shown to cause the formation of visible silicone oil droplets and protein-PDMS particles.[89,90,95] The leaching of PDMS has been linked to the use of surfactants and the surface activity of the therapeutic protein.[64,107] In addition, the air-liquid interface has been proven to contribute to particle formation, where protein formulations maintain contact with the stopper.[89]

Given the increased awareness of the impact of siliconised storage systems on therapeutic protein stability, there has been a move towards silicone-free primary packaging.[73,96] Closure devices have been adapted to have a fluoropolymer laminate film coating on the drug contact surface rather than a PDMS coating.[95,96] Fluorinated coatings have been proven to be compatible with glass packaging systems as they have high lubricity and eliminate the need

for siliconisation.[65,96] Reports also indicate that fluoropolymers represent a suitable alternative to reduce particle formation in glass vial containment systems.[90,95,96] Moreover, they have been shown to reduce the risk of leachables in protein formulations.[65] However, fluoropolymer surfaces such as PTFE have been implicated in causing protein adsorption, unfolding, aggregation and fibrillation.[92,93,324] Further, under stress conditions, fluoropolymer particles can shed into the protein formulation.[90] While fluoropolymer stoppers offer clear advantages over uncoated and siliconised stoppers, limitations still exist where contact between the protein formulation and stopper interface is maintained. The development of adsorption-resistant coatings may address these limitations.

Phospholipid coatings on primary packaging containers have been recently considered to limit non-specific protein-packaging interactions.[329] Phospholipid coatings can act as protein-resistant surfaces owing to the zwitterionic properties of the phosphorylcholine moiety.[330] The phosphorylcholine moiety confers hydrophilicity and has properties in line with Whiteside's rules for protein-resistant surfaces.[100,331,332] Hydrophilic coatings are more suitable for reducing protein adsorption due to the increased energetic cost of interfacial dehydration.[105,206] However, a hydrophobic backbone is required to help maintain their adhesion to the packaging surface. Therefore, to harness the bioinert properties of natural phospholipids, synthetic phosphorylcholine polymers such as 2-methacryloyloxyethyl phosphorylcholine (MPC) have been developed and copolymerized with alkyl methacrylates to create biomimetic protein-resistant coatings.[103,104,333101,334–340] These polymers have a unique hydration state that can prevent proteins from interacting with interfacial water, minimising adsorption to the solid-liquid interface.[37,104,341] Most of the research on MPC has been centred on medical device applications however, its properties align with the requirements of pharmaceutical packaging. [335,336,339,340,342–345]

Coatings applied to pharmaceutical packaging can be deposited using a variety of approaches such as spray-on, dip-coat, surface grafting, cross-linking, bake-on or heat-sealing methods. However, the strength of the coating's adhesion to the surface can be based on the deposition method and may determine the stability and durability of the coating.[346] Other techniques, such as plasma deposition can covalently bond the coating to the substrate. This typically involves plasma functionalisation, a form of surface activation that facilitates covalent polymer immobilisation on the surface, offering enhanced coating stability and

protein-resistant properties.[346,347] There are different types of plasma deposition, yet aerosol-assisted cold plasma offers numerous advantages as a coating deposition technique for pharmaceutical packaging. It offers improved adhesion, is beneficial for temperature-sensitive molecules, and can preserve the chemical stability of the deposited molecules.[348–350] Additionally, as stoppers are stable in high-pressure and vacuum environments, they are suitable for use under plasma functionalisation conditions. Plasma deposition is used commercially by SiO_2 Medical Products for coating polymer storage systems and by SCHOTT Pharma to coat borosilicate glass container systems.[108,109,351,352]

In this study, we investigated poly[MPC-*co*-*n*-BMA] (poly(MPC-*co*-BMA (PMB)) commercially known as Lipidure®-CM5206 (Lipidure®-CM, equivalent to PMB30) as an innovative polymer stopper coating for packaging protein formulations. One of the unique features of this polymer is that the copolymers cannot freely rotate in air, creating a hydrophobic surface.[334,353] However, the copolymers can reorientate at the surface when exposed to water, leading to the rearrangement of the phosphorylcholine moieties towards the interface, rendering the surface hydrophilic.[104,335,343,353] Owing to these surface characteristics, the coating can potentially act as an anti-fouling surface in air and aqueous solution.[353] This approach has previously been demonstrated for PDMS-PEG coatings with biopharmaceutical manufacturing equipment.[206,354] A design of experiment (DoE) approach was used to determine the optimal plasma process parameters required to deposit a uniform poly(MPC-co-BMA) coating on vial stoppers using a novel aerosol-assisted cold plasma deposition process. The coating distribution was assessed by imaging the stopper topography and surface coverage using scanning electron and atomic force microscopy techniques and Raman hyperspectral mapping. Further, the study used a model BSA formulation to benchmark protein formulation compatibility with the poly(MPC-*co*-BMA)-coated stopper against commercial PDMS and ETFE-coated stoppers for the first time.

5.3 Materials & Methods

5.3.1 Materials

Unless otherwise stated, all chemicals and materials were purchased from Merck, Ireland. 24-well and 6-well cell culture plates were purchased from Sarstedt, Germany. Lipidure®-CM5206 (poly(MPC-*co*-BMA) equivalent to PMB30) was purchased from NOF Corp., Japan. SCHOTT 10R/10 mL Fiolax Type 1 Plus® borosilicate vials and 20 mm PDMS injection stoppers were obtained from Adelphi Healthcare Packaging, UK. Uncoated 20 mm small-volume parenteral bromobutyl stoppers and 20 mm ETFE laminate film-coated injection stoppers were obtained from Aptar, France. A schematic of the uncoated stoppers with approximate stopper dimensions and an image of the uncoated stoppers are shown in **Figure S5.1**. Halobutyl rubber locking flange septas were purchased from Fisher Scientific, Ireland.

5.3.2 Methods

Poly(MPC-co-BMA) coating solution preparation

Poly(MPC-*co*-BMA) solutions (2 mg/mL or 8 mg/mL) were prepared in 70% v/v ethanolic solutions in water in 10 mL syringes. Solutions were stored at 5°C for 24 h to ensure complete solubilisation of the polymer before plasma deposition.

C*oating of the vial stoppers*

Plasma deposition coating process

The following plasma treatment procedure was developed with TheraDep Ltd. Vial stoppers were placed in either 24-well or 6-well culture plates and subjected to plasma activation using helium (He) gas. Vial stoppers were activated in a Diener Zepto vacuum activator for 2 min with a He flow rate of 0.5 standard litres per minute (slm) and 100% power. Plasma deposition was carried out using a purpose-built deposition system comprising a G2000 high-voltage power supply (Redline, Baesweiler, Germany) connected to a custom build Teflon deposition unit that encased two metal electrodes, as shown schematically in **Figure S5.2A**. The plasma was operated at a frequency of 20.4 kHz, and an input voltage of either 100 V or 150 V. A pneumatic nebuliser T2100 (Burgener Research, ON, Canada) was placed between the

electrodes, and this was connected to a syringe pump to provide a constant flow of coating solution at 50 µL/min or 100 µL/min. The liquid was nebulised using argon gas with a pressure of 0.31 MPa. In addition, a separate He flow of 6 slm was provided to the metal electrodes to create the plasma discharge. The plasma discharge was combined with the nebulised droplet spray in an acrylic tube (19 mm inner diameter × 35 mm length). To coat the surface evenly, the plasma head was mounted on a computer-controlled X-Y stage that could be moved in a desired pattern. The tops of the stoppers (flange), **Figure S5.2B** and **Figure S5.2C** were coated using a raster pattern (4.5 mm step size and width dependent on size/no. of samples) over the target surface. After determining the optimum deposition parameters, the coating was performed on the drug contact surface (stopper plug) **Figure S5.2D**. Coating was achieved by lowering the plasma head into each individual well and moving the head in a circular pattern. The speed was maintained at 500 mm/min or 2000 mm/min.

Design of experiments to optimise coating deposition using plasma deposition

A complete factorial 2^4 DoE was employed to optimise the coating process using Minitab v20.2. The DoE investigated the effect of poly(MPC-*co*-BMA) concentration on the coating solution at 2 levels (2 mg/mL and 8 mg/mL) and 3 process parameters, each at 2 levels; solution flow rate (50 µL/min and 100 µL/min), atomiser horizontal speed (500 mm/min and 2000 mm/min) and voltage (100 V and 150 V). Six stoppers, n=6, were coated for each run and measured in duplicate. The run number and corresponding level of each variable are summarised in **Table S5.1**. The response metrics included a change in WCA to measure surface hydrophobicity as an indication of coating application. Secondly, the percent relative standard deviation (%RSD) between individual WCA measurements for all stopper samples in each run was used to indicate coating uniformity.

Surface analysis of vial stoppers and flange septas

Water contact angle analysis

Static WCA measurements were conducted using a KRÜSS TVA100 to directly measure the contact angle on the top of the stopper (flange) and within the plug of the stopper. The stopper top and plugs are shown in **Figure S5.2C** and **Figure S5.2D**, respectively. A 0.5 µL droplet of water was deposited on the stopper. Top-view measurements were taken in air at

equilibrium after 30 s, and the WCA data were analysed using the KRÜSS ADVANCE software package. The WCA was measured in duplicate on the flange of coated and uncoated stoppers. WCA analysis was also performed on the coated stopper plugs using the optimum deposition parameters, n=6 independent replicates.

Scanning electron microscopy with energy-dispersive X-ray spectroscopy

Scanning electron microscopy (SEM) images were acquired using a Zeiss Supra 40 at an accelerating voltage of 5-10 kV. Energy-dispersive X-ray spectroscopy (EDX) was performed using an X-Max^N (Oxford Instruments) and elemental analysis was carried out using the Aztec 3.3 software package. A stopper for each condition (uncoated and coated) was mounted on a high-purity aluminium stub using double-sided carbon tape and sputtered coated with gold at approx. 100 nm thickness using a Quorum Q300T D plus. Three areas for each stopper were analysed for SEM with one area analysed by EDX per stopper.

Atomic force microscopy

It was not possible to perform AFM analysis of the stopper plug section (**Figure S5.2D**) owing to the challenges posed by the plug dimensions. Consequently, halobutyl rubber locking flange septas (**Figure S5.3**) were plasma deposited with poly(MPC-*co*-BMA) and used as a surrogate to enable AFM analysis of the coating topology. Polymer coatings were directly deposited onto the flange septas using poly(MPC-*co*-BMA) 2 mg/mL at a flow rate of 100 µL/min, a voltage of 150 V and a duration of 60 s. AFM images were taken in air at ambient temperature using a purpose-built Nanosurf Easyscan 2 instrument. The data acquired was analysed using Easyscan 2 software. AFM was conducted with a z height of 4.9 µm and the tip voltage set at 0 V. The scan range was 50 µm, with overscan enabled at 10%. Analysis was performed in duplicate using n=3 independent replicates.

Spectroscopic analysis of coating

Fourier transform infrared spectroscopy

To assess the impact of the plasma coating process on the chemical stability of poly(MPC-*co*-BMA), FTIR spectroscopy was conducted using a Perkin Elmer Spectrum One operating in single beam mode using 8 scans and a 32 cm^{-1} resolution at a 1 cm^{-1} data interval. Polymer coatings were directly plasma deposited onto NaCl discs using poly(MPC-*co*-BMA) 2 mg/mL at 100 µL/min, 150 V and duration of 60 s. Wet sample controls were deposited under the non-plasma mode (0 V). In this case, the solution was again sprayed at a 100 µL/min flow rate for 60 s and then allowed to dry under ambient conditions. This enabled the evaluation of the plasma discharge's impact on polymer stability during the deposition process. Poly(MPC-*co*-BMA) powder was analysed as a positive control using a Perkin Elmer Spectrum Two in attenuated reflective mode using the same settings. Additionally, a coated stopper was analysed but due to the stopper signal's confounding interference, it was not possible to accurately detect the coating's full spectral response when analysing the coated stoppers due to the low polymer content, **Figure S5.4**.

Raman spectroscopy

Raman spectra and hyperspectral maps were generated using a Renishaw inVia Qontor confocal Raman microscope equipped with a 532 nm, 50 mW diode pumped solid state laser, kinematically attached Rayleigh line rejection filters, an 1800 lines mm^{-1} grating, and a Peltier cooled (-70°C), near infra-red, deep depletion CCD detector (1024 x 256 pixels). Spectra were calibrated with an integrated silica standard of 520.5 cm^{-1}. Single spectra were acquired in Renishaw WiRE 5.5 software using a x20LWD objective to achieve a broad measurement area. Power, residence time and accumulations were calculated to achieve an optimal signal-to-noise ratio. A 'bleach' time of 30 s was used to help reduce autofluorescence. Each spectrum was collected using 5% laser power, 1 s residence time and 100 accumulations. Hyperspectral maps were collected using a x50LWD objective, 10% laser power, and a resolution of 0.7 µm x 0.7 µm at an accumulation rate of 10 spectra per s^{-1}. Maps contained between 400,00 and 500,000 spectra. LiveTrack™ focus tracking technology maintained optimum laser focus on the sample surface. LiveTrack™ focus tracking height data produced images of the surface's 3D morphology.

Individual spectra were processed in Renishaw WiRE 5.6, using minimal smoothing, cosmic ray removal and baseline subtraction. Map data sets were also subjected to cosmic ray removal and baseline subtraction. Data was processed using Renishaw's Empty Modelling™ method. Component spectra and concentration images were iteratively resolved to provide a group of spectra that could be matched to standard spectra generated from known substances. The distribution of these modelled spectra was then introduced to the map using a least squares component analysis that determined the linear superposition of component spectra that best represented the data.

Polymer-coated stopper stability study

Poly(MPC-*co*-BMA)-coated stoppers were subject to various destabilising conditions as outlined in **Table 5.1** and then one spot per stopper was analysed using Raman hyperspectral imaging. These conditions were chosen as they represent common stresses pharmaceutical coatings may be exposed to during storage. For thermal conditions, an APOLLO HP50 orbital shaker oven was used. At the endpoint, the stoppers exposed to the aqueous environment were dried gently under nitrogen.

Table 5.1. Storage conditions to assess coated stopper stability.

Sample	Storage Details
Uncoated	Reference stopper, uncoated, analysed without exposure to stress conditions
Coated	Reference stopper, coated, analysed without exposure to stress conditions
Autoclave	Coated stopper exposed to one autoclave cycle of 121°C for 15 min
Aqueous solution	Coated stopper exposed to deionised water for 24 h under ambient storage conditions
Thermal	Coated stopper exposed to a placebo formulation consisting of 20 mM histidine buffer pH 6 with PS80 2 mg/mL at 40°C shaking at 150 rpm

Protein-stopper compatibility study

Bovine serum albumin formulation preparation

BSA solutions were prepared by adding BSA 100 mg/mL to PBS pH 7.4. The formulation also contained trehalose 10 mg/mL, glycine 5 mg/mL and Pol188 2 mg/mL. Before adding the BSA, the aqueous solution was filtered through a 0.45 µm polyvinylidene fluoride filter. The BSA formulation was filtered through a 0.22 µm polyether sulfone filter into 10R/10 mL Fiolax Type 1 Plus® vials up to a 3 mL fill volume. Samples were then stoppered with a PDMS, ETFE or poly(MPC-*co*-BMA)-coated stopper and crimp sealed.

BSA formulation storage and stress conditions

BSA formulations were packaged in vials with PDMS, ETFE or poly(MPC-*co*-BMA)-coated stoppers and were stored in an inverted position under control (refrigerated) and forced degradation conditions as outlined in **Table 5.2** for 3 months. These conditions were chosen as they represent common stressors protein formulations can be exposed to during storage. For shaking conditions, an IKA-VIBRAX-VXR orbital shaker was used, and for thermal conditions, an APOLLO HP50 orbital shaker oven was used. At the end of the 3 months, the protein samples were retrieved and subject to particle size analysis.

Table 5.2. Storage conditions to assess BSA formulation-stopper compatibility.

Sample	Storage Details
Reference	Freshly prepared BSA formulation
Refrigerated (Control)	Storage at 2°C to 8°C for 3 Months
Freeze-Thaw	5 cycles @ -20°C for 12 h then 2°C to 8°C for 12h Followed by storage at 2°C to 8°C up to 3 month's time point
Shaking	1-week @ 300 rpm then refrigerated storage up to 6 week's time point, 24 h @ 300 rpm at 6 week's time point then refrigerated storage up to 3 month's time point
Thermal	Storage at 40°C for 3 months

Investigation of protein particle formation using dynamic light scattering

The BSA formulation Z-Avg and PDI were measured without dilution or filtration in disposable 1 mL poly(methyl methacrylate) cuvettes with the minimum required volume of 500 µL. The analysis involved 120 s equilibration, 30 s delay between measurements and a minimum of 13 runs of 10 s performed in duplicate using a Zetasizer nano ZS (Malvern Panalytical) operated in protein analysis mode. Sample parameter settings were as follows: protein as material (refractive index 1.450 and absorption 0.001) and water as dispersant (viscosity 0.8872cP, refractive index 1.330) at 25°C. Samples were measured using n=3 independent replicates. A freshly prepared BSA formulation was used as a reference.

Analysis of gel-like particles

For the collection of the visible particles, 2 mL of sample from each independent replicate was collected, collated for each stress condition, and filtered through 0.8 µm Isopore™ polycarbonate membranes in removable filter housing. The filters were dried in a desiccator overnight (approx. 8 h), placed on clear glass slides with a coverslip, and analysed using an Olympus BX43 microscope. Images were captured using a mounted Olympus SC100 camera and were processed with Stream Essentials v2.3.3.

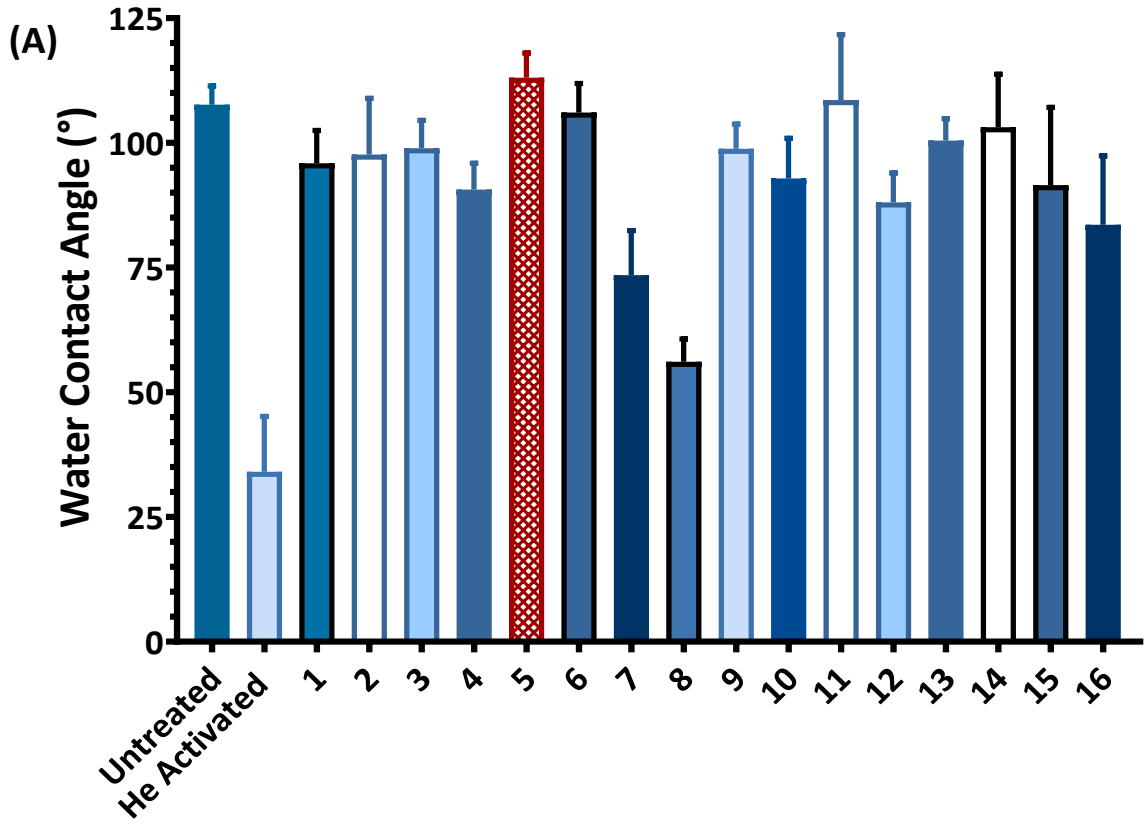
Data process and statistical analysis

The data was processed and graphed in OriginPro® 2022 version 9 or GraphPad Prism 8®. All statistical analysis was performed using GraphPad Prism 8®. The datasets were analysed by conducting a two-way ANOVA (alpha threshold = 0.05; C.I = 95%) and Tukey's post-hoc test.

5.4 Results

5.4.1 Optimizing coating parameters using design of experiments

Static WCA of the uncoated, He activated, and coated bromobutyl rubber stoppers was analysed to understand the changes in stopper surface hydrophobicity due to the poly(MPC-*co*-BMA) coating deposition. Uncoated stoppers showed a WCA of 107.65°, which reduced to 34.07° after He activation, **Figure 5.1A**. After polymer deposition, the WCA was measured for the stoppers coated according to the parameters in **Table S5.1**. The WCA of the coated stoppers was variable and ranged from 56.1° to 113.06° (**Figure 5.1A**). The variability of repeat WCA measurements for each experimental run ranged from 3.6% to 10.1% %RSD (**Figure 5.1B**). The difference in WCA between each analysis site on the stopper flange for runs 1 to 16 can be seen in **Figure S5.5**.



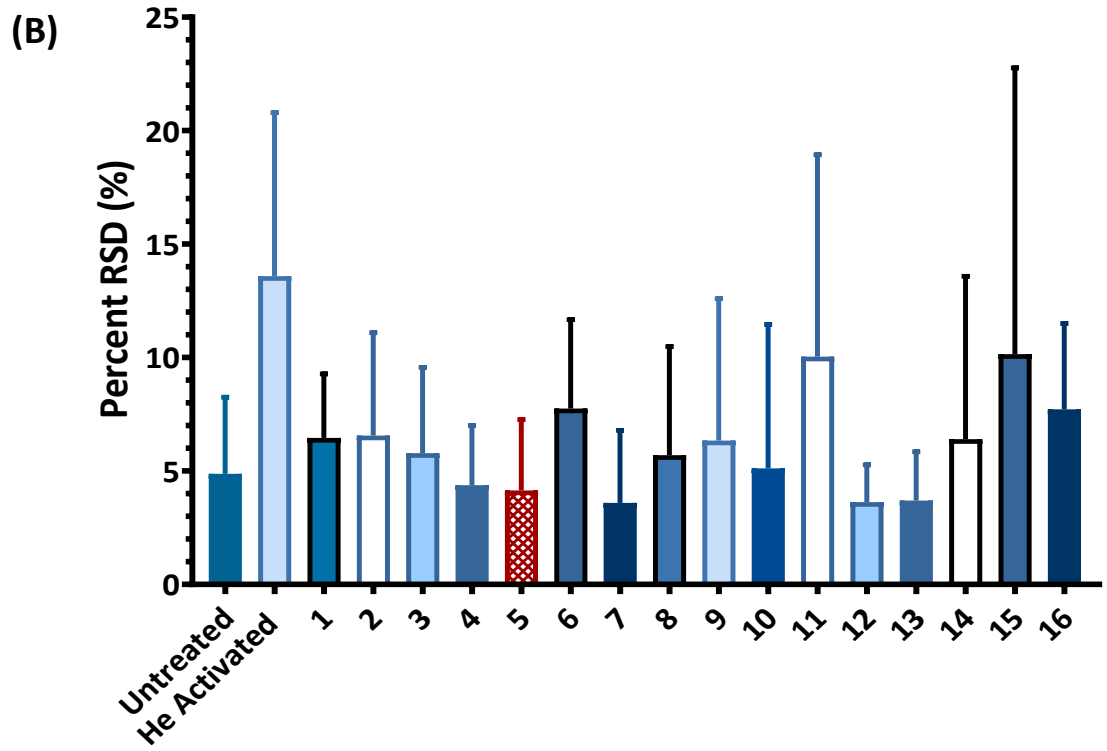
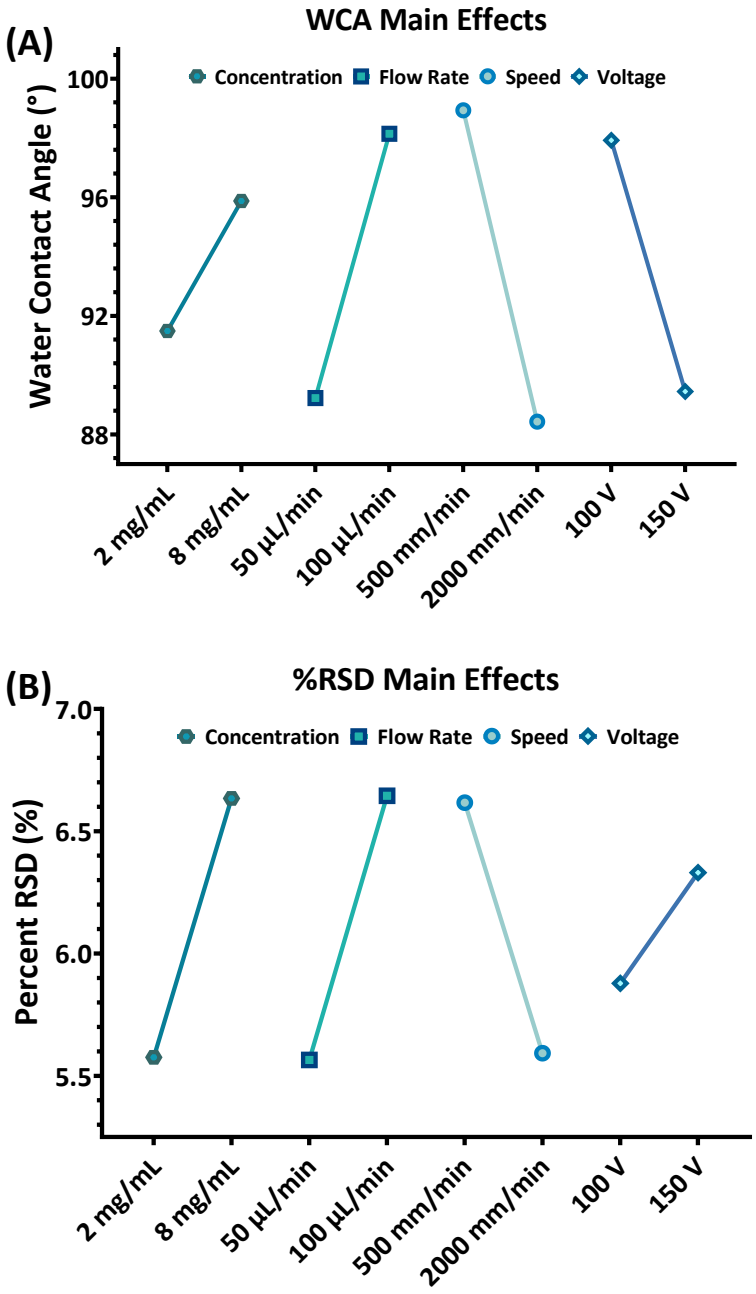


Figure 5.1: WCA measurements (**A**) and %RSD of WCA measurements across six coated stoppers (**B**). Stoppers were coated with poly(MPC-*co*-BMA) according to a 2^4 DoE approach. He activated represents He activated control. Data represents mean ± SD, n=6, each measured in duplicate.

The main effects plots, **Figure 5.2A** and **Figure 5.2B**, for the WCA indicated that the following parameters at an individual level yielded a more hydrophobic surface: polymer concentration 8 mg/mL; voltage 100 V; flow rate 100 µL/min and speed 500 mm/min. Except for the 100 V setting, those parameters also displayed the highest levels of %RSD between WCA measurements, indicating reduced coating uniformity. The two-factor interaction plots, **Figure 5.2C**, **Figure 5.2D** and **Figure 5.2E**, revealed interactive effects between parameters studied, altering the surface coverage as indicated by changes in WCA. The effect of nebuliser speed was found to be one of the most important operating parameters as it displayed significant two-factor interactions with the other plasma process parameters and polymer concentration. Considering the outputs of the main effects and two-factor interactions, response optimisation was performed to identify the combination of parameters which maximise WCA while minimising %RSD to determine the optimum, most statistically significant process parameters for producing a polymer coating with uniform surface

coverage. Run 5 (denoted in **Figure 5.1** by red colouring), corresponding to a polymer concentration of 2 mg/mL, voltage 150 V, flow rate of 100 µL/min and speed of 500 mm/min, was determined to represent the optimum combination of variables with a composite desirability of 0.833. The stopper plug was then coated using the parameters outlined in run 5 and produced near-identical WCA and %RSD values to the stopper flange, **Figure S5.6**.



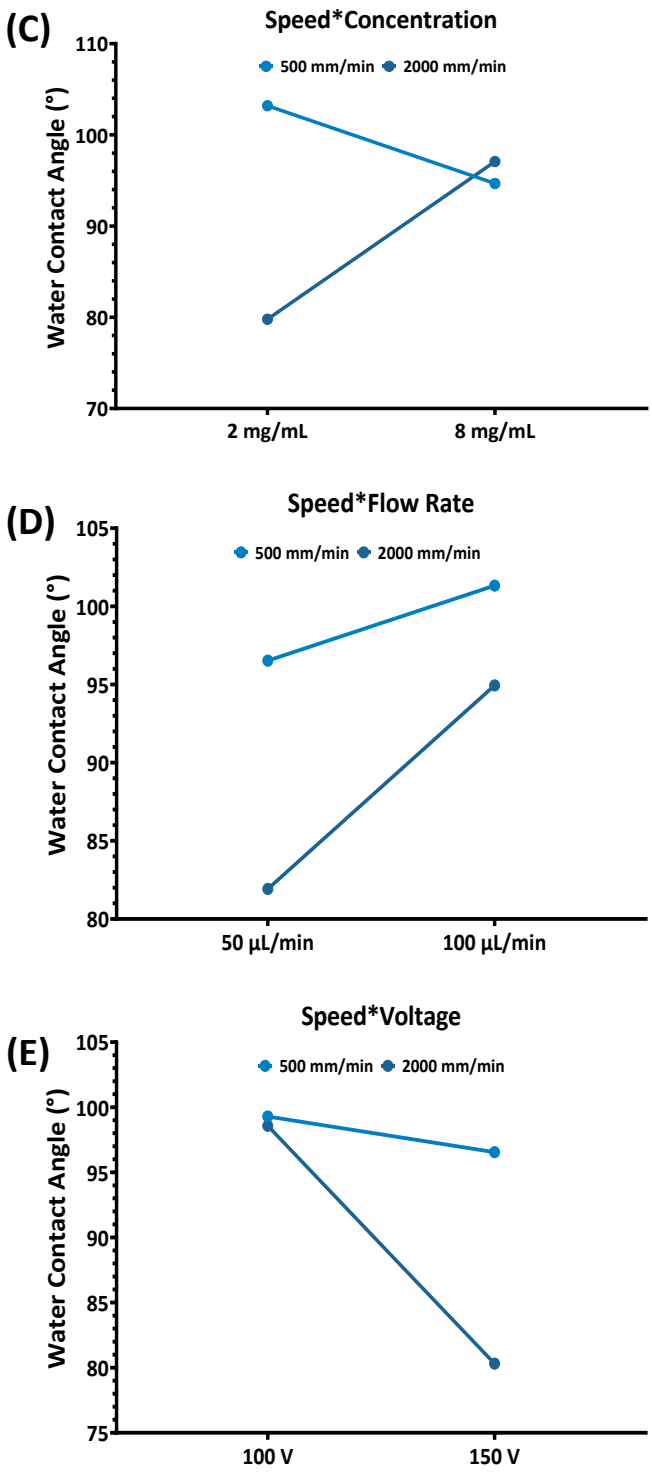
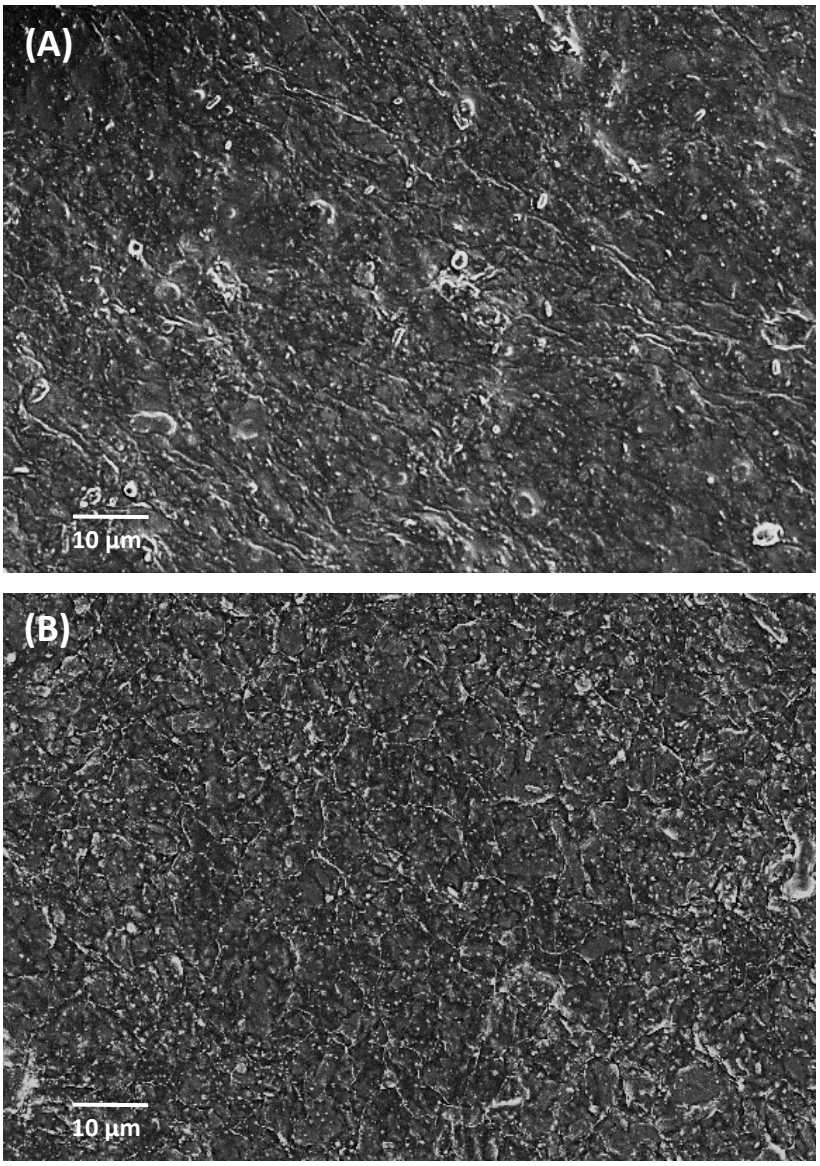


Figure 5.2: Main effects plots for WCA (**A**) and %RSD between repeat WCA measurements for the coated stoppers in each run (**B**) and significant two-factor interaction plots for significant binary mixtures (**C-E**).

5.4.2 Microscopic analysis of poly(MPC-*co*-BMA)-coated stoppers

Scanning electron microscopy with energy-dispersive X-ray spectroscopy

The physical structure of the plasma-deposited poly(MPC-*co*-BMA) coating was compared to an uncoated surface, **Figure 5.3A**, using SEM to identify any changes in the surface features of the stopper. There were no apparent gross changes in the topography of the coated stopper, **Figure 5.3B**. Magnified images of the uncoated stoppers, **Figure 5.3C**, show an irregular surface, whereas the coated surface, **Figure 5.3D**, illustrates that the coating technique produces a polymer coating that aligns closely with the contours of the stopper topology.



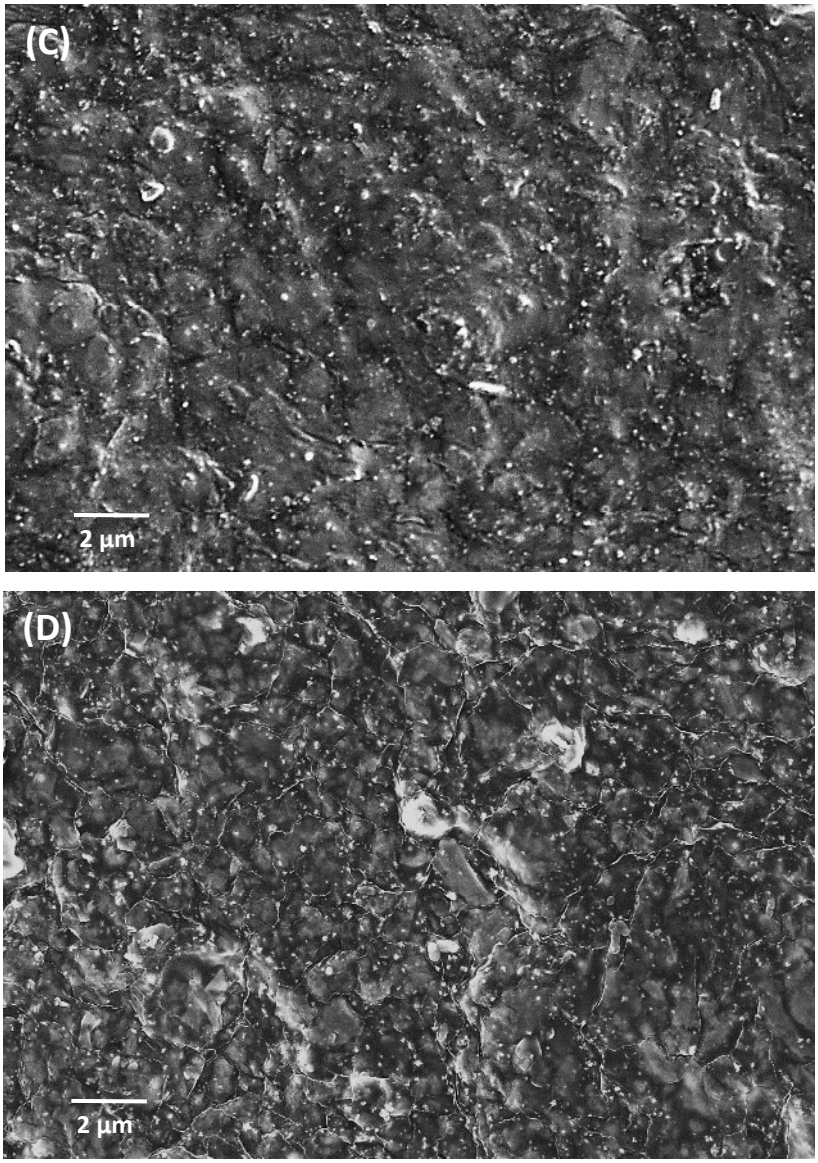


Figure 5.3: SEM images of stopper surfaces. Uncoated (**A**) and poly(MPC-*co*-BMA)-coated stopper (**B**), scale bar 10 µm. Higher magnification images of uncoated (**C**) and poly(MPC-*co*-BMA)-coated (**D**) stoppers, scale bar 2 µm.

EDX elemental maps are shown in **Figure 5.4** for an uncoated and poly(MPC-*co*-BMA)-coated stopper. These maps reveal a shift in surface elemental composition, primarily in the carbon distribution. While the maps suggest some heterogeneity in the coating application, the application of EDX can only be examined qualitatively as phosphorus and nitrogen, two elements present in poly(MPC-*co*-BMA) were undetectable, likely due to the low content of the coating.

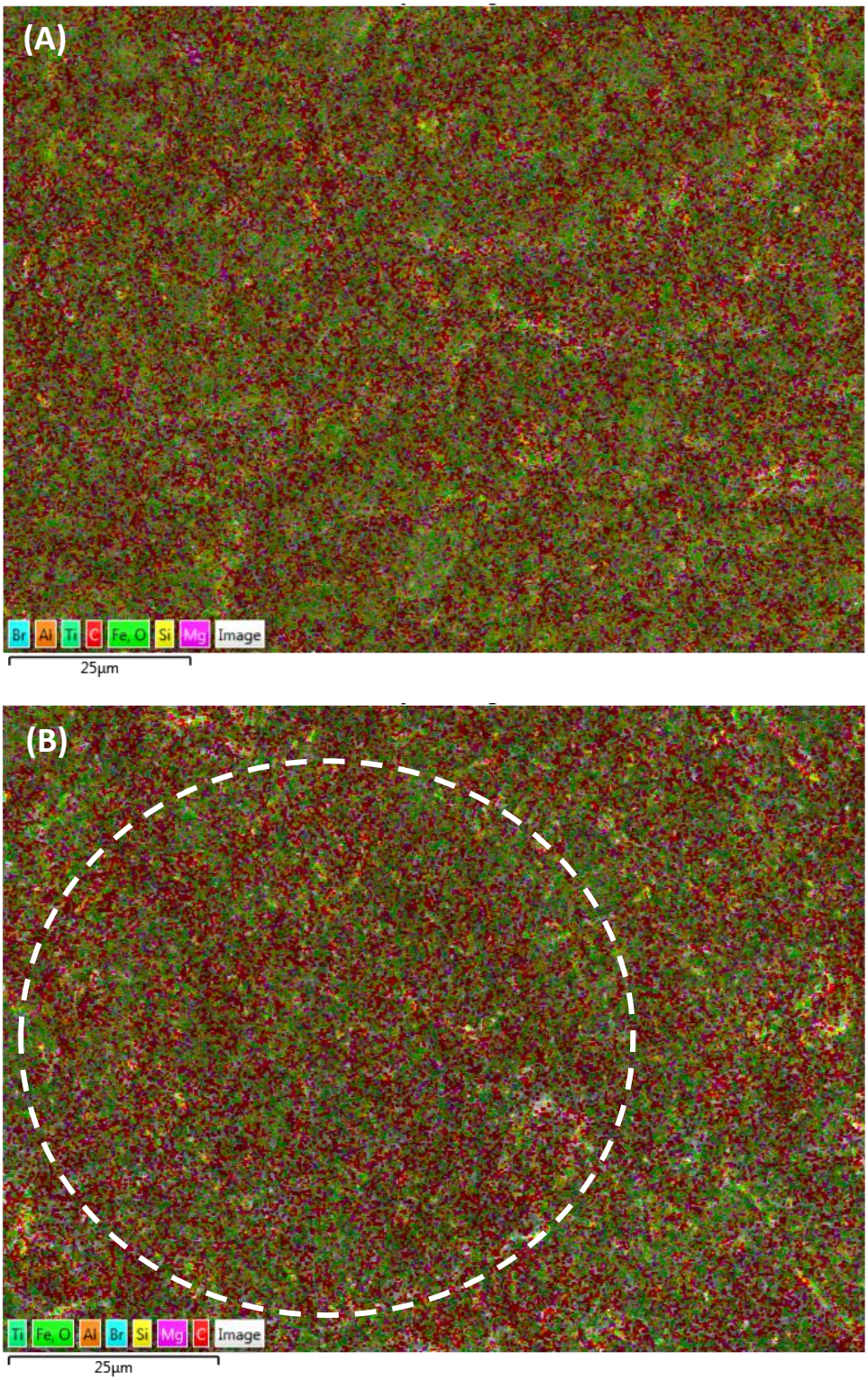


Figure 5.4: EDX elemental maps of uncoated (**A**) and poly(MPC-*co*-BMA)-coated (**B**) stoppers. The encircled area denotes a carbon rich region on the coated stopper with a carbon distribution profile that is dissimilar to that of the uncoated control.

Atomic force microscopy

To ascertain how the plasma polymer deposition technique quantitatively impacted the surface topography of the rubber, AFM was performed on flat, coated sections of halobutyl rubber flange septa. The uncoated rubber surface displayed a textured surface with a roughness of 124 ± 77 nm, manifested by larger peaks and pits, indicating an uneven surface, **Table 5.3** and **Figure 5.5**. The polymer-coated surface showed reduced peaks and pits, corresponding to a decrease in surface roughness to 93 ± 40 nm, **Table 5.3**. This is supported by the representative AFM image, **Figure 5.5B**, which show that the poly(MPC-*co*-BMA) coating smoothed the rubber surface by conforming to the topography of the material.

Table 5.3: AFM analysis of representative uncoated and poly(MPC-*co*-BMA)-coated surfaces. Data represents mean ± SD, n=3.

Characteristic measured	Uncoated control (nm)	Poly(MPC-*co*-BMA)-coated (nm)
Surface Roughness	124 ± 77	93 ± 40
Highest Peak	1564 ± 1145	597 ± 311
Lowest Pit	-908 ± 729	-473 ± 160

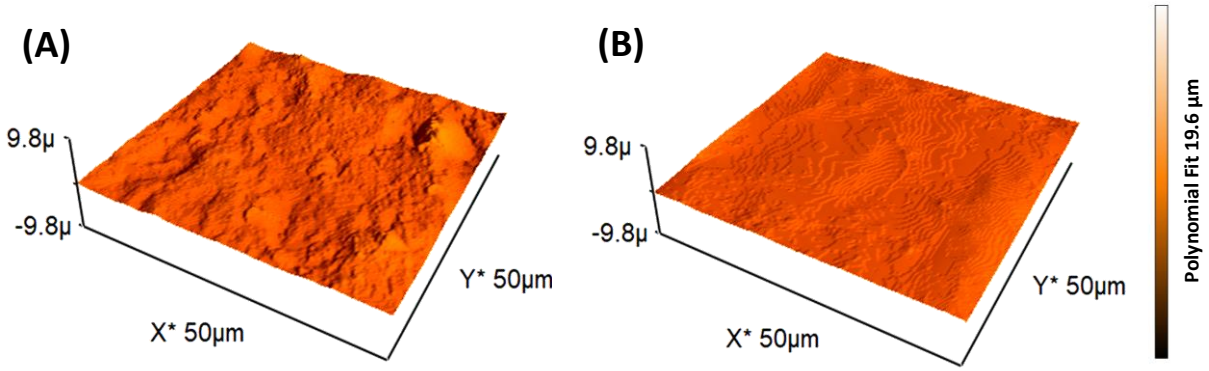
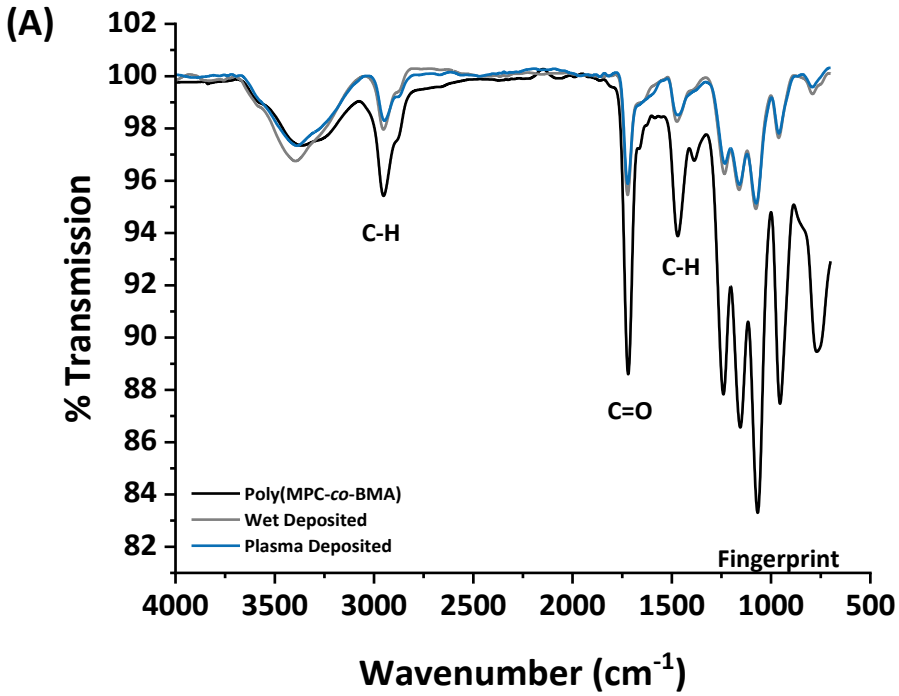


Figure 5.5: Representative AFM images showing 50 x 50 µm area on the uncoated (**A**) and poly(MPC-*co*-BMA)-coated (**B**) surfaces. Each sample was evaluated in duplicate and n=3 independent samples were analysed for the uncoated and coated halobutyl rubber flange septas.

5.4.3 Spectroscopic analysis of poly(MPC-*co*-BMA) coatings

FTIR spectroscopy of poly(MPC-co-BMA) coatings

The impact of deposition parameters on the chemistry of the poly(MPC-*co*-BMA) coating was investigated by comparing FTIR spectra of poly(MPC-*co*-BMA) powder against coatings deposited directly onto NaCl discs using plasma and wet deposition (atomised spray at 0 V) methods. The spectra for both plasma and wet deposit coatings were similar and comparable to the raw material, **Figure 5.6A**. Both spectra showed C-H bonds at approx. 2950 cm^{-1} and 1470 cm^{-1} representative of the alkane functional group. Meanwhile, C=O bonds indicate the ester functional group found in the BMA and MPC monomers are present at 1720 cm^{-1}. Overlapping peaks from the phosphorylcholine moiety are present in the fingerprint region where -$POCH_2$- and -$N^+(CH_3)$ functional groups can be observed.[355,356] Additionally, despite interference from the stopper components masking the full spectral response of the polymer, the ester functional group was observed at approximately 1728 cm^{-1} when analysing the coated stoppers, **Figure 5.6B**. This functional group has also been used to identify MPC-based coatings on other substrates.[357]



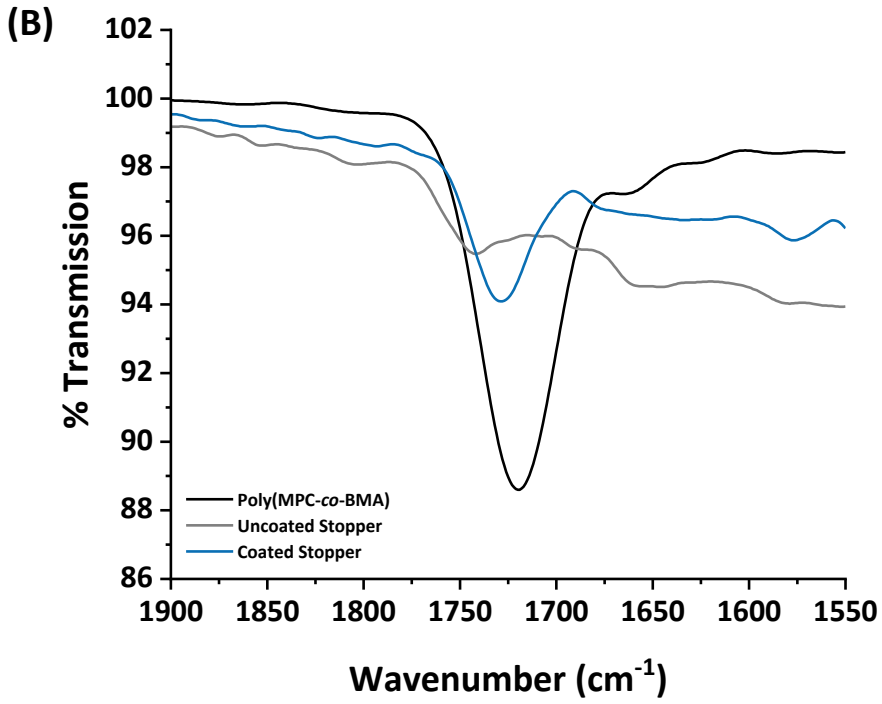


Figure 5.6: Representative FTIR spectra of poly(MPC-*co*-BMA) raw material and coatings produced on NaCl discs by wet and plasma deposition methods (**A**) and poly(MPC-*co*-BMA) immobilised on the stopper surface (**B**). Three independent samples were evaluated for each coating process to the NaCl discs.

Raman hyperspectral imaging of coating deposition

Due to the diverse chemical makeup of pharmaceutical vial stoppers, chemical identification of the polymer coating and subsequent uniformity analysis was challenging due to interference from the rubber formulation components in the stopper substate. Raman spectroscopy identified a TiO_2 signal with Raman shift peaks at 145 cm^{-1}, 397 cm^{-1}, 515 cm^{-1} and 638 cm^{-1} in the uncoated rubber stopper (**Figure S5.7**), which can be attributed to the use of TiO_2 as an inorganic pigment in rubber formulations.[358] The Raman fingerprint for TiO_2 was explored in the stopper, and Raman hyperspectral imaging was performed. Polymer coating uniformity and coverage were visualised indirectly by chemical mapping the TiO_2 signal attenuation using the uncoated stopper as a reference, **Figure 5.7**. Raman maps were generated where red indicated the signal of TiO_2 near the surface, green represented the TiO_2 signal at the midpoint, and blue represented the signal at the lowest depth measured (maximum 2 µm). The black colour represented areas where the Raman signal was oversaturated due to intense autofluorescence. As seen in **Figure 5.7A**, the uncoated stopper showed a significant amount of TiO_2 on the stopper surface, as illustrated by the uniform distribution of red corresponding to the TiO_2 signal near the surface. After poly(MPC-*co*-BMA) coating using the optimised plasma deposition parameters, run 5 (**Table S5.1**), there was a loss in intensity of the TiO_2 signal and only TiO_2 located in the deeper regions of the stopper was detected, **Figure 5.7B**. The impact of high speed on coating deposition is also shown in **Figure S5.8**.

Additionally, Z-track in-focus images were obtained as a by-product of Raman hyperspectral imaging. These images can be superimposed on the spectral data to show additional spatial chemical and micro-topographical information. Qualitatively, the images showed that the surface of the uncoated stopper displayed a variable surface topography, with the appearance of large peaks and pits, **Figure 5.7C**. By comparison, the coated stopper, **Figure 5.7D**, presented a more uniform topography and reduced the number of peaks and pits. Overall, the images suggest a more uniform surface after plasma deposition, which agrees with the AFM findings.

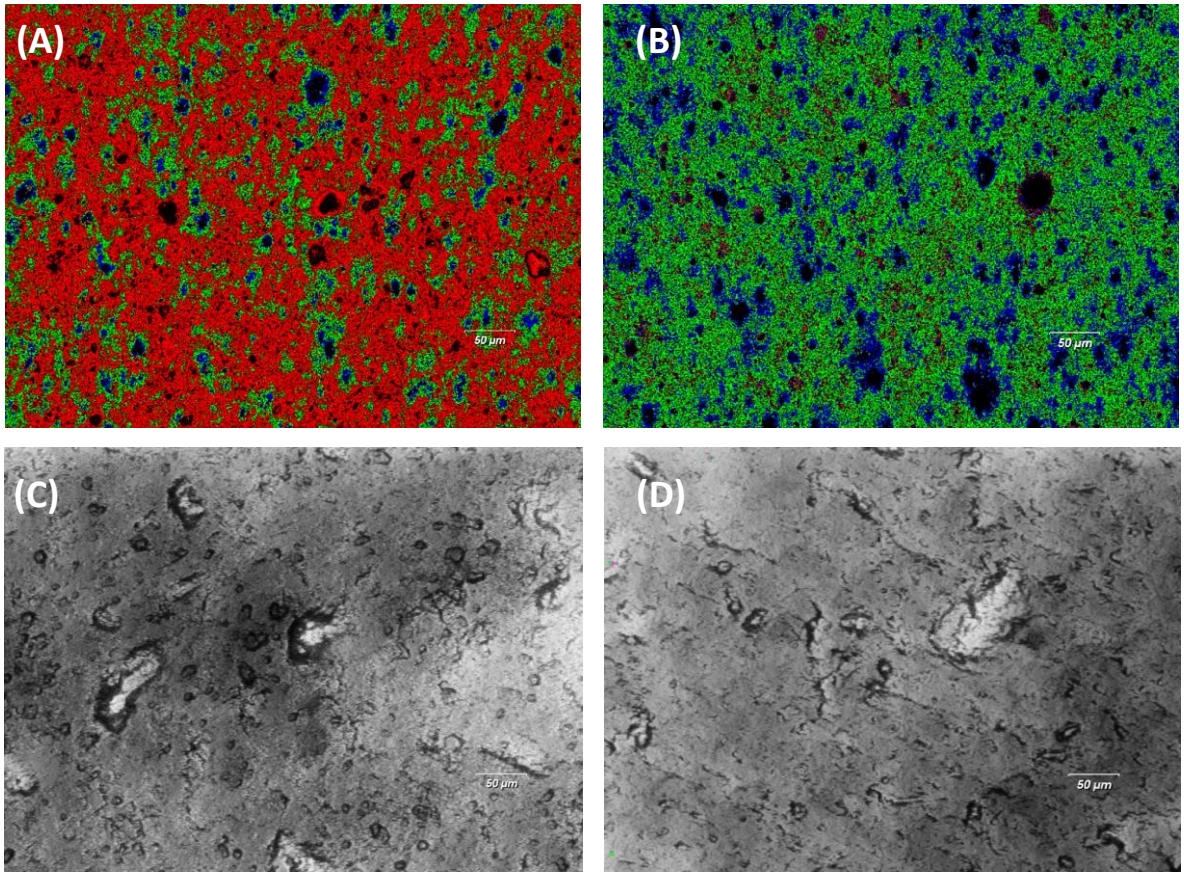


Figure 5.7: Raman hyperspectral images of the drug contact area of uncoated (**A**) and poly(MPC-*co*-BMA)-coated (**B**) stopper plugs. Red colouring indicates the signal of TiO_2 near the surface, green represents the TiO_2 signal at the midpoint, and blue denotes the signal at the lowest depth measured (2 µm). The black represents areas where the Raman signal was oversaturated due to intense autofluorescence. Topographic images of uncoated (**C**) and poly(MPC-*co*-BMA)-coated (**D**) stopper plugs. Scale bar 50 µm in all images.

Assessment of coating stability

Raman hyperspectral imaging was performed to assess the stability of the coated stoppers after exposure to different stress conditions, as outlined in **Table 5.1**. **Figure 5.8** shows that the coating degrades in patches to different extents depending on the solution or environmental stressor. This is indicated by the increased presence of the TiO_2 signal at the surface (highlighted in red) compared to the stopper controls, **Figure 5.8A**, before exposure to the aqueous solution. The sample that was subject to autoclaving, **Figure 5.8B**, exhibited the greatest degree of degradation compared to the samples subjected to the aqueous environment, indicating a potential sensitivity to elevated temperatures.

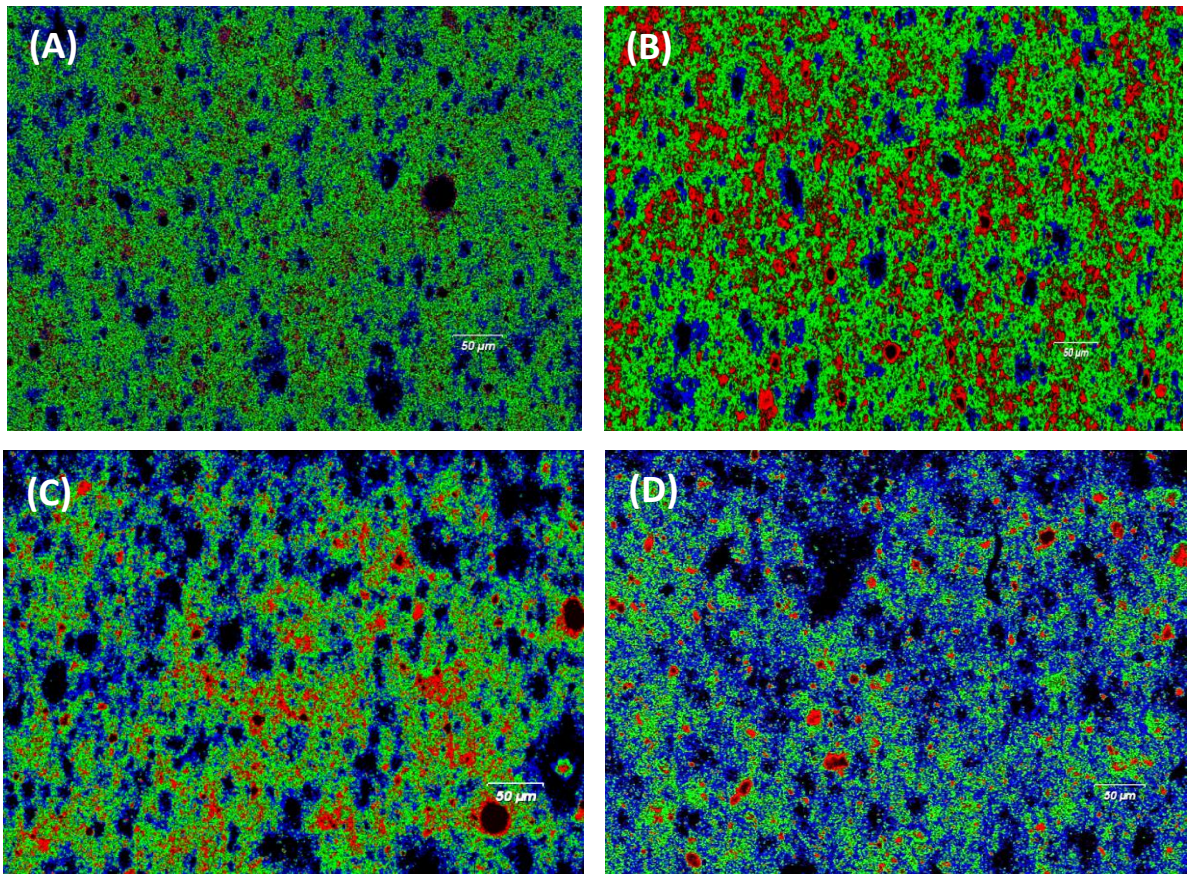


Figure 5.8: Raman hyperspectral image of the reference stopper plug (**A**), after autoclavation at 121°C for 15 minutes (**B**), immersion in water for 24 hours (**C**), and 4 weeks exposure to a placebo formulation under thermal agitation stress (**D**). Red colouring indicates the signal of TiO_2 near the surface, green is the TiO_2 signal at the midpoint, and blue is the signal at the lowest depth measured (2 µm). The black represents areas where the Raman signal was oversaturated due to intense autofluorescence. Scale bar 50 µm in all images.

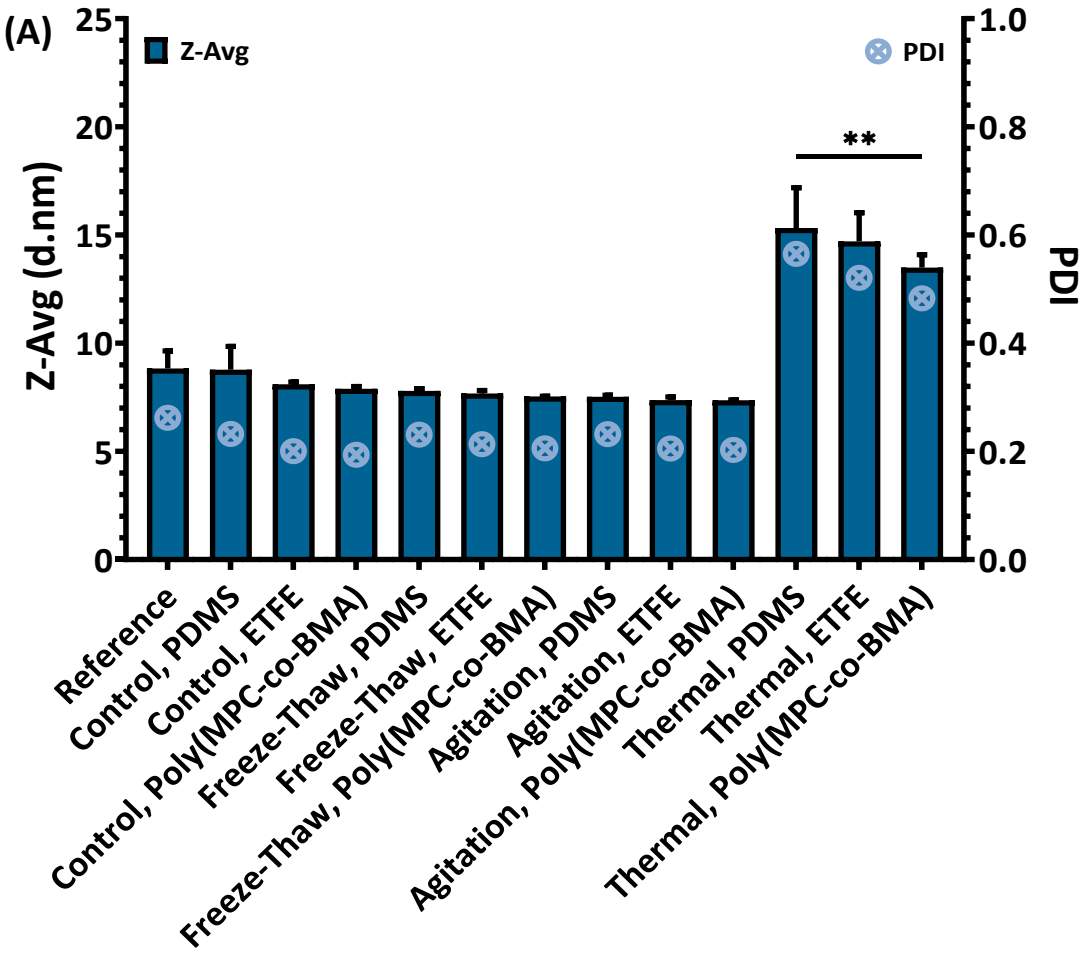
5.4.4 BSA formulation compatibility with coated stoppers

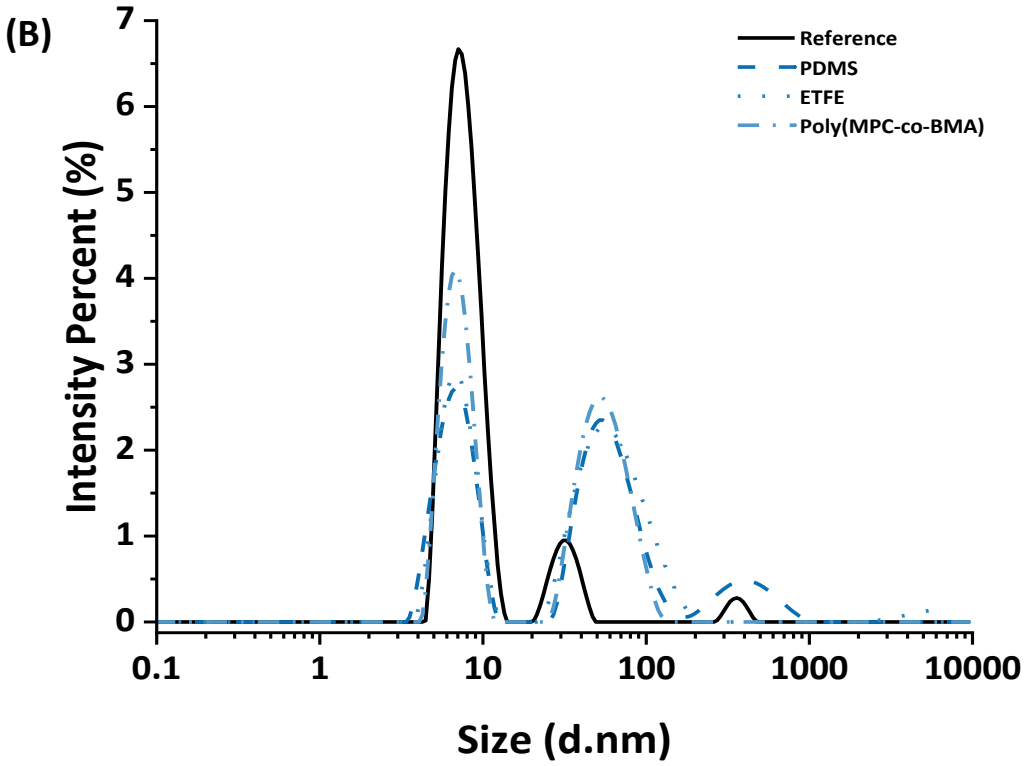
The compatibility of a model BSA formulation with the poly(MPC-*co*-BMA)-coated stoppers was probed using DLS to detect the stability of BSA on contact with the stopper and the possibility of particle generation. A reference sample was prepared to determine the Z-Avg and PDI before storage. The poly(MPC-*co*-BMA)-coated stoppers were benchmarked against commercial PDMS and ETFE-coated stoppers. The model formulation was stored in contact with different stoppers (vial inversion) for 3 months under various storage conditions, **Table 5.2**. Each storage condition was chosen to examine the effect of a range of stress conditions on protein-stopper compatibility. Control samples were refrigerated without freeze-thaw, agitation, or thermal stress to establish the impact of protein-stopper compatibility without exposure to environmental stress.

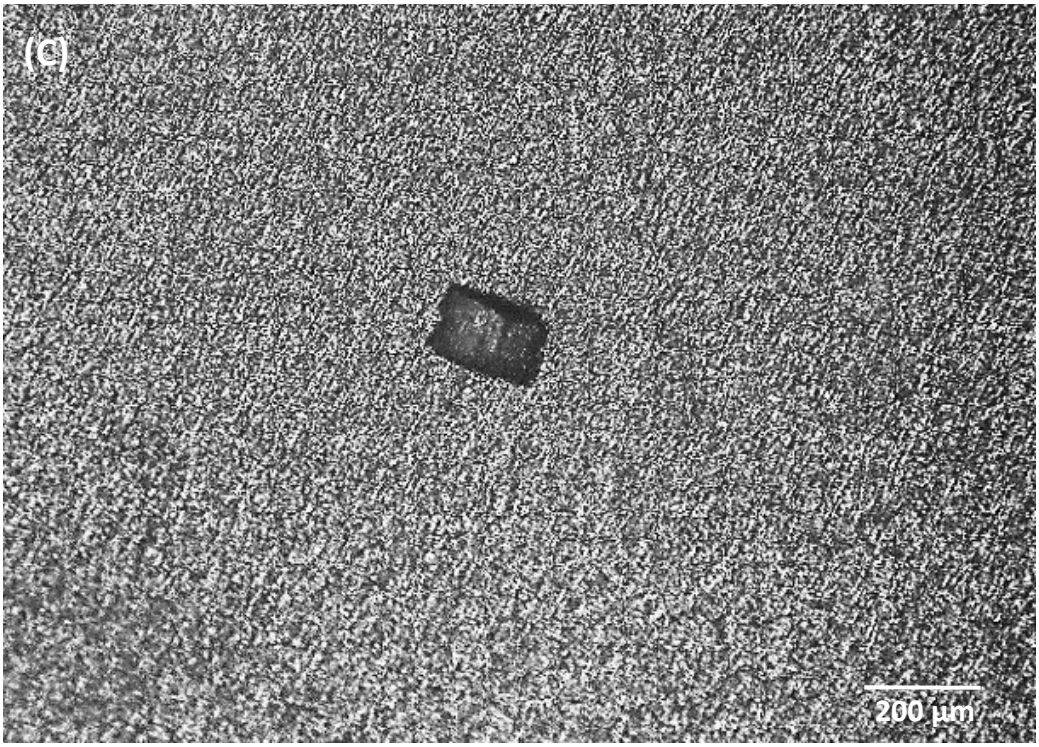
Formulations subjected to refrigeration with or without freeze-thaw or agitation stress displayed no change in Z-Avg or PDI relative to the reference, indicating that the formulation maintained the stability of BSA whilst in contact with the different stoppers investigated in this study, **Figure 5.9A**. However, the thermally stressed samples stored at 40°C for 3 months demonstrated a significant increase in Z-Avg and perturbations in polydispersity irrespective of the stopper type. However, it can be noted that the poly(MPC-*co*-BMA)-coated stopper showed marginally superior stabilising effects on BSA's stability compared to the PDMS-coated stoppers in terms of Z-Avg values. No significant differences were observed for PDI.

To interrogate the changes in Z-Avg observed when stored at 40°C, the intensity plots for the BSA formulations in contact with the different stopper types were examined, **Figure 5.9B**. The intensity plot for the reference sample showed a trimodal distribution, which changed to a bimodal distribution in the case of the formulations stored with the ETFE and Poly(MPC-*co*-BMA)-coated stoppers. The samples in contact with the PDMS stopper maintained a trimodal distribution, but an increase in the polydispersity for the third peak was observed. Additionally, all samples showed a substantial increase in the intensity and size distribution for the second peak. The peak 2 size for the reference sample was 32.6 nm and increased to approx. 55 nm for all formulations in contact with coated stoppers. The derived count rate (DCR) was also studied, identifying more particles for the PDMS and ETFE-coated stoppers than the Poly(MPC-*co*-BMA)-coated stoppers, **Figure S5.9A**. However, the particles did not contribute to the mass of the samples, as seen in the volume plot, **Figure S5.9B**.

For the formulations stored at 40°C, visible particles were observed irrespective of the stopper type, **Figure 5.9C**. Samples were collated from formulations in contact with each stopper type, dried and examined by FTIR (**Figure S5.10**) to determine if leached or detached coating material could be detected in these particles. BSA was identified, but the presence of the stopper coating was not detected. Furthermore, the stability of the poly(MPC-*co*-BMA) coating was examined for the stoppers obtained from refrigerated samples (control) after 3 months employing the Raman hyperspectral approach detailed above. The coating displayed partial degradation in patches, **Figure 5.9E**, as observed by the increased presence of the signal corresponding to TiO_2 near the surface (indicated by red colouring). However, under thermal stress conditions, the coating integrity appears to have been maintained, **Figure 5.9F**.




(B)
Intensity Percent (%)
Size (d.nm)
Reference
PDMS
ETFE
Poly(MPC-co-BMA)
0
1
2
3
4
5
6
7
0.1
1
10
100
1000
10000


(C)
200 µm

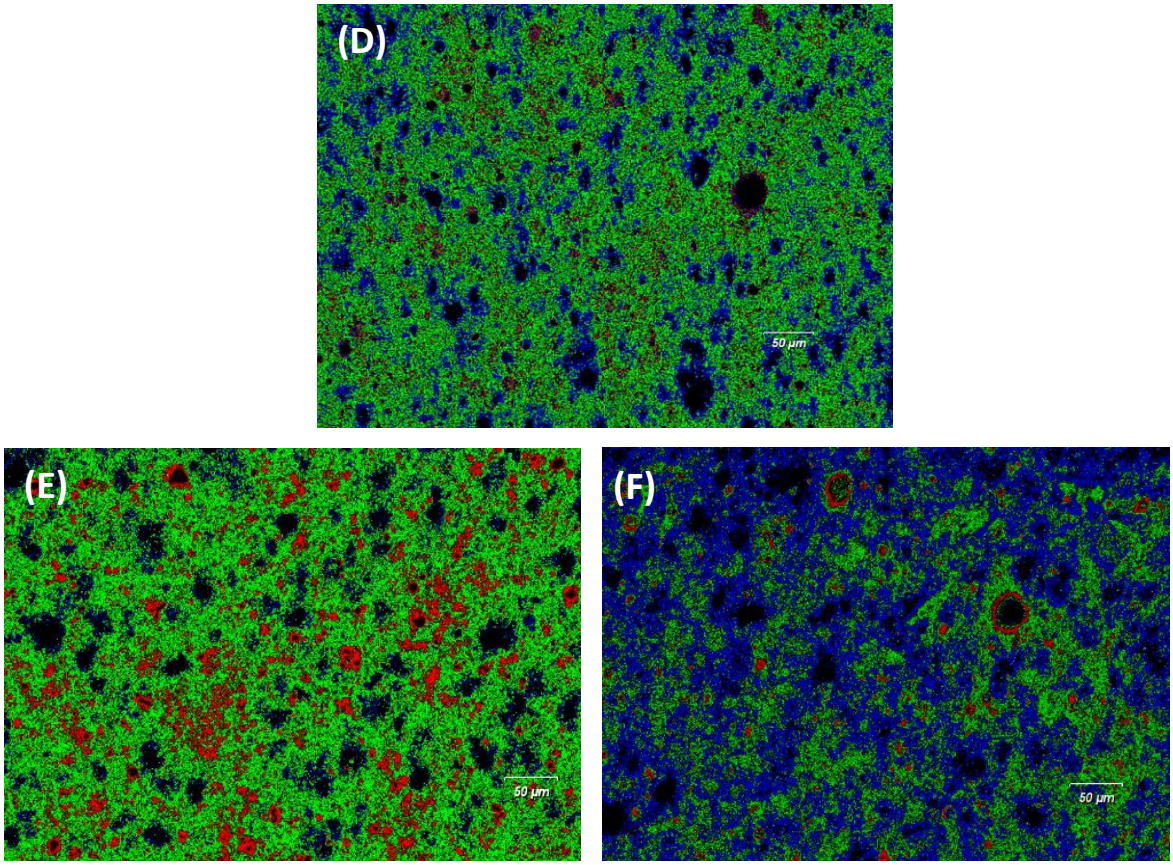


Figure 5.9: Z-Avg (blue bars) and PDI (crossed blue circles) correspond to the left and right axes, respectively (**A**), representative intensity plot of the BSA formulation stored under thermal stress conditions for each stopper type (**B**), representative light microscopy image of an isolated gel-like particle captured on an Isopore™ 0.8 µm polycarbonate membrane, scale bar 200 µm (**C**) and Raman hyperspectral image of reference (**D**), refrigerated (**E**) and thermal stress (**F**) poly(MPC-*co*-BMA)-coated stoppers after 3 months contact with the model formulation, scale bar 50 µm (**D**). Data in (**A**) represents mean ± SD, n=3, measured in duplicate. Statistical analysis was conducted using a two-way ANOVA, correcting for multiple comparisons with Tukey's post-hoc test, **p<0.01.

5.5 Discussion

Pharmaceutical packaging plays a vital role in preserving the sterility and stability of therapeutic protein formulations. However, incompatibilities between protein formulations, container/closure materials, and the coatings applied to them can compromise product integrity.[89] Optimisation of the siliconisation process to pharmaceutical glass has successfully reduced particle formation in pre-filled syringes.[97,98] However, some therapeutic protein moieties are sensitive to siliconised interfaces, prompting the investigation of alternative copolymerised PDMS and silicone-free coatings.[96,105,206] Silicone-free coatings such as fluoropolymer laminate films can reduce leachables and particles generated from packaging interfaces, including vial stoppers, and improve protein stabilisation.[65,95,96] Still, they can impact product integrity through protein adsorption and shedding under thermal stress.[65,90,95,96,324] However, outside of fluoropolymer laminate films, there is a need for viable alternative coatings for elastomeric closures. To address these limitations, this study investigated an alternative copolymer coating, poly(MPC-*co*-BMA). We successfully demonstrated the deposition of this phosphorylcholine coating on pharmaceutical vial stoppers using an innovative aerosol-assisted cold plasma deposition process. A compatibility study showed that BSA stability was retained after 3 months, and the stopper compatibility performed at least as well as commercial stopper materials.

MPC based polymers show promise as protein-resistant materials. Due to their hydration properties and zwitterionic nature, they offer an alternative to other adsorption-resistant coatings, such as PEG. Moreover, they can confer protein-resistant properties at layers as thin as 20 nm.[359] Their hydration occurs through hydration of trimethylammonium's three methyl groups, allowing water molecules to form a clathrate-like hydrogen bond network. This results in the formation of a thick hydration shell that can impair electrostatic interactions. Unlike PEG, MPC-based polymers can avoid issues like hypersensitivity and non-biodegradability.[360] Traditionally, MPC-based coatings are applied via physisorption and surface grafting techniques.[361–363] Film formation using these surface functionalisation techniques can degrade, desorb, or detach over time owing to poor coating adherence. Aerosol-assisted, low-temperature plasma can overcome this issue and is advantageous for pharmaceutical packaging applications, including the processing of temperature-sensitive

molecules, and the versatile technique can be used to coat complex 3D geometries quickly with rapid film drying.[364]

To optimise the poly(MPC-*co*-BMA) coating deposition onto bromobutyl rubber, the impact of plasma process parameters and polymer concentration were assessed using a 2^4 factorial design. Static WCA measurements were employed to monitor the changes in stopper hydrophobicity, and %RSD was used to indicate the uniformity and reproducibility of the coating (**Figure 5.1**). Unsurprisingly, the poly(MPC-*co*-BMA) coating yielded a hydrophobic surface in air post-deposition, which is attributed to the hydrophobic nature of the BMA backbone. For this study, a successful coating was defined as having a WCA ≥90° and an %RSD ≤5%. Of the 16 experimental runs, 4, 5, 10 and 13 were within range for both parameters. The optimum coating parameters were chosen as the variables corresponding to run 5 (2 mg/mL, voltage 150 V, flow rate of 100 µL/min and speed 500 mm/min). *Katayama et al*. also demonstrated that MPC-based coatings deposited on hydrophobic plastic surfaces produced a WCA in the range of 80° to 110°. *The authors* showed that a similar WCA could be anticipated where polymer concentrations greater than 1 mg/mL were used. This is beneficial as it allows for the sustainable use of MPC-based polymers at concentrations as low as 1 mg/mL once instrument parameters are optimised.[334,344] One limitation of this study was that the dynamic WCA was not analysed, so the surface reorientation of the phosphorylcholine moieties and associated WCA properties were not determined. However, these properties are widely reported in the literature.[335,342,343]

The main effects plots (**Figure 5.2**) show that higher polymer concentrations and lower voltages generally resulted in higher WCA values. However, the 8 mg/mL polymer concentration also exhibited the highest %RSD on average, even at 100 V. The difference in WCA between the 2 mg/mL and 8 mg/mL samples was minimal, with the 2 mg/mL concentration offering a significantly lower %RSD. Additionally, when evaluating low speed in conjunction with voltage, no significant differences were observed in the two-factor interaction plot, so there were no additional benefits to using low voltage to obtain a higher WCA. Studies in the literature also confirm the importance of the combination of plasma process parameters on the successful deposition of thin films and highlight the impact on film stability, especially when exposed to the aqueous environment.[106,365]

Determining layer thickness and topological properties of the surface post-deposition was challenging due to the stopper's morphology and coating conformation on the surface. However, SEM surface characterisation studies (**Figure 5.3**) suggested that the poly(MPC-*co*-BMA) coating was uniformly applied, and the surface retained its textured appearance. This was supported by EDX analysis however, the elemental mapping suggested some areas were more concentrated in carbon than others (**Figure 5.4**). It is important to note that elements specific to poly(MPC-*co*-BMA) namely phosphorus and nitrogen were not detected which may have influenced the elemental composition detected on the stopper surface and represents a key imitation of this analytical approach. AFM was performed on coated halobutyl rubber flange septas to overcome imaging challenges associated with the stopper geometry (**Figure 5.5**). AFM complimented SEM-EDX results indicating that the coated surface was uniformly smoother compared the uncoated surface, yet the surface retained its gross macroscopic features. These findings agree with other SEM and AFM results in the literature for plasma-deposited surfaces where the application of thin films did not significantly alter the gross features in the material's topography.[366,367] This smoother surface is potentially beneficial for parenteral protein formulations because the reduction in surface roughness can help minimise protein-surface interactions and adsorption.[368]

Plasma deposition has been shown to have limited effects on the chemical stability of the depositing molecules.[348–350] While the stability of the coating once deposited on the stopper surface could not be accurately assessed, the detection of the ester functional group provided confirmation of the presence of the poly(MPC-*co*-BMA) on the stopper complimenting the WCA measurements (**Figure 5.6A**). FTIR analysis of the polymer coatings on NaCl discs confirmed that the plasma process did not affect the polymer's chemical stability (**Figure 5.6B**). Indeed, other studies in the literature have identified the robustness of MPC-based polymers after surface deposition.[355,356]

It was important to assess the compatibility of the coated stoppers with a model protein formulation to verify its potential use in packaging applications. The poly(MPC-*co*-BMA) surface did not adversely affect the colloidal stability of BSA under refrigerated, agitation, or freeze-thaw conditions, demonstrating compatibility with protein stability, as confirmed by DLS measurements (**Figure 5.9A**). However, gel particle formation occurred due to inherent protein instability under thermal stress (**Figure S5.10**). The poly(MPC-*co*-BMA)-coated

stopper showed a small stabilising effect compared to PDMS commercial stoppers, evidenced by a statistically lower Z-Average value (**Figure 5.9A**). A limitation of this study was that BSA adsorption to the stopper was not performed. However, other studies have shown that BSA adsorption to poly(MPC-*co*-BMA) coatings is minimal and results in marginal changes to the conformational stability of BSA, which is notable since BSA has been observed to undergo conformational changes when adsorbed to both hydrophobic and hydrophilic surfaces.[44,341,363,369] Moreover, the stability study reveals that aggregation and gelation were more influenced by environmental conditions than the stopper interface.

An innovative use of Raman hyperspectral imaging was also used to investigate the coating coverage on the stopper, which otherwise proved challenging due to interference from rubber manufacturing components and the low phosphorylcholine content in the polymer. The novel use of Raman hyperspectral imaging successfully confirmed polymer deposition by monitoring the TiO_2 signal intensity inherent in the rubber and its attenuation due to coating (**Figure 5.7**). This approach allowed indirect imaging of the polymer coating after deposition, confirming the coating's presence. The technique also helped to assess polymer stability after exposure to common stresses encountered by elastomeric closures during biopharmaceutical manufacture and storage, such as autoclavation, and formulation components (**Figure 5.8**). It also assessed the effect of a model BSA formulation for 3 months on the coating integrity (**Figure 5.9E** and **Figure 5.9F**).

In all instances, the polymer coating demonstrated an altered surface topography with the greatest changes observed where autoclavation and contact with the model BSA formulation occurred. The impact of autoclavation was noteworthy as MPC-based coatings have been shown to have high thermal stability (≥250°C) highlighting a potential limitation of the application of this copolymer.[357] The alterations observed in the coating where 3 months of contact was maintained with the model BSA formulation (refrigerated conditions) could be a result of BSA degrading the coating which has been observed in other studies for siliconized primary packaging materials.[107] However, as shown by *Moll et al*. the alterations observed on the microscale may not necessarily indicate macroscopic changes and indeed it is possible similar phenomena occurred here and the total amount of poly(MPC-*co*-BMA) may still be present on the stopper.[221] However, as MPC-based coatings can alter their orientation on the substrate surface depending on the state of hydration, these changes can potentially be

attributed to polymer hydration effects. Analysis of the polymer material using *in-situ* analytical techniques could assist in determining if the signal attenuation is due to the polymer's flexibility on the surface.

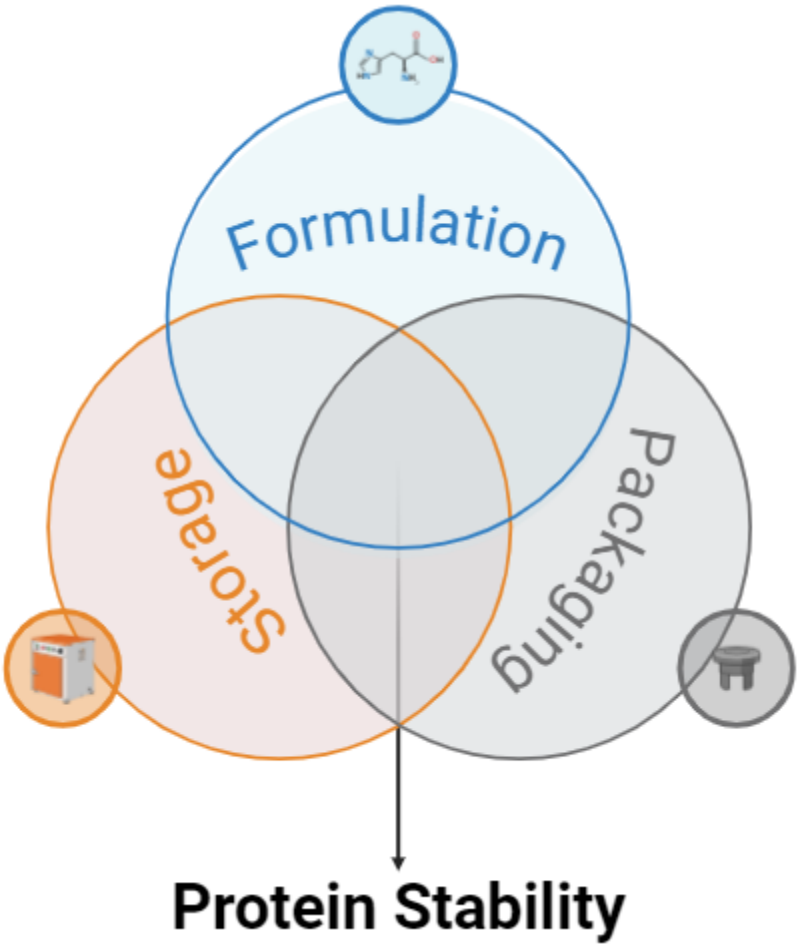
Nonetheless, the changes observed during Raman mapping, whether through hydration effects, desorption, detachment, or degradation represent a significant concern that requires further investigation. It is important to evaluate because exposure to the underlying surface can reduce the coated surface's potential to resist protein adsorption.[370] Additionally, it is crucial to assess how formulation conditions affect polymer stability, as salts can alter the stiffness of the aqueous polymer layer.[371] Further studies are needed to examine the extractables/leachables profile, as plasma activation can alter the substrate composition and lead to the breakdown of silicones and oils used in rubber formulations. More broadly speaking, exploring various MPC-based copolymers, which may also offer potential benefits for pharmaceutical packaging applications, warrants consideration as other hydrophobic backbones exist which may adhere more strongly to the vial stopper. Moreover, changes to the polarity of the deposition solution could also alter the adhesion of the polymer to the stopper and should be investigated. At the same time, an alternative approach to this study could also involve coating fluoropolymer laminate films with phosphorylcholine moieties. The fluoropolymer laminate film would provide a reduction in the leachables and extractables profile and the phosphorylcholine moieties a would confer protein-resistant properties, minimising adsorption.

5.6 Conclusion

The study demonstrated that a novel aerosol-assisted cold plasma deposition technique produced a poly(MPC-*co*-BMA) coating onto a bromobutyl vial stopper. The uniformity of the coating depended on the plasma deposition parameters, which created a uniform hydrophobic coating when optimised. FTIR analysis demonstrated poly(MPC-*co*-BMA) chemical stability following the plasma deposition. The coating produced was smooth and closely followed the contours of the stopper surface, with a reduction in the roughness of the surface due to the infilling of indentations in the stopper surface. A novel Raman imaging approach was utilised to investigate coating coverage by mapping attenuation of the stopper's TiO_2 signal following coating deposition. Interestingly, this approach could also map other polymeric stopper coatings, including commercial materials. The compatibility of the poly(MPC-*co*-BMA) coating with a model BSA formulation was demonstrated for refrigerated samples with equivalent performance compared to commercial PDMS and ETFE-coated stoppers. The study findings highlight the potential of a poly(MPC-*co*-BMA) stopper coating as an alternative to current coatings employed for protein therapeutic packaging. However, further work is required to interrogate issues related to coating integrity during long-term storage. Additionally, the findings demonstrate the capability of an optimised atmospheric aerosol-assisted plasma deposition technique to apply uniform polymer coatings to vial stoppers. Further exploration of this innovative deposition technique's potential will necessitate studies to benchmark it against current coating technologies.

Chapter Six

6. General Discussion



6.1 Research objectives and outcomes

Protein therapies are essential in modern pharmacotherapy, however, exposure to various stresses can significantly undermine their stability.[312] Interfacial hydrophobicity and charge pose significant risks to the quality, safety and efficacy of therapeutic proteins, due to the potential to cause protein unfolding and particle formation.[27] Glass-based packaging and elastomeric closures used to maintain sterility can also destabilise the protein.[65] Glass-based packaging can be ionised in solution, generating a strongly anionic surface which promotes protein adsorption.[114] Furthermore, where the solution conditions are near the protein's IEP, an interplay between electrostatic and hydrophobic interactions occurs during adsorption.[114] Moreover, the elastomeric closures and their coatings are inherently hydrophobic and are known to cause protein adsorption, unfolding, and particle formation and are prone to leaching into solution.[89,90,95]

Despite this understanding, there have been no investigations utilising *in-situ* analysis techniques into the impact of buffering excipients on protein adsorption to borosilicate glass surfaces. This is important because buffering excipients regulate solution pH and can modify the surface charge and hydrophobicity of therapeutic proteins.[50] Furthermore, there is scope to examine novel formulation approaches to replace surfactants in protein formulations. Hydrophobic excipients, such as amino acids, have the potential to alter protein adsorption and stability at hydrophobic interfaces but have received little attention to date. Additionally, elastomeric closures, which are subject to protein interaction during syringe aspiration, have received less attention in the literature compared to glass packaging surface and scope exists to explore protein-resistant coatings for elastomeric closures to minimise adsorption.[105]

Understanding the interactions at the protein-excipient-packaging interface is critical to achieving a successful biotherapeutic product. Therefore, the overall aim of this thesis was to explore the impact of packaging interfaces and formulation on the adsorption and stability of two model proteins, lysozyme and BSA, and develop novel formulation and packaging mitigation strategies to minimise the adverse impact of protein adsorption.

6.1.1 Thesis findings

Formulation effects

Buffering excipients are the most critical excipient class used in protein formulations. Buffers control the pH of the solution, maintain the therapeutic protein's stability and activity, and balance the interactions between proteins and packaging interfaces.[50] However, buffer type is informed by the protein's IEP and trends in commercial formulations but their potential effects on adsorption are not the foremost consideration. This thesis determined that the choice of buffering excipient has limited influence on lysozyme adsorption to borosilicate glass and that solution pH can control the charge of the borosilicate interface and influence protein-glass interactions (**Chapter Three**). Interestingly, in some cases, buffer type affected the type of protein layer formed as shown by QCM-D analysis. Histidine buffer pH 5.5 promoted the formation of a hydrated film as measured by the D/F ratio and variability in the dissipation factor over the measured overtones. This effect has also been reported by *Wang et al*. for lysozyme adsorption to borosilicate.[244] Similar variabilities in the dissipation factor were noted for the citrate buffer at pH 5.5, but the effects were smaller in comparison.

Solution pH had more significant effects on film formation as at pH 3.6, the film was likely sub-monolayer in nature. Low dissipation coupled with low-frequency values has also been identified in the literature to be associated with a sparsely populated protein film.[304] At pH 5.5 and above, a densely packed monolayer was postulated to have formed owing to the low dissipation and high-frequency values, which have also been seen in other literature.[141,304] The poor reversibility of adsorption measured using QCM-D (buffer perfusion step) supports this in addition to the low dissipation values and frequencies obtained. Protein concentration was the other factor that altered the layer formation. Higher concentrations were shown to create a thicker and more hydrated film.[244] The use of histidine buffer at the higher protein concentration continued to produce variability in the dissipation factor measured however the values obtained were larger, signifying viscoelasticity. The pathway to layer formation was also altered as two adsorption events were noted, one at the -10 Hz to -20 Hz range, which produced no change in the dissipation, suggesting a dense and rigid layer formed on the sensor. This was followed by a steep decline in frequency and increased dissipation, indicating that the second layer interacts with the first adsorbed protein layer and incorporates interfacial water.[189]

Interestingly, while not considerably altering the stability of lysozyme, the amino acid buffers were found to increase lysozyme's melt temperature as measured by DSF (**Chapter Three**). Additionally, the solution pH was also found to affect lysozyme stability, with pH 7.4 reducing the protein's thermal stability. This impacted the adsorption behaviour as the lower the thermal stability, the greater the protein adsorption. This work agrees with a study by *Fujita et al*., who correlated protein melt temperatures with adsorption to polyolefin packaging surfaces.[283]

Similarly, the change in pH affected the zeta potential of both the lysozyme and the borosilicate, which acted as the primary driving force for adsorption. Despite the charge inversion effects produced by citrate buffer, the strongly anionic nature of the borosilicate maintained the same quantity of adsorbed protein at pH 5.5 as the histidine buffer. This agrees with *Mathes* and *Friess*, who were the first to identify electrostatic-mediated protein adsorption to borosilicate glass.[114] However, where this study identified the importance of the borosilicate surface charge, *Mathes* and *Friess* identified the importance of the protein surface charge, especially around the solution and surface IEP, as protein adsorption can increase at these values due to a loss in charge repulsion effects. Regardless, both studies reveal the necessity to balance the electrostatic forces between the protein and the surface, with the most suitable mitigation strategy being to have them bear the same net charge or include surface active excipients.

To find alternatives to surfactant stabilisers to control hydrophobic interface-induced instability, novel formulation approaches revealed that prioritising BSA's conformational stability, was important to reduce aggregation at hydrophobic interfaces (**Chapter Four**). Leucine, which has shown promise in protein formulations as an aggregation suppressor, did not stabilise BSA's conformation.[316] Consequently, greater unfolding and aggregation occurred when BSA was exposed to hydrophobic interfaces during inverted storage. Leucine reduced the formation of small aggregates of BSA however, it appeared to do so by altering its aggregation pathway toward forming particles >100 nm in size. This was variable as leucine was found to maintain BSA in near-native conditions at 50 mM and 100 mM based on Z-Avg values for upright storage orientation under thermal agitation stress, suggesting a potential packaging incompatibility concern regarding its use. Despite the limitations, leucine may be effective in combination with other amino acids or for other proteins or destabilising

conditions. Mixtures of aliphatic, hydrophobic amino acids with charged amino acid residues have previously been identified to promote conformational and colloidal stability.[289] Additionally, it may be suitable for protein products stored under refrigerated or ambient conditions to maintain protein stability. Further work is required to elucidate if its weak surfactant-like properties could support its use as an interfacial stabiliser for protein formulations.[250,257]

While not the focus of **Chapter Five**, the effect of a model formulation was examined with different vial stopper materials. The formulation proved capable of maintaining the stability of BSA for three months under refrigerated conditions when exposed to freeze-thaw and agitation stresses. However, intrinsic protein instability was observed at prolonged elevated temperatures, negating the stabilising effects of the formulation, as evidenced by BSA's gelation.

Storage conditions

Preserving a therapeutic protein's physical stability is dependent on how it is transported and stored. Proteins can transition from their native conformation to either an intermediate unfolded or unfolded state on exposure to elevated temperatures (e.g., >40°C).[312] They also aggregate and form soluble and insoluble particles with prolonged heat exposure, interfacial contact with air, or exposure to mechanical stresses such as mixing, stirring, and shaking.[18,20,312] This was evidenced in **Chapter Four**, where BSA was identified to become unstable at 40°C under shaking conditions during short-term (7 days) storage leading to unfolding and aggregation compared to refrigerated or ambient storage conditions. Shaking promotes protein-protein interactions by disrupting Brownian motion and increasing the potential of protein-protein collisions in aqueous solution. Interestingly, sub-visible particles were identified to form in **Chapter Four**, while visible BSA gel particles formed in the samples after three months of quiescent storage at 40°C in **Chapter Five**. Despite differences in the formulation and the absence of agitation (**Chapter Five**) both studies displayed BSA particles of approx. 40-55 nm in size in addition to particles >100 nm in size. This confirms that BSA is an unstable, thermally reactive, aggregate-prone protein with a tendency to gel.

Elevated temperatures are also associated with higher levels of protein adsorption. Increasing the temperature of the storage environment can reduce the solution viscosity.

Consequently, Brownian motion is accelerated, and adsorption is promoted by increasing the diffusivity of the protein toward the surface.[308] This was observed in **Chapter Three**, where increased lysozyme adsorption was measured upon increasing the temperature of the storage environment. This is typically associated with the protein being in an intermediate unfolded state however, for structurally rigid proteins such as lysozyme, increased adsorption can more likely be linked to changes in the solution conditions rather than alterations in the protein's physical stability as suggested by *Forov et al*.[372]

Formulation-packaging interactions

Secondary to rational formulation design is the choice of packaging container. Ideally, the choice of primary container/closure system should go hand in hand with the formulation design. Consideration of packaging interactions during formulation design can highlight excipient-container/closure incompatibility when exposed to external stressors which can adversely affect protein stability.[89,90,95]

Significant differences were observed when examining the changes in protein physical stability using BSA when in contact with different packaging interfaces for **Chapter Four**. While BSA stability is more sensitive to the storage conditions, where contact with the vial stopper was established (inverted storage), BSA was shown to have an altered conformation and presented a greater number of aggregates in aqueous solution under thermal agitation conditions. This behaviour was observed for stoppers with either a thin PDMS or ETFE laminate film coating. These findings agree with those of *Teska et al*. and *Dasnoy et al*., who identified that vial stopper contact and a large vial headspace could induce protein instability in the form of particle formation and precipitation.[95,270] However, in the absence of stress conditions, protein-packaging interactions had no adverse effect on BSA's stability. Comparable findings were obtained in **Chapter Five**, where three vial stopper coatings were evaluated. In the absence of thermal stress conditions, BSA-stopper interactions did not induce instability and maintained BSA in its native conformation. However, prolonged exposure to thermal stress conditions produced BSA gel particles, and the Z-Avg and PDI values obtained were similar to those in **Chapter Four**. Additionally, the formulations in contact with PDMS stoppers in **Chapter Five** had sub-micron particles in solution, which were not observed in **Chapter Four**, highlighting the risks associated with prolonged exposure to

siliconised surfaces at high storage temperatures. This thesis demonstrates that inverted storage under elevated temperatures can be detrimental to protein stability on exposure to external stressors due to the presence of two hydrophobic interfaces, i.e., vial stopper and vial air headspace.

Stoppers represent challenging primary packaging materials that can impact product integrity and safety. They are responsible for maintaining product sterility, yet they can be inherently destabilising packaging interfaces.[65] Their requirement for a surface coating is a significant challenge of their application in pharmaceutical packaging. Typically, stoppers are washed in PDMS to create a thin silicon emulsion film on the surface to enhance the lubricity of the material. However, this approach does not covalently bond the PDMS to the stopper, explaining why silicone oil leachables can be observed in commercial protein formulations.[72] To overcome this issue, fluoropolymer laminates can be bonded to the stopper using heat sealing and have proven effective at preserving product integrity and safety.[65] However, laminate films are susceptible to degradation under thermal stress conditions and in the presence of surfactants.[90] Additionally, they are also susceptible to protein adsorption.[324] Ideally, stopper coatings should be thin, covalently bonded, and adsorption-resistant. To obtain thin film coatings, aerosol-assisted cold plasma is an innovative and viable approach which was employed in **Chapter Five** to create a novel, strongly adherent, adsorption-resistant vial stopper coating using poly[MPC-*co*-*n*-BMA] (poly(MPC-*co*-BMA)).[106]

To determine the parameters which influence plasma deposition a DoE approach was applied for **Chapter Five**. The deposition of the polymer coating was found to be affected primarily by the speed of the nebuliser, especially when coupled with the solution flow rate, applied voltage and polymer concentration. However, when optimised, a uniform coating was achieved on the stopper surface with reduced surface roughness. This is beneficial as reduced roughness will limit the surface area, minimising protein adsorption.[368] However, the stability of the polymer coating appeared to be compromised by elevated temperature (121°C) and the aqueous environment. This presents a potential limitation of the applied approach which requires further investigation to fully elucidate coating stability. However, it can be noted that the poly(MPC-*co*-BMA) coating in the aqueous solution, placebo and model protein formulation showed equivalent stabilities however, it showed greater sensitivity when exposed to BSA.[107] Moreover, even though protein gelation has been reported to occur at

packaging interfaces, owing to the thermal instability exhibited by BSA, gelation was likely initiated in solution and is unlikely to be associated with the stopper interface.[21,373] This is supported by the DLS and SEC studies in **Chapter Four** which showed that BSA can undergo self-association and aggregation in as little as 7 days. However, the innovative use of Raman mapping proved useful in determining the effects of different solution and storage environments on the stopper coating stability.

Analysis techniques

Throughout this thesis, numerous techniques were used to measure protein adsorption and stability when in contact with different commercial packaging materials and formulations. A broad range of techniques (**Table S6.1**) were applied due to the lack of available *in-situ* analysis methods to measure adsorption and stability within the packaging system.[374,375] This thesis demonstrated novel applications for two instruments, the QCM-D (**Chapter Three**) and Raman hyperspectral imaging (**Chapter Four**).

QCM-D is a surface-sensitive microbalance that operates in aqueous conditions. It has predominantly been used to examine the impact of surfactants on protein adsorption to PDMS, SiO_2, borosilicate, PTFE and manufacturing surfaces.[64,244,324] QCM-D has scope for utilisation in other areas of formulation development, such as investigating the optimum solution conditions to minimise adsorption. This would be beneficial for determining the impact of pH and ionic strength on adsorption and the subsequent effect of layer formation on particle formation. As seen in **Chapter Three**, QCM-D was beneficial for determining pH effects on protein adsorption including determining the hydration properties which is a unique feature of this analytical technique. QCM-D even shows promise for use as a predictive tool for protein stability as demonstrated by *Weidman et al*. and more routine use of QCM-D would optimise formulation development studies and circumvent the consequences associated with protein adsorption.[299]

Raman mapping is a standard analytical tool used to understand the distribution of chemical, structural, and spatial arrangement of moieties within a sample. It is primarily employed in the pharmaceutical sector to analyse the surface, depth, and size distribution of active ingredients of solid products.[376] In **Chapter Five**, a novel application of Raman mapping was employed to study pharmaceutical packaging and coatings. It assisted in characterising

the stopper surface and the distribution of the polymer surface coating and identified where changes in coating uniformity occurred. This was achieved by tracking the signal attenuation of TiO_2 in the stopper composition. Additionally, it was able to distinguish the effects of both autoclavation and solution conditions on coating stability. However, the application of Raman mapping has limitations, as seen with the interplay between the interference of the vial stopper components and the thinness of the deposited poly(MPC-*co*-BMA) layer. Combining Raman mapping with additional techniques capable of analysing thin polymeric coatings would be invaluable for packaging manufacturers to determine coating integrity.

Protein stability

Lysozyme and BSA have well-defined physicochemical properties and are widely used as models within protein studies. However, the work presented in this thesis highlighted some interesting findings on the stability behaviour of these two proteins which should be considered when assessing their stability with respect to formulation and packaging design. CD spectroscopy showed that lysozyme, when exposed to elevated temperatures, displayed marginal differences in both the signal intensity and alpha helix content estimated after spectral deconvolution (**Chapter Three**). However, BSA displayed a significant reduction in the spectral intensity and was identified to be in an unfolded state in solution above 40°C and an aggregated state above 60°C (**Chapter Four**). Comparing the thermal stability of both proteins in a 10 mM Na-Phos buffer pH 7/7.4 studies showed lysozyme's melt temperature was 68°C, whereas BSA's melt temperature was within the range of 50-60°C (**Chapter Three** and **Chapter Four**). Additionally, DLS and SEC showed that both proteins also had different native size distributions. Lysozyme was found to be monomeric, but BSA was found to be heterogenous, likely consisting of monomers and small amounts of dimer/trimer (**Chapter Three** and **Chapter Four**).[375,377]

The differences in both proteins can be attributed to their shape and structures. Due to its rigid, compact, ellipsoidal, globular structure, lysozyme can maintain its stability via hydrophobic interactions, van der Waals forces and salt bridges.[141,378] Moreover, due to the asymmetric distribution of its charged and hydrophilic residues, lysozyme can also interact with water in its surrounding environment, promoting stability.[110,111] BSA, however, is more unstable. Compared to lysozyme, BSA is a larger protein with a less compact and elongated

asymmetric structure. As protein shape and size increase, the effectiveness of the internal stabilising forces decreases. Furthermore, BSA is a flexible, elliptical heart-shaped protein consisting of three domains, each with several alpha helices with their own hydrophobic pockets.[115] This conformation makes BSA prone to unfolding and aggregation, as it does not have a well-defined core. BSA also has more charged residues than lysozyme, which makes it highly sensitive to the solution environment.[115] In the design of protein therapeutics, the protein's intrinsic structural stability is critical to consider with respect to storage conditions, formulation and packaging.

6.1.2 Thesis highlights

Highlights of thesis research can be summarised into the following points:

- Lysozyme adsorption to borosilicate is mediated by solution pH. Buffer type and pH can affect layer properties such as hydration. Protein concentration influences the type of layer formed (**Chapter Three**).
- Commercial primary packaging interfaces have a limited impact on BSA's stability however, inverted storage can induce marginally higher unfolding and aggregation because of BSA-stopper interactions. BSA is more likely to unfold and aggregate when exposed to changes in the solution and environmental conditions (**Chapter Four**).
- Atmospheric aerosol-assisted plasma deposition showed promise for depositing a thin poly(MPC-*co*-BMA) film to the surface of vial rubber stoppers. Polymer-coated stoppers performed as well as commercial ETFE stopper coatings performed during the stability study. The application of Raman mapping proved useful for monitoring the uniformity of coatings on the surface of commercial primary packaging systems (**Chapter Five**).

6.1.3 Limitations

Limitations of thesis research can be summarised into the following points:

- This work was performed using model proteins, lysozyme and BSA, which have some similar characteristics to biotherapeutics but are not entirely representative of therapeutic protein adsorption and stability behaviour.

- The structural stability of lysozyme was not examined on the surface of the QCM-D sensor or in contact with commercial borosilicate glass vial packaging (**Chapter Three**).
- In **Chapter 4**, quantitation of BSA adsorption to the different packaging components was not performed, hence its contribution to aggregate formation was not delineated. A simple formulation approach was also undertaken, and a small number of conditions were investigated. A broader investigation of leucine in comparison/combination with other amino acids, cyclodextrins or surfactants might have yielded a more successful formulation. Moreover, examining BSA stability using thermal and agitation stress independently would decouple the effects of each stress condition on aggregation.
- *In-situ* characterisation of the polymer coating to determine its properties in aqueous media and the use of a surface-sensitive technique to analyse specific functional groups in the deposited polymer would have provided more detailed information and complimented the top-view WCA and Raman mapping techniques employed in **Chapter Five**. Additionally, the leachables profile was not investigated.

6.1.4 Future work

The research presented in this thesis suggests that primary packaging interfaces play a minor role in lysozyme and BSA's instability and that the protein's intrinsic characteristics, formulation, and environmental conditions have a more significant impact.

Future work is recommended in the following areas:

- Studies that quantify therapeutic protein adsorption and characterise protein structural stability *in-situ* is a critical area that needs further research. At present, a combination of analytical methods is required to measure both adsorption and stability independently. Of the available techniques reported to analyse both, e.g., QCM-D, the stability data obtained is complex to process and easy to misinterpret. Combining QCM-D with FTIR microspectroscopy could provide a route to assess adsorption and protein stability on the surface accurately.
- Combinations of amino acids have been reported to stabilise protein formulations, effectively replacing surface-active agents. However, further work on hydrophobic

amino acids is required to understand protein-excipient-packaging interactions. Mixtures of hydrophobic amino acids with arginine-glutamate and arginine-aspartate systems in histidine or glycine buffers may provide a simple route to optimal stabilisation of the therapeutic moiety.

- The vial stopper is undeniably a problematic interface and further research into the application of the phosphorylcholine-based polymer is required. The deposition of poly(MPC-*co*-BMA) to uncoated and fluoropolymer-coated stoppers should be compared for protein adsorption and stability with a focus on particle counting technologies using a surface-sensitive therapeutic protein such as Ig. Additionally, the repeated deposition of coatings to increase the thickness and a leachables/extractables study should be performed to determine if noteworthy effects can be observed. Characterisation of the polymer's water-responsive behaviour also requires analysis *in-situ* to understand the hydration properties. Furthermore, different deposition techniques, such as physisorption, should be compared to the plasma-deposited coating for stability. However, it may also be judicious to study the application of plasma deposition for commercial fluoropolymer coatings and examine their stability compared to the laminate film coating.

6.1.5 Conclusions

This thesis explored the impact of packaging interfaces and formulation on protein adsorption and stability and studied novel formulation and packaging mitigation strategies to minimise the adverse effect of protein instability and adsorption. The primary aim of investigating the role of primary packaging interfaces was achieved, and for the model proteins lysozyme and BSA, interfacial stress played a small role in adsorption and stability. Minimal adsorption for lysozyme was noted for the uncoated and SiO_2-coated commercial vials, even under thermal stress conditions however, long-term studies and low protein concentration formulations might present different results. Sustained contact with the vial stopper using inverted vial storage for 7 days was observed to induce more BSA aggregate formation in an aqueous solution compared to upright storage.

However, the combination of the formulation and storage environments had a more significant impact on BSA stability during storage studies compared to packaging

configuration. It was found that the formulation investigated had a marginal impact on lysozyme stability but led to the destabilisation of BSA, highlighting the importance of investigating each protein based on knowledge of its physicochemical properties. However, where contact with the vial stopper is maintained, formulation approaches to maintain protein stability may be negated especially under elevated storage temperatures. This is possibly due to the packaging system's hydrophobic interfaces, i.e., the vial stopper and air headspace. This would suggest that surfactants are still the optimum choice of stabiliser for hydrophobic packaging interfaces.

Novel packaging strategies such as the poly(MPC-*co*-BMA) stopper coating indicated that vial stoppers were suitable for coating with innovative polymers. Moreover, the cold plasma deposition process provided a viable alternative approach for the coating of thin polymer films to the surface of primary packaging surfaces. However, further investigation is warranted to optimise the deposition process and confirm suitability with surface-sensitive therapeutic proteins. Furthermore, confirming the stability of the polymer on the vial stopper has the potential to highlight a superior deposition process. Additional research into the role of the vial stopper and its coatings is essential to preserve the biotherapeutic's medicinal value, safety and efficacy, as they have been demonstrated to compromise product integrity.

References

(1) Gervasi, V.; Dall Agnol, R.; Cullen, S.; McCoy, T.; Vucen, S.; Crean, A. Parenteral Protein Formulations: An Overview of Approved Products within the European Union. Eur J Pharm Biopharm 2018, 131, 8–24. https://doi.org/10.1016/j.ejpb.2018.07.011.
(2) Ebrahimi, S. B.; Samanta, D. Engineering Protein-Based Therapeutics through Structural and Chemical Design. Nat Commun 2023, 14 (1). https://doi.org/10.1038/s41467-023-38039-x.
(3) Wu, J.; Sahoo, J. K.; Li, Y.; Xu, Q.; Kaplan, D. L. Challenges in Delivering Therapeutic Peptides and Proteins: A Silk-Based Solution. Journal of Controlled Release 2022, 345, 176–189. https://doi.org/10.1016/j.jconrel.2022.02.011.
(4) Akbarian, M.; Chen, S.-H. Instability Challenges and Stabilization Strategies of Pharmaceutical Proteins. Pharmaceutics 2022, 14 (11). https://doi.org/10.3390/pharmaceutics14112533.
(5) Wang, W. Protein Aggregation and Its Inhibition in Biopharmaceutics. Int J Pharm 2005, 289 (1–2), 1–30. https://doi.org/10.1016/j.ijpharm.2004.11.014.
(6) Morris, R.; Black, K. A.; Stollar, E. J. Uncovering Protein Function: From Classification to Complexes. Essays Biochem 2022, 66 (3), 255–285. https://doi.org/10.1042/EBC20200108.
(7) Guo, W.; Shea, J.; Berry, R. S. The Physics of the Interactions Governing Folding and Association of Proteins. Ann N Y Acad Sci 2006, 1066 (1), 34–53. https://doi.org/10.1196/annals.1363.025.
(8) Dobson, C. M. Protein Folding and Misfolding. Nature 2003, 426, 884–890. https://doi.org/10.1038/nature02261.
(9) Chiti, F. Relative Importance of Hydrophobicity, Net Charge, and Secondary Structure Propensities in Protein Aggregation. In Protein Misfolding, Aggregation, and Conformational Diseases; Springer US, 2006; Vol. 4, pp 43–59. https://doi.org/10.1007/0-387-25919-8_3.
(10) Pham, N. B.; Meng, W. S. Protein Aggregation and Immunogenicity of Biotherapeutics. Int J Pharm 2020, 585. https://doi.org/10.1016/j.ijpharm.2020.119523.
(11) Tamizi, E.; Jouyban, A. Forced Degradation Studies of Biopharmaceuticals: Selection of Stress Conditions. Eur J Pharm Biopharm 2016, 98, 26–46. https://doi.org/10.1016/j.ejpb.2015.10.016.
(12) Nowak, C.; K. Cheung, J.; M. Dellatore, S.; Katiyar, A.; Bhat, R.; Sun, J.; Ponniah, G.; Neill, A.; Mason, B.; Beck, A.; Liu, H. Forced Degradation of Recombinant Monoclonal Antibodies: A Practical Guide. MAbs 2017, 9 (8), 1217–1230. https://doi.org/10.1080/19420862.2017.1368602.
(13) Campbell, J. M.; Colombo, S.; Doyle, J. L.; Filoti, D. I.; Hübner, G.; Magnenat, L.; Nowinski, A. K.; Pavon, J. A.; Singh, S. M.; Vo, L. R.; Woods, J. M.; Stokes, E. S. E. An Industry Perspective on the Use of Forced Degradation Studies to Assess Comparability of Biopharmaceuticals. J Pharm Sci 2024, 113 (3), 505–512. https://doi.org/10.1016/j.xphs.2023.12.011.
(14) Velankar, K. Y.; Gawalt, E. S.; Wen, Y.; Meng, W. S. Pharmaceutical Proteins at the Interfaces and the Role of Albumin. Biotechnol Prog 2024. https://doi.org/10.1002/btpr.3474.
(15) Philo, J.; Arakawa, T. Mechanisms of Protein Aggregation. Curr Pharm Biotechnol 2009, 10 (4), 348–351. https://doi.org/10.2174/138920109788488932.

(16) Yazdanparast, R.; Esmaeili, M. A.; Khodagholi, F. Control of Aggregation in Protein Refolding: Cooperative Effects of Artificial Chaperone and Cold Temperature. Int J Biol Macromol 2007, 40 (2), 126–133. https://doi.org/10.1016/j.ijbiomac.2006.06.018.
(17) Shah, M.; Rattray, Z.; Day, K.; Uddin, S.; Curtis, R.; van der Walle, C. F.; Pluen, A. Evaluation of Aggregate and Silicone-Oil Counts in Pre-Filled Siliconized Syringes: An Orthogonal Study Characterising the Entire Subvisible Size Range. Int J Pharm 2017, 519 (1–2), 58–66. https://doi.org/10.1016/j.ijpharm.2017.01.015.
(18) Ratanji, K. D.; Derrick, J. P.; Dearman, R. J.; Kimber, I. Immunogenicity of Therapeutic Proteins: Influence of Aggregation. J Immunotoxicol 2014, 11 (2), 99–109. https://doi.org/10.3109/1547691X.2013.821564.
(19) Raut, A. S.; Kalonia, D. S. Pharmaceutical Perspective on Opalescence and Liquid–Liquid Phase Separation in Protein Solutions. Mol Pharm 2016, 13 (5), 1431–1444. https://doi.org/10.1021/acs.molpharmaceut.5b00937.
(20) Amin, S.; Barnett, G. V.; Pathak, J. A.; Roberts, C. J.; Sarangapani, P. S. Protein Aggregation, Particle Formation, Characterization & Rheology. Curr Opin Colloid Interface Sci 2014, 19 (5), 438–449. https://doi.org/10.1016/j.cocis.2014.10.002.
(21) Mehta, S. B.; Lewus, R.; Bee, J. S.; Randolph, T. W.; Carpenter, J. F. Gelation of a Monoclonal Antibody at the Silicone Oil–Water Interface and Subsequent Rupture of the Interfacial Gel Results in Aggregation and Particle Formation. J Pharm Sci 2015, 104 (4), 1282–1290. https://doi.org/10.1002/jps.24358.
(22) Krebs, M. R. H.; Devlin, G. L.; Donald, A. M. Protein Particulates: Another Generic Form of Protein Aggregation? Biophys J 2007, 92 (4), 1336–1342. https://doi.org/10.1529/biophysj.106.094342.
(23) Weiss, W. F.; Young, T. M.; Roberts, C. J. Principles, Approaches, and Challenges for Predicting Protein Aggregation Rates and Shelf Life. J Pharm Sci 2009, 98 (4), 1246–1277. https://doi.org/10.1002/jps.21521.
(24) Lévy, E.; El Banna, N.; Baïlle, D.; Heneman-Masurel, A.; Truchet, S.; Rezaei, H.; Huang, M.-E.; Béringue, V.; Martin, D.; Vernis, L. Causative Links between Protein Aggregation and Oxidative Stress: A Review. Int J Mol Sci 2019, 20 (16). https://doi.org/10.3390/ijms20163896.
(25) Davies, K. J.; Delsignore, M. E.; Lin, S. W. Protein Damage and Degradation by Oxygen Radicals. II. Modification of Amino Acids. Journal of Biological Chemistry 1987, 262 (20), 9902–9907. https://doi.org/10.1016/S0021-9258(18)48019-2.
(26) Hipper, E.; Diederichs, T.; Kaiser, W.; Lehmann, F.; Buske, J.; Hinderberger, D.; Garidel, P. Visible Light Triggers the Formation of Reactive Oxygen Species in Monoclonal Antibody Formulations. Int J Pharm 2024, 661. https://doi.org/10.1016/j.ijpharm.2024.124392.
(27) Pinholt, C.; Hartvig, R. A.; Medlicott, N. J.; Jorgensen, L. The Importance of Interfaces in Protein Drug Delivery - Why Is Protein Adsorption of Interest in Pharmaceutical Formulations?. Expert Opin Drug Deliv 2011, 8 (7), 949–964. https://doi.org/10.1517/17425247.2011.577062.
(28) March, D.; Bianco, V.; Franzese, G. Protein Unfolding and Aggregation near a Hydrophobic Interface. Polymers (Basel) 2023, 15 (9). https://doi.org/10.3390/polym15092053.
(29) Hoehne, M.; Samuel, F.; Dong, A.; Wurth, C.; Mahler, H. C.; Carpenter, J. F.; Randolph, T. W. Adsorption of Monoclonal Antibodies to Glass Microparticles. J Pharm Sci 2011, 100 (1), 123–132. https://doi.org/10.1002/jps.22275.

(30) Rabe, M.; Verdes, D.; Seeger, S. Understanding Protein Adsorption Phenomena at Solid Surfaces. Adv Colloid Interface Sci 2011, 162 (1–2), 87–106. https://doi.org/10.1016/j.cis.2010.12.007.
(31) Rabe, M.; Verdes, D.; Zimmermann, J.; Seeger, S. Surface Organization and Cooperativity during Nonspecific Protein Adsorption Events. Journal of Physical Chemistry B 2008, 112 (44), 13971–13980. https://doi.org/10.1021/jp804532v.
(32) Wahlgren, M.; Elofsson, U. Simple Models for Adsorption Kinetics and Their Correlation to the Adsorption of β-Lactoglobulin A and B. J Colloid Interface Sci 1997, 188 (1), 121–129. https://doi.org/10.1006/jcis.1996.4715.
(33) Nakanishi, K.; Sakiyama, T.; Imamura, K. On the Adsorption of Proteins on Solid Surfaces, a Common but Very Complicated Phenomenon. J Biosci Bioeng 2001, 91 (3), 233–244. https://doi.org/10.1016/S1389-1723(01)80127-4.
(34) Gerlt, M. S.; Meier, E. M.; Dingfelder, F.; Zürcher, D.; Müller, M.; Arosio, P. Microfluidic Stress Device to Decouple the Synergistic Effect of Shear and Interfaces on Antibody Aggregation. J Pharm Sci 2024, 113 (8), 2161–2169. https://doi.org/10.1016/j.xphs.2024.05.024.
(35) Latour, R. A. Fundamental Principles of the Thermodynamics and Kinetics of Protein Adsorption to Material Surfaces. Colloids Surf B Biointerfaces 2020, 191. https://doi.org/10.1016/j.colsurfb.2020.110992.
(36) Mathé, C.; Devineau, S.; Aude, J. C.; Lagniel, G.; Chédin, S.; Legros, V.; Mathon, M. H.; Renault, J. P.; Pin, S.; Boulard, Y.; Labarre, J. Structural Determinants for Protein Adsorption/Non-Adsorption to Silica Surface. PLoS One 2013, 8 (11). https://doi.org/10.1371/journal.pone.0081346.
(37) Vogler, E. A. Protein Adsorption in Three Dimensions. Biomaterials 2012, 33 (5), 1201–1237. https://doi.org/10.1016/j.biomaterials.2011.10.059.
(38) Hawe, A.; Frieß, W. Formulation Development for Hydrophobic Therapeutic Proteins. Pharm Dev Technol 2007, 12 (3), 223–237. https://doi.org/10.1080/10837450701247350.
(39) Moskovitz, Y.; Srebnik, S. Conformational Changes of Globular Proteins upon Adsorption on a Hydrophobic Surface. Physical Chemistry Chemical Physics 2014, 16 (23), 11698–11707. https://doi.org/10.1039/c4cp00354c.
(40) Penna, M. J.; Mijajlovic, M.; Biggs, M. J. Molecular-Level Understanding of Protein Adsorption at the Interface between Water and a Strongly Interacting Uncharged Solid Surface. J Am Chem Soc 2014, 136 (14), 5323–5331. https://doi.org/10.1021/ja411796e.
(41) Yu, J.; Becker, M. L.; Carri, G. A. The Influence of Amino Acid Sequence and Functionality on the Binding Process of Peptides onto Gold Surfaces. Langmuir 2012, 28 (2), 1408–1417. https://doi.org/10.1021/la204109r.
(42) Huber, R. Flexibility and Rigidity, Requirements for the Function of Proteins and Protein Pigment Complexes. Biochem Soc Trans 1987, 15 (6), 1009–1020. https://doi.org/10.1042/bst0151009.
(43) Norde, W. Driving Forces for Protein Adsorption at Solid Surfaces. Macromol Symp 1996, 103 (1), 5–18. https://doi.org/10.1002/masy.19961030104.
(44) Norde, W. My Voyage of Discovery to Proteins in Flatland ...and Beyond. Colloids Surf B Biointerfaces 2008, 61 (1), 1–9. https://doi.org/10.1016/j.colsurfb.2007.09.029.
(45) Norde, W.; Lyklema, J. Why Proteins Prefer Interfaces. J Biomater Sci Polym Ed 1991, 2 (3), 183–202. https://doi.org/10.1080/09205063.1991.9756659.
(46) Norde, W.; Favier, J. P. Structure of Adsorbed and Desorbed Proteins. Colloids and Surfaces 1992, 64 (1), 87–93. https://doi.org/10.1016/0166-6622(92)80164-W.

(47) Norde, W.; Arai, T.; Shirahama, H. Protein Adsorption in Model Systems. Biofouling 1991, 4 (1–3), 37–51. https://doi.org/10.1080/08927019109378193.
(48) Jain, D.; Mahammad, S. S.; Singh, P. P.; Kodipyaka, R. A Review on Parenteral Delivery of Peptides and Proteins. Drug Dev Ind Pharm 2019, 45 (9), 1403–1420. https://doi.org/10.1080/03639045.2019.1628770.
(49) Ohtake, S.; Kita, Y.; Arakawa, T. Interactions of Formulation Excipients with Proteins in Solution and in the Dried State. Adv Drug Deliv Rev 2011, 63 (13), 1053–1073. https://doi.org/10.1016/j.addr.2011.06.011.
(50) Zbacnik, T. J.; Holcomb, R. E.; Katayama, D. S.; Murphy, B. M.; Payne, R. W.; Coccaro, R. C.; Evans, G. J.; Matsuura, J. E.; Henry, C. S.; Manning, M. C. Role of Buffers in Protein Formulations. J Pharm Sci 2016, 106 (3), 713–733. https://doi.org/10.1016/j.xphs.2016.11.014.
(51) Kanthe, A. D.; Krause, M.; Zheng, S.; Ilott, A.; Li, J.; Bu, W.; Bera, M. K.; Lin, B.; Maldarelli, C.; Tu, R. S. Armoring the Interface with Surfactants to Prevent the Adsorption of Monoclonal Antibodies. ACS Appl Mater Interfaces 2020, 12 (8), 9977–9988. https://doi.org/10.1021/acsami.9b21979.
(52) Kapp, S. J.; Larsson, I.; Van De Weert, M.; Cárdenas, M.; Jorgensen, L. Competitive Adsorption of Monoclonal Antibodies and Nonionic Surfactants at Solid Hydrophobic Surfaces. J Pharm Sci 2015, 104 (2), 593–601. https://doi.org/10.1002/jps.24265.
(53) Zoeller, M. P.; Hafiz, S.; Marx, A.; Erwin, N.; Fricker, G.; Carpenter, J. F. Exploring the Protein Stabilizing Capability of Surfactants Against Agitation Stress and the Underlying Mechanisms. J Pharm Sci 2022, 111 (12), 3261–3274. https://doi.org/10.1016/j.xphs.2022.09.004.
(54) Höger, K.; Mathes, J.; Frieß, W. IgG1 Adsorption to Siliconized Glass Vials — Influence of PH, Ionic Strength, and Nonionic Surfactants. J Pharm Sci 2015, 104 (1), 34–43. https://doi.org/10.1002/jps.24239.
(55) Her, C.; Tanenbaum, L.; Bandi, S.; Randolph, T.; Thirumangalathu, R.; Mallela, K.; Carpenter, J.; Elias, Y. Effects of Tubing Type, Operating Parameters and Surfactants on Particle Formation during Peristaltic Filling Pump Processing of a Monoclonal Antibody Formulation. J Pharm Sci 2020, 109 (4), 1439–1448. https://doi.org/10.1016/j.xphs.2020.01.009.
(56) Rospiccio, M.; Arsiccio, A.; Winter, G.; Pisano, R. The Role of Cyclodextrins against Interface-Induced Denaturation in Pharmaceutical Formulations: A Molecular Dynamics Approach. Mol Pharm 2021, 18 (6), 2322–2333. https://doi.org/10.1021/acs.molpharmaceut.1c00135.
(57) Shikiya, Y.; Tomita, S.; Arakawa, T.; Shiraki, K. Arginine Inhibits Adsorption of Proteins on Polystyrene Surface. PLoS One 2013, 8 (8). https://doi.org/10.1371/journal.pone.0070762.
(58) Gliński, J.; Chavepeyer, G.; Platten, J.-K. Surface Properties of Aqueous Solutions of L-Leucine. Biophys Chem 2000, 84 (2), 99–103. https://doi.org/10.1016/S0301-4622(99)00150-7.
(59) Bollenbach, L.; Buske, J.; Mäder, K.; Garidel, P. Poloxamer 188 as Surfactant in Biological Formulations – An Alternative for Polysorbate 20/80?. Int J Pharm 2022, 620. https://doi.org/10.1016/j.ijpharm.2022.121706.
(60) Li, J.; Sonje, J.; Suryanarayanan, R. Role of Poloxamer 188 in Preventing Ice-Surface-Induced Protein Destabilization during Freeze–Thawing. Mol Pharm 2023, 20 (9), 4587–4596. https://doi.org/10.1021/acs.molpharmaceut.3c00312.

(61) Dwivedi, M.; Blech, M.; Presser, I.; Garidel, P. Polysorbate Degradation in Biotherapeutic Formulations: Identification and Discussion of Current Root Causes. Int J Pharm 2018, 552 (1–2), 422–436. https://doi.org/10.1016/j.ijpharm.2018.10.008.
(62) Zürcher, D.; Caduff, S.; Aurand, L.; Palmiero, U. C.; Wuchner, K.; Arosio, P. Comparison of the Protective Effect of Polysorbates, Poloxamer and Brij on Antibody Stability Against Different Interfaces. J Pharm Sci 2023. https://doi.org/10.1016/j.xphs.2023.06.004.
(63) Kim, H. L.; McAuley, A.; Livesay, B.; Gray, W. D.; McGuire, J. Modulation of Protein Adsorption by Poloxamer 188 in Relation to Polysorbates 80 and 20 at Solid Surfaces. J Pharm Sci 2014, 103 (4), 1043–1049. https://doi.org/10.1002/jps.23907.
(64) Kannan, A.; Shieh, I. C.; Negulescu, P. G.; Suja, V. C.; Fuller, G. G. Adsorption and Aggregation of Monoclonal Antibodies at Silicone Oil−Water Interfaces. Mol Pharm 2021, 18 (4), 1656–1665. https://doi.org/10.1021/acs.molpharmaceut.0c01113.
(65) Sacha, G. A.; Saffell-Clemmer, W.; Abram, K.; Akers, M. J. Practical Fundamentals of Glass, Rubber, and Plastic Sterile Packaging Systems. Pharm Dev Technol 2010, 15 (1), 6–34. https://doi.org/10.3109/10837450903511178.
(66) Duerkop, M.; Berger, E.; Dürauer, A.; Jungbauer, A. Impact of Cavitation, High Shear Stress and Air/Liquid Interfaces on Protein Aggregation. Biotechnol J 2018, 13 (7). https://doi.org/10.1002/biot.201800062.
(67) Lopes, A. G. Single-Use in the Biopharmaceutical Industry: A Review of Current Technology Impact, Challenges and Limitations. Food Bioprod Process 2015, 93, 98–114. https://doi.org/10.1016/j.fbp.2013.12.002.
(68) Sürmelioğlu, N.; Nenni, M.; Fırat, A.; Demirkan, K.; Özcengiz, D. Evaluation of Regular Insulin Adsorption to Polypropylene Bag and Polyvinyl Chloride Infusion Set. Int J Clin Pract 2021, 75 (4), 13–16. https://doi.org/10.1111/ijcp.13895.
(69) Yoneda, S.; Torisu, T.; Uchiyama, S. Development of Syringes and Vials for Delivery of Biologics: Current Challenges and Innovative Solutions. Expert Opin Drug Deliv 2021, 18 (4), 459–470. https://doi.org/10.1080/17425247.2021.1853699.
(70) Iacocca, R. G.; Toltl, N.; Allgeier, M.; Bustard, B.; Dong, X.; Foubert, M.; Hofer, J.; Peoples, S.; Shelbourn, T. Factors Affecting the Chemical Durability of Glass Used in the Pharmaceutical Industry. AAPS PharmSciTech 2010, 11, 1340–1349. https://doi.org/10.1208/s12249-010-9506-9.
(71) Allmendinger, A.; Lebouc, V.; Bonati, L.; Woehr, A.; Kishore, R. S. K.; Abstiens, K. Glass Leachables as a Nucleation Factor for Free Fatty Acid Particle Formation in Biopharmaceutical Formulations. J Pharm Sci 2021, 110 (2), 785–795. https://doi.org/10.1016/j.xphs.2020.09.050.
(72) Bee, J. S.; Randolph, T. W.; Carpenter, J. F.; Bishop, S. M.; Dimitrova, M. N. Effects of Surfaces and Leachables on the Stability of Biopharmaceuticals. J Pharm Sci 2011, 100 (10), 4158–4170. https://doi.org/10.1002/jps.22597.
(73) Werner, B. P.; Schöneich, C.; Winter, G. Silicone Oil-Free Polymer Syringes for the Storage of Therapeutic Proteins. J Pharm Sci 2018, 108 (3), 1–13. https://doi.org/10.1016/j.xphs.2018.10.049.
(74) Schaut, R. A.; Peanasky, J. S.; DeMartino, S. E.; Schiefelbein, S. L. A New Glass Option for Parenteral Packaging. PDA J Pharm Sci Technol 2014, 68 (5), 527–534. https://doi.org/10.5731/pdajpst.2014.00998.
(75) Sperry, A.; Imhoff, D.; Traunfeld, J.; Gundagari, S.; Smaga, K.; Singh, G. A Case Study Demonstrating the Importance of Glass Vial Selection for Parenteral Pharmaceutical Products. J Pharm Sci 2024, 113 (9), 2974–2980. https://doi.org/10.1016/j.xphs.2024.06.008.

(76) Ditter, D.; Mahler, H.-C.; Roehl, H.; Wahl, M.; Huwyler, J.; Nieto, A.; Allmendinger, A. Characterization of Surface Properties of Glass Vials Used as Primary Packaging Material for Parenterals. Eur J Pharm Biopharm 2018, 125, 58–67. https://doi.org/10.1016/j.ejpb.2017.12.018.
(77) Rupertus, V.; Hladik, B.; Rothhaar, U.; Scheumann, V. A Quick Test To Monitor the Delamination Propensity of Glass Containers. PDA J Pharm Sci Technol 2014, 68 (4), 373–380. https://doi.org/10.5731/pdajpst.2014.00990.
(78) Pikal-Cleland, K. A.; Rodríguez-Hornedo, N.; Amidon, G. L.; Carpenter, J. F. Protein Denaturation during Freezing and Thawing in Phosphate Buffer Systems: Monomeric and Tetrameric β-Galactosidase. Arch Biochem Biophys 2000, 384 (2), 398–406. https://doi.org/10.1006/abbi.2000.2088.
(79) Boltres, B.; Tratzky, S.; Kass, C.; Eichholz, R.; Nass, P. There Is Still Room for Improvement: Presentation of a Neutral Borosilicate Glass with Improved Chemical Stability for Parenteral Packaging. PDA J Pharm Sci Technol 2016, 70 (4), 346–352. https://doi.org/10.5731/pdajpst.2015.005934.
(80) Iacocca, R. G.; Allgeier, M. Corrosive Attack of Glass by a Pharmaceutical Compound. J Mater Sci 2007, 42, 801–811. https://doi.org/10.1007/s10853-006-0156-y.
(81) Ditter, D.; Mahler, H.-C.; Gohlke, L.; Nieto, A.; Roehl, H.; Huwyler, J.; Wahl, M.; Allmendinger, A. Impact of Vial Washing and Depyrogenation on Surface Properties and Delamination Risk of Glass Vials. Pharm Res 2018, 35. https://doi.org/10.1007/s11095-018-2421-6.
(82) Richter, C.; Lipperheide, C.; Lipke, U.; Lamprecht, A. Impact of Extractables from Rubber Closures on Protein Stability under Heat Stress. Eur J Pharm Biopharm 2018, 130, 22–29. https://doi.org/10.1016/j.ejpb.2018.06.009.
(83) Boven, K.; Stryker, S.; Knight, J.; Thomas, A.; van Regenmortel, M.; Kemeny, D. M.; Power, D.; Rossert, J.; Casadevall, N. The Increased Incidence of Pure Red Cell Aplasia with an Eprex Formulation in Uncoated Rubber Stopper Syringes. Kidney Int 2005, 67 (6), 2346–2353. https://doi.org/10.1111/j.1523-1755.2005.00340.x.
(84) Qi, L.; Liu, J.; Ronk, M.; Gallegos, A.; Fujimori, K.; Luo, Y.; Li, K.; Lee, H.; Nashed-Samuel, Y. A Holistic Approach of Extractables and Leachables Assessment of Rubber Stoppered Glass Vial Systems for Biotechnology Products. J Pharm Sci 2021, 110 (11), 3580–3593. https://doi.org/10.1016/j.xphs.2021.07.015.
(85) Wakankar, A. A.; Wang, Y. J.; Canova-Davis, E.; Ma, S.; Schmalzing, D.; Grieco, J.; Milby, T.; Reynolds, T.; Mazzarella, K.; Hoff, E.; Gomez, S.; Martin-Moe, S. On Developing a Process for Conducting Extractable–Leachable Assessment of Components Used for Storage of Biopharmaceuticals. J Pharm Sci 2010, 99 (5), 2209–2218. https://doi.org/10.1002/jps.22012.
(86) Singh, R.; Waxman, L.; Fang, L.; Zhao, C. An Investigation to Examine the Effect of the Elastomeric Surface Treatment on Protein Stability. PDA J Pharm Sci Technol 2021, 75 (3), 230–244. https://doi.org/10.5731/pdajpst.2020.012120.
(87) Sharma, B. Immunogenicity of Therapeutic Proteins. Part 2: Impact of Container Closures. Biotechnol Adv 2007, 25 (3), 318–324. https://doi.org/10.1016/j.biotechadv.2007.01.006.
(88) Kiminami, H.; Takeuchi, K.; Nakamura, K.; Abe, Y.; Lauwers, P.; Dierick, W.; Yoshino, K.; Suzuki, S. Low Leachable Container System Consisting of a Polymer-Based Syringe with Chlorinated Isoprene Isobutene Rubber Plunger Stopper. PDA J Pharm Sci Technol 2015, 69 (6), 713–724. https://doi.org/10.5731/pdajpst.2015.01080.

(89) Soeda, K.; Arai, K.; Yamamoto, T.; Ofuji, K.; Fukuda, M.; Hashimoto, D.; Yamanaka, Y. Mechanism of Protein–PDMS Visible Particles Formation in Liquid Vial Monoclonal Antibody Formulation. J Pharm Sci 2022, 112 (3), 653–664. https://doi.org/10.1016/j.xphs.2022.09.027.
(90) Grapentin, C.; Müller, C.; Kishore, R. S. K.; Adler, M.; ElBialy, I.; Friess, W.; Huwyler, J.; Khan, T. A. Protein-Polydimethylsiloxane Particles in Liquid Vial Monoclonal Antibody Formulations Containing Poloxamer 188. J Pharm Sci 2020, 109 (8), 2393–2404. https://doi.org/10.1016/j.xphs.2020.03.010.
(91) Britt, K. A.; Schwartz, D. K.; Wurth, C.; Mahler, H.; Carpenter, J. F.; Randolph, T. W. Excipient Effects on Humanized Monoclonal Antibody Interactions with Silicone Oil Emulsions. J Pharm Sci 2012, 101 (12), 4419–4432. https://doi.org/10.1002/jps.23318.
(92) Jorgensen, L.; Bennedsen, P.; Hoffmann, S. V.; Krogh, R. L.; Pinholt, C.; Groenning, M.; Hostrup, S.; Bukrinsky, J. T. Adsorption of Insulin with Varying Self-Association Profiles to a Solid Teflon Surface - Influence on Protein Structure, Fibrillation Tendency and Thermal Stability. Eur J Pharm Sci 2011, 42 (5), 509–516. https://doi.org/10.1016/j.ejps.2011.02.007.
(93) Kueltzo, L. A.; Wang, W. e. i.; Randolph, T. W.; Carpenter, J. F. Effects of Solution Conditions, Processing Parameters, and Container Materials on Aggregation of a Monoclonal Antibody during Freeze-Thawing. J Pharm Sci 2008, 97 (5), 1801–1812. https://doi.org/10.1002/jps.21110.
(94) Zardeneta, G.; Mukai, H.; Marker, V.; Milam, S. B. Protein Interactions with Particulate Teflon: Implications for the Foreign Body Response. Journal of Oral and Maxillofacial Surgery 1996, 54 (7), 873–878. https://doi.org/10.1016/S0278-2391(96)90540-6.
(95) Teska, B. M.; Brake, J. M.; Tronto, G. S.; Carpenter, J. F. Aggregation and Particle Formation of Therapeutic Proteins in Contact With a Novel Fluoropolymer Surface Versus Siliconized Surfaces: Effects of Agitation in Vials and in Prefilled Syringes. J Pharm Sci 2016, 105 (7), 2053–2065. https://doi.org/10.1016/j.xphs.2016.04.015.
(96) Moll, F.; Bechtold-Peters, K.; Friess, W. Evaluation of a Novel Silicone Oil Free Primary Packaging System with PTFE-Based Barrier Stopper for Biologics. Eur J Pharm Biopharm 2023, 190, 206–219. https://doi.org/10.1016/j.ejpb.2023.07.015.
(97) Thakare, V.; Schmidt, T.; Rupprechter, O.; Leibold, J.; Stemmer, S.; Mischo, A.; Bhattacharjee, D.; Prazeller, P. Can Cross-Linked Siliconized PFS Come to the Rescue of the Biologics Drug Product?. J Pharm Sci 2020, 109 (11), 3340–3351. https://doi.org/10.1016/j.xphs.2020.08.018.
(98) Depaz, R. A.; Chevolleau, T.; Jouffray, S.; Narwal, R.; Dimitrova, M. N. Cross-Linked Silicone Coating: A Novel Prefilled Syringe Technology That Reduces Subvisible Particles and Maintains Compatibility with Biologics. J Pharm Sci 2014, 103 (5), 1384–1393. https://doi.org/10.1002/jps.23947.
(99) Chapman, R. G.; Ostuni, E.; Yan, L.; Whitesides, G. M. Preparation of Mixed Self-Assembled Monolayers (SAMs) That Resist Adsorption of Proteins Using the Reaction of Amines with a SAM That Presents Interchain Carboxylic Anhydride Groups. Langmuir 2000, 16 (17), 6927–6936. https://doi.org/10.1021/la991579l.
(100) Ostuni, E.; Chapman, R. G.; Holmlin, R. E.; Takayama, S.; Whitesides, G. M. A Survey of Structure-Property Relationships of Surfaces That Resist the Adsorption of Protein. Langmuir 2001, 17 (18), 5605–5620. https://doi.org/10.1021/la010384m.
(101) Murphy, E. F.; Lu, J. R.; Lewis, A. L.; Brewer, J.; Russell, J.; Stratford, P. Characterization of Protein Adsorption at the Phosphorylcholine Incorporated Polymer−Water Interface. Macromolecules 2000, 33 (12), 4545–4554. https://doi.org/10.1021/ma991642d.

(102) Ekblad, T.; Liedberg, B. Protein Adsorption and Surface Patterning. Curr Opin Colloid Interface Sci 2010, 15 (6), 499–509. https://doi.org/10.1016/j.cocis.2010.07.008.
(103) Ishihara, K. Revolutionary Advances in 2-Methacryloyloxyethyl Phosphorylcholine Polymers as Biomaterials. J Biomed Mater Res A 2019, 107 (5), 933–943. https://doi.org/10.1002/jbm.a.36635.
(104) Ishihara, K.; Mu, M.; Konno, T.; Inoue, Y.; Fukazawa, K. The Unique Hydration State of Poly(2-Methacryloyloxyethyl Phosphorylcholine). J Biomater Sci Polym Ed 2017, 28 (10–12), 884–899. https://doi.org/10.1080/09205063.2017.1298278.
(105) Höger, K.; Becherer, T.; Qiang, W.; Haag, R.; Frieß, W.; Küchler, S. Polyglycerol Coatings of Glass Vials for Protein Resistance. Eur J Pharm Biopharm. 2013, 85 (3, Pt A), 756–764. https://doi.org/10.1016/j.ejpb.2013.04.005.
(106) Palumbo, F.; Porto, C. Lo; Fracassi, F.; Favia, P. Recent Advancements in the Use of Aerosol-Assisted Atmospheric Pressure Plasma Deposition. Coatings 2020, 10 (5). https://doi.org/10.3390/COATINGS10050440.
(107) Moll, F.; Bechtold-Peters, K.; Friess, W. The Silicone Depletion in Combination Products Induced by Biologics. Eur J Pharm Biopharm 2024, 203. https://doi.org/10.1016/j.ejpb.2024.114418.
(108) Schwarzenbach, M. S.; Reimann, P.; Thommen, V.; Hegner, M.; Mumenthaler, M.; Schwob, J.; Güntherodt, H.-J. Interferon Alpha-2a Interactions on Glass Vial Surfaces Measured by Atomic Force Microscopy. PDA J Pharm Sci Technol 2002, 56 (2), 78–89.
(109) Vieregg, J. R.; Martin, S. J.; Breeland, A. P.; Weikart, C. M.; Tirrell, M. V. Inhibiting Sterilization-Induced Oxidation of Large Molecule Therapeutics Packaged in Plastic Parenteral Vials. PDA J Pharm Sci Technol 2018, 72 (1), 35–43. https://doi.org/10.5731/pdajpst.2017.008011.
(110) Komorek, P.; Wałek, M.; Jachimska, B. Mechanism of Lysozyme Adsorption onto Gold Surface Determined by Quartz Crystal Microbalance and Surface Plasmon Resonance. Bioelectrochemistry 2020, 135. https://doi.org/10.1016/j.bioelechem.2020.107582.
(111) Komorek, P.; Jachimska, B.; Brand, I. Adsorption of Lysozyme on Gold Surfaces in the Presence of an External Electric Potential. Bioelectrochemistry 2021, 142. https://doi.org/10.1016/j.bioelechem.2021.107946.
(112) Cao, X. M.; Tian, Y.; Wang, Z. Y.; Liu, Y. W.; Wang, C. X. Effects of Protein and Phosphate Buffer Concentrations on Thermal Denaturation of Lysozyme Analyzed by Isoconversional Method. Bioengineered 2016, 7 (4), 235–240. https://doi.org/10.1080/21655979.2016.1197629.
(113) Venkataramani, S.; Truntzer, J.; Coleman, D. R. Thermal Stability of High Concentration Lysozyme across Varying PH: A Fourier Transform Infrared Study. J Pharm Bioallied Sci 2013, 5 (2), 148–153. https://doi.org/10.4103/0975-7406.111821.
(114) Mathes, J.; Friess, W. Influence of PH and Ionic Strength on IgG Adsorption to Vials. Eur J Pharm Biopharm 2011, 78 (2), 239–247. https://doi.org/10.1016/j.ejpb.2011.03.009.
(115) Jachimska, B.; Pajor, A. Physico-Chemical Characterization of Bovine Serum Albumin in Solution and as Deposited on Surfaces. Bioelectrochemistry 2012, 87, 138–146. https://doi.org/10.1016/j.bioelechem.2011.09.004.
(116) Li, R.; Wu, Z.; Wangb, Y.; Ding, L.; Wang, Y. Role of PH-Induced Structural Change in Protein Aggregation in Foam Fractionation of Bovine Serum Albumin. Biotechnol Rep 2016, 9, 46–52. https://doi.org/10.1016/j.btre.2016.01.002.

(117) Jiang, B.; Jain, A.; Lu, Y.; Hoag, S. W. Probing Thermal Stability of Proteins with Temperature Scanning Viscometer. Mol Pharm 2019, 16 (8), 3687–3693. https://doi.org/10.1021/acs.molpharmaceut.9b00598.
(118) Sarkar, S.; Kundu, S. Protein (BSA) Adsorption on Hydrophilic and Hydrophobic Surfaces. Mater Today Proc 2023. https://doi.org/10.1016/j.matpr.2023.04.200.
(119) Majorek, K. A.; Porebski, P. J.; Chruszcz, M.; Almo, S. C.; Minor, W. Crystal Structure of Bovine Serum Albumin; 2011; Vol. 52. https://doi.org/https://doi.org/10.2210/pdb3v03/pdb.
(120) Diamond, R.; Phillips, D. C.; Blake, C. C. F.; North, A. C. T. Real-Space Refinement of the Structure of Hen Egg-White Lysozyme; 1975; Vol. 82. https://doi.org/https://doi.org/10.2210/pdb1lyz/pdb.
(121) Manning, M. C.; Patel, K.; Borchardt, R. T. Stability of Protein Pharmaceuticals. Pharm Res 1989, 6 (11), 903–918. https://doi.org/10.1023/A:1015929109894.
(122) Doran, P. M. Loss of Secreted Antibody from Transgenic Plant Tissue Cultures Due to Surface Adsorption. J Biotechnol 2006, 122 (1), 39–54. https://doi.org/10.1016/j.jbiotec.2005.08.029.
(123) Li, J.; Krause, M. E.; Chen, X.; Cheng, Y.; Dai, W.; Hill, J. J.; Huang, M.; Jordan, S.; LaCasse, D.; Narhi, L.; Shalaev, E.; Shieh, I. C.; Thomas, J. C.; Tu, R.; Zheng, S.; Zhu, L. Interfacial Stress in the Development of Biologics: Fundamental Understanding, Current Practice, and Future Perspective. AAPS Journal 2019, 21 (3). https://doi.org/10.1208/s12248-019-0312-3.
(124) Deiringer, N.; Friess, W. Afraid of the Wall of Death? Considerations on Monoclonal Antibody Characteristics That Trigger Aggregation during Peristaltic Pumping. Int J Pharm 2023, 633. https://doi.org/10.1016/j.ijpharm.2023.122635.
(125) Castañeda Ruiz, A. J.; Shetab Boushehri, M. A.; Phan, T.; Carle, S.; Garidel, P.; Buske, J.; Lamprecht, A. Alternative Excipients for Protein Stabilization in Protein Therapeutics: Overcoming the Limitations of Polysorbates. Pharmaceutics 2022, 14 (12). https://doi.org/10.3390/pharmaceutics14122575.
(126) Hollowell, P.; Li, Z.; Hu, X.; Ruane, S.; Kalonia, C.; van der Walle, C. F.; Lu, J. R. Recent Advances in Studying Interfacial Adsorption of Bioengineered Monoclonal Antibodies. Molecules 2020, 25 (9). https://doi.org/10.3390/molecules25092047.
(127) Kopp, M. R. G.; Grigolato, F.; Zürcher, D.; Das, T. K.; Chou, D.; Wuchner, K.; Arosio, P. Surface-Induced Protein Aggregation and Particle Formation in Biologics: Current Understanding of Mechanisms, Detection and Mitigation Strategies. J Pharm Sci 2022, 112 (2), 377–385. https://doi.org/10.1016/j.xphs.2022.10.009.
(128) Adler, M.; Allmendinger, A. Filling Unit Operation for Biological Drug Products: Challenges and Considerations. J Pharm Sci 2024, 113 (2), 332–344. https://doi.org/10.1016/j.xphs.2023.11.017.
(129) Vitharana, S.; Stillahn, J. M.; Katayama, D. S.; Henry, C. S.; Manning, M. C. Application of Formulation Principles to Stability Issues Encountered During Processing, Manufacturing, and Storage of Drug Substance and Drug Product Protein Therapeutics. J Pharm Sci 2023, 112 (11), 2724–2751. https://doi.org/10.1016/j.xphs.2023.08.003.
(130) Sampathkumar, K.; Kerwin, B. A. Roadmap for Drug Product Development and Manufacturing of Biologics. J Pharm Sci 2024, 113 (2), 314–331. https://doi.org/10.1016/j.xphs.2023.11.004.
(131) Wang, M.; Li, Y.; Srinivasan, P.; Hu, Z.; Wang, R.; Saragih, A.; Repka, M. A.; Murthy, S. N. Interactions Between Biological Products and Product Packaging and Potential Approaches to Overcome Them. AAPS PharmSciTech 2018, 19 (8), 3681–3686. https://doi.org/10.1208/s12249-018-1184-z.

(132) Castro-Muñoz, R.; Serna-Vázquez, J.; García-Depraect, O. Current Evidence in High Throughput Ultrafiltration toward the Purification of Monoclonal Antibodies (MAbs) and Biotechnological Protein-Type Molecules. Crit Rev Biotechnol 2022, 42 (6), 827–837. https://doi.org/10.1080/07388551.2021.1947182.
(133) Migliorini, E.; Weidenhaupt, M.; Picart, C. Practical Guide to Characterize Biomolecule Adsorption on Solid Surfaces (Review). Biointerphases 2018, 13 (6). https://doi.org/10.1116/1.5045122.
(134) Adamczyk, Z. Protein Adsorption: A Quest for a Universal Mechanism. Curr Opin Colloid Interface Sci 2019, 41, 50–65. https://doi.org/10.1016/j.cocis.2018.11.004.
(135) Latour, R. A. The Langmuir Isotherm: A Commonly Applied but Misleading Approach for the Analysis of Protein Adsorption Behavior. J Biomed Mater Res A 2015, 103 (3), 949–958. https://doi.org/10.1002/jbm.a.35235.
(136) Kim, J. Mathematical Modeling Approaches to Describe the Dynamics of Protein Adsorption at Solid Interfaces. Colloids Surf B Biointerfaces 2018, 162, 370–379. https://doi.org/10.1016/j.colsurfb.2017.12.006.
(137) Penna, M.; Ley, K.; MacLaughlin, S.; Yarovsky, I. Surface Heterogeneity: A Friend or Foe of Protein Adsorption-Insights from Theoretical Simulations. Faraday Discuss 2016, 191, 435–464. https://doi.org/10.1039/c6fd00050a.
(138) Weltz, J. S.; Schwartz, D. K.; Kaar, J. L. Surface-Mediated Protein Unfolding as a Search Process for Denaturing Sites. ACS Nano 2016, 10 (1), 730–738. https://doi.org/10.1021/acsnano.5b05787.
(139) Quan, X.; Liu, J.; Zhou, J. Multiscale Modeling and Simulations of Protein Adsorption: Progresses and Perspectives. Curr Opin Colloid Interface Sci 2019, 41, 74–85. https://doi.org/10.1016/j.cocis.2018.12.004.
(140) Yano, Y. F. Kinetics of Protein Unfolding at Interfaces. J Condens Matter Phys 2012, 24. https://doi.org/10.1088/0953-8984/24/50/503101.
(141) Komorek, P.; Martin, E.; Jachimska, B. Adsorption and Conformation Behavior of Lysozyme on a Gold Surface Determined by QCM-D, MP-SPR, and FTIR. Int J Mol Sci 2021, 22 (3). https://doi.org/10.3390/ijms22031322.
(142) Asanov, A. N.; Delucas, L. J.; Oldham, P. B.; Wilson, W. W. Interfacial Aggregation of Bovine Serum Albumin Related to Crystallization Conditions Studied by Total Internal Reflection Fluorescence. J Colloid Interface Sci 1997, 196 (1), 62–73. https://doi.org/10.1006/jcis.1997.5182.
(143) Roach, P.; Farrar, D.; Perry, C. C. Interpretation of Protein Adsorption: Surface-Induced Conformational Changes. J Am Chem Soc 2005, 127 (22), 8168–8173. https://doi.org/10.1021/ja042898o.
(144) Barberi, J.; Spriano, S. Titanium and Protein Adsorption: An Overview of Mechanisms and Effects of Surface Features. Materials 2021, 14 (7). https://doi.org/10.3390/ma14071590.
(145) Wood, C. V.; McEvoy, S.; Razinkov, V. I.; Qi, W.; Furst, E. M.; Roberts, C. J. Kinetics and Competing Mechanisms of Antibody Aggregation via Bulk- and Surface-Mediated Pathways. J Pharm Sci 2020, 109 (4), 1449–1459. https://doi.org/10.1016/j.xphs.2020.01.005.
(146) Griffin, V. P.; Merritt, K.; Vaclaw, C.; Whitaker, N.; Volkin, D. B.; Ogunyankin, M. O.; Pace, S.; Dhar, P. Evaluating the Combined Impact of Temperature and Application of Interfacial Dilatational Stresses on Surface-Mediated Protein Particle Formation in Monoclonal Antibody Formulations. J Pharm Sci 2022, 111 (3), 680–689. https://doi.org/10.1016/j.xphs.2021.10.038.

(147) Pardeshi, N.; Marsiglio, D.; Padmakumar, V.; Bernacki, J.; Rathore, N. Investigating and Addressing Challenges Associated with Filling Protein Drug Products. J Pharm Sci 2023, 112 (4), 954–962. https://doi.org/10.1016/j.xphs.2022.11.017.
(148) Sediq, A. S.; van Duijvenvoorde, R. B.; Jiskoot, W.; Nejadnik, M. R. No Touching! Abrasion of Adsorbed Protein Is the Root Cause of Subvisible Particle Formation During Stirring. J Pharm Sci 2016, 105 (2), 519–529. https://doi.org/10.1016/j.xphs.2015.10.003.
(149) Sarin, D.; Krishna, K.; Nejadnik, M. R.; Suryanarayanan, R.; Rathore, A. S. Impact of Excipient Extraction and Buffer Exchange on Recombinant Monoclonal Antibody Stability. Mol Pharm 2024, 21 (4), 1872–1883. https://doi.org/10.1021/acs.molpharmaceut.3c01157.
(150) Tsukamoto, K.; Hamamoto, R.; Oguri, R.; Miura, A.; Iwasaki, T.; Sukegawa, T. Size-based Analysis of Virus Removal Filter Fouling Using Fractionated Protein Aggregates. Biotechnol Prog 2024, 40 (1). https://doi.org/10.1002/btpr.3391.
(151) Arsiccio, A.; Pisano, R. The Ice-Water Interface and Protein Stability: A Review. J Pharm Sci 2020, 109 (7), 2116–2130. https://doi.org/10.1016/j.xphs.2020.03.022.
(152) Schwegman, J. J.; Carpenter, J. F.; Nail, S. L. Evidence of Partial Unfolding of Proteins at the Ice/Freeze-Concentrate Interface by Infrared Microscopy. J Am Pharm Assoc 2009, 98 (9), 3239–3246. https://doi.org/10.1002/jps.21843.
(153) Minatovicz, B.; Sun, L.; Foran, C.; Chaudhuri, B.; Tang, C. (Xiaolin); Shameem, M. Freeze-Concentration of Solutes during Bulk Freezing and Its Impact on Protein Stability. J Drug Deliv Sci Technol 2020, 58. https://doi.org/10.1016/j.jddst.2020.101703.
(154) Duarte, A.; Rego, P.; Ferreira, A.; Dias, P.; Geraldes, V.; Rodrigues, M. A. Interfacial Stress and Container Failure During Freezing of Bulk Protein Solutions Can Be Prevented by Local Heating. AAPS PharmSciTech 2020, 21 (7). https://doi.org/10.1208/s12249-020-01794-x.
(155) Authelin, J.-R.; Rodrigues, M. A.; Tchessalov, S.; Singh, S. K.; McCoy, T.; Wang, S.; Shalaev, E. Freezing of Biologicals Revisited: Scale, Stability, Excipients, and Degradation Stresses. J Pharm Sci 2020, 109 (1), 44–61. https://doi.org/10.1016/j.xphs.2019.10.062.
(156) Jain, K.; Salamat-Miller, N.; Taylor, K. Freeze–Thaw Characterization Process to Minimize Aggregation and Enable Drug Product Manufacturing of Protein Based Therapeutics. Sci Rep 2021, 11 (1). https://doi.org/10.1038/s41598-021-90772-9.
(157) Peláez, S. S.; Mahler, H.-C.; Huwyler, J.; Allmendinger, A. Directional Freezing and Thawing of Biologics in Drug Substance Bottles. Eur J Pharm Biopharm 2024, 203. https://doi.org/10.1016/j.ejpb.2024.114427.
(158) Peláez, S. S.; Mahler, H.-C.; Vila, P. R.; Huwyler, J.; Allmendinger, A. Characterization of Freezing Processes in Drug Substance Bottles by Ice Core Sampling. AAPS PharmSciTech 2024, 25. https://doi.org/10.1208/s12249-024-02818-6.
(159) Khanal, O.; Singh, N.; Traylor, S. J.; Xu, X.; Ghose, S.; Li, Z. J.; Lenhoff, A. M. Contributions of Depth Filter Components to Protein Adsorption in Bioprocessing. Biotechnol Bioeng 2018, 115 (8), 1938–1948. https://doi.org/10.1002/bit.26707.
(160) Mahler, H. C.; Huber, F.; Kishore, R. S. K.; Reindl, J.; Rückert, P.; Müller, R. Adsorption Behavior of a Surfactant and a Monoclonal Antibody to Sterilizing-Grade Filters. J Pharm Sci 2010, 99 (6), 2620–2627. https://doi.org/10.1002/jps.22045.
(161) Deiringer, N.; Leitner, I.; Friess, W. Effect of the Tubing Material Used in Peristaltic Pumping in Tangential Flow Filtration Processes of Biopharmaceutics on Particle Formation and Flux. J Pharm Sci 2022, 112 (3), 665–672. https://doi.org/10.1016/j.xphs.2022.10.005.

(162) Liu, L.; Randolph, T. W.; Carpenter, J. F. Particles Shed from Syringe Filters and Their Effects on Agitation-Induced Protein Aggregation. J Pharm Sci 2012, 101 (8), 2952–2959. https://doi.org/10.1002/jps.23225.
(163) Fröhlich, H.; Villian, L.; Melzner, D.; Strube, J. Membrane Technology in Bioprocess Science. Chem Ing Tech 2012, 84 (6), 905–917. https://doi.org/10.1002/cite.201200025.
(164) van Reis, R.; Zydney, A. Bioprocess Membrane Technology. J Memb Sci 2007, 297 (1–2), 16–50. https://doi.org/10.1016/j.memsci.2007.02.045.
(165) Schick, A. J.; Yi, L.; Lam, P.; Pallante, P.; Swanson, N.; Tyler, J. Y. Understanding Loss of Soluble High Molecular Weight Species during Filtration of Low Concentration Therapeutic Monoclonal Antibodies. J Pharm Sci 2021, 110 (5), 1997–2004. https://doi.org/10.1016/j.xphs.2021.02.015.
(166) Ren, J.; Zhang, Y.; Wang, C. Understanding Adsorption Behavior of Polysorbate-20 to Sterile Filters in Therapeutic Proteins Final Filtration Process. Biotechnol Prog 2024, 40 (2). https://doi.org/10.1002/btpr.3401.
(167) Van den Oetelaar, P. J. M.; Mentink, I. M.; Brinks, G. J. Loss of Peptides and Proteins Upon Sterile Filtration Due to Adsorption to Membrane Filters. Drug Dev Ind Pharm 1989, 15 (1), 97–106. https://doi.org/10.3109/03639048909040198.
(168) Hamamoto, R.; Ito, H.; Hirohara, M.; Chang, R.; Hongo-Hirasaki, T.; Hayashi, T. Interactions between Protein Molecules and the Virus Removal Membrane Surface: Effects of Immunoglobulin G Adsorption and Conformational Changes on Filter Performance. Biotechnol Prog 2018, 34 (2), 379–386. https://doi.org/10.1002/btpr.2586.
(169) Haindl, S. M. H.; Doppleb, O.; Förster, L.; Wraage, S.; Reiche, A. Study of Protein Adsorption During Sterile Filtration of Protein Formulations by ILC. Chem Ing Tech 2020, 92 (8), 1109–1121. https://doi.org/10.1002/cite.201900185.
(170) Huang, M.; Horwitz, T. S.; Zweiben, C.; Singh, S. K. Impact of Extractables/Leachables from Filters on Stability of Protein Formulations. J Pharm Sci 2011, 100 (11), 4617–4630. https://doi.org/10.1002/jps.22670.
(171) Arunkumar, A.; Singh, N.; Schutsky, E. G.; Peck, M.; Swanson, R. K.; Borys, M. C.; Li, Z. J. Effect of Channel-Induced Shear on Biologics during Ultrafiltration/Diafiltration (UF/DF). J Memb Sci 2016, 514, 671–683. https://doi.org/10.1016/j.memsci.2016.05.031.
(172) Yun, K. H.; Sharma, K.; Kim, H. U.; Bae, T.-H. Modification of a PES Microfiltration Membrane to Enhance Sterile Filtration by Inhibiting Protein Adsorption. J Ind Eng Chem 2023, 123, 311–319. https://doi.org/10.1016/j.jiec.2023.03.048.
(173) Li, G.; Li, T.; Li, Y.; An, L.; Li, W.; Zhang, Z. Preparation of PH-Controllable Nanofibrous Membrane Functionalized with Lysine for Selective Adsorption of Protein. Colloids Surf A Physicochem Eng Asp 2017, 531, 173–181. https://doi.org/10.1016/j.colsurfa.2017.08.003.
(174) Rajesh, S.; Crandall, C.; Schneiderman, S.; Menkhaus, T. J. Cellulose-Graft-Polyethyleneamidoamine Anion-Exchange Nanofiber Membranes for Simultaneous Protein Adsorption and Virus Filtration. ACS Appl Nano Mater 2018, 1 (7), 3321–3330. https://doi.org/10.1021/acsanm.8b00519.
(175) Fu, Q.; Wang, X.; Si, Y.; Liu, L.; Yu, J.; Ding, B. Scalable Fabrication of Electrospun Nanofibrous Membranes Functionalized with Citric Acid for High-Performance Protein Adsorption. ACS Appl Mater Interfaces 2016, 8 (18), 11819–11829. https://doi.org/10.1021/acsami.6b03107.
(176) Ma, N.; Cao, J.; Li, H.; Zhang, Y.; Wang, H.; Meng, J. Surface Grafting of Zwitterionic and PEGylated Cross-Linked Polymers toward PVDF Membranes with Ultralow Protein

Adsorption. Polymer (Guildf) 2019, 167, 1–12. https://doi.org/10.1016/j.polymer.2019.01.053.
(177) Samaras, J. J.; Micheletti, M.; Ding, W. Transformation of Biopharmaceutical Manufacturing Through Single-Use Technologies: Current State, Remaining Challenges, and Future Development. Annu Rev Chem Biomol Eng 2022, 13, 73–97. https://doi.org/10.1146/annurev-chembioeng-092220-030223.
(178) Uettwiller, I.; Dubut, D.; Voute, N. Quantification of Protein Adsorption onto the Surface of Single-Use Flexible Containers. Bioprocess Int 2006, 4 (6), 22–26.
(179) Rathore, N.; Rajan, R. S. Current Perspectives on Stability of Protein Drug Products during Formulation, Fill and Finish Operations. Biotechnol Prog 2008, 24 (3), 504–514. https://doi.org/10.1021/bp070462h.
(180) Thite, N. G.; Ghazvini, S.; Wallace, N.; Feldman, N.; Calderon, C. P.; Randolph, T. W. Interfacial Adsorption Controls Particle Formation in Antibody Formulations Subjected to Extensional Flows and Hydrodynamic Shear. J Pharm Sci 2023, 112 (11), 2766–2777. https://doi.org/10.1016/j.xphs.2023.07.010.
(181) Saller, V.; Matilainen, J.; Grauschopf, U.; Bechtold-Peters, K.; Mahler, H.-C.; Friess, W. Particle Shedding from Peristaltic Pump Tubing in Biopharmaceutical Drug Product Manufacturing. J Pharm Sci 2015, 104 (4), 1440–1450. https://doi.org/10.1002/jps.24357.
(182) Saller, V.; Hediger, C.; Matilainen, J.; Grauschopf, U.; Bechtold-Peters, K.; Mahler, H.-C.; Friess, W. Influence of Particle Shedding from Silicone Tubing on Antibody Stability. J Pharm Pharmacol 2018, 70 (5), 675–685. https://doi.org/10.1111/jphp.12603.
(183) Deiringer, N.; Friess, W. Proteins on the Rack: Mechanistic Studies on Protein Particle Formation During Peristaltic Pumping. J Pharm Sci 2022, 111 (5), 1370–1378. https://doi.org/10.1016/j.xphs.2022.01.035.
(184) Deiringer, N.; Friess, W. Reaching the Breaking Point: Effect of Tubing Characteristics on Protein Particle Formation during Peristaltic Pumping. Int J Pharm 2022, 627. https://doi.org/10.1016/j.ijpharm.2022.122216.
(185) Deiringer, N.; Rüdiger, D.; Luxbacher, T.; Zahler, S.; Frieß, W. Catching Speedy Gonzales: Driving Forces for Protein Film Formation on Silicone Rubber Tubing During Pumping. J Pharm Sci 2022, 111 (6), 1577–1586. https://doi.org/10.1016/j.xphs.2022.02.013.
(186) Wu, H.; Randolph, T. W. Aggregation and Particle Formation During Pumping of an Antibody Formulation Are Controlled by Electrostatic Interactions Between Pump Surfaces and Protein Molecules. J Pharm Sci 2020, 109 (4), 1473–1482. https://doi.org/10.1016/j.xphs.2020.01.023.
(187) Chandrasekaran, N.; Dimartino, S.; Fee, C. J. Study of the Adsorption of Proteins on Stainless Steel Surfaces Using QCM-D. Chem Eng Res Des 2013, 91 (9), 1674–1683. https://doi.org/10.1016/j.cherd.2013.07.017.
(188) Bee, J. S.; Davis, M.; Freund, E.; Carpenter, J. F.; Randolph, T. W. Aggregation of a Monoclonal Antibody Induced by Adsorption to Stainless Steel. Biotechnol Bioeng 2010, 105 (1), 121–129. https://doi.org/10.1002/bit.22525.
(189) Kalonia, C. K.; Heinrich, F.; Curtis, J. E.; Raman, S.; Miller, M. A.; Hudson, S. D. Protein Adsorption and Layer Formation at the Stainless Steel-Solution Interface Mediates Shear-Induced Particle Formation for an IgG1 Monoclonal Antibody. Mol Pharm 2018, 15 (3), 1319–1331. https://doi.org/10.1021/acs.molpharmaceut.7b01127.
(190) Dreckmann, T.; Boeuf, J.; Ludwig, I.-S.; Lümkemann, J.; Huwyler, J. Low Volume Aseptic Filling: Impact of Pump Systems on Shear Stress. Eur J Pharm Biopharm 2020, 147, 10–18. https://doi.org/10.1016/j.ejpb.2019.12.006.

(191) Nayak, A.; Colandene, J.; Bradford, V.; Perkins, M. Characterization of Subvisible Particle Formation During the Filling Pump Operation of a Monoclonal Antibody Solution. J Pharm Sci 2011, 100 (10), 4198–4204. https://doi.org/10.1002/jps.22676.
(192) Thomas, C. R.; Geer, D. Effects of Shear on Proteins in Solution. Biotechnol Lett 2011, 33 (3), 443–456. https://doi.org/10.1007/s10529-010-0469-4.
(193) Cromwell, M. E. M.; Hilario, E.; Jacobson, F. Protein Aggregation and Bioprocessing. AAPS J 2006, 8. https://doi.org/10.1208/aapsj080366.
(194) Bee, J. S.; Stevenson, J. L.; Mehta, B.; Svitel, J.; Pollastrini, J.; Platz, R.; Freund, E.; Carpenter, J. F.; Randolph, T. W. Response of a Concentrated Monoclonal Antibody Formulation to High Shear. Biotechnol Bioeng 2009, 103 (5), 936–943. https://doi.org/10.1002/bit.22336.
(195) Jaspe, J.; Hagen, S. J. Do Protein Molecules Unfold in a Simple Shear Flow? Biophys J 2006, 91 (9), 3415–3424. https://doi.org/10.1529/biophysj.106.089367.
(196) Roffi, K.; Li, L.; Pantazis, J. Adsorbed Protein Film on Pump Surfaces Leads to Particle Formation during Fill-Finish Manufacturing. Biotechnol Bioeng 2021, 118 (8), 2947–2957. https://doi.org/10.1002/bit.27801.
(197) Grigolato, F.; Arosio, P. Synergistic Effects of Flow and Interfaces on Antibody Aggregation. Biotechnol Bioeng 2020, 117 (2), 417–428. https://doi.org/10.1002/bit.27212.
(198) Moino, C.; Artusio, F.; Pisano, R. Shear Stress as a Driver of Degradation for Protein-Based Therapeutics: More Accomplice than Culprit. Int J Pharm 2024, 650. https://doi.org/10.1016/j.ijpharm.2023.123679.
(199) Defante, A. P.; Kalonia, C. K.; Keegan, E.; Bishop, S. M.; Satish, H. A.; Hudson, S. D.; Santacroce, P. V. The Impact of the Metal Interface on the Stability and Quality of a Therapeutic Fusion Protein. Mol Pharm 2020, 17 (2), 569–578. https://doi.org/10.1021/acs.molpharmaceut.9b01000.
(200) Corvari, V.; Narhi, L. O.; Spitznagel, T. M.; Afonina, N.; Cao, S.; Cash, P.; Cecchini, I.; DeFelippis, M. R.; Garidel, P.; Herre, A.; Koulov, A. V.; Lubiniecki, T.; Mahler, H.-C.; Mangiagalli, P.; Nesta, D.; Perez-Ramirez, B.; Polozova, A.; Rossi, M.; Schmidt, R.; Simler, R.; Singh, S.; Weiskopf, A.; Wuchner, K. Subvisible (2–100 Mm) Particle Analysis during Biotherapeutic Drug Product Development: Part 2, Experience with the Application of Subvisible Particle Analysis. Biologicals 2015, 43 (6), 457–473. https://doi.org/10.1016/j.biologicals.2015.07.011.
(201) Fanthom, T. B.; Wilson, C.; Gruber, D.; Bracewell, D. G. Solid-Solid Interfacial Contact of Tubing Walls Drives Therapeutic Protein Aggregation During Peristaltic Pumping. J Pharm Sci 2023, 112 (12), 3022–3034. https://doi.org/10.1016/j.xphs.2023.08.012.
(202) Eisner, D. R.; Hubbard, A.; Eppler, K.; Tegoulia, V.; Maa, Y. F. Vapor-Phase Hydrogen Peroxide Uptake by Silicone Tubing and Primary Packaging Components during Protein Drug Product Aseptic Filling: Impact of Pretreatment and Sterilization Process. PDA J Pharm Sci Technol 2019, 73 (5), 443–458. https://doi.org/10.5731/pdajpst.2019.009928.
(203) Hubbard, A.; Roedl, T.; Hui, A.; Knueppel, S.; Eppler, K.; Lehnert, S.; Maa, Y.-F. Vapor Phase Hydrogen Peroxide Decontamination or Sanitization of an Isolator for Aseptic Filling of Monoclonal Antibody Drug Product—Hydrogen Peroxide Uptake and Impact on Protein Quality. PDA J Pharm Sci Technol 2018, 72 (4), 348–366. https://doi.org/10.5731/pdajpst.2017.008326.
(204) Tyagi, A. K.; Randolph, T. W.; Dong, A.; Maloney, K. M.; Jr, C. H.; Carpenter, J. F. IgG Particle Formation during Filling Pump Operation: A Case Study of Heterogeneous Nucleation on Stainless Steel Nanoparticles. J Pharm Sci 2009, 98 (1), 94–104. https://doi.org/10.1002/jps.21419.

(205) Roffi, K.; Sebastião, I.; Morel, A. Engineering a Ceramic Piston Pump to Minimize Particle Formation for a Therapeutic Immunoglobulin: A Combined Factorial and Modeling Approach. J Adv Manuf Process 2022, 5 (1). https://doi.org/10.1002/amp2.10142.
(206) Deiringer, N.; Aleshkevich, S.; Müller, C.; Friess, W. Modification of Tubings for Peristaltic Pumping of Biopharmaceutics. J Pharm Sci 2022, 111 (12), 3251–3260. https://doi.org/10.1016/j.xphs.2022.08.037.
(207) Murphy, M. I.; Leissa, J. A.; Plata, S. B.; Chamberlin, A. L.; Patel, S. M. Effect of Various Silicone Oil And Tungsten Levels on the Stability of a Monoclonal Antibody in Nine Commercially Available Prefilled Syringes. J Pharm Sci 2023, 112 (6), 1586–1594. https://doi.org/10.1016/j.xphs.2023.03.009.
(208) Jiang, Y.; Nashed-Samuel, Y.; Li, C.; Liu, W.; Pollastrini, J.; Mallard, D.; Wen, Z.-Q.; Fujimori, K.; Pallitto, M.; Donahue, L.; Chu, G.; Torraca, G.; Vance, A.; Mire-Sluis, T.; Freund, E.; Davis, J.; Narhi, L. Tungsten-Induced Protein Aggregation: Solution Behavior. J Pharm Sci 2009, 98 (12), 4695–4710. https://doi.org/10.1002/jps.21778.
(209) Solomun, L.; Ibric, S.; Boltic, Z.; Djuric, Z.; Stupar, B. The Impact of Primary Packaging on the Quality of Parenteral Products. J Pharm Biomed Anal 2008, 48 (3), 744–748. https://doi.org/10.1016/j.jpba.2008.07.025.
(210) Sluzky, V.; Klibanov, A. M.; Langer, R. Mechanism of Insulin Aggregation and Stabilization in Agitated Aqueous Solutions. Biotechnol Bioeng 1992, 40 (8), 895–903. https://doi.org/10.1002/bit.260400805.
(211) Ludwig, D. B.; Carpenter, J. F.; Hamel, J. B.; Randolph, T. W. Protein Adsorption and Excipient Effects on Kinetic Stability of Silicone Oil Emulsions. J Pharm Sci 2010, 99 (4), 1721–1733. https://doi.org/10.1002/jps.21982.
(212) Gerhardt, A.; McGraw, N. R.; Schwartz, D. K.; Bee, J. S.; Carpenter, J. F.; Randolph, T. W. Protein Aggregation and Particle Formation in Prefilled Glass Syringes. J Pharm Sci 2014, 103 (6), 1601–1612. https://doi.org/10.1002/jps.23973.
(213) Funke, S.; Matilainen, J.; Nalenz, H.; Bechtold-Peters, K.; Mahler, H. C.; Friess, W. Silicone Migration From Baked-on Silicone Layers. Particle Characterization in Placebo and Protein Solutions. J Pharm Sci 2016, 105 (12), 3520–3531. https://doi.org/10.1016/j.xphs.2016.08.031.
(214) Shen, K.; Hu, X.; Li, Z.; Liao, M.; Zhuang, Z.; Ruane, S.; Wang, Z.; Li, P.; Micciulla, S.; Kasinathan, N.; Kalonia, C.; Lu, J. R. Competitive Adsorption of a Monoclonal Antibody and Nonionic Surfactant at the PDMS/Water Interface. Mol Pharm 2023, 20 (5), 2502–2512. https://doi.org/10.1021/acs.molpharmaceut.2c01099.
(215) Song, J.; Hu, G.; Hamzaoui, H.; Krishnamachari, Y.; Persak, S. C.; Xi, H.; Su, Y. The Impact of Syringe Age Prior to Filling on Migration of Subvisible Silicone-Oil Particles into Drug Product. J Pharm Sci 2022, 111 (12), 3191–3194. https://doi.org/10.1016/j.xphs.2022.09.015.
(216) Gentile, K.; Huang, C.; Liu, X.; Whitty-Léveillé, L.; Hamzaoui, H.; Cristofolli, E.; Rayfield, W.; Afanador, N. L.; Mittal, S.; Krishnamachari, Y.; Xi, H.; Zhao, X. Variables Impacting Silicone Oil Migration and Biologic Drug Product in Prefilled Syringes. J Pharm Sci 2023, 112 (8), 2203–2211. https://doi.org/10.1016/j.xphs.2023.05.017.
(217) Gerhardt, A.; Nguyen, B. H.; Lewus, R.; Carpenter, J. F.; Randolph, T. W. Effect of the Siliconization Method on Particle Generation in a Monoclonal Antibody Formulation in Pre-Filled Syringes. J Pharm Sci 2015, 104 (5), 1601–1609. https://doi.org/10.1002/jps.24387.
(218) Majumdar, S.; Ford, B. M.; Mar, K. D.; Sullivan, V. J.; Ulrich, R. G.; D'souza, A. J. M. Evaluation of the Effect of Syringe Surfaces on Protein Formulations. J Pharm Sci 2011, 100 (7), 2563–2573. https://doi.org/10.1002/jps.22515.

(219) Funke, S.; Matilainen, J.; Nalenz, H.; Bechtold-Peters, K.; Mahler, H.-C.; Friess, W. Optimization of the Bake-on Siliconization of Cartridges. Part I: Optimization of the Spray-on Parameters. Eur J Pharm Biopharm 2016, 104, 200–215. https://doi.org/10.1016/j.ejpb.2016.05.007.
(220) Funke, S.; Matilainen, J.; Nalenz, H.; Bechtold-Peters, K.; Mahler, H.-C.; Vetter, F.; Müller, C.; Bracher, F.; Friess, W. Optimization of the Bake-on Siliconization of Cartridges. Part II: Investigations into Burn-in Time and Temperature. Eur J Pharm Biopharm 2016, 105, 209–222. https://doi.org/10.1016/j.ejpb.2016.05.015.
(221) Moll, F.; Bechtold-Peters, K.; Friess, W. Impact of Autoclavation on Baked-on Siliconized Containers for Biologics. Eur J Pharm Biopharm 2023, 187, 184–195. https://doi.org/10.1016/j.ejpb.2023.04.018.
(222) Thirumangalathu, R.; Krishnan, S.; Ricci, M. S.; Brems, D. N.; Randolph, T. W.; Carpenter, J. F. Silicone Oil- and Agitation-Induced Aggregation of a Monoclonal Antibody in Aqueous Solution. J Pharm Sci 2009, 98 (9), 3167–3181. https://doi.org/10.1002/jps.21719.
(223) Nayef, L.; Khan, M. F.; Brook, M. A. The Stability of Insulin Solutions in Syringes Is Improved by Ensuring Lower Molecular Weight Silicone Lubricants Are Absent. Heliyon 2017, 3 (3). https://doi.org/10.1016/j.heliyon.2017.e00264.
(224) Yoneda, S.; Maruno, T.; Mori, A.; Hioki, A.; Nishiumi, H.; Okada, R.; Murakami, M.; Zekun, W.; Fukuhara, A.; Itagaki, N.; Harauchi, Y.; Adachi, S.; Okuyama, K.; Sawaguchi, T.; Torisu, T.; Uchiyama, S. Influence of Protein Adsorption on Aggregation in Prefilled Syringes. J Pharm Sci 2021, 110 (11), 3568–3579. https://doi.org/10.1016/j.xphs.2021.07.007.
(225) Krayukhina, E.; Tsumoto, K.; Uchiyama, S.; Fukui, K. Effects of Syringe Material and Silicone Oil Lubrication on the Stability of Pharmaceutical Proteins. J Pharm Sci 2015, 104 (2), 527–535. https://doi.org/10.1002/jps.24184.
(226) Waxman, L.; Vilivalam, V. D. A Comparison of Protein Stability in Prefillable Syringes Made of Glass and Plastic. PDA J Pharm Sci Technol 2017, 71 (6), 462–477. https://doi.org/10.5731/pdajpst.2016.007146.
(227) Funatsu, K.; Kiminami, H.; Abe, Y.; Carpenter, J. F. Impact of Ethylene Oxide Sterilization of Polymer-Based Prefilled Syringes on Chemical Degradation of a Model Therapeutic Protein During Storage. J Pharm Sci 2019, 108 (1), 770–774. https://doi.org/10.1016/j.xphs.2018.09.029.
(228) Masato, A.; Kiichi, F.; Uchiyama, S. Suppression of Methionine Oxidation of a Pharmaceutical Antibody Stored in a Polymer-Based Syringe. J Pharm Sci 2016, 105 (2), 623–629. https://doi.org/10.1002/jps.24675.
(229) Weikart, C. M.; Pantano, C. G.; Shallenberger, J. R. Performance Stability of Silicone Oxide–Coated Plastic Parenteral Vials. PDA J Pharm Sci Technol 2017, 71 (4), 317–327. https://doi.org/10.5731/pdajpst.2016.007278.
(230) Wu, H.; Chisholm, C. F.; Puryear, M.; Movafaghi, S.; Smith, S. D.; Pokhilchuk, Y.; Lengsfeld, C. S.; Randolph, T. W. Container Surfaces Control Initiation of Cavitation and Resulting Particle Formation in Protein Formulations After Application of Mechanical Shock. J Pharm Sci 2020, 109 (3), 1270–1280. https://doi.org/10.1016/j.xphs.2019.11.015.
(231) Torisu, T.; Maruno, T.; Yoneda, S.; Hamaji, Y.; Honda, S.; Ohkubo, T.; Uchiyama, S. Friability Testing as a New Stress-Stability Assay for Biopharmaceuticals. J Pharm Sci 2017, 106 (10), 2966–2978. https://doi.org/10.1016/j.xphs.2017.05.035.
(232) Dill, S.; Brees, K.; Stahly, A.; Cheng, E.; Carpenter, J.; Caplan, L. Mechanical Shock During Shipping of Medications: The Roles of Packaging and Transportation Vendors. J Pharm Sci 2020, 109 (1), 670–676. https://doi.org/10.1016/j.xphs.2019.10.050.

(233) Jiao, N.; Barnett, G. V.; Christian, T. R.; Narhi, L. O.; Joh, N. H.; Joubert, M. K.; Cao, S. Characterization of Subvisible Particles in Biotherapeutic Prefilled Syringes: The Role of Polysorbate and Protein on the Formation of Silicone Oil and Protein Subvisible Particles After Drop Shock. J Pharm Sci 2020, 109 (1), 640–645. https://doi.org/10.1016/j.xphs.2019.10.066.
(234) Thakral, S.; Sonje, J.; Munjal, B.; Suryanarayanan, R. Stabilizers and Their Interaction with Formulation Components in Frozen and Freeze-Dried Protein Formulations. Adv Drug Deliv Rev 2021, 173, 1–19. https://doi.org/10.1016/j.addr.2021.03.003.
(235) Lee, H. J.; McAuley, A.; Schilke, K. F.; McGuire, J. Molecular Origins of Surfactant-Mediated Stabilization of Protein Drugs. Adv Drug Deliv Rev 2011, 63 (13), 1160–1171. https://doi.org/10.1016/j.addr.2011.06.015.
(236) Bai, L.; Zhang, Y.; Zhang, C.; Lu, Y.; Li, Z.; Huang, G.; Meng, B. Investigation of Excipients Impact on Polysorbate 80 Degradation in Biopharmaceutical Formulation Buffers. J Pharm Biomed Anal 2023, 233. https://doi.org/10.1016/j.jpba.2023.115496.
(237) Goli, V. A. R.; Butreddy, A. Biosimilar Monoclonal Antibodies: Challenges and Approaches towards Formulation. Chem Biol Interact 2022, 366. https://doi.org/10.1016/j.cbi.2022.110116.
(238) Ghosh, I.; Gutka, H.; Krause, M. E.; Clemens, R.; Kashi, R. S. A Systematic Review of Commercial High Concentration Antibody Drug Products Approved in the US: Formulation Composition, Dosage Form Design and Primary Packaging Considerations. MAbs 2023, 15 (1). https://doi.org/10.1080/19420862.2023.2205540.
(239) Her, C.; Carpenter, J. F. Effects of Tubing Type, Formulation, and Postpumping Agitation on Nanoparticle and Microparticle Formation in Intravenous Immunoglobulin Solutions Processed With a Peristaltic Filling Pump. J Pharm Sci 2020, 109 (1), 739–749. https://doi.org/10.1016/j.xphs.2019.05.013.
(240) Tomlinson, A.; Zarraga, I. E.; Demeule, B. Characterization of Polysorbate Ester Fractions and Implications in Protein Drug Product Stability. Mol Pharm 2020, 17 (7), 2345–2353. https://doi.org/10.1021/acs.molpharmaceut.0c00093.
(241) Lebar, B.; Lekić, T.; Košir, P.; Kastelic, M.; Zidar, M.; Mravljak, J.; Pajk, S. Polysorbate Stability: Effects of Packaging Materials, Buffers, Counterions, and PH. Int J Pharm 2024, 665. https://doi.org/10.1016/j.ijpharm.2024.124598.
(242) Poumarede, L.; Audat, H.; Pellet, C.; de la Motte Saint Pierre, M.; Narradon, C.; Bensaid, F.; Nakach, M.; Authelin, J.-R.; Wils, P. Impact of Tubing Material on Stability and Filling Accuracy of Biologic Drug Product. Int J Pharm 2024, 654. https://doi.org/10.1016/j.ijpharm.2024.123927.
(243) Bensaid, F.; Dagallier, C.; Authelin, J.-R.; Audat, H.; Filipe, V.; Narradon, C.; Guibal, P.; Clavier, S.; Wils, P. Mechanistic Understanding of Metal-Catalyzed Oxidation of Polysorbate 80 and Monoclonal Antibody in Biotherapeutic Formulations. Int J Pharm 2022, 615. https://doi.org/10.1016/j.ijpharm.2022.121496.
(244) Wang, W.; Zheng, S.; Li, J. Adsorption of Lysozyme and Antibodies at Material Surfaces: Implications to Material Compatibility for Development of Biologics. J Drug Deliv Sci Technol 2022, 73. https://doi.org/10.1016/j.jddst.2022.103416.
(245) Mahler, H.-C.; Printz, M.; Kopf, R.; Schuller, R.; Müller, R. Behaviour of Polysorbate 20 During Dialysis, Concentration and Filtration Using Membrane Separation Techniques. J Pharm Sci 2008, 97 (2), 764–774. https://doi.org/10.1002/jps.21029.
(246) Zhou, J.; Qiu, J.; Jiang, G.; Zhou, C.; Bingham, N.; Yeung, H.; Dransart, B.; Wadhwa, M.; Tressel, T. Non-Specific Binding and Saturation of Polysorbate-20 with Aseptic Filter

Membranes for Drug Substance and Drug Product during MAb Production. J Memb Sci 2008, 325 (2), 735–741. https://doi.org/10.1016/j.memsci.2008.08.046.
(247) Shi, G. H.; Gopalrathnam, G.; Shinkle, S. L.; Dong, X.; Hofer, J. D.; Jensen, E. C.; Rajagopalan, N. Impact of Drug Formulation Variables on Silicone Oil Structure and Functionality of Prefilled Syringe System. PDA J Pharm Sci Technol 2018, 72 (1), 50–61. https://doi.org/10.5731/pdajpst.2017.008169.
(248) Richard, C. A.; Wang, T.; Clark, S. L. Using First Principles to Link Silicone Oil/Formulation Interfacial Tension With Syringe Functionality in Pre-Filled Syringes Systems. J Pharm Sci 2020, 109 (10), 3006–3012. https://doi.org/10.1016/j.xphs.2020.06.014.
(249) Wang, T.; Richard, C. A.; Dong, X.; Shi, G. H. Impact of Surfactants on the Functionality of Prefilled Syringes. J Pharm Sci 2020, 109 (11), 3413–3422. https://doi.org/10.1016/j.xphs.2020.07.033.
(250) Soeda, K.; Fukuda, M.; Takahashi, M.; Imai, H.; Arai, K.; Saitoh, S.; Kishore, R. S. K.; Oltra, N. S.; Duboeuf, J.; Hashimoto, D.; Yamanaka, Y. Impact of Poloxamer 188 Material Attributes on Proteinaceous Visible Particle Formation in Liquid Monoclonal Antibody Formulations. J Pharm Sci 2022, 111 (8), 2191–2200. https://doi.org/10.1016/j.xphs.2022.04.012.
(251) Katz, J. S.; Chou, D. K.; Christian, T. R.; Das, T. K.; Patel, M.; Singh, S. N.; Wen, Y. Emerging Challenges and Innovations in Surfactant-Mediated Stabilization of Biologic Formulations. J Pharm Sci 2022, 111 (4), 919–932. https://doi.org/10.1016/j.xphs.2021.12.002.
(252) Yue, L.; Yan, Z.; Li, H.; Liu, X.; Sun, P. Brij-58, a Potential Injectable Protein-Stabilizer Used in Therapeutic Protein Formulation. Eur J Pharm Biopharm 2020, 146, 73–83. https://doi.org/10.1016/j.ejpb.2019.12.001.
(253) Brosig, S.; Cucuzza, S.; Serno, T.; Bechtold-Peters, K.; Buecheler, J.; Zivec, M.; Germershaus, O.; Gallou, F. Not the Usual Suspects: Alternative Surfactants for Biopharmaceuticals. ACS Appl Mater Interfaces 2023, 15 (29), 34540–34553. https://doi.org/10.1021/acsami.3c05610.
(254) Prashar, D.; Cui, D.; Bandyopadhyay, D.; Luk, Y. Y. Modification of Proteins with Cyclodextrins Prevents Aggregation and Surface Adsorption and Increases Thermal Stability. Langmuir 2011, 27 (21), 13091–13096. https://doi.org/10.1021/la203271u.
(255) Zhang, H.; Hong, S.; Si Kai Tan, S.; Peng, T.; Yuan Hao Goh, L.; Lam, K. H.; Chow, K. T.; Gokhale, R. Polysorbates versus Hydroxypropyl Beta-Cyclodextrin (HPβCD): Comparative Study on Excipient Stability and Stabilization Benefits on Monoclonal Antibodies. Molecules 2022, 27 (19). https://doi.org/10.3390/molecules27196497.
(256) Stolzke, T.; Krieg, F.; Peng, T.; Zhang, H.; Häusler, O.; Brandenbusch, C. Hydroxylpropyl-β-Cyclodextrin as Potential Excipient to Prevent Stress-Induced Aggregation in Liquid Protein Formulations. Molecules 2022, 27 (16). https://doi.org/10.3390/molecules27165094.
(257) Serno, T.; Härtl, E.; Besheer, A.; Miller, R.; Winter, G. The Role of Polysorbate 80 and HPβCD at the Air-Water Interface of IgG Solutions. Pharm Res 2013, 30, 117–130. https://doi.org/10.1007/s11095-012-0854-x.
(258) Callahan, D. J.; Stanley, B.; Li, Y. Control of Protein Particle Formation During Ultrafiltration/Diafiltration Through Interfacial Protection. J Pharm Sci 2014, 103 (3), 862–869. https://doi.org/10.1002/jps.23861.
(259) Cucuzza, S.; Brosig, S.; Serno, T.; Bechtold-Peters, K.; Cerar, J.; Kammüller, M.; Gallou, F. Modular and Tunable Alternative Surfactants for Biopharmaceuticals Provide Insights into

Surfactant's Structure-Function Relationship. Int J Pharm 2024, 650. https://doi.org/10.1016/j.ijpharm.2023.123692.
(260) Kale, S. S.; Akamanchi, K. G. Trehalose Monooleate: A Potential Antiaggregation Agent for Stabilization of Proteins. Mol Pharm 2016, 13 (12), 4082–4093. https://doi.org/10.1021/acs.molpharmaceut.6b00686.
(261) King, T. E.; Humphrey, J. R.; Laughton, C. A.; Thomas, N. R.; Hirst, J. D. Optimizing Excipient Properties to Prevent Aggregation in Biopharmaceutical Formulations. J Chem Inf Model 2024, 64 (1), 265–275. https://doi.org/10.1021/acs.jcim.3c01898.
(262) Roy, I.; Wuchner, K.; Stahl, P.; Tran, T.; Yaragudi, N. A Comparison of Polysorbates and Alternative Surfactants for Interfacial Stress Protection and Mitigation of Fatty Acid Particle Formation in the Presence of an Esterase. J Pharm Sci 2024, 113 (9), 2688–2698. https://doi.org/10.1016/j.xphs.2024.07.010.
(263) Huang, J.; Hong, S.; Goh, L. Y. H.; Zhang, H.; Peng, T.; Chow, K. T.; Gokhale, R.; Tuliani, V. Investigation on the Combined Effect of Hydroxypropyl Beta-Cyclodextrin (HPβCD) and Polysorbate in Monoclonal Antibody Formulation. Pharmaceuticals 2024, 17 (4). https://doi.org/10.3390/ph17040528.
(264) Papadopoulos, E.; Arrahmani, B. C.; Beck, K.; Friess, W. Lyso-Phosphatidylcholine as an Interfacial Stabilizer for Parenteral Monoclonal Antibody Formulations. European Journal of Pharmaceutics and Biopharmaceutics 2024, 204. https://doi.org/10.1016/j.ejpb.2024.114514.
(265) Katz, J. S.; Nolin, A.; Yezer, B. A.; Jordan, S. Dynamic Properties of Novel Excipient Suggest Mechanism for Improved Performance in Liquid Stabilization of Protein Biologics. Mol Pharm 2019, 16 (1), 282–291. https://doi.org/10.1021/acs.molpharmaceut.8b00984.
(266) Kanthe, A. D.; Carnovale, M. R.; Katz, J. S.; Jordan, S.; Krause, M. E.; Zheng, S.; Ilott, A.; Ying, W.; Bu, W.; Bera, M. K.; Lin, B.; Maldarelli, C.; Tu, R. S. Differential Surface Adsorption Phenomena for Conventional and Novel Surfactants Correlates with Changes in Interfacial MAb Stabilization. Mol Pharm 2022, 19 (9), 3100–3113. https://doi.org/10.1021/acs.molpharmaceut.2c00152.
(267) Katz, J. S.; Tan, Y.; Kuppannan, K.; Song, Y.; Brennan, D. J.; Young, T.; Yao, L.; Jordan, S. Amino-Acid-Incorporating Nonionic Surfactants for Stabilization of Protein Pharmaceuticals. ACS Biomater Sci Eng 2016, 2 (7), 1093–1096. https://doi.org/10.1021/acsbiomaterials.6b00245.
(268) Hanson, M. G.; Katz, J. S.; Ma, H.; Putterman, M.; Yezer, B. A.; Petermann, O.; Reineke, T. M. Effects of Hydrophobic Tail Length Variation on Surfactant-Mediated Protein Stabilization. Mol Pharm 2020, 17 (11), 4302–4311. https://doi.org/10.1021/acs.molpharmaceut.0c00737.
(269) Fares, H. M.; Carnovale, M.; Tabouguia, M. O. N.; Jordan, S.; Katz, J. S. Novel Surfactant Compatibility with Downstream Protein Bioprocesses. J Pharm Sci 2023, 112 (7), 1811–1820. https://doi.org/10.1016/j.xphs.2023.04.011.
(270) Dasnoy, S.; Illartin, M.; Queffelec, J.; Nkunku, A.; Peerboom, C. Combined Effect of Shaking Orbit and Vial Orientation on the Agitation-Induced Aggregation of Proteins. J Pharm Sci 2024, 113 (3), 669–679. https://doi.org/10.1016/j.xphs.2023.08.016.
(271) Jorgensen, L.; Hostrup, S.; Moeller, E. H.; Grohganz, H. Recent Trends in Stabilising Peptides and Proteins in Pharmaceutical Formulation - Considerations in the Choice of Excipients. Expert Opin Drug Deliv 2009, 6 (11), 1219–1230. https://doi.org/10.1517/17425240903199143.

(272) Mozgovicz, M.; Fischer, A.; Brocard, C.; Jungbauer, A.; Lingg, N. L-Arginine Sulfate Reduces Irreversible Protein Binding in Immobilized Metal Affinity Chromatography. J Chromatogr A 2023, 1706. https://doi.org/10.1016/j.chroma.2023.464246.
(273) Arakawa, T.; Ejima, D.; Tsumoto, K.; Obeyama, N.; Tanaka, Y.; Kita, Y.; Timasheff, S. N. Suppression of Protein Interactions by Arginine: A Proposed Mechanism of the Arginine Effects. Biophys Chem 2007, 127 (1–2), 1–8. https://doi.org/10.1016/j.bpc.2006.12.007.
(274) Kim, N. A.; Hada, S.; Thapa, R.; Jeong, S. H. Arginine as a Protein Stabilizer and Destabilizer in Liquid Formulations. Int J Pharm 2016, 513 (1–2), 26–37. https://doi.org/10.1016/j.ijpharm.2016.09.003.
(275) Fukuda, M.; Kameoka, D.; Torizawa, T.; Saitoh, S.; Yasutake, M.; Imaeda, Y.; Koga, A.; Mizutani, A. Thermodynamic and Fluorescence Analyses to Determine Mechanisms of IgG1 Stabilization and Destabilization by Arginine. Pharm Res 2014, 31, 992–1001. https://doi.org/10.1007/s11095-013-1221-2.
(276) Raza, M. A.; Hallett, P. D.; Liu, X.; He, M.; Afzal, W. Surface Tension of Aqueous Solutions of Small-Chain Amino and Organic Acids. J Chem Eng Data 2019, 64 (12), 5049–5056. https://doi.org/10.1021/acs.jced.9b00026.
(277) Horn, J.; Tolardo, E.; Fissore, D.; Friess, W. Crystallizing Amino Acids as Bulking Agents in Freeze-Drying. Eur J Pharm Biopharm 2018, 132, 70–82. https://doi.org/10.1016/j.ejpb.2018.09.004.
(278) Wendorf, J. R.; Radke, C. J.; Blanch, H. W. Reduced Protein Adsorption at Solid Interfaces by Sugar Excipients. Biotechnol Bioeng 2004, 87 (5), 565–573. https://doi.org/10.1002/bit.20132.
(279) Evers, F.; Steitz, R.; Tolan, M.; Czeslik, C. Reduced Protein Adsorption by Osmolytes. Langmuir 2011, 27 (11), 6995–7001. https://doi.org/10.1021/la2010908.
(280) McArthur, S. L.; McLean, K. M.; Kingshott, P.; St John, H. A. W.; Chatelier, R. C.; Griesser, H. J. Effect of Polysaccharide Structure on Protein Adsorption. Colloids Surf B Biointerfaces 2000, 17 (1), 37–48. https://doi.org/10.1016/S0927-7765(99)00086-7.
(281) Rösch, C.; Kratz, F.; Hering, T.; Trautmann, S.; Umanskaya, N.; Tippkötter, N.; Müller-Renno, C.; Ulber, R.; Hannig, M.; Ziegler, C. Albumin-Lysozyme Interactions: Cooperative Adsorption on Titanium and Enzymatic Activity. Colloids Surf B Biointerfaces 2017, 149, 115–121. https://doi.org/10.1016/j.colsurfb.2016.09.048.
(282) Tarelli, E.; Mire-Sluis, A.; Tivnann, H. A.; Bolgiano, B.; Crane, D. T.; Gee, C.; Lemercinier, X.; Athayde, M. L.; Sutcliffe, N.; Corran, P. H.; Rafferty, B. Recombinant Human Albumin as a Stabilizer for Biological Materials and for the Preparation of International Reference Reagents. Biologicals 1998, 26 (4), 331–346. https://doi.org/10.1006/biol.1998.0163.
(283) Fujita, R.; Nagatoishi, S.; Adachi, S.; Nishioka, H.; Ninomiya, H.; Kaya, T.; Takai, M.; Arakawa, T.; Tsumoto, K. Control of Protein Adsorption to Cyclo Olefin Polymer by the Hofmeister Effect. J Pharm Sci 2019, 108 (5), 1686–1691. https://doi.org/10.1016/j.xphs.2018.12.023.
(284) Ukidve, A.; Rembert, K. B.; Vanipenta, R.; Dorion, P.; Lafarguette, P.; McCoy, T.; Saluja, A.; Suryanarayanan, R.; Patke, S. Succinate Buffer in Biologics Products: Real-World Formulation Considerations, Processing Risks and Mitigation Strategies. J Pharm Sci 2023, 112 (1), 138–147. https://doi.org/10.1016/j.xphs.2022.05.026.
(285) Tomlinson, A.; Demeule, B.; Lin, B.; Yadav, S. Polysorbate 20 Degradation in Biopharmaceutical Formulations: Quantification of Free Fatty Acids, Characterization of Particulates, and Insights into the Degradation Mechanism. Mol Pharm 2015. https://doi.org/10.1021/acs.molpharmaceut.5b00311.

(286) Fish, R.; Lin, J.; Doshi, N. Impact of Silicone Oil on Free Fatty Acid Particle Formation Due to Polysorbate 20 Degradation. Pharm Res 2020, 37. https://doi.org/10.1007/s11095-020-02936-3.
(287) Härtl, E.; Dixit, N.; Besheer, A.; Kalonia, D.; Winter, G. Weak Antibody–Cyclodextrin Interactions Determined by Quartz Crystal Microbalance and Dynamic/Static Light Scattering. Eur J Pharm Biopharm 2013, 85 (3), 781–789. https://doi.org/10.1016/j.ejpb.2013.04.021.
(288) Munjal, B.; Patel, S. M.; Suryanarayanan, R. Role of Arginine Salts in Preventing Freezing-Induced Increase in Subvisible Particles in Protein Formulations. Int J Pharm 2022, 619. https://doi.org/10.1016/j.ijpharm.2022.121694.
(289) Paik, S. H.; Kim, Y. J.; Han, S. K.; Kim, J. M.; Huh, J. W.; Park, Y. I. Mixture of Three Amino Acids as Stabilizers Replacing Albumin in Lyophilization of New Third Generation Recombinant Factor VIII GreenGene F. Biotechnol Prog 2012, 28 (6), 1517–1525. https://doi.org/10.1002/btpr.1640.
(290) Baldursdottir, S.; Tauhaybeche, M.; Pajander, J.; Bukrinski, J. T.; Jorgensen, L. Screening of Formulation Parameters for Stabilizing Recombinant Human Serum Albumin (RHSA) in Liquid Formulations. J Drug Deliv Sci Technol 2016, 34, 1–9. https://doi.org/10.1016/j.jddst.2016.05.001.
(291) Hawe, A.; Friess, W. Stabilization of a Hydrophobic Recombinant Cytokine by Human Serum Albumin. J Pharm Sci 2007, 96 (11), 2987–2999. https://doi.org/10.1002/jps.20909.
(292) Hawe, A.; Friess, W. Development of HSA-Free Formulations for a Hydrophobic Cytokine with Improved Stability. Eur J Pharm Biopharm 2008, 68 (2), 169–182. https://doi.org/10.1016/j.ejpb.2007.04.018.
(293) Haeuser, C.; Goldbach, P.; Huwyler, J.; Friess, W.; Allmendinger, A. Excipients for Room Temperature Stable Freeze-Dried Monoclonal Antibody Formulations. J Pharm Sci 2020, 109 (1), 807–817. https://doi.org/10.1016/j.xphs.2019.10.016.
(294) Gray, J. J. The Interaction of Proteins with Solid Surfaces. Curr Opin Struct Biol 2004, 14 (1), 110–115. https://doi.org/10.1016/j.sbi.2003.12.001.
(295) Arai, T.; Norde, W. The Behavior of Some Model Proteins at Solid-Liquid Interfaces 1. Adsorption from Single Protein Solutions. Colloids and Surfaces 1990, 51, 1–15. https://doi.org/10.1016/0166-6622(90)80127-P.
(296) Wang, W.; Ohtake, S. Science and Art of Protein Formulation Development. Int J Pharm 2019, 568, 118505. https://doi.org/10.1016/j.ijpharm.2019.118505.
(297) Meissner, J.; Prause, A.; Bharti, B.; Findenegg, G. H. Characterization of Protein Adsorption onto Silica Nanoparticles: Influence of PH and Ionic Strength. Colloid Polym Sci 2015, 293 (11), 3381–3391. https://doi.org/10.1007/s00396-015-3754-x.
(298) Roberts, D.; Keeling, R.; Tracka, M.; van der Walle, C. F.; Uddin, S.; Warwicker, J.; Curtis, R. Specific Ion and Buffer Effects on Protein–Protein Interactions of a Monoclonal Antibody. Mol Pharm 2015, 12 (1), 179–193. https://doi.org/10.1021/mp500533c.
(299) Weidman, J.; Mathews, L.; Gokhale, K. Quartz Crystal Microbalance as a Predictive Tool for Drug-Material of Construction Interactions in Intravenous Protein Drug Administration. J Pharm Sci 2023, 112 (12), 3154–3163. https://doi.org/10.1016/j.xphs.2023.07.019.
(300) Greenfield, N. J. Using Circular Dichroism Spectra to Estimate Protein Secondary Structure. Nat Protoc 2007, 1 (6), 2876–2890. https://doi.org/10.1038/nprot.2006.202.
(301) Reviakine, I.; Johannsmann, D.; Richter, R. P. Hearing What You Cannot See and Visualizing What You Hear: Interpreting Quartz Crystal Microbalance Data from Solvated Interfaces. Anal Chem 2011, 83 (23), 8838–8848. https://doi.org/10.1021/ac201778h.

(302) Saurabh, S.; Kalonia, C.; Li, Z.; Hollowell, P.; Waigh, T.; Li, P.; Webster, J.; Seddon, J. M.; Lu, J. R.; Bresme, F. Understanding the Stabilizing Effect of Histidine on MAb Aggregation: A Molecular Dynamics Study. Mol Pharm 2022, 19 (9), 3288–3303. https://doi.org/10.1021/acs.molpharmaceut.2c00453.
(303) Couston, R. G.; Lamprou, D. A.; Uddin, S.; van der Walle, C. F. Interaction and Destabilization of a Monoclonal Antibody and Albumin to Surfaces of Varying Functionality and Hydrophobicity. Int J Pharm 2012, 438 (1–2), 71–80. https://doi.org/10.1016/j.ijpharm.2012.09.002.
(304) Nezu, T.; Taira, M.; Saitoh, S.; Sasaki, K.; Araki, Y. Viscoelastic Adlayers of Collagen and Lysozyme Studied Using Quartz Crystal Microbalance with Dissipation Monitoring. Int J Biol Macromol 2010, 46 (4), 396–403. https://doi.org/10.1016/j.ijbiomac.2010.02.005.
(305) Glomm, W. R.; Halskau, , Øyvind; Hanneseth, A.-M. D.; Volden, S. Adsorption Behavior of Acidic and Basic Proteins onto Citrate-Coated Au Surfaces Correlated to Their Native Fold, Stability, and PI. J Phys Chem B 2007, 111 (51), 14329–14345. https://doi.org/10.1021/jp074839d.
(306) Wei, T.; Kaewtathip, S.; Shing, K. Buffer Effect on Protein Adsorption at Liquid/Solid Interface. Journal of Physical Chemistry C 2009, 113 (6), 2053–2062. https://doi.org/10.1021/jp806586n.
(307) Hlady, V.; Buijs, J.; Jennissen, H. P. Methods for Studying Protein Adsorption. Methods Enzymol 1999, 309, 402–429. https://doi.org/10.1016/S0076-6879(99)09028-X.
(308) Kiesel, I.; Paulus, M.; Nase, J.; Tiemeyer, S.; Sternemann, C.; Rüster, K.; Wirkert, F. J.; Mende, K.; Büning, T.; Tolan, M. Temperature-Driven Adsorption and Desorption of Proteins at Solid-Liquid Interfaces. Langmuir 2014, 30 (8), 2077–2083. https://doi.org/10.1021/la404884a.
(309) Raman, B.; Ramakrishna, T.; Rao, Ch. M. Refolding of Denatured and Denatured/Reduced Lysozyme at High Concentrations. Journal of Biological Chemistry 1996, 271 (29), 17067–17072. https://doi.org/10.1074/jbc.271.29.17067.
(310) Strickley, R. G.; Lambert, W. J. A Review of Formulations of Commercially Available Antibodies. J Pharm Sci 2021, 110 (7), 2590-2608.e56. https://doi.org/10.1016/j.xphs.2021.03.017.
(311) Falconer, R. J. Advances in Liquid Formulations of Parenteral Therapeutic Proteins. Biotechnol Adv 2019, 37 (7). https://doi.org/10.1016/j.biotechadv.2019.06.011.
(312) Manning, M. C.; Holcomb, R. E.; Payne, R. W.; Stillahn, J. M.; Connolly, B. D.; Katayama, D. S.; Liu, H.; Matsuura, J. E.; Murphy, B. M.; Henry, C. S.; Crommelin, D. J. A. Stability of Protein Pharmaceuticals: Recent Advances. Pharm Res 2024, 41, 1301–1367. https://doi.org/10.1007/s11095-024-03726-x.
(313) Mollmann, S. H.; Jorgensen, L.; Bukrinsky, J. T.; Elofsson, U.; Norde, W.; Frokjaer, S. Interfacial Adsorption of Insulin: Conformational Changes and Reversibility of Adsorption. Eur J Pharm Sci 2006, 27 (2–3), 194–204. https://doi.org/10.1016/j.ejps.2005.09.010.
(314) Gerhardt, A.; Mcumber, A. C.; Nguyen, B. H.; Lewus, R.; Schwartz, D. K.; Carpenter, J. F.; Randolph, T. W. Surfactant Effects on Particle Generation in Antibody Formulations in Pre-Filled Syringes. J Pharm Sci 2015, 104 (12), 4056–4064. https://doi.org/10.1002/jps.24654.
(315) Härdter, N.; Menzen, T.; Winter, G. Minimizing Oxidation of Freeze-Dried Monoclonal Antibodies in Polymeric Vials Using a Smart Packaging Approach. Pharmaceutics 2021, 13 (10). https://doi.org/10.3390/pharmaceutics13101695.

(316) Szenczi, Á.; Kardos, J.; Medgyesi, G. A.; Závodszky, P. The Effect of Solvent Environment on the Conformation and Stability of Human Polyclonal IgG in Solution. Biologicals 2006, 34 (1), 5–14. https://doi.org/10.1016/j.biologicals.2005.06.007.
(317) Wang, S.; Zhang, N.; Hu, T.; Dai, W.; Feng, X.; Zhang, X.; Qian, F. Viscosity-Lowering Effect of Amino Acids and Salts on Highly Concentrated Solutions of Two IgG1 Monoclonal Antibodies. Mol Pharm 2015, 12 (12), 4478–4487. https://doi.org/10.1021/acs.molpharmaceut.5b00643.
(318) Kheddo, P.; Tracka, M.; Armer, J.; Dearman, R. J.; Uddin, S.; van der Walle, C. F.; Golovanov, A. P. The Effect of Arginine Glutamate on the Stability of Monoclonal Antibodies in Solution. Int J Pharm 2014, 473 (1–2), 126–133. https://doi.org/10.1016/j.ijpharm.2014.06.053.
(319) Stroppel, L.; Schultz-Fademrecht, T.; Cebulla, M.; Blech, M.; Marhöfer, R. J.; Selzer, P. M.; Garidel, P. Antimicrobial Preservatives for Protein and Peptide Formulations: An Overview. Pharmaceutics 2023, 15 (2). https://doi.org/10.3390/pharmaceutics15020563.
(320) Qureshi, M. A.; Javed, S. Aflatoxin B1 Induced Structural and Conformational Changes in Bovine Serum Albumin: A Multispectroscopic and Circular Dichroism-Based Study. ACS Omega 2021, 6 (28), 18054–18064. https://doi.org/10.1021/acsomega.1c01799.
(321) Callow, M. E.; Fletcher, R. L. The Influence of Low Surface Energy Materials on Bioadhesion — a Review. Int Biodeterior Biodegradation 1994, 34 (3–4), 333–348. https://doi.org/10.1016/0964-8305(94)90092-2.
(322) Sharma, L. G.; Pandey, L. M. Thermomechanical Process Induces Unfolding and Fibrillation of Bovine Serum Albumin. Food Hydrocoll 2021, 112. https://doi.org/10.1016/j.foodhyd.2020.106294.
(323) Oom, A.; Poggi, M.; Wikström, J.; Sukumar, M. Surface Interactions of Monoclonal Antibodies Characterized by Quartz Crystal Microbalance with Dissipation: Impact of Hydrophobicity and Protein Self-Interactions. J Pharm Sci 2012, 101 (2), 519–529. https://doi.org/10.1002/jps.22771.
(324) Vermeer, A.; Giacomelli, C. E.; Norde, W. Adsorption of IgG onto Hydrophobic Teflon. Differences between the Fab and Fc Domains. Biochimica et Biophysica Acta (BBA) - General Subjects 2001, 1526 (1), 61–69. https://doi.org/10.1016/S0304-4165(01)00101-5.
(325) Vermeer, A. W. P.; Bremer, M. G. E. G.; Norde, W. Structural Changes of IgG Induced by Heat Treatment and by Adsorption onto a Hydrophobic Teflon Surface Studied by Circular Dichroism Spectroscopy. Biochimica et Biophysica Acta (BBA) - General Subjects 1998, 1425 (1), 1–12. https://doi.org/10.1016/S0304-4165(98)00048-8.
(326) Mahler, H.-C.; Müller, R.; Frieβ, W.; Delille, A.; Matheus, S. Induction and Analysis of Aggregates in a Liquid IgG1-Antibody Formulation. Eur J Pharm Biopharm 2005, 59 (3), 407–417. https://doi.org/10.1016/j.ejpb.2004.12.004.
(327) Borzova, V. A.; Markossian, K. A.; Chebotareva, N. A.; Kleymenov, S. Yu.; Poliansky, N. B.; Muranov, K. O.; Stein-Margolina, V. A.; Shubin, V. V.; Markov, D. I.; Kurganov, B. I. Kinetics of Thermal Denaturation and Aggregation of Bovine Serum Albumin. PLoS One 2016, 11 (4). https://doi.org/10.1371/journal.pone.0153495.
(328) Ma, G. J.; Yoon, B. K.; Sut, T. N.; Yoo, K. Y.; Lee, S. H.; Jeon, W.; Jackman, J. A.; Ariga, K.; Cho, N. Lipid Coating Technology: A Potential Solution to Address the Problem of Sticky Containers and Vanishing Drugs. View 2021, 3 (3). https://doi.org/10.1002/viw.20200078.
(329) Kim, K.; Kim, C.; Byun, Y. Biostability and Biocompatibility of a Surface-Grafted Phospholipid Monolayer on a Solid Substrate. Biomaterials 2004, 25 (1), 33–41. https://doi.org/10.1016/S0142-9612(03)00469-1.

(330) Le, T. C.; Penna, M.; Winkler, D. A.; Yarovsky, I. Quantitative Design Rules for Protein-Resistant Surface Coatings Using Machine Learning. Sci Rep 2019, 9, 1–12. https://doi.org/10.1038/s41598-018-36597-5.
(331) Chapman, R. G.; Ostuni, E.; Takayama, S.; Holmlin, R. E.; Yan, L.; Whitesides, G. M. Surveying for Surfaces That Resist the Adsorption of Proteins. J Am Chem Soc 2000, 122 (34), 8303–8304. https://doi.org/10.1021/ja000774f.
(332) Goda, T.; Ishihara, K.; Miyahara, Y. Critical Update on 2-Methacryloyloxyethyl Phosphorylcholine (MPC) Polymer Science. J Appl Polym Sci 2015, 132 (16). https://doi.org/10.1002/app.41766.
(333) Katayama, R.; Ikeda, M.; Shiraishi, K.; Matsumoto, A.; Kojima, C. Formation of Hydrophobic Domains on the Poly(MPC- Co-Dodecyl Methacrylate)-Coated Surface Recognized by Macrophage-like Cells. Langmuir 2019, 35 (37), 12229–12235. https://doi.org/10.1021/acs.langmuir.9b00178.
(334) Katayama, R.; Tanaka, N.; Takagi, Y.; Shiraishi, K.; Tanaka, Y.; Matsumoto, A.; Kojima, C. Characterization of the Hydration Process of Phospholipid-Mimetic Polymers Using Air-Injection-Mediated Liquid Exclusion Methods. Langmuir 2020, 36 (20), 5626–5632. https://doi.org/10.1021/acs.langmuir.0c00953.
(335) Ishihara, K.; Ziats, N. P.; Tierney, B. P.; Nakabayashi, N.; Anderson, J. M. Protein Adsorption from Human Plasma Is Reduced on Phospholipid Polymers. J Biomed Mater Res 1991, 25 (11), 1397–1407. https://doi.org/10.1002/jbm.820251107.
(336) Chen, S.; Zheng, J.; Li, L.; Jiang, S. Strong Resistance of Phosphorylcholine Self-Assembled Monolayers to Protein Adsorption: Insights into Nonfouling Properties of Zwitterionic Materials. J Am Chem Soc 2005, 127 (41), 14473–14478. https://doi.org/10.1021/ja054169u.
(337) Schlenoff, J. B. Zwitteration: Coating Surfaces with Zwitterionic Functionality to Reduce Nonspecific Adsorption. Langmuir 2014, 30 (32), 9625–9636. https://doi.org/10.1021/la500057j.
(338) Sibarani, J.; Takai, M.; Ishihara, K. Surface Modification on Microfluidic Devices with 2-Methacryloyloxyethyl Phosphorylcholine Polymers for Reducing Unfavorable Protein Adsorption. Colloids Surf B Biointerfaces 2007, 54 (1), 88–93. https://doi.org/10.1016/j.colsurfb.2006.09.024.
(339) Ishihara, K.; Iwasaki, Y. Reduced Protein Adsorption on Novel Phospholipid Polymers. J Biomater Appl 1998, 13 (2). https://doi.org/10.1177/088532829801300203.
(340) Ishihara, K.; Nomura, H.; Mihara, T.; Kurita, K.; Iwasaki, Y.; Nakabayashi, N. Why Do Phospholipid Polymers Reduce Protein Adsorption? J Biomed Mater Res 1998, 39 (2), 323–330. https://doi.org/10.1002/(SICI)1097-4636(199802)39:2<323::AID-JBM21>3.0.CO;2-C.
(341) Yamasaki, A.; Imamura, Y.; Kurita, K.; Iwasaki, Y.; Nakabayashi, N.; Ishihara, K. Surface Mobility of Polymers Having Phosphorylcholine Groups Connected with Various Bridging Units and Their Protein Adsorption-Resistance Properties. Colloids Surf B Biointerfaces 2003, 28 (1), 53–62. https://doi.org/10.1016/S0927-7765(02)00130-3.
(342) Ho, S. P.; Nakabayashi, N.; Iwasaki, Y.; Boland, T.; LaBerge, M. Frictional Properties of Poly(MPC-Co-BMA) Phospholipid Polymer for Catheter Applications. Biomaterials 2003, 24 (28), 5121–5129. https://doi.org/10.1016/S0142-9612(03)00450-2.
(343) Ueda, T.; Oshida, H.; Kurita, K.; Ishihara, K.; Nakabayashi, N. Preparation of 2-Methacryloyloxyethyl Phosphorylcholine Copolymers with Alkyl Methacrylates and Their Blood Compatibility. Polym J 1992, 24, 1259–1269. https://doi.org/https://doi.org/10.1295/polymj.24.1259.

(344) Ishihara, K. Blood-Compatible Surfaces with Phosphorylcholine-Based Polymers for Cardiovascular Medical Devices. Langmuir 2019, 35 (5), 1778–1787. https://doi.org/10.1021/acs.langmuir.8b01565.
(345) Frazier, R. A.; Matthijs, G.; Davies, M. C.; Roberts, C. J.; Schacht, E.; Tendler, S. J. B. Characterization of Protein-Resistant Dextran Monolayers. Biomaterials 2000, 21 (9), 957–966. https://doi.org/10.1016/S0142-9612(99)00270-7.
(346) Elam, J. H.; Nygren, H.; Stenberg, M. Covalent Coupling of Polysaccharides to Silicon and Silicon Rubber Surfaces. J Biomed Mater Res 1984, 18 (8), 953–959. https://doi.org/10.1002/jbm.820180809.
(347) O'Sullivan, D.; O'Neill, L.; Bourke, P. Direct Plasma Deposition of Collagen on 96-Well Polystyrene Plates for Cell Culture. ACS Omega 2020, 5 (39), 25069–25076. https://doi.org/10.1021/acsomega.0c02073.
(348) O'Neill, L.; Twomey, B.; Tan, F.; O'Donoghue, J.; Hunt, J. A. Collagen Coating of Titanium Implants Using Nonthermal Plasma. Plasma Med 2021, 11 (2), 63–79. https://doi.org/10.1615/PlasmaMed.2021039685.
(349) Olayiwola, B.; O'Neill, F.; Frewen, C.; Kavanagh, D. F.; O'Hara, R.; O'Neill, L. Cold Plasma Deposition of Tobramycin as an Approach to Localized Antibiotic Delivery to Combat Biofilm Formation. Pathogens 2024, 13 (4). https://doi.org/10.3390/pathogens13040326.
(350) Regis, F.; Arsiccio, A.; Bourlès, E.; Scutellà, B.; Pisano, R. Surface Treatment of Glass Vials for Lyophilization: Implications for Vacuum-Induced Surface Freezing. Pharmaceutics 2021, 13 (11). https://doi.org/10.3390/pharmaceutics13111766.
(351) Kuhr, M.; Bauer, S.; Rothhaar, U.; Wolff, D. Coatings on Plastics with the PICVD Technology. Thin Solid Films 2003, 442 (1–2), 107–116. https://doi.org/10.1016/S0040-6090(03)00956-8.
(352) Lee, J.; Yi, S.; Hong, K. D.; Seo, J. H. Copolymerization of Zwitterionic Carboxybetaine and Various Hydrophobic Groups to Optimize Antifouling and Biocompatible Properties. J Ind Eng Chem 2021, 96, 284–293. https://doi.org/10.1016/j.jiec.2021.01.034.
(353) Gökaltun, A.; Kang, Y. B. (Abraham); Yarmush, M. L.; Usta, O. B.; Asatekin, A. Simple Surface Modification of Poly(Dimethylsiloxane) via Surface Segregating Smart Polymers for Biomicrofluidics. Sci Rep 2019, 9. https://doi.org/10.1038/s41598-019-43625-5.
(354) Kyomoto, M.; Moro, T.; Saiga, K.; Miyaji, F.; Kawaguchi, H.; Takatori, Y.; Nakamura, K.; Ishihara, K. Lubricity and Stability of Poly(2-Methacryloyloxyethyl Phosphorylcholine) Polymer Layer on Co–Cr–Mo Surface for Hemi-Arthroplasty to Prevent Degeneration of Articular Cartilage. Biomaterials 2010, 31 (4), 658–668. https://doi.org/10.1016/j.biomaterials.2009.09.083.
(355) Han, G.; Liu, J. T.; Lu, K. J.; Chung, T.-S. Advanced Anti-Fouling Membranes for Osmotic Power Generation from Wastewater via Pressure Retarded Osmosis (PRO). Environ Sci Technol 2018, 52 (11), 6686–6694. https://doi.org/10.1021/acs.est.7b05933.
(356) Ye, F.; Chen, Z.; Li, C.; Chen, J.; Yi, G. A Study of the Phosphorylcholine Polymer Coating of a Polymethylpentene Hollow Fiber Membrane. Polymers (Basel) 2023, 15 (13). https://doi.org/10.3390/polym15132881.
(357) Datta, J.; Kosiorek, P.; Włoch, M. Effect of High Loading of Titanium Dioxide Particles on the Morphology, Mechanical and Thermo-Mechanical Properties of the Natural Rubber-Based Composites. Iranian Polymer Journal 2016, 25 (12), 1021–1035. https://doi.org/10.1007/s13726-016-0488-7.
(358) Inoue, Y.; Onodera, Y.; Ishihara, K. Preparation of a Thick Polymer Brush Layer Composed of Poly(2-Methacryloyloxyethyl Phosphorylcholine) by Surface-Initiated Atom

Transfer Radical Polymerization and Analysis of Protein Adsorption Resistance. Colloids Surf B Biointerfaces 2016, 141, 507–512. https://doi.org/10.1016/j.colsurfb.2016.02.015.
(359) Bento, C.; Katz, M.; Santos, M. M. M.; Afonso, C. A. M. Striving for Uniformity: A Review on Advances and Challenges To Achieve Uniform Polyethylene Glycol. Org Process Res Dev 2024, 28 (4), 860–890. https://doi.org/10.1021/acs.oprd.3c00428.
(360) Zhong, Q.; Yan, J.; Qian, X.; Zhang, T.; Zhang, Z.; Li, A. Atomic Layer Deposition Enhanced Grafting of Phosphorylcholine on Stainless Steel for Intravascular Stents. Colloids Surf B Biointerfaces 2014, 121, 238–247. https://doi.org/10.1016/j.colsurfb.2014.06.022.
(361) Montaño-Machado, V.; Noël, C.; Chevallier, P.; Turgeon, S.; Houssiau, L.; Pauthe, E.; Pireaux, J.-J.; Mantovani, D. Interaction of Phosphorylcholine with Fibronectin Coatings: Surface Characterization and Biological Performances. Appl Surf Sci 2017, 396, 1613–1622. https://doi.org/10.1016/j.apsusc.2016.11.224.
(362) Nagahashi, K.; Teramura, Y.; Takai, M. Stable Surface Coating of Silicone Elastomer with Phosphorylcholine and Organosilane Copolymer with Cross-Linking for Repelling Proteins. Colloids Surf B Biointerfaces 2015, 134, 384–391. https://doi.org/10.1016/j.colsurfb.2015.07.040.
(363) O'Neill, L.; O'Sullivan, C. Polymeric Coatings Deposited From an Aerosol-Assisted Non-thermal Plasma Jet. Chemical Vapor Deposition 2009, 15 (1–3), 21–26. https://doi.org/10.1002/cvde.200806699.
(364) Treglia, A.; Palumbo, F.; Gristina, R.; Calvano, C. D.; Cataldi, T.; Fracassi, F.; Favia, P. Novel Aerosol Assisted Plasma Deposition of PEG Containing Coatings for Non-Fouling Application. Appl Surf Sci 2020, 527. https://doi.org/10.1016/j.apsusc.2020.146698.
(365) O'Sullivan, D.; McArdle, H.; Ng, S. W.; Bourke, P.; Forster, R.; O'Neill, L. Deposition of Cell Culture Coatings Using a Cold Plasma Deposition Method. Applied Sciences 2020, 10 (19). https://doi.org/10.3390/APP10196670.
(366) O'Sullivan, D.; McArdle, H.; O'Reilly, J. A.; O'Kennedy, R. J.; Forster, R.; O'Neill, L. Plasma Deposition of Collagen for Cell-Culture Applications. Plasma Processes and Polymers 2020, 17 (3). https://doi.org/10.1002/ppap.201900147.
(367) Rechendorff, K.; Hovgaard, M. B.; Foss, M.; Zhdanov, V. P.; Besenbacher, F. Enhancement of Protein Adsorption Induced by Surface Roughness. Langmuir 2006, 22 (26), 10885–10888. https://doi.org/10.1021/la0621923.
(368) Iwasaki, Y.; Ishihara, K. Phosphorylcholine-Containing Polymers for Biomedical Applications. Anal Bioanal Chem 2005, 381, 534–546. https://doi.org/10.1007/s00216-004-2805-9.
(369) Österberg, E.; Bergström, K.; Holmberg, K.; Schuman, T. P.; Riggs, J. A.; Burns, N. L.; Van Alstine, J. M.; Harris, J. M. Protein-rejecting Ability of Surface-bound Dextran in End-on and Side-on Configurations: Comparison to PEG. J Biomed Mater Res 1995, 29 (6), 741–747. https://doi.org/10.1002/jbm.820290610.
(370) Zhang, Z.; Moxey, M.; Alswieleh, A.; Morse, A. J.; Lewis, A. L.; Geoghegan, M.; Leggett, G. J. Effect of Salt on Phosphorylcholine-Based Zwitterionic Polymer Brushes. Langmuir 2016, 32 (20), 5048–5057. https://doi.org/10.1021/acs.langmuir.6b00763.
(371) Forov, Y.; Paulus, M.; Dogan, S.; Salmen, P.; Weis, C.; Gahlmann, T.; Behrendt, A.; Albers, C.; Elbers, M.; Schnettger, W.; Egger, S.; Zwar, E.; Rehage, H.; Kiesel, I.; Riedl, T.; Tolan, M. Adsorption Behavior of Lysozyme at Titanium Oxide-Water Interfaces. Langmuir 2018, 34 (19), 5403–5408. https://doi.org/10.1021/acs.langmuir.8b00280.
(372) Mehta, S. B.; Carpenter, J. F.; Randolph, T. W. Colloidal Instability Fosters Agglomeration of Subvisible Particles Created by Rupture of Gels of a Monoclonal Antibody

Formed at Silicone Oil-Water Interfaces. J Pharm Sci 2016, 105 (8), 2338–2348. https://doi.org/10.1016/j.xphs.2016.06.010.
(373) ElKassas, K.; Chullipalliyalil, K.; McAuliffe, M.; Vucen, S.; Crean, A. Fluorescence Spectroscopy for the Determination of Reconstitution Time of an In-Vial Lyophilised Product. Int J Pharm 2021, 597. https://doi.org/10.1016/j.ijpharm.2021.120368.
(374) Chullipalliyalil, K.; Elkassas, K.; McAuliffe, M. A. P.; Vucen, S.; Crean, A. In-Vial Detection of Protein Denaturation Using Intrinsic Fluorescence Anisotropy. Anal Chem 2023, 95 (5), 2774–2782. https://doi.org/10.1021/acs.analchem.2c03912.
(375) Gordon, K. C.; McGoverin, C. M. Raman Mapping of Pharmaceuticals. Int J Pharm 2011, 417 (1–2), 151–162. https://doi.org/10.1016/j.ijpharm.2010.12.030.
(376) Molodenskiy, D.; Shirshin, E.; Tikhonova, T.; Gruzinov, A.; Peters, G.; Spinozzi, F. Thermally Induced Conformational Changes and Protein–Protein Interactions of Bovine Serum Albumin in Aqueous Solution under Different PH and Ionic Strengths as Revealed by SAXS Measurements. Physical Chemistry Chemical Physics 2017, 19 (26), 17143–17155. https://doi.org/10.1039/C6CP08809K.
(377) Pace, C. N.; Fu, H.; Fryar, K. L.; Landua, J.; Trevino, S. R.; Shirley, B. A.; Hendricks, M. M.; Iimura, S.; Gajiwala, K.; Scholtz, J. M.; Grimsley, G. R. Contribution of Hydrophobic Interactions to Protein Stability. J Mol Biol 2011, 408 (3), 514–528. https://doi.org/10.1016/j.jmb.2011.02.053.

Appendix

S3 Supplementary Information for Chapter Three

S3.1 Supporting Methods

In QCM-D, the relationship between mass change and frequency shift for a rigid adsorbed layer can be described by the Sauerbrey equation (Eq. 1):

Equation 1

$$\textbf{\textit{Eq. 1:}}\ \Delta m = -C\frac{\Delta f}{n}$$

Δm is the mass gain of each sensor, Δf is the frequency reduction observed, n is the overtone number, and C is the mass sensitivity constant (~17.7 ng cm^{-2} Hz^{-1} for a 5 MHz quartz resonator).

Regarding the viscoelastic property of the adsorbed lysozyme layer, dissipation (D) is expressed as proportional to the energy dissipated over the energy stored in the oscillating system (Eq. 2):

Equation 2

$$\textbf{\textit{Eq. 2:}}\ D = \frac{E_d}{2\pi E_s}$$

D is the dissipation, and E_d and E_s are the energy dissipated and stored in the oscillating system.

S3.2 Supporting Results

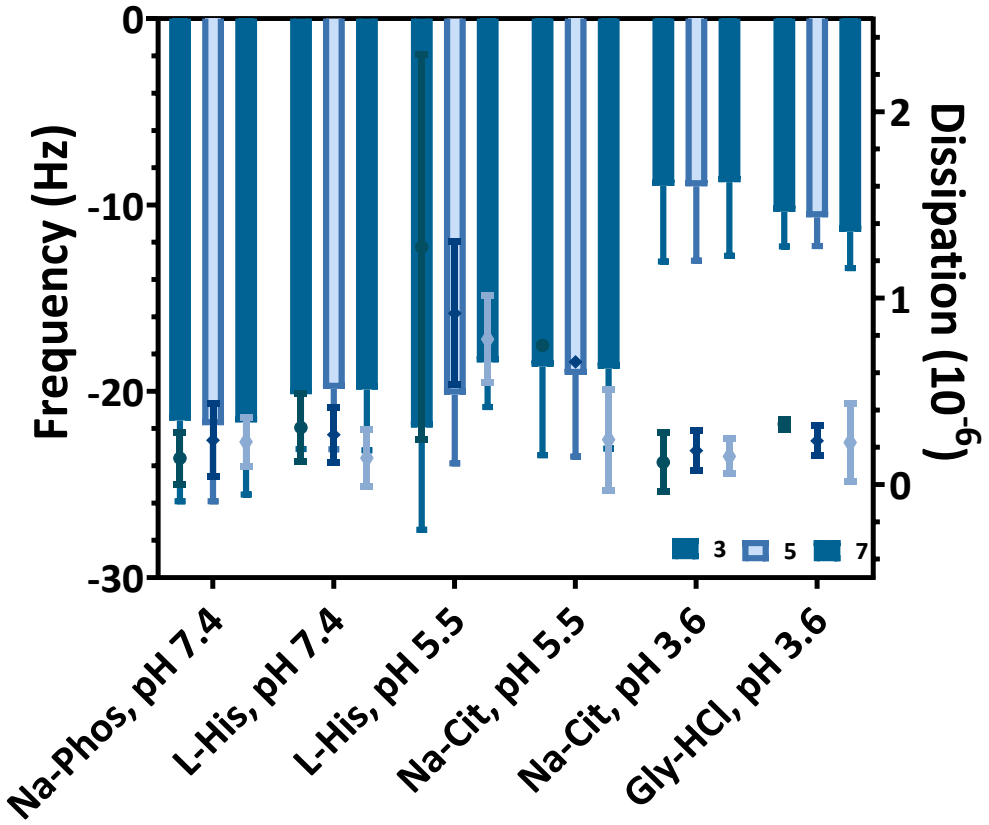


Figure S3.1: Overtone comparison for frequency and dissipation after data acquisition at time=30 min. Frequency and dissipation correspond to the left and right y axes, respectively. Data represents mean ± SD, n=3 for frequency and at least n=2 for dissipation.

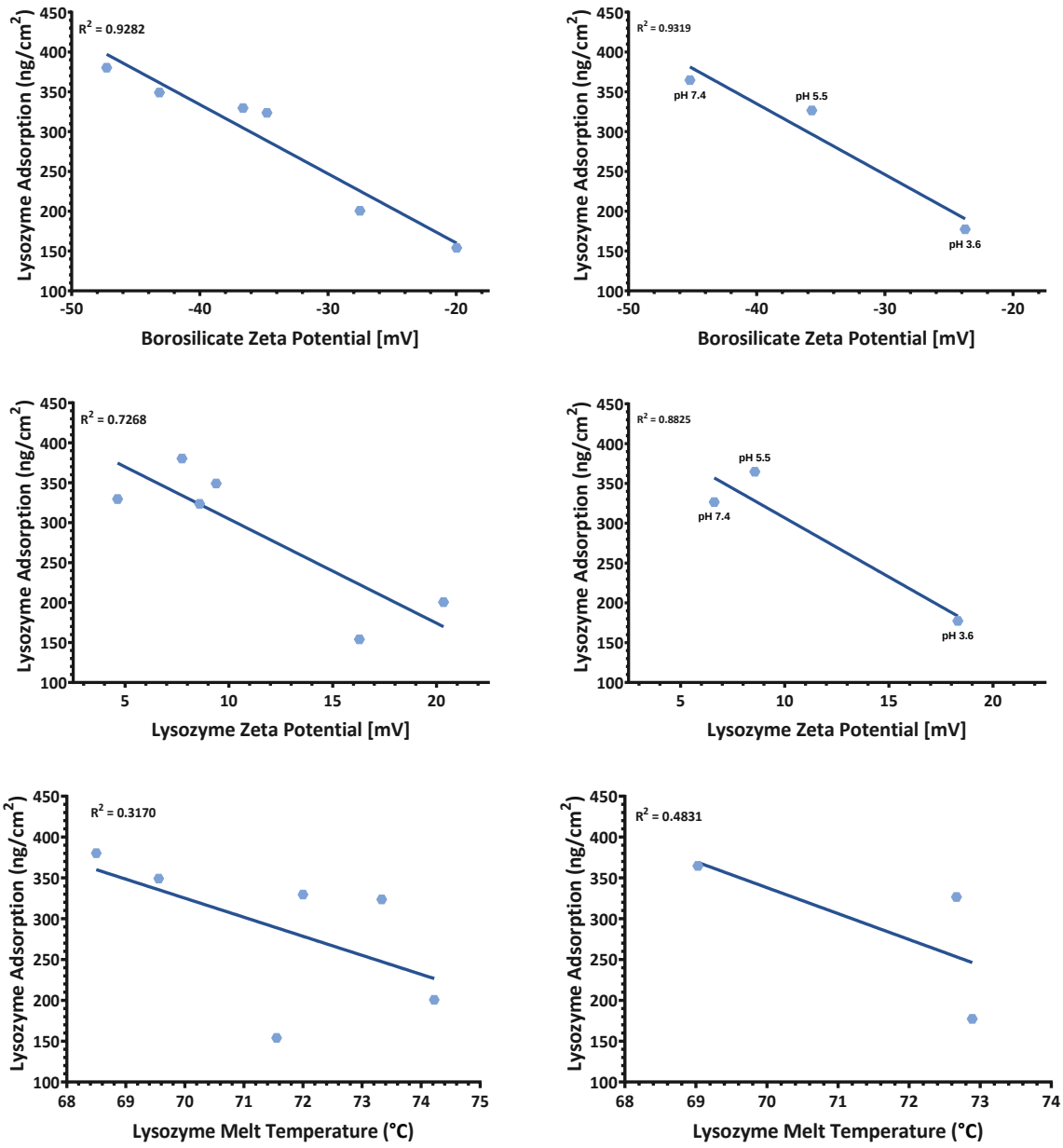


Figure S3.2: Linear regression of the adsorption data obtained by QCM-D from the 1 mg/mL buffered solutions graphed as a function of zeta potential, thermal melt temperature and pH.

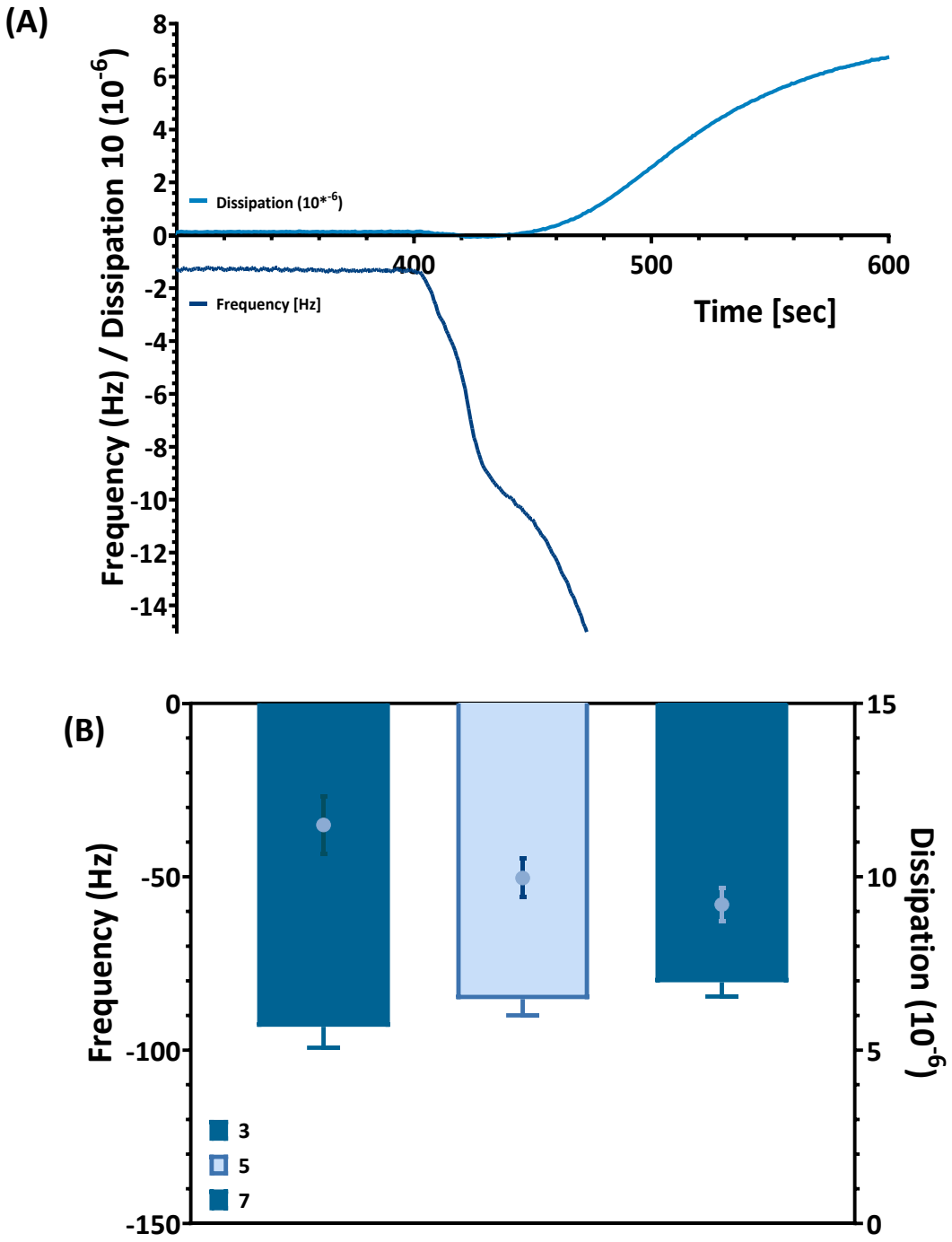


Figure S3.3: Two-step adsorption process observed during QCM-D analysis of 25 mg/mL lysozyme (**A**) and overtone analysis of the frequency and dissipation values after data acquisition at time=30 min (**B**). Frequency (blue bars) and dissipation (blue circles) correspond to the left and right y axes, respectively. Data represents mean ± SD, n=3.

S4 Supplementary Information for Chapter Four

S4.1 Supporting Methods

Linear regression analysis for upright vial orientation

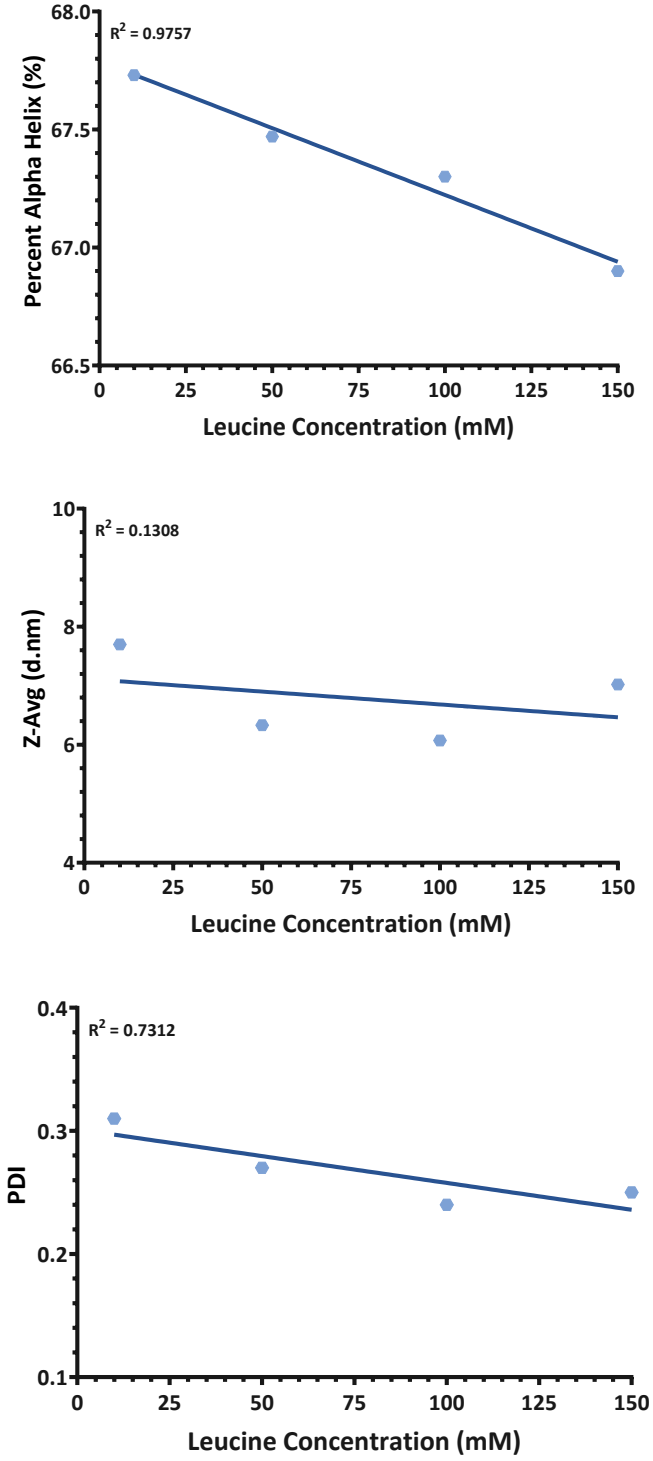


Figure S4.1: Linear regression of the stability data obtained by CD spectroscopy and DLS graphed as a function of leucine concentration.

Linear regression analysis for inverted vial orientation

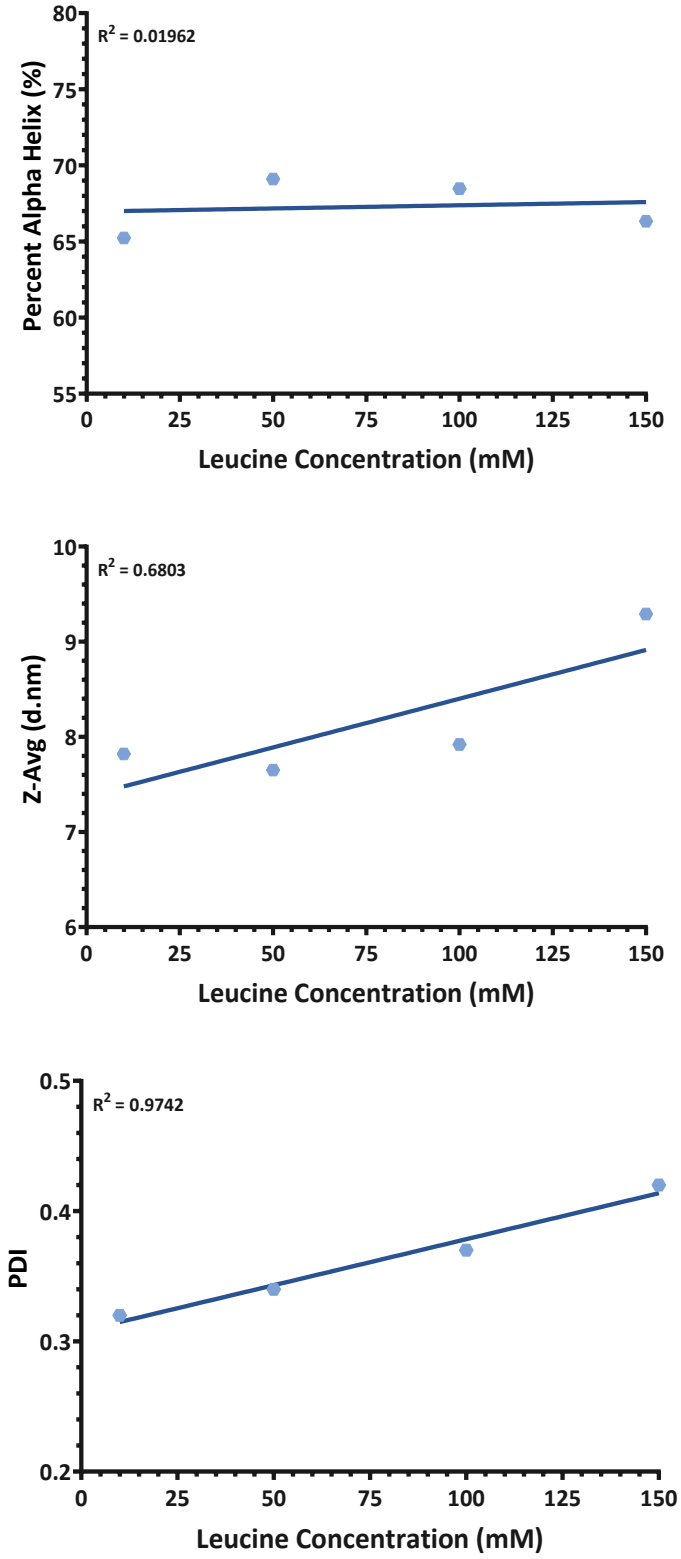


Figure S4.2: Linear regression of the stability data obtained by CD spectroscopy and DLS graphed as a function of leucine concentration.

S5 Supplementary Information for Chapter Five

S5.1 Supporting Methods

Fourier transform infrared (FTIR) spectroscopy for the protein gels was conducted using a Perkin Elmer Spectrum Two instrument operating in single beam mode, using 4 scans, a 16 cm^{-1} resolution, and a 2 cm^{-1} data interval.

S5.2 Supporting Results

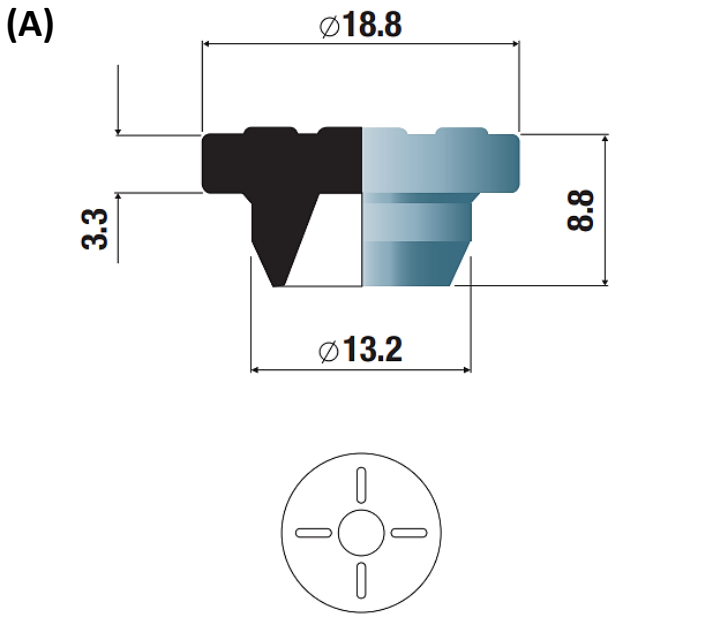
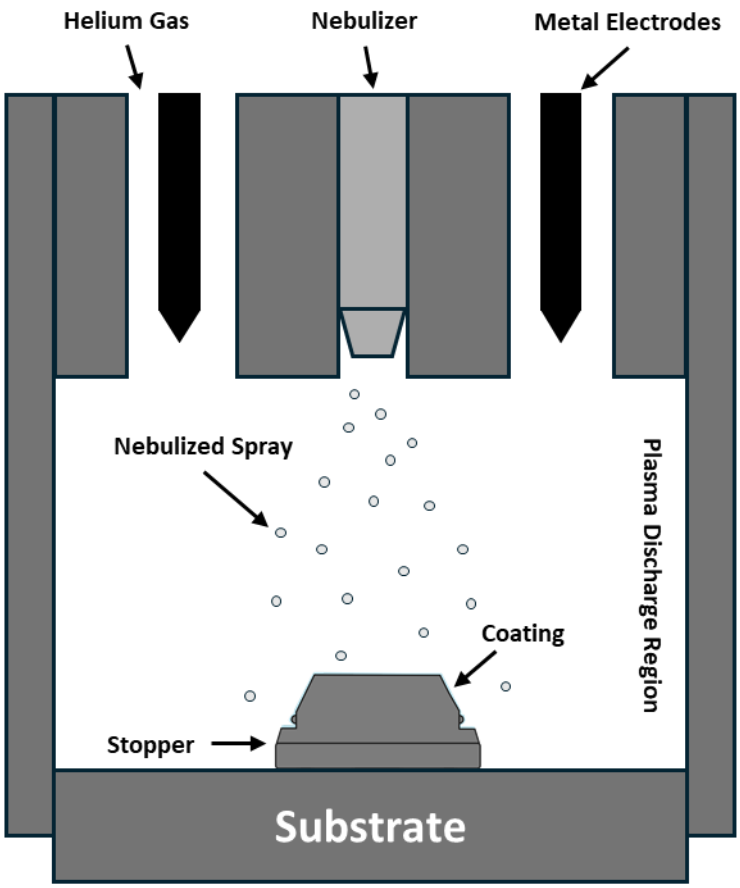
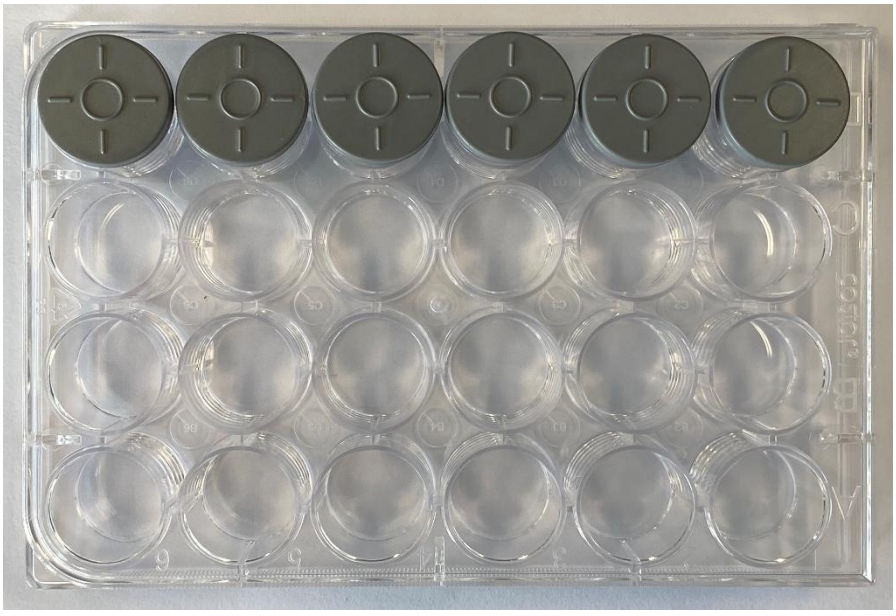


Figure S5.1: Schematic of uncoated, small volume bromobutyl stopper (**A**) and an image of an uncoated bromobutyl stopper used in this study (**B**).

(A)


Helium Gas
Nebulizer
Metal Electrodes
Nebulized Spray
Plasma Discharge Region
Coating
Stopper
Substrate

(B)



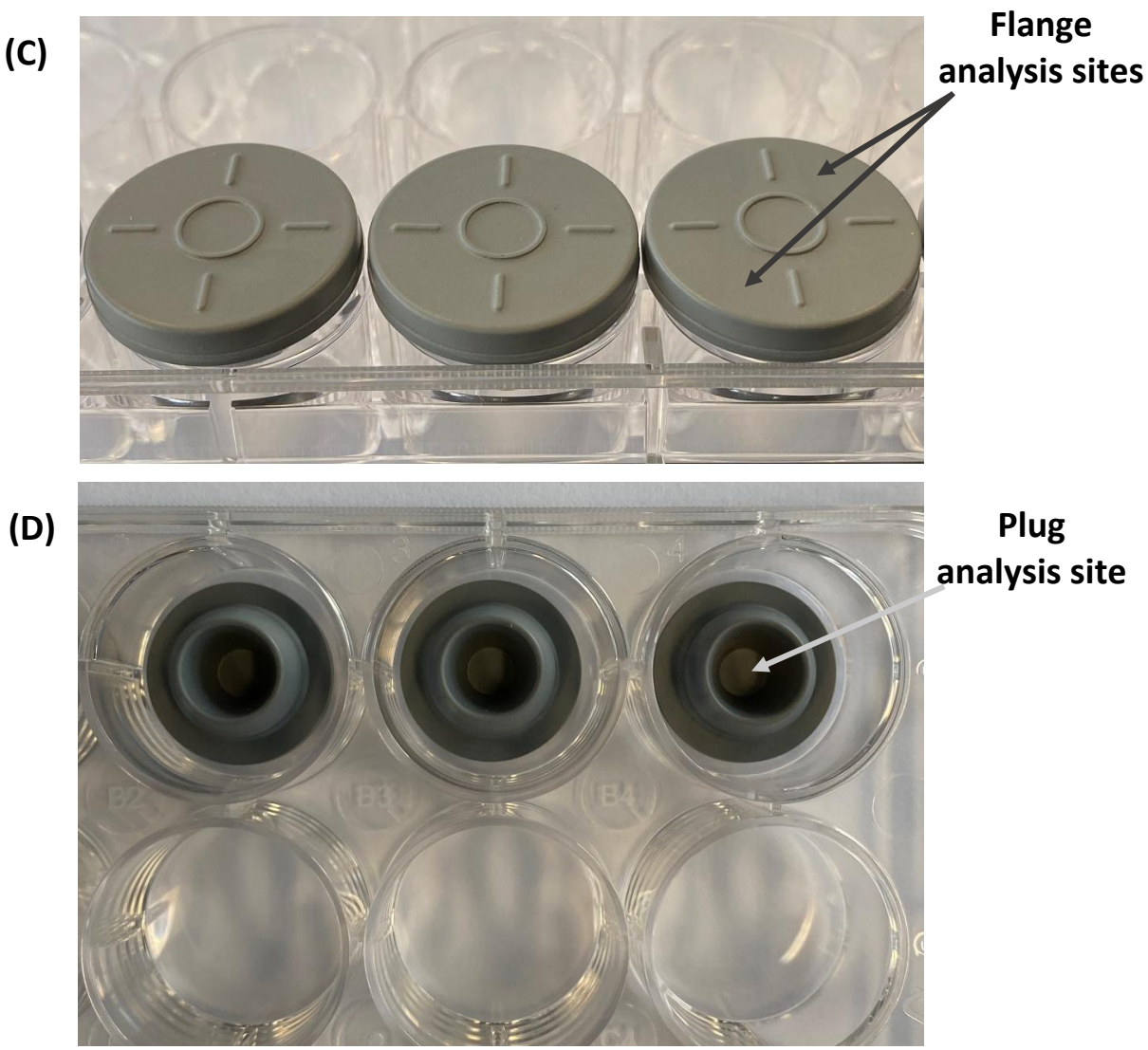


Figure S5.2: Schematic diagram of plasma deposition system (**A**), substrate set-up for the DoE (**B**), close-up view of the top of the stoppers showing flange sites analysed (**C**) and substrate set-up used in the study to coat the drug contact side (plug) of the stopper vial (**D**).

Table S5.1: Variables and corresponding run number for the full factorial 2^4 design.

Concentration (mg/mL)	Flow Rate (µL/min)	Voltage (V)	Speed (mm/min)	Run number
2	50	100	500	**1**
2	100	100	500	**2**
2	100	100	2000	**3**
2	50	100	2000	**4**
2	100	150	500	**5**
2	50	150	500	**6**
2	100	150	2000	**7**
2	50	150	2000	**8**
8	100	150	2000	**9**
8	50	150	2000	**10**
8	100	100	2000	**11**
8	50	100	2000	**12**
8	50	100	500	**13**
8	100	100	500	**14**
8	100	150	500	**15**
8	50	150	500	**16**

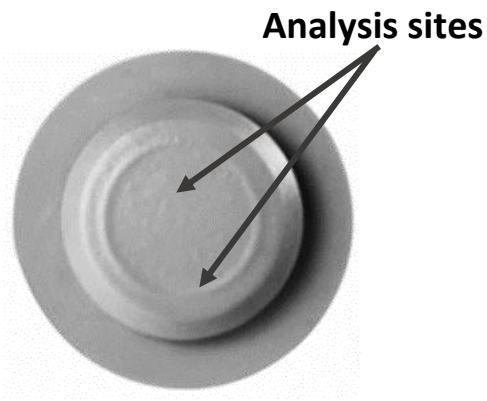


Figure S5.3: Halobutyl locking flange septa used for AFM analysis showing analysis site locations.

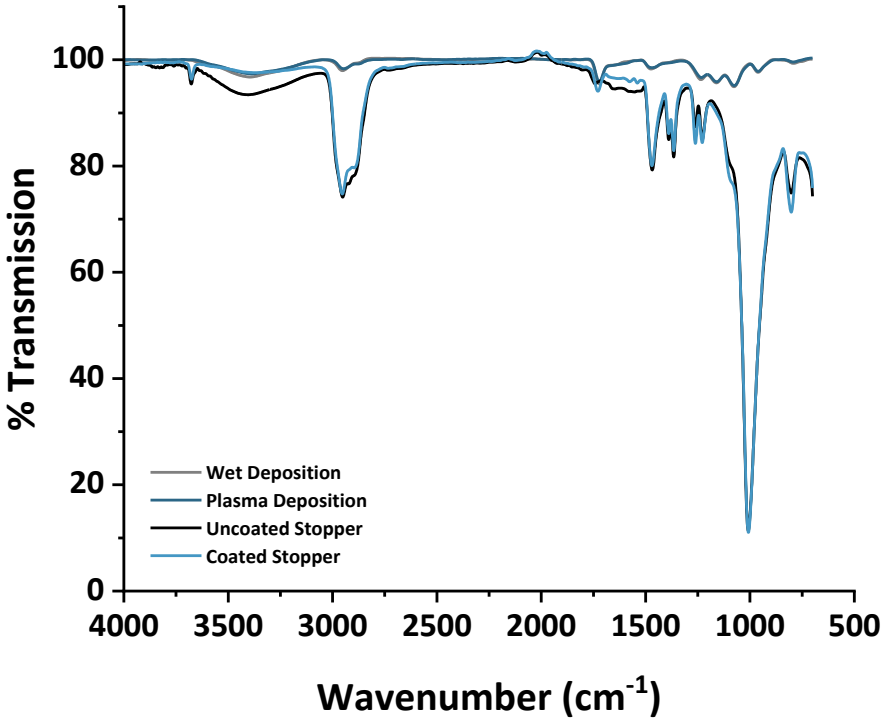


Figure S5.4: FTIR spectra of uncoated stopper, poly(MPC-*co*-BMA)-coated stopper and coatings produced on NaCl discs by wet and plasma deposition methods.

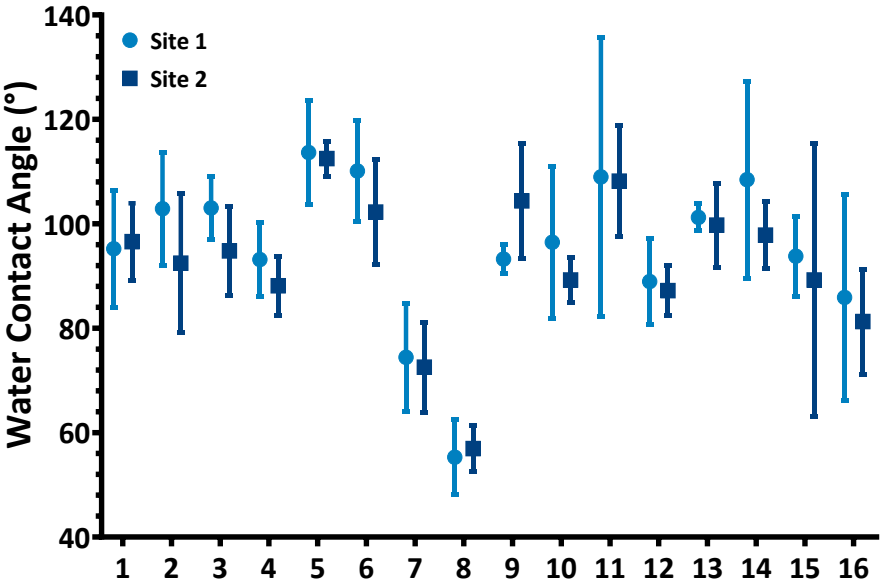


Figure S5.5: In-air static WCA measurements for each site measured on the stopper flange for runs 1 to 16. Data represents mean ± SD, n=6.

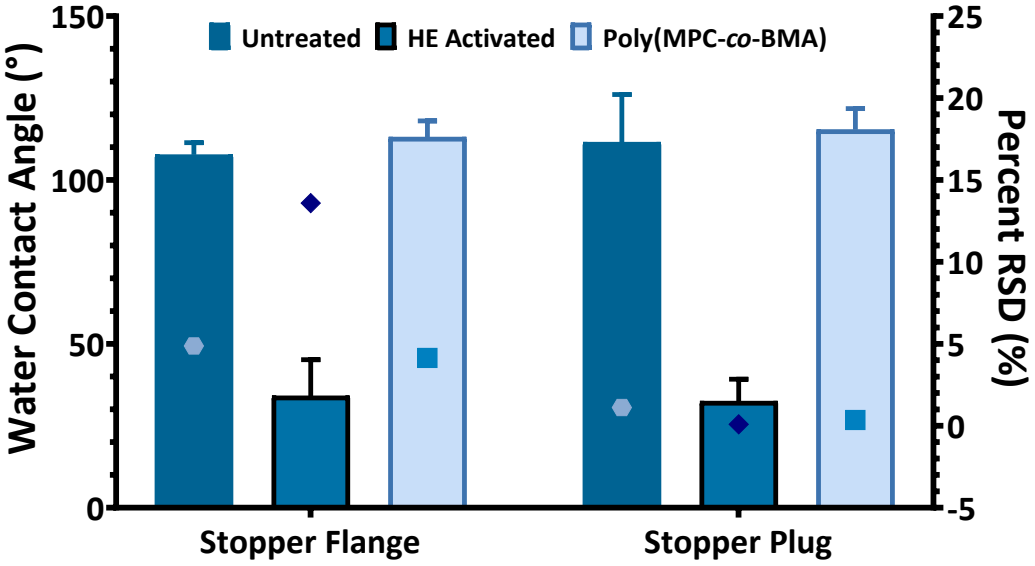


Figure S5.6: Comparison of the WCA (blue bars, x axis) measurements and %RSD (blue symbols, y axis) conducted on top of the stopper versus the drug contact surface (plug). He activated represents He activated control. Data represents mean ± SD, n=6 for the stopper flange and n=3 for the stopper plug.

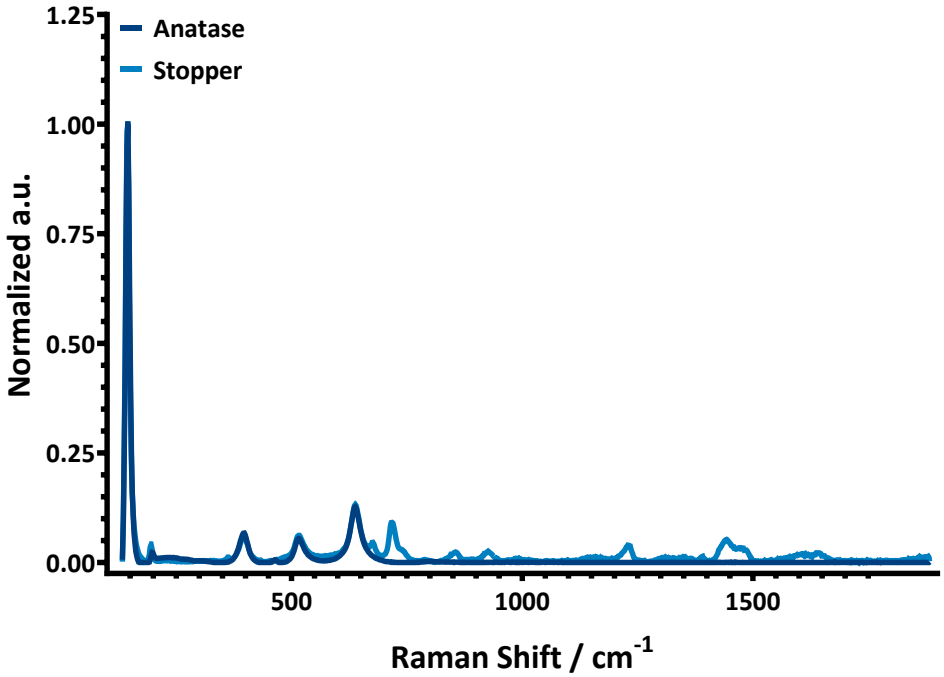


Figure S5.7: Raman spectra of titanium dioxide (TiO_2, Anatase) reference vs TiO_2 signal obtained from an uncoated stopper. The component was generated by reviewing <400,000 spectra using Renishaw's Empty Modelling™ algorithm.

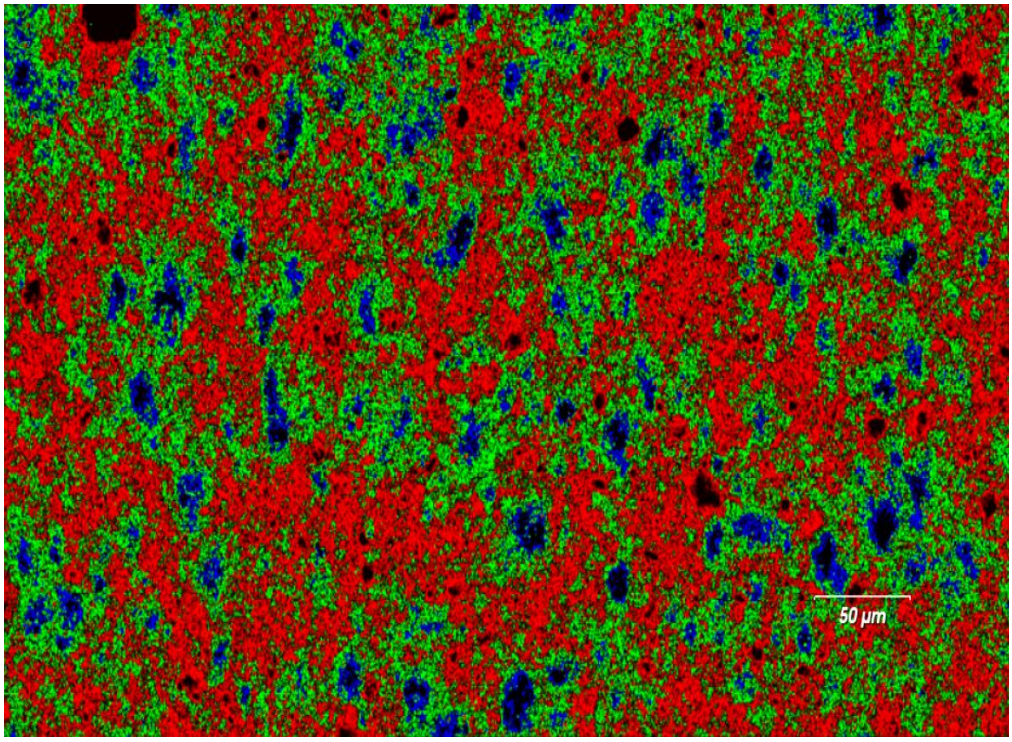


Figure S5.8: Raman hyperspectral images of the drug contact area of poly(MPC-*co*-BMA)-coated stopper plugs deposited using the parameters from run 7 (polymer concentration 2 mg/mL, voltage 150 V, flow rate of 100 µL/min and speed 2000 mm/min) in **Table 3**, scale bar 50 µm. Red coloring indicates the signal of TiO_2 near the surface, green represents the TiO_2 signal at the midpoint and blue denotes the signal at the lowest depth measured (2 µm). The black color represents areas where the Raman signal was oversaturated due to intense autofluorescence.

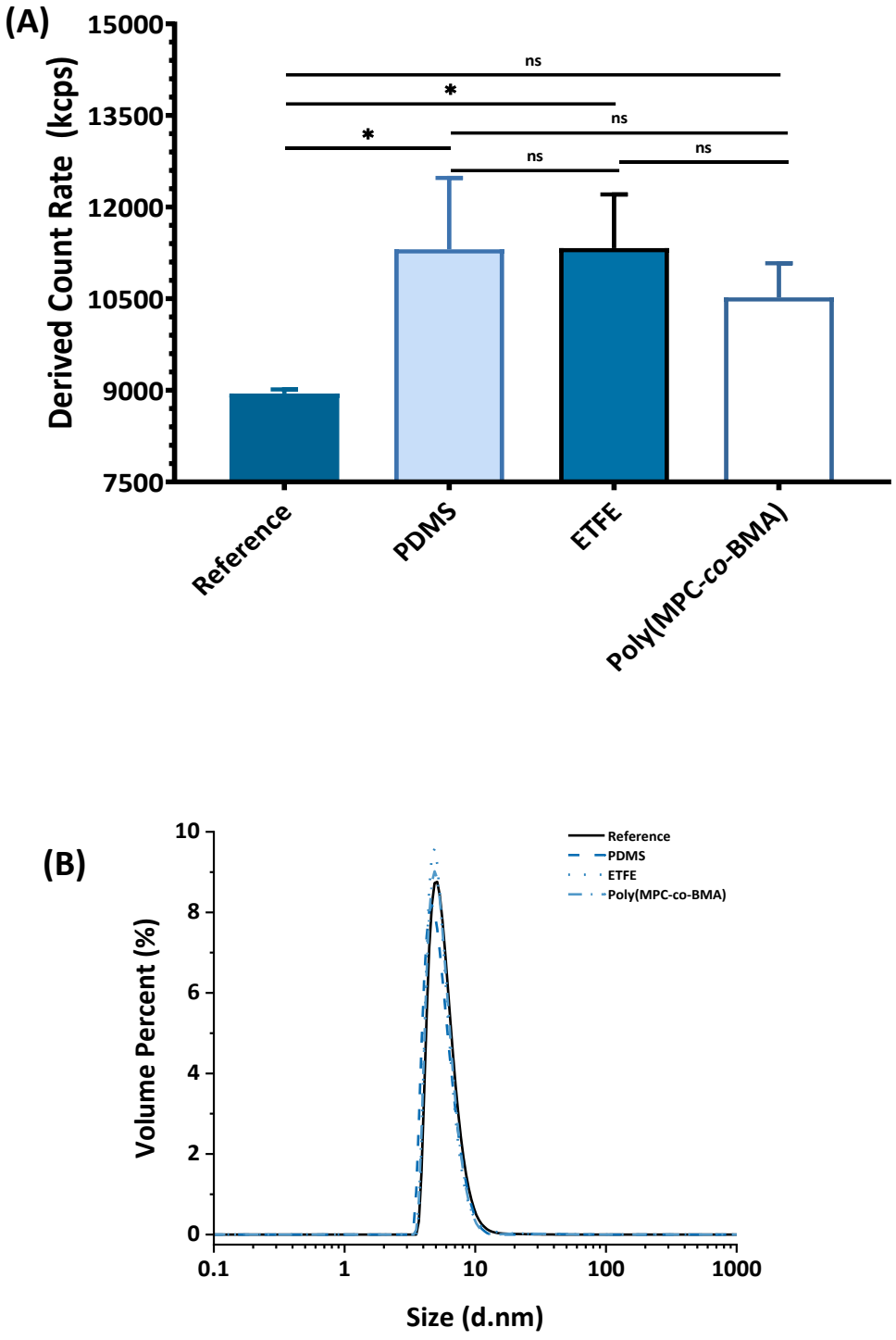


Figure S5.9: Derived count rate (**A**) and volume plot (**B**) of BSA 100 mg/mL formulation after 3 months inverted storage with PDMS, ETFE or Poly(MPC-*co*-BMA)-coated stoppers under thermal stress conditions (40°C). All measurements were performed using three independent replicates, n=3, measured in duplicate. Statistical analysis was conducted on data in (**A)** using a one-way ANOVA with Tukey's post hoc analysis, *p<0.05.

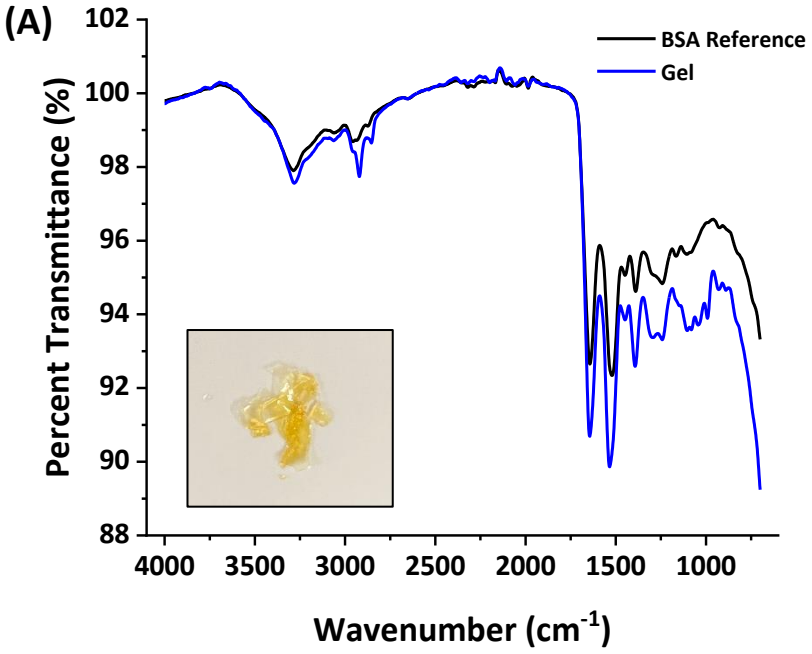


Figure S5.10: FTIR spectra of BSA gel particles after water removal by desiccation for 8 h. The gel spectra are representative of the gel particulates collected from formulations in contact with PDMS, ETFE and poly(MPC-*co*-BMA)-coated stoppers following storage at 40°C for 3 months. The inset shows collated gel particles before water removal.

S6 Supplementary Information for Chapter Six

Table S6.1: Techniques commonly applied to study protein adsorption and stability.

Technique	Signal measured	Data obtained	Considerations
UV-Vis Spectroscopy	Absorbance of UV and visible light	Quantitation of protein concentration Qualitative estimation of tertiary stability using second derivative UV Estimation of aggregation using Aggregation Index Can monitor opalescence and precipitation using turbidity	Second derivative UV only works with proteins that have several aromatic residues Low sensitivity
Raman Spectroscopy	Measures inelastic scattering of monochromatic light	Qualitative identification of protein secondary structure changes Can quantify changes in peak position of amide bands and aromatic amino acid residues	Complete analysis of secondary structure and amide bands Complex data analysis Analysis depends on the substrate on which the sample is placed for analysis
Differential Scanning Fluorimetry	Measures fluorescence changes in response to protein-dye binding	Can determine protein thermal properties Can examine protein-excipient interactions	Uses hydrophobic dyes which are incompatible with hydrophobic excipients It is difficult to obtain a signal for proteins with low internal stability

Circular Dichroism Spectroscopy	Measures the differential absorption of left and right circularly polarised light	Qualitative assessment of protein secondary structure Qualitative identification of tertiary structure Can determine thermal properties. Quantitative measurement of aggregation kinetics by transmittance Quantitative analysis of secondary structure components	Sensitive to buffer composition, pH, salt composition, ionic strength and additives which alter hydration Tertiary structure is challenging to investigate Physical properties of the protein must be known High sensitivity/specificity to protein size, shape and secondary structure
Quartz Crystal Microbalance	Measures change in frequency and dissipation energy of a quartz crystal resonator	Can quantify the amount of adsorbed protein *in-situ* Can measure adsorption kinetics Can determine layer properties Can assess protein stability in the adsorbed state Can determine formulation effects on protein adsorption Can quantify and probe desorption mechanism	High sensitivity Compatible with various surfaces Very sensitive to mechanical vibrations and environmental conditions The determination of arial mass is coupled with the solution conditions Dissipation affects the mass calculation Viscoelastic modelling is very complex
X-ray Photoelectron Spectroscopy	Measures the kinetic energy of electrons emitted from a surface under X-ray irradiation	Analyses the surface chemistry of a material, mainly its elemental composition, chemical state, and electronic state	Samples must be compatible with a vacuum environment

HPLC	Uses chromatographic separation techniques	Reverse phase quantifies bulk protein and desorbed protein concentration in addition to changes in hydrophobicity Size exclusion can quantify aggregation and fragmentation	Dependent on protein properties. Requires extensive validation procedures Sensitive to impurities Size exclusion can incorrectly report size distribution
Tensiometry	Measures the change in surface tension. Measure changes in surface contact angle	Measures dynamics of protein adsorption at the air-liquid interface It can be used to measure excipient effects on protein adsorption It can be used to measure changes in surface chemistry	Requires high sample volume Low specificity Insensitive
IR Spectroscopy	Infrared light absorption to identify molecular vibrations	Qualitative identification of changes in protein secondary Track changes in amide band peak position to monitor chemical stability Quantitation of protein concentration	Complete analysis of amide bands Complex quantitative analysis Requires D_2O Protein concentration analysis requires a specialised instrument
Microscopy e.g., fluorescence, light, electron	Uses various types of light and electron interactions to produce detailed images	High resolution imaging of biological molecules and particles	Low specificity Can measure protein adsorption and stability *in-situ*

Fluorescence Spectroscopy	Emission of light by excited fluorescent molecules	Qualitative information on protein tertiary structure Can quantify changes in fluorescence intensity and monitor stability using F_{max}	High sensitivity Low specificity
Dynamic Light Scattering	Measures fluctuations in light scattering due to particle Brownian motion	Quantifies the size of native proteins, aggregates and sub-visible to visible particles Can quantify polydispersity Measures thermal properties, aggregation and aggregation kinetics	Particles greater than 2 µm can be incorrectly identified. High sensitivity Z-Avg, PDI, DCR, %Int can hide the effects of particle size distribution Low specificity Sensitive to molecules which alter the protein hydration shell It requires a spherical or near-spherical shape for accurate analysis